



US Army Corps
of Engineers



TECHNICAL REPORT GL-85-5

(6)

THE VAIONT SLIDE, A GEOTECHNICAL ANALYSIS BASED ON NEW GEOLOGIC OBSERVATIONS OF THE FAILURE SURFACE

Volume I
MAIN TEXT

by

A. J. Hendron, Jr., F. D. Patton

AD-A158 192

DTIC FILE COPY



June 1985

Final Report
(In Two Volumes)

Approved For Public Release, Distribution Unlimited

DTIC
SELECTED
AUG 21 1985
S E

Prepared for DEPARTMENT OF THE ARMY

US Army Corps of Engineers
Washington, DC 20314-1000

Under Contract No. DACW39-79-C-0063

Monitored by Geotechnical Laboratory
US Army Engineer Waterways Experiment Station
PO Box 631, Vicksburg, Mississippi 39180-0631

85 8 19 070

**Destroy this report when no longer needed. Do not return
it to the originator.**

**The findings in this report are not to be construed as an official
Department of the Army position unless so designated
by other authorized documents.**

**The contents of this report are not to be used for
advertising, publication, or promotional purposes.
Citation of trade names does not constitute an
official endorsement or approval of the use of
such commercial products.**

Unclassified

SECURITY CLASSIFICATION OF THIS PAGE (When Data Entered)

REPORT DOCUMENTATION PAGE		READ INSTRUCTIONS BEFORE COMPLETING FORM
1. REPORT NUMBER Technical Report GL-85-5	2. GOVT ACCESSION NO.	3. RECIPIENT'S CATALOG NUMBER
4. TITLE (and Subtitle) THE VAIONT SLIDE, A GEOTECHNICAL ANALYSIS BASED ON NEW GEOLOGIC OBSERVATIONS OF THE FAILURE SURFACE; Volume I: MAIN TEXT		5. TYPE OF REPORT & PERIOD COVERED Final report
7. AUTHOR(s) A. J. Hendron, Jr. F. D. Patton		6. PERFORMING ORG. REPORT NUMBER Contract No. DACW39-79-C-0063
9. PERFORMING ORGANIZATION NAME AND ADDRESS		10. PROGRAM ELEMENT, PROJECT, TASK AREA & WORK UNIT NUMBERS
11. CONTROLLING OFFICE NAME AND ADDRESS DEPARTMENT OF THE ARMY US Army Corps of Engineers Washington, DC 20314-1000		12. REPORT DATE June 1985
14. MONITORING AGENCY NAME & ADDRESS (if different from Controlling Office) US Army Engineer Waterways Experiment Station Geotechnical Laboratory PO Box 631, Vicksburg, Mississippi 39180-0631		13. NUMBER OF PAGES 324
16. DISTRIBUTION STATEMENT (of this Report) Approved for public release; distribution unlimited.		15. SECURITY CLASS. (of this report) Unclassified
17. DISTRIBUTION STATEMENT (of the abstract entered in Block 20, if different from Report)		<i>Abstract containing color prints; all DDCR reproductions of this document will be in black and white.</i>
18. SUPPLEMENTARY NOTES Available from National Technical Information Service, 5285 Port Royal Road, Springfield, Virginia 22161. Appendices A through G are contained in Volume II.		
19. KEY WORDS (Continue on reverse side if necessary and identify by block number) Landslides--Italy (LC) Vaiont Slide (WES) Slopes (Soil mechanics) (LC) Toc, Mount (Italy) (LC) Geology, Structural (LC)		
20. ABSTRACT (Continue on reverse side if necessary and identify by block number) The large volume and high velocity of the Vaiont Slide combined with the great destruction and loss of life that occurred make it a key precedent landslide, particularly for slides caused by reservoir filling. Engineers and geologists are now generally obliged to examine the slopes of proposed reservoirs for the owners. When the identified slides are large and the effects on the project could be significant, there is an obligation to explain why such (Continued)		

DD FORM 1 JAN 73 EDITION OF 1 NOV 65 IS OBSOLETE

Unclassified

SECURITY CLASSIFICATION OF THIS PAGE (When Data Entered)

Unclassified

SECURITY CLASSIFICATION OF THIS PAGE(When Data Entered)

20. ABSTRACT (Continued).

slopes are different from and safer than the Vajont slopes. Such technical evaluations and comparisons require detailed knowledge of the Vajont Slide, its geology, and the geotechnical evaluations made prior to and following the slide. If the engineers cannot give a reasonably complete and consistent explanation for the Vajont Slide, in terms of currently available stability analyses, then it is difficult to see how they can feel confident about their comparative evaluation of other reservoir slopes. The disturbing aspect of previous reviews of the Vajont Slide is that there are gross inconsistencies when the field data, slide behavior, and the results of analyses are compared.

This report describes the efforts to confirm the existence and nature of clay seams in the slide mass and to confirm the possible existence of an "old" slide at the site. These efforts were made by (a) firsthand field observations of the geology, (b) an examination of preslide and postslide airphotographs, (c) laboratory testing of samples of failure plane materials, and (d) an examination and translation of geologic and other documents related to preslide and postslide conditions. Stability analyses of the Vajont Slide are presented in the report which are relatively consistent with all the observed facts.

The study confirmed that the Vajont Slide was a reactivation of an old slide. The slide moved upon one or more clay layers which were continuous over large areas of the surface of sliding. Three-dimensional stability analyses were required due to the magnitude of the upstream inclination of the clay layers forming the base of the slide. The angle of shearing resistance of the clay layers was determined to be about 12 degrees. The fluid pressure distributions used were consistent with the only piezometric data available before the 1963 slide and with an interpretation of the local groundwater flow system including the presence of karstic terrain above the slide. Results of the analyses completed for key periods in the history of the slide agree with the known slide behavior during these periods. The results also indicate that the reduction in the factor of safety caused by reservoir filling alone was approximately 12 percent, while the reduction caused by rainfall or snowmelt ranged from 10 to 18 percent.

Correlations made between cumulative precipitation, reservoir levels, and slide movement records provide a well-defined "failure" envelope. These results explain why the slide was unstable at a given reservoir level and later stable at the same level. Conclusions from these correlations are consistent with the results of the stability analyses. The results of the study also suggest that the slide could have been stabilized by drainage.

Unclassified

SECURITY CLASSIFICATION OF THIS PAGE(When Data Entered)

PREFACE

The study reported herein was performed under Contract No. DACW39-79-C-0063 (Negotiated), dated 06 July 1979, as part of the work being performed at the U.S. Army Engineer Waterways Experiment Station (WES) in Rock Mechanics and Engineering Geology.

This report was prepared by Dr. Alfred J. Hendron, Jr., and Dr. Franklin D. Patton. The authors acknowledge our principal consultants, Dr. Donald L. Anderson and Professor Edoardo Semenza. Dr. Anderson undertook several original analyses at our request. Professor Semenza, with the assistance of his colleague Professor Daniele Rossi, prepared the preslide and postslide geologic cross sections for this study. Dr. Semenza also showed the authors outcrops which were representative of the principal stratigraphic units of the area.

Valuable assistance was given to the writers by Mr. H. Rodney Smith and Dr. Gabriel Fernandez. Both accompanied the writers during our principal field investigation in 1979, and both were involved in the compilations and calculations leading to the final report.

Dr. Camillo Lina'ì and his colleagues at Ente Nazionale per L'Energia Elettrica (ENEL), Venice, Italy were very cooperative in supplying relevant material from ENEL's files. The writers were also accompanied by Dr. Luciano Broili during one of their earlier field trips to the slide.

The contribution of Mr. James F. Patterson of the Hydroelectric Design Division of the British Columbia Hydro and Power Authority is acknowledged for supporting the writers in an earlier review of the Vajont Slide. B. C. Hydro has kindly allowed the authors to use the data gathered in this earlier review.

Editorial assistance for the report was provided by Wendy Patton and is gratefully acknowledged. Typing was provided by Mary Ann Speck.

The contract monitor for this study was Dr. Don Banks. The writers acknowledge Dr. Banks and Dr. Paul Fisher for their administrative support and technical interest in this study. The review of the draft report for this study provided by Dr. D. C. Banks, Dr. P. Fisher and Dr. Paul F. Hadala, Mr. Walter C. Sherman, and Dr. George Kiersch was very helpful and appreciated.

Finally, we wish to thank our families, friends, and colleagues who throughout this study provided the necessary moral support, suggestions, and patience during the period 1973 to 1984 in which this work was accomplished.

The Commanders and Directors of WES during the period of the study and the preparation and publication of this report were COL John L. Cannon, CE; COL Nelson P. Conover, CE; COL Tilford C. Creel, CE; and COL Robert C. Lee, CE. Technical Directors of WES were Mr. Fred R. Brown and Dr. Robert W. Whalin.

Accession For	
NTIS GRA&I	<input checked="" type="checkbox"/>
DTIC TAB	<input type="checkbox"/>
Unannounced	<input type="checkbox"/>
Justification _____	
By _____	
Distribution/ _____	
Availability Codes	
Dist	Avail and/or Special
A-1	



CONTENTS

	Page
PART I: INTRODUCTION.....	1
Importance of the Vajont Slide.....	1
Technical Literature.....	2
Objectives of This Study.....	3
Activities Undertaken.....	5
Organization of Report.....	5
Previous W.E.S. Publication.....	6
Terminology Used.....	7
PART II: DESCRIPTION OF THE SLIDE.....	8
The Wave and Resulting Losses.....	8
Features of the Slide Area.....	9
PART III: GEOLOGY.....	11
Previous Geologic Studies.....	11
General Geologic Setting.....	12
Erto syncline.....	12
Monocline.....	12
Bedrock units.....	13
Prehistoric slides and possible tectonic faulting.....	13
Vajont Valley.....	14
General Stratigraphy.....	15
Clay Interbeds and Layers.....	15
Existence.....	15
Location.....	16
Characteristics.....	17
Stratigraphic continuity.....	18
Differences in terminology.....	19
Evidence from drillholes.....	20
Conclusion.....	21
Structural Geology.....	21
Geologic maps.....	22
Section 2.....	23
Section 5.....	23
Section 10A.....	24
Sections 16 and 17.....	25
Bedding Plane Fault of Possible Tectonic Origin.....	25

Contents	Page
Minor Structures.....	26
Striated rock surfaces.....	26
Folds.....	27
Cascade structures and monoclines.....	27
Faults.....	28
Geomorphology.....	29
Previous studies.....	29
Evidence from airphotos.....	30
Recognition of an old slide.....	30
Karstic topography above slide.....	31
Other airphoto observations.....	31
Hydrogeology.....	32
Rainfall.....	32
Groundwater data.....	32
Groundwater flow systems.....	33
Solution cavities.....	35
Adits.....	35
Artesian pressures.....	36
PART IV: PHYSICAL PROPERTIES OF THE CLAYS.....	37
Introduction.....	37
Grain-Size Analyses.....	37
Atterberg Limits.....	37
Shear Strength Tests.....	38
Clay Mineral Analyses.....	39
PART V: CHRONOLOGY OF SIGNIFICANT EVENTS.....	40
PART VI: CORRELATIONS BETWEEN RESERVOIR LEVEL, PRECIPITATION, AND RATE OF MOVEMENT.....	51
First Reservoir Filling.....	51
Construction of the Bypass Tunnel.....	52
Second Reservoir Filling.....	52
Third Reservoir Filling.....	53
Erroneous Assumptions Regarding the Effect of Reservoir Levels..	53
Combined Effects of Precipitation and Reservoir Level.....	55
PART VII: ASSUMPTIONS FOR THE STABILITY ANALYSES.....	59
Introduction.....	59
Shear Strength.....	59
Water Pressures.....	62

Contents	Page
Geometry of the Failure Plane.....	63
Slide Movements.....	64
PART VIII: STABILITY ANALYSES.....	66
Purpose and Scope.....	66
Periods Examined for Stability.....	67
Basic Assumptions and Sections Analyzed.....	67
Upstream dip of failure surface.....	68
Schematic illustration of the three-dimensional slide.....	69
Angles of shearing resistance.....	69
Section locations and orientations.....	69
Two-Dimensional Stability Analyses.....	70
Cases Analyzed.....	71
Results of Two-Dimensional Stability Calculations.....	72
Influence of reservoir and groundwater levels.....	73
Forces required to maintain equilibrium.....	73
Discussion.....	74
Three-Dimensional Nature of the Slide Surface.....	74
Forces acting on planes parallel to sections.....	74
Factors of safety.....	75
Results.....	77
Discussion of Three-Dimensional Analyses.....	77
Adjustments for non-uniform rainfall.....	77
Uniform behavior of the slide.....	79
PART IX: KINEMATIC CHARACTERISTICS OF THE VAIONT SLIDE.....	80
Introduction.....	80
Mechanisms Investigated.....	80
Loss of Strength and Maximum Velocity of the Slide.....	81
Bounding toe conditions.....	82
Definition of loss of strength.....	82
Results of calculations.....	83
Mechanisms of Strength Losses.....	83
Reduction of friction angle.....	83
Reduction of shear strength at the eastern slide boundary...	85
Heat-generated pore pressures.....	87
Analytical model.....	88
Input and results of heat generation analysis.....	89

Contents	Page
PART X: CONCLUSIONS.....	91
General Geology.....	91
Hydrogeology.....	93
Shear Strength of Clays.....	94
Stability Analyses.....	94
Precipitation and Reservoir Levels.....	95
Slide Velocity Studies.....	96
General Conclusions and Remarks.....	96
PART XI: LITERATURE CITED.....	99
Tables 1-13	
Figures 1-43	
Photos 1-52	
APPENDICES*	
A PRECIPITATION RECORDS ERTO 1960 TO 1963.....	A1
B STATIC SLOPE ANALYSIS METHOD USED FOR THE VAIONT SLIDE ANALYSES by D. L. Anderson.....	B1
C SECTIONS USED IN STABILITY ANALYSES.....	C1
D THREE-DIMENSIONAL SLOPE STABILITY CALCULATIONS.....	D1
E CALCULATION OF SLIDE VELOCITIES by D. L. Anderson.....	E1
F HEAT GENERATED POKE PRESSURE MECHANISMS by D. L. Anderson.....	F1
G SUMMARY OF GEOLOGICAL STUDIES ON THE SLIDE AT VAIONT, 1959-1964 by E. Semenza.....	G1

* Appendices A-G are contained in Volume II.

LIST OF TABLES

No.

- 1 Summary of Observations in Clay Layers and Related Features, Vaiont Slide
- 2 Atterberg Limits on Clay Samples from the Vaiont Slide
- 3 Summary of Direct Shear Test Results on Remolded Vaiont Clays. Tests by: Thurber Consultants Ltd., Edmonton, Canada
- 4 Summary of Direct Shear Test Results on Remolded Vaiont Clay. Tests by: Engineering Geology Lab, Department of Geology, University of Illinois, Urbana
- 5 Summary of Direct Shear Test Results on Remolded Vaiont Clays. Tests by: Waterways Experiment Station, Vicksburg, Mississippi
- 6 Summary of Clay Mineral Analyses on Vaiont Samples
- 7 Precipitation at ERT0 Station at Different Periods Before Slope Movement
- 8 Precipitation at ERT0 Station for Periods Preceding "Safe Arrivals" to Elevations Where Movements Had Previously Accelerated
- 9 Results of Previous Stability Analyses, From Müller (1968)
- 10 Vaiont Slide, Calculated Factors of Safety
- 11 Vaiont Slide, Force Per Unit Width Required to Maintain Equilibrium of the Slide
- 12 Vaiont Slide, Calculations of Maximum Velocities
- 13 Vaiont Slide, Movement Characteristics

Tables in Appendices*

- A1 Daily precipitation record, Erto - 1960
- A2 Daily precipitation record, Erto - 1961
- A3 Daily precipitation record, Erto - 1962
- A4 Daily precipitation record, Erto - 1963
- D1 Static Factors of Safety and Equilibrium Forces, F_s , for Two-Dimensional Cross-Sections Analyzed

* Appendices are contained in Volume II.

LIST OF FIGURES

No.

- 1 Location maps of the Vajont region, Italy
 - 2 Topography of the Vajont Valley before reservoir filling
 - 3 Topography of the Vajont Valley after October 9, 1963
 - 4 Longitudinal profile along the Vajont Valley, looking north
 - 5 Plan view prior to slide of October 9, 1963
 - 6 Regional north-south geologic section through Vajont Slide
 - 7 East-west geologic section through the toe of the slide
 - 8a Geologic sections of other investigators
 - 8b Additional geologic sections of other investigators
 - 9 Geologic column, Vajont Valley
 - 10 Geologic section looking upstream showing old slide mass covering buried alluvium
 - 11 Geologic map of the Vajont Slide, before the slide of October 9, 1963 in pocket
 - 12 Geologic map of the Vajont Slide, after the slide of October 9, 1963 in pocket
 - 13 Photomosaic of the upper portion of the Vajont Slide in pocket
 - 14 Sketch of outcrop of Lower Cretaceous rocks southwest of Casso
 - 15 Geologic Section 2, Vajont Slide, before October 9, 1963
 - 16 Geologic Section 2, Vajont Slide, after October 9, 1963
 - 17 Geologic Section 5, Vajont Slide, before October 9, 1963
 - 18 Geologic Section 5, Vajont Slide, after October 9, 1963
 - 19 Geologic Section 10A, Vajont Slide, before October 9, 1963
 - 20 Geologic Section 10A, Vajont Slide, after October 9, 1963
 - 21 Geologic Section 16, Vajont Slide
 - 22 Geologic Section 17, Vajont Slide
 - 23 Schematic block diagram illustrating the formation of cascade structures, Vajont Slide

No.

- | | | |
|-----|--|-----------|
| 24a | Airphoto of the Vaiont Dam and Reservoir taken in 1960 | in pocket |
| 24b | Airphoto of the Vaiont Dam and Reservoir taken in 1960
(stereopair to Figure 24a) | in pocket |
| 25a | Geomorphic features, Vaiont Slide, delineated from the
1960 airphotos | |
| 25b | Geomorphic features, Vaiont Slide, delineated from the
1960 airphotos (transparent overlay to Figure 24a) | in pocket |
| 26 | Sketches showing a possible explanation for water levels
recorded in P-2 | |
| 27 | Schematic section through Vaiont Slide showing estimated
regional groundwater flow system | |
| 28 | Plasticity chart, clay samples, Vaiont Slide | |
| 29 | Vaiont Slide, comparison of water levels, movements, and
precipitation, 1960 through 1963 | |
| 30 | Stability of Vaiont Slide for reservoir elevation vs.
7-day precipitation | |
| 31 | Stability of Vaiont Slide for reservoir elevation vs.
15-day precipitation | |
| 32 | Stability of Vaiont Slide for reservoir elevation vs.
30-day precipitation | |
| 33 | Stability of Vaiont Slide for reservoir elevation vs.
45-day precipitation | |
| 34 | Slip surfaces of Vaiont Slide assumed by previous authors | |
| 35 | Schematic illustration of the three-dimensional nature of
the Vaiont Slide mass | |
| 36 | Selection of typical slices and forces acting on a
typical slice | |
| 37 | Schematic representation of normal forces on slide cross-
section developed by the upstream dip of the sliding
surface | |
| 38 | Vaiont Slide, schematic illustration of the three blocks
used in the three-dimensional stability analysis | |
| 39 | Vaiont Slide showing pre- and post-slide ground profiles,
assumed failure surface, water and piezometric levels | |
| 40 | Vaiont Slide, assumed geometry as slide movement
progresses | |
| 41 | Vaiont Slide, velocity profiles | |

No.

- 42 Assumptions used in calculations of slide induced fluid pressures
- 43 Vajont Slide, results of the heat generation analysis

Figures in Appendices*

- B1 Subdivision of slide into slices
- B2 Forces on a typical slice of the slide
- B3 Illustration of method for assigning direction of frictional forces between slices
- B4 Treatment of forces acting on the toe of a slide
- C1 Vajont Slide - Semenza Section 2, No reservoir, no rainfall
- C2 Vajont Slide - Semenza Section 2, No reservoir, rainfall
- C3 Vajont Slide - Semenza Section 2, 650 m reservoir, November 1960, no rainfall
- C4 Vajont Slide - Semenza Section 2, 650 m reservoir, November 1960, with rain
- C5 Vajont Slide - Semenza Section 2, 710 m reservoir, October 1963, no rainfall
- C6 Vajont Slide - Semenza Section 2, 710 m reservoir, October 1963, with rainfall
- C7 Vajont Slide - Semenza Section 5, No reservoir, no rainfall
- C8 Vajont Slide - Semenza Section 5, No reservoir, with rainfall
- C9 Vajont Slide - Semenza Section 5, 650 m reservoir, November 1960, no rain
- C10 Vajont Slide - Semenza Section 5, 650 m reservoir, November 1960, with rain
- C11 Vajont Slide - Semenza Section 5, 710 m reservoir, October 1963, no rain
- C12 Vajont Slide - Semenza Section 5, 710 m reservoir, October 1963, with rainfall
- C13 Vajont Slide - Semenza Section 10 Extended, Shallow, No reservoir, no rainfall
- C14 Vajont Slide - Semenza Section 10 Extended, Shallow, No reservoir, with rainfall

* Appendices are contained in Volume II.

No.

- C15 Vajont Slide - Semenza Section 10 Extended, Shallow, 650 m reservoir, November 1960, no rain
- C16 Vajont Slide - Semenza Section 10 Extended, Shallow, 650 m reservoir, November 1960, with rain
- C17 Vajont Slide - Semenza Section 10 Extended, Shallow, 710 m reservoir, October 1963, no rain
- C18 Vajont Slide - Semenza Section 10 Extended, Shallow, 710 m reservoir, October 1963, with rain
- E1 Slide at various stages of movement
- E2 Selection of typical slices and forces acting on a typical slice
- F1 Idealization of vertical deformation with lateral restraint (uniaxial compression test)
- G1 to G16 Refer to Appendix G

LIST OF PHOTOS

No.

- 1 Location 8-1 with respect to the Vajont Dam
- 2 Outcrop 8-1
- 3 Close-up of three of the five clay interbeds at Outcrop 8-1
- 4 Location 10-2A
- 5 Location 10-3A
- 6 Location 10-4
- 7 Location 10-4A
- 8 Location 11-1
- 9 Location 11-3
- 10 Location 11-4
- 11 Location 11-7
- 12 Location 11-7B
- 13 Location 11-8A
- 14 Location 11-10
- 15 Location 11-10A
- 16 Location 12-1
- 17 Location 12-3
- 18 Location 12-4
- 19 Location 12-4A
- 20 Location 12-5
- 21 Location 18-8
- 22 Location 18-14
- 23 Location 22-1A
- 24 Location 22-3
- 25 Location 18-9
- 26 Location 18-9
- 27 Location 22-3A

No.

- 28 Location 22-3A
- 29 Location 22-6
- 30 Location 22-6A
- 31 Location 22-7
- 32 Location 22-7B
- 33 Location 22-8
- 34 Location 23-11
- 35 Location 23-12
- 36 Location 24-3
- 37 Location 24-7
- 38 Location 12-1A
- 39 Location 12-3
- 40 Location 12-3
- 41 Location 18-10
- 42 Located approximately half-way up western part of slide
- 43 Locations 9-2 and 522-6
- 44 Location 22-1
- 45 Location 12-2A
- 46 Location above 18-6
- 47 Location above 18-10
- 48 Float boulder of partly cemented breccia
- 49 Toe of 1963 slide mass
- 50 Malm formation in small excavation above right abutment
of dam
- 51 Location 9-3B
- 52 Location 22-4

THE VAIONT SLIDE
A GEOTECHNICAL ANALYSIS BASED ON
NEW GEOLOGIC OBSERVATIONS OF THE FAILURE SURFACE

PART I: INTRODUCTION

Importance of the Vaiont Slide

The large volume and high velocity of the Vaiont Slide combined with the great destruction and loss of life that occurred make it a key precedent landslide, particularly for slides caused by reservoir filling. The Vaiont Slide is frequently cited as illustrating one of the hazards caused by dam construction even when the dam itself is shown to be safe. In fact, the 1963 Vaiont Slide marked a turning point in the relative emphasis given in hydro projects to the reservoir slopes as compared to the damsite itself. The authors are aware of major dam projects that were delayed or significantly altered in Mexico, Taiwan and Canada, apparently as a direct result of the Vaiont Slide. Modifications were made in many projects around the world. Gruner (1969) noted that in the post-Vaiont period, between 1964 and 1967, new regulations concerning reservoirs were introduced in France, Germany, Italy, Japan, and the United States, and new recommendations were published by UNESCO.

Engineers and geologists are now generally obliged to examine the slopes of proposed reservoirs for the owners. Where unstable slopes are identified, their impact on the project must be explained. When the identified slides are large and the effects on the project could be significant, there is an obligation to explain why such slopes are different from and safer than the Vaiont slopes. Such technical evaluations and comparisons require detailed knowledge of the Vaiont Slide, its geology, and the geotechnical evaluations made prior to and following the slide. If the engineers cannot give a reasonably complete and consistent explanation of the Vaiont Slide, in terms of the currently

available methods of stability analyses, then it is difficult to see how they can feel confident about their evaluation of other reservoir slopes. The disturbing aspect of previous reviews of the Vajont Slide is that there are gross inconsistencies when the field data, slide behavior, and the results of analyses are compared.

Technical Literature

The technical literature on Vajont is abundant, perhaps as a result of the inconsistencies noted. It is likely that more information has been published and more analyses have been made of the Vajont data than for any other slide in the world. However, in spite of this attention, most fundamental questions regarding the failure mechanism and characteristics of the slide have not been satisfactorily explained. For example, an analysis has not been presented which takes into account: (a) the obvious three-dimensional shape of the slide surface, (b) the actual laboratory shear strengths from representative samples of the material on the slide surface, and (c) reasonable piezometric levels related to both rainfall records and reservoir levels. A believable set of analyses must take into account these factors and permit the calculation of credible factors of safety at various key moments in the history of slide movements.

In addition, there are many contradictory statements and conclusions in the literature concerning the Vajont Slide. For example, many authors have claimed or accepted the claims of others that there were no significant clays or clayey units present along the failure surface. These include Broilli (1967), Müller (1967, 1968), Trollope (1977), and Chowdhury (1978). In fact, Müller (1967, 1968) made a point of dismissing the influence of clay interbeds. He stated: "Clay and loam, however, were not present in the stratification joints of the Mount Toc, contrary to some publications" (Müller, 1967). Yet others have tested or described clay beds in the stratigraphic section or attributed them to the failure surface. These include Giudici and Semenza (1960), Carloni and Mazzanti (1964a, 1964b), Kiersch (1964), Selli and

Trevisan (1964), Semenza (1965b), Skempton (1966), Kenney (1967a, 1967b), and Nonveiller (1967a, 1967b).

Another essential factor in an evaluation of the Vaiont Slide is the determination of whether the 1963 slide was a new slide or whether it resulted from the reactivation of a prehistoric slide. Giudici and Semenza (1960) mapped and projected the outcrop of a failure surface along the left (south) side of the Vaiont Gorge before the slide occurred. At the same time, they also mapped a unit of an "old" slide mass on the right (north) side of the gorge near the dam. The existence or absence of an "old" slide was discussed by Müller (1968) and dismissed. He wrote that if one were present, it would not be sufficiently large to be coincident with the actual slide's slip surface.

Objectives of This Study

Finding answers to these questions concerning the clays and the possible existence of an "old" slide was one of the major objectives of this study. It was felt that these and other questions could be answered by: (a) first-hand field observations of the geology, (b) an examination of preslide and postslide airphotos, (c) laboratory testing of samples of failure plane materials, and (d) an examination and translation of geologic and other documents related to preslide and postslide conditions.

Another objective of this study was to perform stability analyses of the Vaiont Slide which were relatively consistent with all the observed facts. Many back-calculations of shear strength parameters for the conditions at failure have been conducted by various investigators on the basis of two-dimensional cross sections. Most of the back-calculated angles of shearing resistance in terms of "effective" stresses, assuming zero cohesion, ranged between 17° and 22° and several were higher. Even the highest values have been considered by some to be too low (Chowdhury, 1978).

In those instances where direct shear tests were made on clay materials found in the slide debris (Kenney, 1967b; Nonveiller, 1967b),

the residual shear strength values of the clays were between 5° and 22°. If the clays are moderately continuous, such low values for shear strength as measured in the tests could not readily be reconciled with the results obtained from the analysis of two-dimensional cross sections used by all previous investigators. This is because the calculations show that the slide would be unstable, even without a reservoir, if a shear strength much less than 17° were used. For example, Kenney (1967a) and Nonveiller (1967a) back-calculated angles of shearing resistance of 19° to 22° and 17° to 39°, respectively, which were considerably higher than the angles of shearing resistance they had measured on samples from Vajont.

The problem was compounded when the water pressures used in many of the analyses appeared to be too low. This meant that even higher strengths were required if the analyses were to achieve the calculated factors of safety. The enigma was confirmed when the authors, prior to this study, briefly visited Vajont on two occasions (Patton in 1975 and both authors in 1976). On both occasions extensive exposures of clay were found along the failure surface. Not only was clay present, it was a clay with a low angle of shearing resistance.

It became obvious that additional investigations were required before analyses could be made that were consistent with all known observations and laboratory data. It was necessary to:

- a. Make a direct examination of many locations on the sliding surface to confirm the actual presence or absence of clay.
- b. Obtain samples of the clays for shear strength tests, Atterberg limits, and clay mineral analyses.
- c. Obtain a more complete history of the chronology of slide related events.
- d. Make geological field observations which would determine whether the 1963 event was a first-time slide or the reactivation of an old slide.
- e. Make field observations that would help confirm the actual directions of slide movements.
- f. Define by field observation any geometrical aspects of the structural geology which would necessitate changes in or invalidate the two-dimensional analyses.

- g. Collect data and make field observations to improve the assessment of water-pressure conditions within the slide.

Activities Undertaken

In order to investigate the items listed above, the following activities were undertaken for this study:

- a. An extensive literature search was undertaken and all available data on Vajont were collected.
- b. The authors, accompanied by H. R. Smith and G. Fernandez, made a one-month field visit to Vajont during the summer of 1979. During this visit the slide surface was traversed at numerous locations and extensive samples and measurements were taken.
- c. Dr. Edoardo Semenza was contacted. He provided numerous documents on the geology of the Vajont region for preslide as well as postslide studies. Dr. Semenza also accompanied the authors during some of their field studies in 1976 and 1979 and undertook several special assignments. Dr. Luciano Broili assisted the writers during their visit to the slide in 1976.
- d. ENEL (Ente Nazionale per l'Energia Elettrica, Compartimento di Venezia) representatives were contacted and they kindly supplied both engineering and geological documents of pre- and postslide conditions.
- e. Laboratory tests were conducted on clay samples recovered from the failure plane.
- f. Additional analyses were conducted which utilize the more detailed knowledge of the three-dimensional structural control of the slide movements and the shear strength data obtained from clay samples.

Organization of Report

The remainder of this report describes the results of these activities. A general description of the slide is given in Part II, and in Part III the significant geological features are discussed. The physical properties of the clays are given in Part IV. A chronology of slide related events is provided in Part V, and important correlations

established between reservoir level, rainfall, and rate of movement are discussed in Part VI. In Part VII assumptions required for the stability analysis are outlined. Static stability analyses of the slide, are provided in Part VIII. The preferred analysis accounts for the three-dimensional effect caused by the upstream dip of the failure plane in the lower part of the slide. In Part IX the kinematics of the slide are addressed and possible mechanisms are discussed which would have resulted in the loss of shear strength necessary for the slide to have moved so rapidly. The conclusions which can be drawn from this study are given in Part X. Literature Cited is presented in Part XI.

Tables 1 to 13 are presented at the end of the text. These are followed by Figures 1 to 43 and Photos 1 to 52. The photos were taken by the authors during their 1979 field trip to the slide.

Appendices A to G provide some of the background material on which this report is based. Appendix A is a list of the rainfall data available for the town of Erto. The method of stability analysis used is described in Appendix B. This method was devised at the request of the authors by Dr. Donald L. Anderson to meet the specific needs of the Vajont Slide and other slides under study by the authors. Details of cross sections and water levels used in the two-dimensional stability calculations are given in Appendix C. Details of the three-dimensional stability analysis undertaken by the authors are given in Appendix D. In Appendix E the dynamics of the slide movements are examined using the same cross sections and initial shear strength mechanism considered in the static stability analysis. Appendix F is a report by Anderson on a model he developed to account for pore pressures induced on the failure surface due to heat generated from sliding. The appendices conclude with a translation of the Semenza (1965b) summary report of geological investigations on the Vajont Slide from 1959 to 1964.

Previous W.E.S. Publication

Previous publications of the U.S. Army Corps of Engineers on the Vajont Slide are limited to a translation of a paper by Schnitter (1973) which was issued as Translation No. 73-6 of the Waterways Experiment

Station. This is principally a short review of the history of the project, a brief chronology of the legal events that followed the slide, and a discussion of the legal implications for practicing engineers. Neither the geology nor mechanics of the slide are addressed.

Terminology Used

A major part of the recent field investigations described in this study took place on newly exposed rock faces above the main mass of the slide where outcrops of the surface of sliding utilized by the 1963 slide could be examined. The composite subplanar rock surfaces that form the slide scarp are among the most prominent features of the slide today. In many areas slabs of the actual surface of sliding have slid down in post October 9, 1963 slides. Moreover, these surfaces are flatter than most slide scarps. In spite of these factors, it is convenient to occasionally call this exposed surface of sliding the "scarp" and to reserve the term "headscarp" for the steeper true scarp along the upper limit of the slide.

The terms "failure surface," "failure plane," and "surface of sliding" are used interchangeably throughout this report.

The term "clay layer" has been used to denote the clay-rich units that are present in the lower portion of the slide debris and along most of the surface of sliding. Although these layers generally conform with adjacent bedding planes, there are many occasions when they cut across bedding planes. In many areas the clay layers resemble a clayey gouge from past landslide or tectonic activity. The term "clay interbed" is used whenever the clay layer in question appears to be a relatively undisturbed stratigraphic unit.

Vajont is spelled with an i rather than with a j as in Vajont. Both spellings appear in the literature on the slide. The spelling Mt. Toc has been used rather than Mt. Toch. It has been convenient to retain the Italian place names for local landmarks rather than translate them to their English language equivalents.

PART II: DESCRIPTION OF THE SLIDE

On October 9, 1963, approximately 270 million m³ (350 million yd³) of rock slid from the side of Mt. Toc into the Vajont Reservoir. The Vajont Slide is located east of Longarone, which is situated on the Piave River some 100 km north of Venice, Italy (see Figure 1). The slide developed along the north slopes of Mt. Toc where the Vajont River had cut a canyon more than 300 m deep just above its junction with the Piave River. The topography of the Vajont Valley before the slide and before the reservoir was filled behind the Vajont Dam is shown in Figure 2. As a result of the slide, the topography underwent enormous changes along the foot of Mt. Toc as shown in Figure 3.

The slide moved a 250-m-thick mass of rock some 300 to 400 m horizontally and is estimated to have reached a velocity of 20 to 30 m/sec before running up and stopping against the opposite side of the Vajont valley wall. The new slide displaced an old slide mass, which had been isolated on the north side of the valley, some 100 to 150 m above its original position before the slide mass slumped backwards 30 to 40 m to the south (Semenza, 1965b). The uppermost portion of the eastern half of the slide apparently moved over the main slide mass in a separate and slightly later movement. The slide filled the lower half of the Vajont Reservoir (which had been drawn down to elevation 700 m from a level of 710 m just prior to the slide) in a matter of a few tens of seconds.

The Wave and Resulting Losses

The wave resulting from the displaced water propagated both upstream and downstream. The wave eroded trees and soil on the north side of the Vajont Valley up to a maximum elevation of 935 m or 235 m above the reservoir level. The wave swept across the dam reaching over 100 m above its crest (435 m above the downstream base of the dam) and down the Vajont Gorge to the Piave River, where it had a height of some 70 m at the confluence with the Piave Valley, destroying most of the

town of Longarone and parts of other towns in the Piave Valley (see Figure 4). Some 2043 persons died and many others were injured, almost all from the effects of the wave. Most of the loss of life occurred in Longarone, but the loss was also severe in nearby villages, especially Pirago (see Figure 1). Forty-five men, who were part of a work force of engineers, technicians, and laborers living in barracks situated on the dam crest, were also killed. Over 16 million dollars was reported paid for civil suits for personal injury and loss of life. Tens of millions of dollars of property damage resulted. The 100-million dollar dam and reservoir were abandoned. The destruction associated with the Vajont Slide and wave have been described by Ajemian (1963), Kiersch (1964), Müller (1964a), Weber (1964), Weiss (1964), Jaeger (1965a), Gervasoni (1969), and many others. The Vajont Slide was a major tragedy of the 1960's.

If both volume and velocity of slide movement are considered, the Vajont Slide has been exceeded in historic times in only a few instances, such as the 1974 Mantaro Slide in Peru and the 1911 Pamir Slide in the U.S.S.R. However, many other prehistoric slides of greater volume than the Vajont Slide have been recognized, and many recent and prehistoric high-velocity slides of smaller volume are known.

Features of the Slide Area

A plan view of the immediate area of the slide prior to October 9, 1963 is given in Figure 5. This plan shows the M-shaped outline of the slide (when facing Mt. Toc from Casso) in relation to the Vajont Dam and the maximum proposed reservoir level (el. 722.5 m). Figures 2 and 5 also show details of the cultural and surface features of the slide area which will be referred to later. Prior to the slide, the principal feature in this area was the central north-south trending dry valley called the "Massalezza Ditch." On the left side of the Vajont River and just downstream from the junction with the Massalezza Ditch was a prominent bluff at el 777 m called the "Punta del Toc." A prominent bench at about el 840 to 850 m was present part way up the western side of

the slide. This was called the "Pian della Pozza" or "Pozza." This plain contained several enclosed depressions similar to those found in karstic regions or in areas with old landslide debris. Along the toe of the slide the Vajont River varied in elevation from 500 m near the dam to 560 m at the upstream side of the slide.

A few people lived on what became the slide area, but the closest town was Casso which is perched above a cliff opposite the slide at about el 940 to 980 m (see Figures 4 and 5). The lowest two buildings in Casso were damaged by water or by the air blast generated by the wave. The remainder of Casso escaped damage. The larger town of Erto is located on the north side of the Vajont Valley some 3-1/2 km upstream from the dam and 1-1/2 km from the slide mass (see Figures 2 and 3). Most of Erto escaped damage from the wave as the town is over 760 m in elevation. The wave at Erto reached about 740 m in elevation or 40 m above the reservoir elevation as shown on Figure 4.

PART III: GEOLOGY

Previous Geologic Studies

The starting point for detailed geologic studies of the Vajont Slide is the 1960 report prepared in 1959-1960 by Giudici and Semenza (1960). Following the 1963 slide many other geologic studies were made for one or the other of the investigative commissions and for ENEL, the hydroelectric authority which had taken over control of the project prior to the slide. Of these postslide studies, the report by Semenza (1965b) is particularly helpful as it provides a history of the geological and geophysical studies from 1959 to 1964. A translation of this report was prepared for this study and a completed version is given in Appendix G. This translation contains the key pre-slide geologic map and sections prepared by Giudici and Semenza (1960).

Following the slide other important geological studies were published. These include Selli and Trevisan (1964), Carloni and Mazzanti (1964b), Martinis (1964), Rossi and Semenza (1965a), Broili (1967), Müller (1964a, 1968), and Loriga and Mantovani (1965, 1970). Of these, only Broili's and Müller's reports were published in English. Kiersch (1964) wrote a brief summary in English providing an early account of the slide, its causes and associated flooding as well as the general geologic features noted following the slide. Because of the timely nature of Kiersch's article, it received widespread attention in North America. The collected works of Selli and Trevisan (1964), Carloni and Mazzanti (1964b) and Ciabatti (1964) constitute essential documents on the geology, slide observations, seismological data, and dynamic evaluation of the slide.

The original geologic mapping of the Vajont Valley was undertaken by Boyer (1913). Boyer prepared a cross section from Mt. Toc to Mt. Borga across the Vajont Valley in the vicinity of the Vajont Slide. However, his section does not indicate the ancestral slide. Müller

(1964a) reports that a geologic study of the reservoir sides conducted by Dal Piaz (1928) did not indicate any valley wall movements. The regional geology of the Vajont area has been studied in more recent times by Rossi and Semenza (1964, 1965a, 1965b, 1967), Semenza (1967), Leonardi and Semenza (1967) and others. Many of these are in the beautifully illustrated two-volume compendium on the geology of the Dolomites, "Le Dolomiti," edited by Leonardi (1967).

General Geologic Setting

The Vajont Slide is located in the southeastern part of the Dolomite Region of the Italian Alps. The mountains in this area are characterized by massive near-vertical cliffs formed by the Jurassic Dogger formation and underlying Triassic formations. The local valleys tend to be associated with outcrops of the weaker formations, particularly the Upper and Lower Cretaceous and Tertiary units which contain more clays and are more thinly bedded.

Erto syncline

The Vajont Valley has been eroded along the axis of an east-west trending, asymmetrical syncline plunging upstream to the east. This has been called the Erto syncline. The syncline is shown extending under Mt. Borga north of the slide on Figure 6. The upstream plunge is shown in Figure 7 on a section made by Broili (1967) through the toe of the slide.

Monocline

An abrupt monoclinal flexure on the south limb of the Erto syncline forms a distinctive and important aspect of the geology of the slide. The axis of the lower fold of the monocline is aligned sub-parallel to the Vajont River, which is some 400 to 800 m to the north. Between this axis, which forms the rear of the "seat of the chair," and the river there is a 9° to 20° eastward dip of the beds down the plunge of the syncline. South of this axis the beds dip to the north towards the Vajont River at 25° to 45°. These beds form the "back" of the slide.

Most sections of the slide are drawn down the maximum dip of the steeper exposed bedding planes located at the "back" of the slide. A number of these sections are given on Figure 8. These sections, which show the flat apparent dip of the "seat" of the slide, are misleading because the true dip of the beds along the seat is 9° to 22° to the east as noted above. This aspect of the geometry of the geologic structure had a significant effect on the behavior of the slide.

Bedrock units

The bedrock in the slide area consists of a thick succession of limestone and marly limestone beds of Upper Jurassic and Lower and Upper Cretaceous ages. Brecciated limestones are present, frequently with chert nodules, in addition to lesser amounts of dolomites. Some of the limestone and dolomite beds are locally porous due to solution features. Occasional clay interbeds are found in the Malm formation of Middle Jurassic age, but are particularly common in the Lower Cretaceous rocks. A simplified stratigraphic column, prepared by Carloni and Mazzanti (1964b), of the rocks exposed in the slide area is shown in Figure 9a, and an abbreviated geologic column is shown in Figure 9b. The base of the Vajont Slide lies within the Lower Cretaceous (c_1 unit of Carloni and Mazzanti) and perhaps in part of the upper part of the Malm formation which overlies the massive oolitic beds of the Dogger formation. The thickness of the beds at the base of the slide averages about 5 to 10 cm but varies from 1 to 20 cm. However, the Dogger limestone (see Figure 9b), which lies a short distance below the failure plane, is "massive" and the thickness of the beds generally exceeds 0.5 to 1.0 m.

Prehistoric slides and possible tectonic faulting

Evidence was found suggesting that the 1963 surface of sliding had a complex origin and corresponded with more than one previous period of rupture. These periods include both a prehistoric landslide or landslides and possibly a much older period of tectonic faulting. The locii of these different periods of shearing displacements were the weak clay interbeds in the Lower Cretaceous units. The outcrop of these previous

rupture surfaces prior to 1963 corresponds with the one shown on Figure 5 as mapped by Giudici and Semenza (1960) along the left side of the Vajont River gorge and described by Semenza (1965b). The elevation of this plane varies from 700 m near the dam to 540 m about 1 km east of the dam. There it rises slowly to el 650 to 660 m in the next 700 m upstream to join the east side of the slide. This surface of rupture generally tends to follow the bedding planes on the downstream (western) side of the slide but appears to cut across or step up to successively higher clay interbeds on the upstream (eastern) side of the slide. It seems unlikely that the surface of sliding would cut smoothly across the bedding as shown by Broili on Figure 7. The eastern side of the slide appears to follow in part a fault that was oriented roughly perpendicular to the river (see Figure 5). Faults have also been mapped along the headscarp of the slide, and some have been mapped along the western side of the slide.

Vajont Valley

The Vajont Valley is an unusual feature. It has an extremely deep and narrow inner gorge some 300 m deep which was eroded within a broader glaciated valley (see Carloni and Mazzanti, 1964b). Following deglaciation, a predecessor to the present Vajont Canyon was eroded into the syncline thereby releasing one or more prehistoric rock slides. Part of one of these slides buried alluvium that was infilling a deep bedrock channel, possibly a preglacial valley. This channel and the overlying slide mass were first mapped by Giudici and Semenza (1960). After these early events, the present canyon was eroded at the site of the Vajont Reservoir. Figure 10, from Selli and Trevisan, is a geologic section showing the alluvium of this earlier buried valley covered by material from a prehistoric slide originating on the north side of the canyon. Figure 15 by Rossi and Semenza shows another interpretation of this old slide mass. It would appear that the present canyon resulted from down-cutting and erosion of the river through an old slide mass which had originated from the south side of the valley. This set the stage for a repeat performance of the prehistoric slide. There is evidence that

further movements of the old slide on the south side of the Vajont River occurred as the canyon was being eroded to its 1963 preslide configuration. This evidence, which involves the presence of talus breccia of several ages infilling a crevass or graben at the head of the slide, is discussed later in this section of the report.

General Stratigraphy

The succession of stratigraphic units in the Vajont Valley has been the subject of many reports and published papers. The first study containing details of the stratigraphy relevant to the slide is the Giudici and Semenza (1960) report which included a brief stratigraphic sequence based upon a review of literature and field work in the summer of 1959 and spring of 1960. They described the Jurassic-Cretaceous-Eocene sequence of rocks present. The principal units were described in more detail by Semenza (1965b). This was based upon work by Rossi and Semenza (1964, 1965a, 1965c), an unpublished stratigraphic column prepared with the help of R. Dal Cin, M. Novi and A. Venturini, and the very detailed micropaleontological studies by Loriga and Mantovani (1965, 1970). In addition, several independent inquiries gathered information relevant to the slide. These included the stratigraphic studies of Martinis (1964), Carloni and Mazzanti (1964a, 1964b), and Selli and Trevisan (1964).

Semenza's (1965b) stratigraphic description is given in Appendix G. The symbols used in Appendix G are the same as those used in the geologic maps by Rossi and Semenza (1965a). Figures 11 and 12 in this report are a reproduction of these maps and show the geology before and after the slide of October 9, 1963, respectively. Figure 12 also includes an abbreviated geologic column.

Clay Interbeds and Layers

Existence

The most significant aspects of the stratigraphy are the location, continuity, and physical properties of the clay interbeds in the rock column. This topic has been a controversial one and was the subject of

an extensive report and technical paper by Broili (1967) on work undertaken at the direction of L. Müller at the Institute for Soil Mechanics and Rock Mechanics, Karlsruhe. Broili's work was based upon a review of the logs of the core obtained from drillholes which were made for a study conducted by ENEL after the slide. The micropaleontological and petrographic studies of these cores were undertaken by G. A. Venzo and A. Fuganti of the Geology Institute of Trieste University. Further studies of geologic sections in the slide area were also made by these geologists. Broili (1967, p. 80) concluded that "... the succession does not include any clay beds or intercalations which some authors consider may have been responsible for some aspects of the phenomenon." Broili's work was cited by Müller (1968) to support his contention that "contrary to several publications, no clay existed on the slip surface."

Consequently the authors were surprised during preliminary examinations of the failure surface in 1975 and 1976 to note extensive clay interbeds and layers of clay intimately associated with the surface of the 1963 slide. In July 1979 the authors, accompanied by H. R. Smith and G. Fernandez, had a further opportunity to examine and sample the exposed portions of the failure surfaces during a three week period. The locations where observations were noted and samples taken are shown on the photomosaic of the upper portion of the Vajont Slide which is reproduced as Figure 13.

Location

Not all of the failure surfaces examined resulted from the October 9, 1963 slide. Many of the rock faces visible on Figure 13 were formed by later slides involving slabs of rock which "broke down" to one of the many adjacent underlying clay interbeds.

The numbers of the locations noted in Figure 13 are keyed to photographs of the clay layers and other features (see Photos 1 to 52). Where the surface of sliding is overlain by slide debris, the clays were generally found preserved (for example, see Photos 4, 6, 7, 9, 10, 11, 13, 16, 17, 18, 20, 24, 25, 26, 27). However, where the failure plane has been exposed, the clays are rapidly eroded by rainfall and by debris

flows from the large catchment surfaces (see Photos 11 and 25). Small folds and faulted monoclinal (cascade) structures, which are present in many areas of the slide but are not visible at the scale of the photo-mosaic (Figure 13), have served to protect and preserve small portions of the clay interbeds which are stratigraphically continuous with large adjacent areas of the 1963 sliding surface (for example, see Photos 12, 21, 22, 29, 31, 32, 34, 35, and 36).

The lower 10 to 30 m portion of slide debris exposed along the base of the rock outcrops on the west side of the slide consists of an uncemented angular gravel and sand-sized breccia with frequent layers of clay and breccia with a clay matrix (for example, see Photos 4, 5, 6, 8, 9, 14, 15, 16, 17, 23, 27, and 28). The clay layers in this breccia frequently show structures which suggest shearing of the upper layers over the lower layers (see Photos 15, 27, and 28). Although the clays are often mixed with angular breccia, layers and interbeds of clay without noticeable sand-sized particles were observed with thicknesses of 10 to 15 cm and occasionally more (see Photos 5, 14, 15, 17, 28 and 33). The clay layers in the breccia are commonly 1 to 4 cm thick (see Photos 5, 6, 27, and 28). Lumps of clay were reported on the surface of the slide by Nonveiller (1967a), who tested the strength of one of these lumps. Similar lumps were found by the authors at numerous locations on the surface of the slide debris. Clay layers along the surface of sliding of the 1963 slide are commonly 1 to 2 cm thick but vary from 0.5 to 10 cm or more.

Characteristics

The numbers of the locations noted in Figure 13 can be used to find the abbreviated descriptions of the clay layers given in Table 1. The descriptions in Table 1 include the thickness, number, and the position of the clay layers and interbeds.

When exposed in the field in a destressed condition, the clay is generally very soft and sticky and has a slight "popcorn" or cracked and fluffy surface because it has been subjected to frequent wetting and drying cycles. Such characteristics are typical of montmorillonitic

clays. The location of the clay layers in the field can often be inferred from the presence of small slumps whose failure surface corresponds to one of the clay layers. When these slumps are trenched and examined, the soft, sticky clays can be readily identified. The dry clay fragments slake rapidly in fresh water. Where the clay interbeds remain in their original stratigraphic position within the undeformed bedrock, the material is much firmer. The thickness and frequency of clay interbeds seemed to diminish with increasing distance below the bedrock-slide debris contact. Thick layers of clay were found in the slide mass at the contact with the underlying bedrock surface. In isolated areas of partly displaced slide debris at the top of the slide, clays were found indicating that at least one layer of clay occurred several metres above the surface of sliding of the 1963 slide. This clay layer was thicker than any found at the base of the 1963 slide.

Stratigraphic continuity

Evidence of the stratigraphic continuity of the clay interbeds found in the slide was sought away from the slide, particularly in the valley of the Mesazzo Torrent just east of the slide and on the slopes above the dam on the north side of the Vajont Valley south and west of Casso. In the latter case a series of five continuous clay interbeds varying from 0.5 to 17.5 cm thick was located within 20 to 30 m of the same stratigraphic position as the surface of sliding of the Vajont Slide. The location of this outcrop is shown on Figure 12 and Photo 1. This outcrop lies just above the main path leading to Casso from the west at about el 940 m. Samples taken from these clay interbeds have similar Atterberg limits to those taken from the failure surface of the slide (Table 2). A sketch of this outcrop is given in Figure 14. Photo 2 shows the outcrop with respect to the slide in the background. Photo 3 is a closeup photograph of the outcrop showing three of the clay interbeds. Two natural benches located on the hillside just above and below this outcrop suggest that the clay interbeds, which may be thicker than the ones examined, may be hidden beneath the overburden. The lower bench, which is the larger and appears to be covered by a mantle of slide

debris, is likely to be associated with especially weak or thick clay interbeds.

Differences in terminology

Some of the confusion concerning the clay layers seems to result from differences in terminology. Broili (1967, Tables 3 and 4) summarized some of the different descriptions and terminology. Giudici and Semenza (1960) wrote in reference to the Lower Cretaceous rocks that "numerous intercalations of greenish clay, with thicknesses a few centimeters, are present" (translated from Italian). Kiersch (1964) mentions clay seams, claystone interbeds, marl, and clay partings in the Malm and Lower Cretaceous beds. Other descriptions of the clays mention "milonitic" and "ultramylonitic facies" (Semenza, 1965b). Martinis (1964) described "reddish or greenish calcareous marls in the form of streaks or extremely thin layers" and "limestone interbedded with greenish foliated marls." Others have described the clayey materials as "thin films of pelitic material."

Any clay bed in a folded stratigraphic sequence of alternating hard and softer units will be subjected to differential shearing displacements along bedding planes due to the flexural-slips as described by Skempton (1966) and Patton and Deere (1970). Hence, a sheared and slickensided structure would be expected in portions of all such clay beds. When fault displacements have occurred along the same beds, more sheared and slickensided clays can be expected. It seems to be of little consequence with respect to the slide to argue whether the layers are clay, pelite, argillite, foliated marl, clayey marl, marly clay, soft calcareous marl, biomictite, or largely argillaceous. All such materials when sheared would result in a clay-rich slickensided material.

It is clear that numerous stratigraphically continuous layers of uncemented clay-rich materials are present. The clay content is variable. It varies from: 16 percent, (Müller, 1968) to 35 to 38 percent montmorillonite (Broili, 1967), to 50 to 80 percent (this study and Kenney, 1967b). Because the predominant clay mineral is a calcium

montmorillonite, all of the preceding percentages are sufficient to produce soil mixtures which have very low values of the residual angle of shearing resistance.

Evidence from drillholes

Broili (1967), after his study of the core from postslide drillholes, seemed to dismiss the influence of clay along the surface of sliding. However, the core recovery was very poor (0 to 20 percent) in the lower Cretaceous materials, and often remained poor (20 to 30 percent) in the Malm and Dogger units below the failure surface. Under these circumstances of low core recovery, little clay was recovered from the drill core. Furthermore, for the first few years after the slide, many of the excellent outcrops now present were covered by the slide material. Thus, the number and thickness of the clay layers and interbeds may have been difficult to ascertain immediately after the slide.

During this study the geologic logs of the holes drilled after the slide were examined. The locations of the ENEL post-slide borings are shown on Figures 11 and 12. It is believed to be significant that the ENEL boring P-2 (not to be confused with the SADE boring P-2 drilled prior to the slide), located on the north side of the valley some 450 m upstream from the right abutment of the dam, encountered a series of layers of brecciated debris. In some of these layers, clay was noted. These clayey layers varied from 1 to 3 m in thickness. These layers are in the stratigraphic position of the extension of the basal rupture plane of Giudici and Semenza (1960); the area was mapped as old slide material by Rossi and Semenza (1965a) as shown in Figure 11.

Although the core recovery was extremely poor in most other post-slide drillholes made in the slide debris, the following observations are noted on the ENEL logs drilled after the slide: Drillhole S5A encountered detritus with clay in the lower 7 m of the slide mass; drillhole S58" encountered clayey debris near the base of the slide, and further encountered 3.5 m of calcareous chert intercalated with clay just above the in-situ rock; drillhole S6C encountered 4 m of clay with rock fragments 0.7 m above the base of the slide mass; drillhole S58'

encountered 31.5 m of clayey debris; drillhole S5C' encountered two zones of "argilla" (clay) with detritus, at depths of 48 to 71 m and 91 to 107 m; and drillhole S4B encountered 5 m of reddish clayey rock fragments just above the in-situ rock. Hence, it would appear that there is considerable evidence of clay and clayey debris at the base of the slide mass, in spite of the fact that soft clay with rock fragments can be very difficult to recover.

Conclusion

In conclusion, it is clear that multiple layers of weak clays were present along much of the surface of sliding. These clays are largely stratigraphic in origin, although undoubtedly some shearing and development of slickensides had occurred prior to the sliding activity. This conclusion is not in agreement with the conclusions given in the principal technical papers on the slide in English by Müller (1964a, 1968) and Broili (1967). Rather, we are in general agreement with a conclusion of the Frattini Commission (1964) wherein they noted:

Yet in the material accumulated by the slide we can see clay beds, a few centimeters thick, separated by small or less flinty, nodular calcareous strata.

In our opinion, these strata, of a really clayey nature, cannot be considered the product of sliding; they may rather be of sedimentary origin....The malm and the base of the Lower Cretaceous, which are calcareous-nodular, with flint nodules or beds and clay interstrata, forms a mass that can be easily deformed, minutely cracked and subject to cataclasis.

Structural Geology

The basic structures affecting the slide are: (a) the steep back of the slide which provided the driving forces, (b) the pronounced eastward dip of the seat of the slide, (c) the continuous layers of very weak clays within the bedded rocks, and (d) the faults along the eastern boundary of the slide.

Giudici and Semenza (1960) mapped the outcrop of a prehistoric failure surface along the Vajont Canyon walls, showed its limits at both

ends, and indicated that the entire area was a zone of possible sliding. They showed no uphill limit to the base of this zone which ended in question marks. However, a simple extension of their projected "line of movement" or surface of sliding would extend to or beyond the depression of the Pozza. The steep back and flat toe (on a north-south section) of the slide was established by their mapping and by their interpretation of the Dogger-Malm contact. From their geologic map the upstream dip of the failure surface along the walls of the canyon could be determined. They had also clearly established the existence of a block of old slide material on the right abutment and stated that it had come from the south side of the valley in a previous slide. It is now known that the outcrop of the failure surface mapped by Giudici and Semenza was nearly coincident with the 1963 surface of sliding.

Geologic maps

The two geologic maps (Figures 11 and 12) by Rossi and Semenza (1965a) provide an accurate and detailed picture of the geologic structures present before and after the slide. These maps show a large number of lines (from 1 to 15) representing traces of proposed north-south geologic sections which were to be published by Rossi and Semenza. Their original sections, based upon surface mappings, were modified to accommodate the postslide drillhole information. This information continued to be generated until at least December 1966.

In the course of this study, the authors developed a particular interest in Sections 2, 5, and 10. These were chosen as representative sections for use in stability analyses. To avoid the bend in the middle of Section 10, a modification was made and the resulting section is labelled Section 10A. These sections were chosen because they appeared to be oriented relatively closely to the direction of the original movement of the slide.

At the request of the authors, Rossi and Semenza undertook to interpret the geology along these sections both before and after the 1963 slide. Their interpretations are presented as Figures 15 through

20. The symbols used for the units on these sections correspond to those used on Figures 11 and 12.

Section 2

Figure 15 shows Section 2 before October 9, 1963. Two different minor variations in the interpreted surface of sliding are shown along the steeply inclined portion of the slide. Figure 15 also indicates a fault at the top of the slide area and some previous sliding within the future slide mass, as well as a portion of the old remnant block of slide material on the right-hand side of the Vajont Valley. The ground surface after the slide of November 4, 1960 is shown by the dashed surface above the canyon wall. This surface approximates the surface of sliding of this precursor slide.

Figure 16 shows Section 2 after October 9, 1963. It indicates a moderately simple downhill translation of the slide. It also shows a remarkable upward displacement of the old slide material on the right-hand valley wall and some of the post October 9, 1963 debris and alluvial fans covering portions of the surface of the main mass. Figure 16 shows the failure plane is parallel to the bedding in the upper part of the slide but cuts across the bedding in the lower part of the back of the slide. The authors agree with the general position and orientation of the slide surface shown for the exposed portions of the failure surface. Whether at depth the surface of sliding cuts across beds or not is a matter of interpretation. Appreciably more drillholes would be required to better define the degree of conformity of the failure surface to the bedding.

Section 5

Figure 17 shows Section 5 before October 9, 1963. It illustrates a section with a large stabilizing toe relative to the small volume which acts as a driving force. Some uncertainty about the structures at the base of the slide along the monoclinal axis is noted.

Figure 18 shows Section 5 after October 9, 1963. This shows almost complete removal of the activating forces after the slide. Just after the slide Semenza (1965b) saw evidence of a 30 to 40 m southern

movement of the mass after it had reached its maximum northern limit. This backward movement is shown by the two directions of movement noted on the planes of sliding at the toe. A comparison of Figures 17 and 18 shows only modest changes in the structure of the majority of the displaced rock mass other than translational and rotational movements.

Section 10A

Geologic Section 10A given on Figure 19 shows the geologic structure of a representative section of the eastern side of the slide taken in the approximate direction of initial movement of the main slide mass. Most sections of this part of the slide presented in previous investigations have been oriented some 10° to 20° counterclockwise in plan view to give more emphasis to the direction of movement of the top of the eastern portion of the slide. On Figures 19 and 20 Rossi and Semenza called this upper part of the slide the "Eastern Lobe" and show it in the area A-B before the slide. Postslide surface depositional features suggest that the Eastern Lobe did not complete its movement until after the main slide mass had completed most of its movement. From this evidence the authors have assumed that the two slide movements were essentially independent and that the Eastern Lobe followed the movement of the main slide and formed the slide material shown in the area A-B on Figure 20. Rossi and Semenza have also speculated on the existence of a "tectonized" zone shown by the hatching along the failure surface on Figures 19 and 20. By comparing Figure 19 to Figure 20, it can be seen that, except for the deposit of the Eastern Lobe, there is relatively little deformation of the surface of the majority of the sliding mass which is not accounted for by a translational and rotational displacement. Figure 20 also shows the near-horizontal surface of the slide mass following the 1963 slide. This is believed to reflect the very low shear strength along the base of the slide. On Figure 20 Rossi and Semenza note that a portion of the front of the pre-1963 canyon wall is missing. They have suggested that this portion fell into the gorge and was covered and spread by the slide movement. Presumably, part of this missing volume may also have been removed by "wave action".

Sections 16 and 17

An appreciation of the upstream dip of the seat of the slide cannot be obtained without an examination of the east-west sections. Sections 16 and 17 shown in Figures 21 and 22 are east-west sections based upon information obtained from drillholes made after the slide. The location of these sections is given in Figures 11 and 12. The dip of the beds along the seat of the slide is steeper (17° to 22°) on the west end near the dam, and flatter (9° to 11°) in the central portion of the slide. The bedding steepens again to 30° to 40° just east of the slide (not shown on these sections). An interpretation of the stair-stepped seat of the slide on its eastern side is shown on Figures 21 and 22. The shapes of these steps are not known in detail. However, several drillholes provide local control points. A portion of one step was observed at location 24-2. The treads of these steps will form in the weakest clay units, while the risers will form along pre-existing faults and major joints wherever possible.

Bedding Plane Fault of Possible Tectonic Origin

Delineation of the potentially unstable slopes prior to the 1963 slide was essentially defined by what appears to be an ancestral tectonic bedding-plane fault whose locus was most likely the weakest clay units in the pre-existing stratigraphic section. Such ancient tectonic structures in the Costa Delle Ortiche region just east of the slide are discussed in Rossi and Semenza (1967). The distance travelled by such detached blocks is unknown, but is likely to be large since Rossi and Semenza (1964) report significant differences in the stratigraphic columns from their work in the Costa Delle Ortiche. The differences in the stratigraphy were attributed to the two areas being portions of two different tectonic blocks.

A cemented calcareous breccia associated with the surface of sliding is found at numerous locations throughout the exposed failure surface. Twenty locations are listed in Table 1. However, the best exposure found by the authors was at location 12-3 shown on Photo 39.

This substantial outcrop is near the base of the in-situ rock exposures near the east side of the slide. The large grooves visible in Photo 39 have an amplitude of about 15 cm and a wave length of 1 to 2 m. The axis of the grooves is 353° Az and plunges 15° N. This axis is essentially parallel to the sides of the tectonic block as plotted on the regional geologic map by Leonardi et al (1967). The most recent striations on the surface of this outcrop, which are shown in Photo 40, are apparently due to the sliding of the Eastern Lobe and are oriented at 316° Az and plunge 20° north. On the western portion of the slide, the direction of the 1963 slide movement more nearly agrees with the axis of the grooves noted above (353°). Photo 38 of location 12-1A shows another outcrop of the striated surface of the tectonic breccia. This outcrop is located at the base of the eastern wall of the slide. The striations on this outcrop are aligned at 338° Az and plunge 30° N.

The origin of the cemented breccia has not been established and may have been the result of landslide processes. However, the cemented breccia does appear to be older than the overlying slide debris and has features that are more characteristic of tectonic faulting than the authors have observed at the base of other slide masses.

Minor Structures

Striated rock surfaces

There are a number of minor geologic structures that can be observed on and adjacent to the surface of sliding which are less significant to an understanding of the slide than the structures previously described. Generally, striated rock surfaces are notable for their absence except for those associated with the cemented breccia noted previously. An exception to this general case is the slickensided and striated surface at location 18-10 near the top of the western portion of the slide. These striations, shown on Photo 41, are aligned at 308° Az and plunge 26° N. Slickensided and striated surfaces appear to be absent elsewhere because of the presence of clay interbeds which would serve to protect the surfaces during slide movements. The

striations at location 18-10 probably were produced by post-1963 sliding of rock slabs below the 1963 rupture surface.

Folds

A number of folded structures were observed. One of these consisted of small, accordian-like, alternating synclines and anticlines with amplitudes of 2 to 15 m and wave lengths of 5 to 25 m. One of the more pronounced of these folds is shown in Photo 42 which was taken half-way up one of the gullies on the western half of the slide scarp. The axis of these folds tends to be aligned at about 220° to 230° Az which is within 10° to 15° of the initial direction of movement of the slide mass. Hence, these folds have a minimal effect on the shearing resistance of the base of the slide. However, they have had a significant effect on the distribution of the slide debris left on the in-situ bedrock surfaces. These folds underlie several of the ribs of debris which remain on the rock surfaces, especially in the western part of the slide scarp (see Figure 13). The folds may have served to slightly increase the shearing resistance by adding a small geometrical component to the frictional resistance when they are not aligned exactly in the direction of movement.

Cascade structures and monoclines

Perhaps the most frequently encountered structures on the exposed bedrock surfaces are the small folds and structures described as "a cascata" by Giudici and Semenza (1960). These are called "cascade" structures in this report. The small monoclines and cascade structures bear a dragfold relationship to the larger monocline forming the "back" of the slide. Examples of these structures are shown in Photos 43 and 44. Photo 43 shows a small monocline running parallel to the strike of the beds half-way up the most westerly rock face (locations 9-2 and 522-6). As the monoclinal structures develop, and are subjected to continual shearing displacements, they turn into nappes which are faulted on their bases. The stratigraphic unit forming the top of the nappes continues below the cascade on the surface, but at a lower position. The deformation within the cascade structure can be complex in detail.

Photos 44 and 45 show exposed sections of the interior of one of the cascade structures.

Carloni and Mazzanti (1964a) have illustrated folding of surface structures which would in a general way account for the cascade structures noted on the base of the slide. Most of the structures observed on the exposed in-situ bedding planes are thought to be more related to the deformation of layered rocks adjacent to the tectonic basal fault or to deformation shortly after deposition of the original sediments.

Carloni and Mazzanti's interpretation is given on Figure 23.

Small monoclines and cascade structures may serve to slightly increase the shearing resistance along the failure plane by introducing localized points of higher normal stresses which would result in some rock-to-rock contacts. However, in general, the small monoclines are aligned in a stair-step fashion so that interruptions in the continuity of the clay layers are minimized with respect to slide movements to the north. The overall shear strength along a clay layer with a small monocline or cascade structure may be somewhat higher than for a smooth, continuous, uniformly dipping clay layer.

Another aspect of these folds, which was incidental to the slide but important to this study, is that they have served to preserve fragments of the clay layers which otherwise would have been eroded off of exposed bedding plane surfaces. Photos 12, 19, 29, 30, 31, 32, 33, 34, 35 and 36 are examples of clay layers preserved in such structures. Because of local increases in shearing resistance, the monoclinal and cascade structures also tend to collect the slide debris overlying them.

Faults

The fault and associated dragfold found at the headscarp at the top of the western half of the slide are shown in Photos 46 and 47. The beds steepen appreciably close to the headscarp where they turn vertical or are faulted. Photo 46, taken above location 18-6, shows that the recent headscarp is the lower portion of an older scarp whose shape is evident on the vegetated cliffs above. Fragments of partly cemented talus breccia are found along the new headscarp indicating that a

peripheral crack had previously been opened prior to the 1960-1963 slide movements. Photo 47, taken above location 18-10, shows the new scarp and the old scarp and a thick uncemented to poorly cemented talus deposit which has filled a portion of an old peripheral crack. This crack opened up in 1960 and 1963. These old talus deposits are considered the best diagnostic evidence encountered for previous periods of movement of the Vajont Slide in prehistoric and perhaps during or since Roman times. A close-up view of the partly cemented talus material from the old bergschrund-like crevass at the scarp of the slide is shown in Photo 48.

Photo 49 shows the contorted structures in the toe of the slide mass. This rock mass has probably undergone tectonic deformation as well as a repeated series of landslides, at least one of which (1963) was a high-velocity slide. Yet the bedding is relatively continuous, and small outcrops of such rocks could easily pass as in-situ bedrock if the slide event was not well known. Photo 50 shows the bedding and dark chert layers in the Malm formation in a small rock cut above the right abutment of the dam. The weak clay interbeds occur above this part of the Malm.

Geomorphology

Previous studies

Previous studies of the geomorphology of the Vajont Slide have been undertaken by Giudici and Semenza (1960), Semenza (1967), Rossi and Semenza (1964, 1965a), Carloni and Mazzanti (1964a, 1964b), Selli and Trevisan (1964) and others. Perhaps the most significant question to be addressed by such studies is whether or not there is geomorphological evidence of a pre-1960 slope movement. A related and very practical question is: Could one have recognized the Vajont Slide as an old slide area prior to 1961 by using conventional airphoto interpretation techniques? The latter question is particularly important to other studies of reservoir slopes, for such reviews are done principally by airphoto studies (Patton and Hendron, 1974) followed by field geologic mapping.

Evidence from airphotos

To answer these questions the authors examined stereoscopic pairs of vertical airphotos taken in 1960 and another set taken a few days after the slide of October 9, 1963. The 1960 airphotos are included as Figures 24a and 24b. Figure 24b is included in the pocket so it can be used to obtain a stereoscopic view of the slide. The scale of these airphotos is about 1:30,000. Figure 25b is a transparent overlay to the airphoto in Figure 24a. Some of the major topographical features related to the slide have been depicted on Figures 25a and 25b. These include depressions and scarps, streams, gullies, and sinkholes. Also outlined are the dam, reservoir, roads, and visible traces of trails.

Recognition of an old slide

Two geomorphological factors on Figures 25a and 25b are of particular interest. The first is the series of depressions within the slide. These occur in three areas: (a) the Pozzo plain, (b) the area between the "Altoplano" or high plateau above the Pozzo and the cliff that traces the location of the dragfold, monocline or fault at what will develop into the headscarp of the western side of the 1963 slide, and (c) the area of large scarps, one below the other, and small depressions on the eastern half of the slide. The eastern and western limits of the 1963 slide are defined on the 1960 airphotos by an abrupt change in morphology or by airphoto lineaments. The depressions in the three areas appear to be primarily the result of previous slide movements which occurred several thousand years ago. However, the depressions no doubt were enlarged by solution of the carbonate rocks present. Kiersch (1964) mapped a number of these depressions within the slide boundary and described them as sinkholes. Sufficient time has elapsed to subdue the original landslide topography so that the evidence is not particularly obvious. However, it seems likely that after detailed study an experienced airphoto interpreter would recognize the area as a possible or probable landslide. Certainly, on-the-ground field investigations would be required to confirm such an interpretation. The appearance of the slopes above the slide and west and

northwest of the slide suggest that they have been denuded by previous slides.

Karstic topography above slide

The second geomorphical feature of particular interest, and one of the most surprising aspects of the airphoto study, was the substantial area of pronounced karstic topography in a basin above the slide and to the west of the peak of Mt. Toc. Other small incipient sinkholes are present in the surface of the Dogger beyond the western and southern limits of the slide. These apparent kettles or sinkholes, which sometimes form small elongated doline-like depressions, are mapped on Figure 25. Their implications with respect to groundwater conditions of the slide are discussed in the section on hydrogeology.

Other airphoto observations

The area of old slide material mapped by Giudici and Semenza (1960) and Rossi and Semenza (1965a) on the right side of the valley can be recognized on the airphotos as a morphologically distinct area, but it is unlikely to be identified as an old slide mass from the airphotos alone. However, small strips of landslide topography are present on the hillside above the right abutment of the dam. These shallow slide areas occupy a series of benches which appear to be formed by weaker stratigraphic units in the rock sequence. These benches further suggest that clay interbeds are present, particularly considering the relatively low dip, 10° to 20°, of the rocks. One of these benches is associated with location 8-1 (Figures 11 and 12).

The light colored scar on the side of Mt. Borga, which extends downslope just east of Casso, is the site of active talus cones resulting from a series of fairly recent rock slides from the slopes above. From the vegetation, it would appear that some of these slides have occurred in the last several hundred years and others are forthcoming. At the top of the rock slide area there is an area of cracked rock which has not yet come down.

Hydrogeology

Rainfall

The principal reason for studying the groundwater conditions within a slide is to determine the distribution of the water pressures acting along the surfaces of sliding. When the average rainfall of an area is in the range of 1200 to 2300 mm/year and the terrain is mountainous, there is a potential for significant fluctuations in groundwater pressures and levels to occur. The detailed rainfall records for the village of Erto for the years 1960 to 1964 have been supplied by ENEL and are given in Tables A1 through A5, Appendix A.

Groundwater data

The groundwater data available for the Vajont Slide area are sparse and unfortunately questionable. The data consist of water levels measured in three drillholes (P1, P2, and P3) from the summer of 1961 until October 1963. Water level measurements were made inside pipes placed in open drillholes. The annulus between the pipe and the rock was not sealed so that the water pressures at different elevations in the rock would be expected to be connected (see Figure 26b). As a result, the water levels recorded inside the casing could reflect some average value of the different water pressures and hydraulic conductivities of the units encountered. However, if a natural seal developed on the outside of the pipe (for example, by the squeezing around the pipe of a soft clayey layer), then the water level inside the pipe would reflect average hydraulic pressure conditions in the formations below the seal as shown in Figure 26c. Such a seal could conceivably provide water pressure readings in the vicinity of the base of the slide as precise as if a fully sealed standpipe piezometer, such as that shown on Figure 26a, had been installed. With continued but small displacements of the slide, the seal around the pipe could be eroded or the pipe could be pulled apart and start to leak as indicated in Figures 26d to 26f.

From early November 1961, when P2 was first read, until later January 1962 the water level in P2 was 25 to 90 m above the reservoir levels. During this period the slide moved 5 to 10 cm. From February

1962 to July 1962 piezometer P2 showed levels lower than previously indicated but still 2 to 10 m higher than piezometers P1 and P3. In this interval the slide had moved from 20 to 25 cm (since P2 was installed). After July 1962 the water levels recorded in P2 were generally within 1 to 2 m of those recorded in P1 and P3. Thus, the total displacement of the slide since P2 was installed was about 30 cm by July 1962. It would appear that this much displacement was sufficient to pull out, rupture or pinch the end of the pipe in the manner suggested on Figures 26e and 26f.

Although this type of piezometer construction would not be considered good practice today, similar fully interconnecting but more elaborate "piezometers" were still being routinely installed by some major engineering firms fifteen years after P1 through P3 were placed. Also, considering the difficulty in drilling, the extremely low core recovery, and the problem in placing a good seal under these conditions, it is noteworthy that any pipe was installed at Vajont. It would appear that one piezometer (P2) out of the three was partially sealed and for a period of about two months gave more representative water pressures of conditions near the surface of sliding than the others. The other piezometers, P1 and P3, probably gave reasonably accurate measurements of the groundwater table in the highly fractured rock mass above the basal clay-rich zone. The groundwater pressures in the bulk of the rock debris appear to have varied directly with reservoir levels, maintaining a slight (3 to 10 m) increase above reservoir levels. So far as the authors can determine, no groundwater data were obtained from the holes drilled after the 1963 slide.

Groundwater flow systems

The scarcity of groundwater data makes it important to develop a reliable concept of the basic hydrogeologic conditions at the slide in order to make reasonable assumptions of water pressures for stability analyses. A knowledge of groundwater flow systems can be used to predict the typical pressure distributions to be expected.

Figure 27 shows the general groundwater flow system that might be expected on a section through Mt. Toc, assuming a relatively homogeneous and isotropic distribution of hydraulic conductivities within the mountain. If on the northern slopes of Mt. Toc there was a tendency for higher conductivities along the bedding than across the bedding, there would be a corresponding tendency for the higher fluid potentials originating from infiltration in the area of the karstic topography on the upper slopes of the mountain to be transmitted to the region of the Vajont Slide with minimal head losses. At the base of the Vajont slide mass high fluid potentials would be held beneath the clay layers, whereas in the highly fractured rock above the more continuous clay layers the fluid potential would be much lower, reflecting the fluid potential base level in the valley. The base level for the local groundwater pressures in the portion of the slide above a clay interbed would be either the elevation of the intersection of the top of the clay with the valley wall or the reservoir level, whichever is highest. Beneath and within the zone of clay interbeds the water pressures should vary with changes in the groundwater conditions (or levels) at the top of the mountain and with changes in the outlet pressure conditions in the valley at the base of the mountain. Hence, the water pressures below the clay layers should directly reflect changes in infiltration rates because of rainfall or snowmelt above the slide and changes in reservoir levels. Kiersch (1964) was the first to comment on the importance of infiltration on the stability of the slide mass.

Initial fluid pressures recorded in P2, which were about 90 m above reservoir level, occurred in a period of moderately low precipitation. These fluid pressures increased approximately 20 m during a period when a 20 m rise occurred in the reservoir level. This implies that the relatively closed groundwater flow system described above was present near the base of the slide. In such a system changes in the outlet pressure could have an effect at appreciable distances away from the reservoir. Thus, the hydrogeological conditions present appear to provide the opportunity for large groundwater pressure fluctuations to

occur around the base of Mt. Toc. The very limited piezometric measurements available support this view.

During a conversation with the authors, E. Semenza recalled that he had observed springs and moist areas in the two areas in 1959 and 1960 where he and Giudici had mapped the exposed shear zone that forms the outcrop of basal failure plane in the Vajont Canyon. The outcrop of the remainder of this plane was beneath a rock talus formed by the ravelling slopes above. Semenza's description of these groundwater discharge areas is consistent with the hydrogeologic picture noted above.

Solution Cavities

Solution cavities were observed at four locations on the exposed scarp, 9-3B, 22-4, 24-2 and 24-3, in the rocks immediately below the failure surface. Two of these areas are shown in Photos 51 and 52. The cavity shown in Photo 51 ranged from 10 to 15 cm across, and on Photo 52 the cavity ranged from 0.5 to 1.0 cm across. Unfortunately, photos are not available of the largest solution cavities, 10 to 50 cm wide, which were observed near locations 24-2 and 24-3. The solution cavities would suggest that hydraulic connections existed beneath portions of the failure surface. Undoubtedly, other solution cavities could have been located if time was spent investigating these features. They are likely to be associated with small faults and folds in the bedding. The traces of the lines visible on the rock surfaces in Figure 13 indicate the location of such folds and faults.

Adits

During field visits to the Vajont Slide the authors observed that during moderate to heavy rainfalls no water flowed from the Massalezza Ditch onto the slide scarp, although many of the drainage paths down the scarp became torrents. This lack of flow in the Massalezza is believed to be indicative of the very high infiltration of precipitation into the karstic bedrock on the slopes above the slide scarp. Presumably water would flow in the upper Massalezza Ditch after heavy and prolonged rainfalls. But when this happens, the groundwater pressures in the

underlying rocks would have to be much higher than when the Massalezza runs dry.

One of the main purposes of the adits placed in 1960-61 on either side of the Massalezza Ditch was to investigate the possibility of draining the slide (Müller, 1964a). One of these adits was encountered by the authors at location 23-13 on the east side of the Massalezza (see Figure 13). The top of the portal of this adit had approximately 1 m of cover below the exposed failure surface. As these adits were so close to the Massalezza, which generally was dry, it is not surprising that very little water was encountered in them. Apparently the adits were located too high in the slide and too close to the ground surface to encounter the high water pressures that were undoubtedly present at greater depths and in other portions of the slide. This was unfortunate, as conclusions drawn from the lack of water encountered in adits were reportedly responsible for the 1961 decision that it was not practical to stabilize the slide by drainage (Müller, 1961).

In 1979 E. Semenza described for the authors the sheared clay-rich zones (ultramylonites) that were exposed in the adits of the western side of the Massalezza. These are noted in Semenza (1965b) and in Appendix G. These clay-rich zones have not been given sufficient attention in the technical literature. They no doubt represent previous or potential slide planes.

Artesian pressures

Lo et al (1972) and others speculated on the probable existence along the base of the slide of "artesian pressures". This would appear to refer to pressures in excess of a hydrostatic condition. Generally they assumed that the pressure distribution along the failure surface followed a straight line from the reservoir to the top of the slide. These values of water pressure distribution are much higher than the initial readings of "piezometer" P-2 would indicate.

The water pressure distributions used in the analyses for this report were made to agree with the initial P-2 record for low rainfall conditions and were increased for high rainfall conditions. These assumptions are discussed in more detail in Part VII.

PART IV: PHYSICAL PROPERTIES OF THE CLAYS

Introduction

The properties of the clayey materials found along the failure surface of the Vajont Slide were tested by soil laboratories in several different countries during the course of this study. The following laboratories were employed:

Waterways Experiment Station, Vicksburg, Mississippi, USA

University of Illinois, Urbana, Illinois, USA

Thurber Consultants Ltd., Edmonton, Alberta, Canada

Instituto Di Scienza e Tecnica Delle Construzioni

Del Politecnico de Milano, Milan, Italy.

The tests were conducted over a five-year period from 1976 to 1981. The initial tests in 1976 and 1977 were made for work undertaken by the authors for the British Columbia Hydro and Power Authority. The results of all of these tests are presented in this section together with the results of tests on the Vajont clay layers published by others. The tests performed include grain-size analyses, Atterberg limits, direct shear strength tests, and clay mineral analyses.

Grain-Size Analyses

A grain-size analysis was completed on the clay sample tested by Thurber Consultants. A summary of these results is presented on Table 3. This sample contained 51 percent clay, 36 percent silt, 7 percent sand and 6 percent gravel. Samples of the Vajont clays were also examined by Kenney (1967b). He reported similar results in that 52 to 70 percent of his samples were less than 2 microns in size.

Atterberg Limits

Atterberg limits are more directly related to the strength properties of the soil than are the grain-size analyses. Hence, most samples were tested for their liquid and plastic limits. These results are presented on Table 2. Figure 28 is a Plasticity Chart which shows the Atterberg limits of the clay samples obtained for this study.

The samples fall within two general groups. One group plots nearly on the A-line and the soils are classified as CL, ML and MH. Thus, these soils are inorganic clay of low plasticity and inorganic clayey silts of low to high plasticity. The liquid limits of this group vary from 33 to 60 and the plasticity indices vary from 9 to 27. The other group falls within the area of the Plasticity Chart distinctly above the A-line. These are classified as clays of high plasticity (CH soils). In this second group, the soils had liquid limits that varied from 57 to 91 and plasticity indices that varied from 30 to 61.

Results of tests by Kenney (1967b) and Nonveiller (1967b) for clay samples from the Vajont Slide are also shown on Figure 28. The liquid limits (29 to 116) and plasticity indices (15 to 71) of some of these samples exceed those measured in this study, but are consistent with the character of the clays noted in the field observations for this study.

Shear Strength Tests

Shear strength tests were run by Dr. P. K. Chatterji of Thurber Consultants, by Dr. A. Nieto of the University of Illinois, and by the staff of the Waterways Experiment Station. These results are summarized on Tables 3, 4, and 5, respectively. Tests by Thurber and WES were conducted by reversing the direction of movement in a direct shear box, whereas the tests by Nieto were made with a direct shear box which permitted approximately 5 cm of travel in one direction. All shear strength tests were made on samples of the remolded clayey soils.

Two series of tests were undertaken by Thurber Consultants on one sample. These tests were made at stress levels of 103 to 6,200 kPa (15 to 900 psi) and the surfaces of sliding were pre-cut. The first series of tests were conducted on that portion of the sample (83 to 87 percent by weight) passing the No. 10 sieve size. The second series of tests were conducted on the material which passed the No. 4 sieve. The thickness of the samples was 7 to 11 mm and the rate of shearing varied from 1 to 0.003 mm per minute. The area of the samples was 25.8 cm².

The significance of these test results is covered in Part VII in the discussion of the assumptions of the shear strength properties appropriate for stability analyses.

Clay Mineral Analyses

Clay mineral analyses were made by the Alberta Research Council on the sample tested by Thurber; by Dr. D. Eberl of the Department of Geology, University of Illinois on the sample tested by Nieto; and by A. D. Buck of the WES Materials and Concrete Analysis Group, Concrete Technology Branch on the sample tested by WES. In addition, WES personnel examined a limestone sample to see if clay minerals were present in the unsheared rock. The results of these tests are presented on Table 6 together with the results of Kenney (1967b).

The clay mineral analyses indicate that some 50 to 80 percent of the whole samples are clay minerals. These clay minerals are predominantly of the type generally known in soil mechanics as calcium montmorillonites. However, in detail the clays are composed of 25 to 75 percent of a mixed layer vermiculite/smectite composition with the remainder of hydrous mica illite to smectite composition containing something on the order of 60 percent smectite. An illite/corrensite composition is reported in one set of analyses. Such clay minerals have an expanding lattice, are associated with low shear strengths, and exhibit swelling properties when stresses are reduced and water is present. The residual angles of shearing resistance obtained from these samples compare favorably with the 8° to 10° reported by Olson (1974) for calcium montmorillonite. Olson's tests were run with stress levels of 350 to 500 kPa.

PART V: CHRONOLOGY OF SIGNIFICANT EVENTS

In this part of the report the authors have attempted to provide a chronological list of the events leading up to and following the Vajont Slide. These events include natural events, construction activities, and the activities of engineers and geologists investigating the slide area. The authors believe that an understanding of this sequence of events is necessary to develop an understanding of many of the technical aspects of the slide.

This list is as complete as possible considering the nature of the data available. Despite any errors and omissions, the authors believe this list will help the reader to understand the major events and decisions prior to the slide and the events in the years following.

- 1928 Prof. Giorgio Dal Piaz examined the stability of the future banks of the reservoir. At that time no question was raised about the area of the 1963 slide (Müller, 1964a, p. 154). The Bozzi Commission (1964) indicated that while Dal Piaz described a general phenomena of deep fissures near the Casso bridge, nevertheless the reservoir conditions were no worse than those met on the great majority of the mountain basins throughout the Venetian area.
- 1956-57 Excavation at the dam (Müller, 1964a, p. 155)
- 1957 (July) Construction of the dam began.
- 1957 Müller was consulted on problems of stability of the rock abutments of the dam and on how the stability of the future reservoir banks should be determined. On the basis of a short inspection of the rock fabrics, Müller (1964a, p. 156) thought it possible that the reservoir "would cause slides, some of which might be perhaps as much as 1 million m³ in some parts of the future banks."

1958 Dal Piaz re-examined the stability of the left valley slopes between the Pineda and the dam in connection with the construction of the new road along this bank. He concluded that the rock was fractured but it was in place and showed no signs of an earlier movement with the exception of a small strip 500 m east of the Pozza where the rock was covered with moraine-like materials. Dal Piaz concluded that only local detachments of such materials could be expected; however, these would not be of a serious magnitude (Müller, 1964a, p. 157). The Bozzi Commission (1964) noted a discussion of fissures, possibly deep, in the area of the Pozza in this report of Dal Piaz.

Spring
1959 Dr. Carlo Semenza, designer of the dam, invited Dr. Müller and Dr. E. Semenza, geologist, to inspect the banks of the future storage reservoir (Semenza, 1965b). Semenza noted that following this visit, Müller, in his report No. 6 of 1959 outlined a general investigation program to assess the stability of the Vajont banks.

Summer
1959 F. Giudici and E. Semenza (1960) conducted a geological survey of the banks of this proposed reservoir. Field observations made during this survey led to the first doubts regarding the stability of the left bank (Semenza, 1965b) (Much of the earlier concern had been for the Erto area). An uncemented mylonitic zone, extending some 1-1/2 km along the left wall of the Vajont Canyon, was identified during this survey. Question marks on the geologic sections indicated the authors' uncertainty about the upslope extent of a possible slide mass associated with this fault.

Rock masses with disturbed bedding were found lying on gravel and sand deposits on the righthand side of the

Vaiont Valley. On the basis of these facts it was then hypothesized that the area from the Pozza down to the Vaiont River represented the mass of an old prehistoric slide that moved down Mt. Toc in a northeast direction.

Oct.-Nov. 1959 Prof. Caloi started a seismic survey of the Massalezza area along a profile that lay roughly parallel to the Massalezza Ditch and extended from the Vaiont Gorge to el 850 m. The total length of the two traverses completed came to about 1.0 km. The results he interpreted to be proof that the left valley wall consisted of "extraordinarily firm in-situ rock - covered with only 10 to 20 m of a loose slide material" (Müller, 1964a, p. 159). "Thus the hypothesis of an ancient very deep slide of the in-situ rock became improbable" (Müller, 1964a, p.159).

In a letter to his father, Carlo Semenza, in April 1960, E. Semenza differed with the conclusions of Prof. Caloi (Semenza, 1965b). Semenza indicated that in his opinion the left side of the valley was a large rock mass that had slid in the past in a northeast direction. This opinion was discussed by Giudici and Semenza in their report submitted in June 1960 and was also noted by Müller (1964a, p. 159).

Feb. 1960 Filling of the reservoir began.

Spring 1960 Borings S-1, S-2, S-3 (see Figure 5) were drilled to depths of 172, 71 and 105 m, respectively, in the toe of the western side of the slide under the supervision F. Giudici and E. Semenza.

Trenches were excavated in the depression south of the Pozza. Heavily fractured and highly permeable (water

circulation was frequently lost) green and pink marly-calcareous materials were found towards the bottom of the borings. No traces of the Dogger and Malm formations and of the old sliding plane were found in these borings. The borings could not be drilled any deeper because of continuous collapse of the borehole walls (Semenza, 1965b). In the trenches well-stratified cherty limestones with open cracks were found.

- March 1960 Reservoir was filled to el 595 m. Small rockfalls took place just east and west of the mouth of the Massalezza Ditch.
- May 1960 The first survey reference points were installed on the left slopes of the Vajont Valley.
- June 1960 Giudici and Semenza (1960) submitted their formal report which establishes the presence of "numeous intercalations of greenish clay, with thickness of a few centimeters" in the Lower and Upper Cretaceous material at the site. The presence of the various mylonitic zones in the left slope, particularly a mylonitic zone below the mouth of the Massalezza at an approximate elevation of 625 m, together with the rock debris remaining on the right valley slope was considered by Giudici and Semenza as evidence of an ancient slide in the left slope. They pointed out that the whole mass below Pian del Toc, between Casera Pierin and Colomber, could slide if the surface of the prehistoric slide was inclined towards the lake. Furthermore, they indicated this movement could be produced by the reservoir filling.
- July 1960 Dal Piaz submitted another geological report in which he re-examined the stability of the reservoir banks. He found no evidence of a past movement in the rock of the left bank.

A similar large occurrence in the future was not considered possible. The report mentioned the possibility of smaller slides developing in loose layers near the surface between Pineda and the Pian della Pozza only. Partial and localized detachments of rock glebes and slices along the edge of the Pian della Pozza, which would not extend to the Pozza itself, were predicted. "It was finally admitted that such detachments would help the area to reach a sure equilibrium" (Müller, 1964a, p. 160).

- Summer 1960 Studies by E. Semenza were made to define the boundary of the old slide mass.
- Sept. 1960 The dam was completed.
- June 1960 to Oct. 1960 Reservoir level was raised from 595 to 635 m. Movements were recorded on the slope along the canyon wall from the dam to 350 m west of Massalezza Ditch. This is the region of the November 1960 slide noted below.
- Oct. 1960 Reservoir filled to el 635 m. Benchmark movements accelerated and a crack over 2 km long (see Figure 5) formed in the approximate location of the perimeter of the October 1963 slide. Approximately 500 mm of rain, the largest rainfall in the life of the reservoir, was measured at the Erto Station during this month (Appendix A). Cumulative movements of the sliding mass measured between the Massalezza Ditch and the dam exhibited an average of 1.0 m and a maximum of 1.4 m (Müller, 1964b).
- Nov. 4, 1960 With the reservoir at el 645 m, a 700,000 m³ slide occurred on the left side of the valley just upstream from the dam (see Figure 5). This collapse produced a 2 m high wave in the reservoir.

Nov. 8 to Müller, E. Semenza, Broili, and others were called to Vajont 16, 1960 to investigate the movements of late October and early November 1960. In his Report No. 15 Müller (1961) outlined the nature of the movements, the various causes responsible for the movements, and suggested a series of potential remedial measures. He concluded that the sliding mass followed basically two types of movements: (a) a glacier-type of movement that took place at the lower part of the slope between the dam and the Massalezza Ditch, and (b) a rigid block ("en block") type of movement that took place in the rest of the slide. He also concluded that it was not possible to stop the movements completely, and the only alternative was to maintain the slide under control by limiting the size of the sliding mass as well as the velocity of displacements. It was assumed that slow and controlled mass displacements would eventually build a passive resistance at the toe of the slide large enough to provide a stable equilibrium. To gain control of the sliding movement Müller recommended: (a) a slow and controlled lowering of the reservoir level, and (b) lowering and leveling of the phreatic level by means of two drainage tunnels driven underneath the sliding mass. These adits would start in the vicinity of the Massalezza Ditch at an approximate elevation of 900 m and run east and west, respectively. (Note, it is now known that the 900 m elevation was above most of the slide mass.) Other remedial measures, such as: (a) rock removal to reduce the weight of the "driving" mass, (b) cementation of the sliding plane to improve the friction resistance along the sliding plane, and (c) attempts to stop or considerably reduce the amount of water infiltrating the sliding mass, were considered either too expensive or beyond human endeavor.

- Nov.-Dec. 1960 Reservoir lowered from 650 to 600 m; slide movements were reduced.
- Dec. 1960 Professor Caloi completed a second seismic investigation. This investigation was more extensive than the first and included two traverses from an elevation of 750 m to the perimetral crack at the top of the slide. One traverse was about 200 m west of the Massalezza Ditch, the other was about 400 m east of the ditch. This survey coincided with the 1959 survey in only one location along the 1.8 km length of the two traverses (see Figure 5). This time an upper layer of loose rock 30 to 50 m thick was found in the eastern part and a similar layer 70 to 150 m thick was found in the western part. Caloi concluded that there had been a deterioration in the rock quality since his first survey (Müller 1964a, p. 168).
- Late 1960 Hydraulic model studies of the slide induced reservoir wave phenomena were requested by C. Semenza (E. Semenza, 1965b).
- Early 1961 Exploration adits were driven in the Massalezza Ditch at about el 920 to 950 m (see Figure 5).
- In April 1961 Broili and Weber visited the exploration adits. They determined that the lower portion of the moving mass was at the contact between the Dogger and the Malm formations. They also determined that the movements did not take place along a single plane, but rather along a series of planes (passing through the fractured material) with clay layers sandwiched between solid pieces of rock (Müller, 1964b, p. 25). Semenza indicates that during the course of numerous visits to the adits it was possible to determine that after a few tens of meters inside the underground

openings, the loose materials present at the entrance changed into fractured rocks with folded stratification. Further on into the adit, after a section where a series of ultramylonitic facies were present, a sound uniformly bedded rock was found (Semenza 1965b, and Appendix G). These strata dipped approximately 30° to 40° north and apparently represented the undisturbed beds beneath the zone of failure.

- Early 1961 Bench mark system was extended over the total area included in the October 1960 movements.
- Feb.-Oct. 1961 A bypass tunnel was constructed on the right bank to regulate the reservoir level in the Erto area in the event of a slide that would divide the reservoir (see Figure 5). The reservoir was held down between el 585 and 600 m during this period.
- Sept.-Oct. 1961 Piezometers P1, P2, P3, and P4 were installed under the supervision of E. Semenza and F. Giudici (see Figure 5).
- Oct. 1961 Carlo Semenza, designer of the dam, died.
- Oct. 1961 - Feb. 1962 The water level in the reservoir was raised from 590 m to 650 m. Mass movements during this period were almost negligible and the speed of movement remained below 0.1 cm/day (Müller, 1964b, p. 37). Water level in the reservoir reached 635 m elevation in December 1961, the level at which the October 1960 movements and perimetral crack that outlined the 1963 slide developed. Movements were very small.
- Oct. 1961 - Sept. 1963 Studies of the slide were generally limited to routine monitoring of slide movements and to observations of groundwater levels.

- Feb. 1962 - Oct. 1962 The water level in the reservoir continued to rise from 650 to 695 m. Around the first of October, when the water level in the reservoir was at an elevation of 695 m, the maximum speed of movement measured was still below 1 cm/day (Müller, 1964b, p. 37).
- April 20 1962 Prof. Dal Piaz died.
- Nov. 1962 The water level in the reservoir was raised to el 700 m. Records indicate heavy rainfalls, 414 mm, during this month (230 mm in the first ten days) and the rate of movement increased up to 1.2 cm/day (Müller, 1964b, p. 37).
- Dec. 1962 - March 1963 The reservoir level was lowered very slowly to an elevation of 650 m. By the middle of February 1963 the reservoir level was at an elevation of 675 m, and the maximum rate of movement was 0.3 cm/day (Müller, 1964b, p. 38). By the end of March the reservoir level was at 650 m and the movements were almost nil. At the end of this period, the slide between the Massalezza Ditch and the dam had moved approximately 2.3 m. Bench marks at points of maximum displacements indicated total cumulative movements approximately equal to 3 m (Müller, 1964b, p. 37). East of the Massalezza the magnitude of movements was smaller.
- April - May 1963 From the first of April to the end of May the reservoir level was raised from an elevation of 650 m to 696 m. Bench marks indicated a slight increase in the rate of movement up to 0.3 cm/day (Müller, 1964b, p. 40).
- June - July 1963 During this period the water level in the reservoir had reached an elevation of 705 m by the middle of July. The

maximum rate of movement measured at this time (middle of July) remained below 0.5 cm/day (Müller, 1964b, p. 41).

- Aug.-Sept.
1963 From the middle of August to early September the water level in the reservoir was raised from 705 to 710 m elevation. Heavy rainfalls were measured in the middle of August (close to 200 mm between August 10 and 20). Unusually heavy rainfall (200 mm) was also measured in the following 20 days.
- Sept.
1963 The rate of movement greatly increased during the first days of September, while the reservoir level was slowly rising to a level of 710 m. The rate of movement reached values similar to those reached in October 1960 and in November of 1962. By the middle of September 1963 the maximum rate of movement measured at the lower west portion of the sliding mass reached a value of 3.5 cm/day.
- By the end of the month a maximum rate of movement of 3.25 cm/day was measured at points located in both the upper and lower parts of the western portion of the slide mass (Müller, 1964b, p. 43). A slow drawdown to minimize the rate of movement of the sliding mass was started during the last days of September. Rainfall records at Erto indicate 164 mm of rain during this month.
- Oct. 1-8
1963 A drawdown of the reservoir level continued at the rate of about 1 m per day. Records indicate relatively heavy rainfalls of 29 and 22 mm on October 3 and 4. The rate of movement increased during the first days in October. According to the Bozzi Commission (1964) the rate of movement on October 9 reached a value of 20 cm/day.
- Oct. 9,
1963 A five-member board of advisors formed by the Italian Government in 1962 was evaluating conditions on a day-to-day

basis. Prof. Penta, the geologist member, was scheduled to visit the slide area on Oct. 10 (Kiersch, personal communication).

- Oct. 9, 1963 At 10:39 pm, October 9, with the reservoir level at el 700.4 m, the Vajont Slide took place (Bozzi Commission, 1964).
- Oct. 10, 1963 The Minister of Public Works appointed an Inquiry Commission with Carlo Bozzi as chairman. The other members were: Engr. Giuseppe Merla, Prof. Livio Trevisan, Prof. Raimondo Selli and Prof. M. Viparelli. Their report was submitted January 16, 1964.
- Oct. 10, 1963 E. Semenza made his first visit to the site after the slide. An extensive geological study of the slide mass and surrounding areas was undertaken by Semenza and Rossi for E.N.E.L. The study continued into 1964.
- Oct. 23-27, 1963 Müller and Broili together with Engr. H. Maier and Prof. G. A. Kiersch made their first visit to the site after the slide. Extensive investigations for E.N.E.L. began and continued into 1964.
- Nov. 1, 1963 A commission was appointed by E.N.E.L. to "ascertain the causes of the Vajont disaster". The members of this commission were: Avv. Marcello Frattini, Prof. Filippo Arredi, Prof. Alfredo Boni, Prof. Costantino Fasso, and Prof. Francesco Scarsella. Prof. Filippo Falini, also a member of this commission, died in a helicopter accident in the Vajont area while investigating the slide in November. The commission was commonly known as the "Frattini Commission" (1964) and submitted its report in January 1964.

PART VI: CORRELATIONS BETWEEN RESERVOIR LEVEL, PRECIPITATION, AND RATE OF MOVEMENT

First Reservoir Filling

Comparisons between precipitation in 10-day intervals with reservoir level, rate of slide movement, and water level in the piezometers for the four-year period from 1960 through 1963 are given on Figure 29.

There was a small slide in March 1960 at the toe of the east end of the overall slide. The outline of this slide is shown on Figure 5. The time of this slide, which occurred before displacement measurements were made, is shown on Figure 29. The March 1960 slide occurred without a noticeably high 10-day incremental rainfall, although there were substantial 3-day rainfalls. This early slide also could be associated with a period of snowmelt and probably was strongly influenced by the rising reservoir.

The first major slope movement that was monitored occurred in October 1960 during the first filling when the reservoir level had reached an elevation of about 650 m. By late October 1960 the displacements were sufficient to result in a series of cracks which essentially outlined the perimeter of the entire slide as it subsequently developed in 1963. The perimeter "crack" is shown on Figures 5 and 11 together with the outline of the October 9, 1963 slide. It can be seen on Figure 29 that the development of the perimeter crack coincided with the maximum 10-day precipitation for the year. Also, the onset of significant movement coincided with the start of a period of unusually heavy and prolonged precipitation which followed an exceptionally wet July and August. The slide continued to move after the perimeter crack opened, reaching a maximum rate of 3 to 4 cm/day at the end of October 1960.

On November 4, a major slide occurred along the toe of the future Vajont Slide and some 700,000 m³ of material slid into the reservoir. The outline of this slide is shown on Figures 5 and 15. The reservoir level was lowered immediately after the November 4 slide from a maximum

level of 650 m and reached el 600 m by early January 1961. Thereafter slide movements decreased rapidly to less than 0.1 cm/day. The slide essentially stopped moving when the reservoir level was below el 600 m and when the precipitation was low.

At the end of the first drawdown, the average total displacement on the western half of the slide area was 100 cm, and the total movement east of the Massalezza Ditch was less than 20 cm.

It is apparent from Figure 29 that the decline in the rate of movement of the slide from November 1 to 4, 1960 corresponded to the end of the abnormally high rainfall. At this point the reservoir level was still rising.

Construction of the Bypass Tunnel

The reservoir was held between el 585 and 600 m from early January 1961 until early October 1961. During this period the bypass tunnel was driven in the right bank of the valley opposite the 1963 slide area. This was a period of moderately low precipitation except for one wet 10-day period in May 1961. The rate of movement of the slide during this period was negligible. Piezometers P1, P2, and P3 were installed in this period and water level readings commenced as shown on Figure 29. The probable significance of the high piezometric levels recorded in P2 has been discussed earlier.

Second Reservoir Filling

The second filling of the reservoir began in October of 1961, and near the end of January 1962 the reservoir elevation was again at 650 m. As Figure 29 indicates, the rate of movement corresponding to the second filling to el 650 m was negligible and the velocity was less than 0.1 cm/day. This behavior was in sharp contrast to the 3.5 cm/day velocity observed when the reservoir was just below el 650 m during the first filling. Even as the reservoir approached el 700 m at the beginning of November 1962, the velocity was only about 0.2 to 0.3 cm/day. The rate of movement increased abruptly to about 1.2 cm/day at the end of November 1962, although the reservoir remained nearly constant at the

700 m elevation. This increased movement followed a period of record precipitation for the four-year period shown on Figure 29. The reservoir was lowered to 650 m by the end of March 1963 and the movement stopped. But the movements which occurred during the second filling and drawdown to el 650 m amounted to 130 cm. These were in addition to the 100 cm of movement which occurred due to the first filling.

Third Reservoir Filling

The third filling of the reservoir began in April 1963, and the reservoir reached approximately el 695 m by early June 1963. At this time the slide velocity was about 0.3 cm/day (see Figure 29). The reservoir reached 705 m in the middle of July 1963, and the rate of movement increased to about 0.4 to 0.5 cm/day.

In mid-August the reservoir started to rise from el 705 m and reached 710 m in early September. There was an immediate increase in the rate of slope movement from 0.5 to 1.0 cm/day. This rate continued to increase throughout September reaching 2 to 4 cm/day in the first days of October. In early October lowering of the reservoir began. The elevation of the reservoir had dropped to about 700 m by October 9, 1963 when the major slide occurred. According to the report of the Bozzi Commission (1964), the velocity of the slide by October 9, 1963 was about 20 cm/day.

It is important to note on figure 29 that the final acceleration of movement began in late August 1963 and coincided with a period of near-record precipitation for the four-year period.

Erroneous Assumptions Regarding the Effect of Reservoir Levels

If other factors governing stability remain constant, then it is reasonable to assume that similar rates of movement should be observed for similar reservoir levels. The empirical observations at Vajont, which showed that the movement of the slide in October 1960 was 3.5 cm/day when the elevation of the reservoir was at 650 m, seemed at variance with the observation of a negligible slide velocity in January 1962 when the reservoir was also raised to el 650 m. Moreover, the rate

of movement of 1.2 cm/day, which accompanied the reservoir elevation of 702 m in November 1962, was below the rate of 3.5 cm/day observed for the 650 m reservoir elevation in October 1960. Having such data available, Müller (1964a, p. 178) stated:

The experiences gathered during the second period of storage seemed also to confirm the assumption, developed in the meantime, according to which it was considered possible to control the velocity of the slide by the effect of the water on the sliding mass itself. The observation that the movements generally had a higher velocity only if a new portion was wetted for the first time, whereas they remained always smaller than the previous one if a layer once wetted was flooded a second time, led authorities and technicians to the conviction that a gradual stabilization of the moving mass would be brought about by raising the water level in individual steps. It was assumed that the mass would eventually reach a certain equilibrium, or, at least would keep moving so slowly that no serious problems would occur.

The erroneous assumption which led to the conclusions quoted above was that all other factors were remaining constant and the reservoir level was the main variable controlling the stability of the slide. In fact, rainfall was significant and was not remaining constant.

Inspection of Figure 29 reveals that there were periods of high precipitation preceding all the major slide movements; that is, October 1960, November 1962, and October 1963. Also, where there are different movement rates for similar reservoir levels, the higher movement rate correlates with a higher precipitation rate. For example, the second time the reservoir reached el 650 m in January 1962 there was negligible movement because of the low precipitation at that time and in the preceding months. Another example can be seen by comparing the rates of movement for June 1963 when the reservoir was at el 700 m with those for November 1962 at the same reservoir level. The rate of movement was accelerating in November 1962 following a period of record

precipitation, whereas in June 1963, with near normal precipitation, the rate of movement was nearly constant and at half the rate observed in November of 1962. Thus, it would appear from an evaluation of the records on Figure 29 that rainfall is as important as the reservoir level in determining the rate of movement of the slide.

Combined Effects of Precipitation and Reservoir Level

The history of the slide movements above can be explained by considering the combined effects of precipitation and reservoir elevation. It is not necessary to consider another mechanism, such as "creep" (Müller, 1967) or "thixotropy" (Müller 1968), because the behavior only appears to be anomalous when the movements are correlated with reservoir levels without considering precipitation.

As indicated in Part III, the karst-like topography in the Dogger formation above the slide area (see Figure 25a) should permit rainfall and snowmelt to infiltrate rapidly into the bedrock. Some of the resulting groundwater no doubt drains towards the north slopes of Mt. Toc and the Vaiont Valley, moving beneath the many inclined clay interbeds in the Malm and Lower Cretaceous formations. These clays served as aquitards or low permeability barriers to confine the subsurface flow. Thus, as heavy rainfall penetrated into the slope mass above and beneath the failure surface, uplift pressures could be generated on the failure surface corresponding to piezometric levels much higher than the reservoir level. At low reservoir levels very heavy rainfalls would be required to develop uplift pressures large enough to cause instability of the slide mass. As the reservoir level increased, the piezometric gradients towards the reservoir would tend to be maintained so as to transport the same amount of water through the bedrock. Therefore, as reservoir levels increase, the piezometric pressures should also increase so that progressively smaller amounts of rain can produce unstable conditions.

Precipitation records from three stations in the vicinity of the Vaiont Dam were examined. The records cover the period from 1960 through 1964. Two of the stations, Erto and Cimolais, are located east

of the dam at el 726 m and 652 m, respectively. The third station at Longarone is at an approximate elevation of 474 m. A study of the precipitation records shows that the upstream stations of Erto and Cimolais (see locations in Figure 1) recorded much more precipitation than the station at Longarone. The records also show reasonably similar rainfalls at Erto and Cimolais. Since the Erto station was closest to the Vaiont slide, the Erto records, which are presented in Appendix A, were chosen to represent precipitation at the slide. However, it seems likely that the actual precipitation on and above the slide would be higher than at Erto.

In the winter months (November to March or April) the correlation between precipitation and slide movement would not be expected to be as reliable as when the precipitation was all rainfall. This is because much of the precipitation would be snow which would produce almost no immediate infiltration. However, once the snow begins to melt large amounts of infiltration could occur even though there was no precipitation.

The amount of precipitation which occurred during various time intervals immediately preceding the three dates approximating the time of the maximum rate of movement (October 31, 1960; November 30, 1962; and October 9, 1963) is shown in Table 7. Table 7 shows precipitation measured during intervals of 7, 15, 21, 30 and 45 days preceding the day that the maximum rate of movement took place. The reservoir elevations and dates of maximum movements are also shown. As indicated in Table 7, substantial amounts of precipitation, from 80 to 170 mm in the 15-day periods preceding the movements, were measured before the movements took place. Table 7 also suggests that the amount of precipitation necessary to induce significant movements gradually decreased for higher reservoir elevations. As indicated in Table 7, precipitation during a 15-day period preceding movements was 170 mm for a reservoir elevation of 645 m. The precipitation during a 15-day period preceding movements ranged from 81 to 94 mm when the reservoir elevation was at 700 m.

Table 8 shows precipitation for various intervals preceding the dates at which the reservoir level was again raised to those elevations where movements had previously accelerated. For these "safe arrival" dates, no significant rates of movement were observed. For the 15-day interval preceding December 15, 1961, the date at which the reservoir approached el 645 m, the precipitation was 50 mm. This compares with the 170 mm recorded in the 15-day interval immediately preceding October 31, 1960, the date at which the reservoir first reached 645 m and significant movements occurred. Rainfall in the 15-day interval preceding June 30, 1963, which corresponded to a reservoir level of about 700 m, was 29.8 mm. This compares with the 94.3 mm precipitation recorded for the 15-day period prior to November 30, 1962 when the reservoir was also near 700 m. Thus, for these examples, it is clear that the 15-day precipitation immediately preceding a significant movement at a given reservoir elevation was greater than three times the 15-day precipitation preceding the dates when the reservoir was at the same elevation but when no significant movements were observed.

Graphical representations of rainfall and reservoir data, including the values in Tables 7 and 8, are shown in Figures 30 to 33. On these figures the water level in the reservoir is plotted vs the amount of precipitation measured during periods of 7, 15, 30 and 45 days preceding the arrival of the reservoir at those elevations. It was believed that the "rain period" affecting the uplift pressures along the sliding plane would be bracketed between these intervals, although longer term climatic effects could also be significant. The solid and half-filled dots on Figures 30 to 33 correspond to those occasions where accelerating movements exceeded 0.5 cm/day. The solid line through the lower range of these points would represent a "failure envelope" corresponding to those combinations of water level and precipitation required for the slope to become unstable. The extremes of this failure envelope if extended would correspond to:

- a. the reservoir elevation that would develop enough uplift pressure to make the slope unstable without any rainfall or snowmelt (approximately 710 to 720 m), and

- b. the rainfall or snowmelt required to make the slope unstable without the reservoir present (approximately 180 mm/7 days, 350 mm/15 days, 700 mm/30 days and 1100 mm/45 days).

Various combinations of reservoir elevation and preceding precipitation which correspond to different situations during the lifetime of the reservoir (impoundments as well as drawdowns) are represented in Figures 30 to 33 by the points plotted. As indicated on each figure, the combinations represented by open triangular points correspond to relatively "stable" conditions. Open circles indicate when the rate of movement is less than 0.5 cm/day. These points plot generally below the "failure envelope" and there is a tendency for the rate of movement (given by the number in parentheses) to increase for those combinations closer to the failure envelope.

It is clear that the two main variables affecting the stability of the slide were the reservoir level and the precipitation in the preceding interval. Figures 30 through 33 suggest that the slide would have failed with no rainfall or snowmelt when the reservoir levels reached the vicinity of the proposed full supply level, el 722.5 m. The data also indicate that slide movements could be triggered by very high rainfalls or snowmelts, the magnitude of which were in the range of 130 to 200 percent of the 7 to 45 day precipitations recorded for the period from 1960 to 1964. Hence, it is quite likely that slope movements have resulted from the maximum precipitation occurring within 100-year or 1000-year intervals in the past. This would appear to provide quantitative verification of the stories attributed to the local inhabitants about the occurrence of slope movements from time-to-time.

PART VII: ASSUMPTIONS FOR THE STABILITY ANALYSES

Introduction

The differences between the analyses presented in this study and those of previous investigators lie principally in the differences in the assumptions used for the input parameters. Although these assumptions have been mentioned throughout this report, they are repeated and discussed in this section.

Shear Strength

The shear strength along the base of the slide was assumed to be related more to the residual shear strength of the multiple layers of clay found along the basal surface of sliding than to the higher shear strengths of the rock-to-rock contacts. This is a basic departure from previous stability analyses, such as those of Müller (1964a and 1968), Lo et al (1972), Chowdhury (1978), and others. The bases for this assumption are the authors' field observations presented in Table 1, Figure 13, and Photos 1 to 37, and the results of the laboratory shear strength tests, and Atterberg limit tests summarized on Tables 2, 3, 4, and 5, and Figure 28. Also, Rossi and Semenza (1965a) indicated the correlation of the Lower Cretaceous and Malm stratigraphic units with the base of the slide. This is shown in the cross sections, Figures 15 to 20, which Rossi and Semenza completed for this report. This correlation was independently verified by the authors' field studies and by a review of the drillhole logs and other preslide and postslide geological evidence.

Essentially all peak strengths and most increases in strength caused by irregular geometric effects were assumed to have been lost because of prehistoric slide movements or tectonic movements. Thus, the residual strength, ϕ_r , of the failure plane materials was assumed to be the most significant factor in these analyses. However, modest strength increases, as indicated by the results of laboratory residual strength tests of the weakest clays, could be expected because of the substantial

number of rock-to-rock contacts which occur along the basal sliding surface. These occur because of the existence of (a) localized areas of shearing across bedding planes, (b) areas where clays do not occur, and (c) areas where clays are squeezed and forced to flow into voids that develop as a result of the displacement of irregular surfaces on either side of the clay beds. Also, small increases in shear strength could be expected as a result of the introduction of brecciated rock fragments into the clays along the surface of sliding.

The residual angle of shearing resistance, ϕ_r , of the clays as determined from the laboratory tests was 5° to 16° , with an average value of 8° to 10° (see Tables 3, 4, and 5). However, because of the factors noted above, it seems quite reasonable to accept a mean value for ϕ_r along the basal surface of sliding of 10° to 12° . Cohesion is, of course, assumed to be essentially zero. The basal surface of sliding also is assumed to closely correspond to the old rupture surface described by Semenza (1967) and possibly to a tectonic décollement fault, the traces of which have been mapped on the exposed portion of the failure surface (see Figures 5 and 11). The previous assumptions are in agreement with the occurrence of an uncemented basal fault or rupture surface.

In addition to the shearing that occurs along the base of the slide, deformations occur within the slide mass as it moves over irregularities and across gross changes in inclination of the failure plane. In a highly disturbed rock mass, such as the Vajont Slide, much if not all of these deformations will occur along pre-existing discontinuities, such as joints and faults. In this study the angle of shearing resistance, β , acting along the discontinuities which cross bedding planes within the slide mass, was chosen on the basis of the authors' experience and their field observations on the type of materials present. It was apparent that deformation along these planes would require shearing across thinly bedded limestones, cherts and clay interbeds of the Lower and Upper Cretaceous formations. On a large scale these beds can deform locally and would be expected to develop an angle of shearing

resistance, β , of 30° to 40° . This potential shearing resistance is not mobilized except where there is a tendency for adjacent slices to move relative to each other as described by Mencl (1966). With the geometry of the failure surface established, the largest amount of relative movement of slices would occur at the junction between the "back" and the "seat" of the slide. The analyses have indicated that the stability of the slide is quite sensitive to the value of β .

Since there is no practical way to measure β in the field, the analytical procedure was arranged so that the effect of various assumed values of β could be determined. It should be noted that the field values of β could drop significantly if a pre-existing, near-vertical, fault surface was to coincide with the junction between the back and the seat of the slide. However, field mapping of the exposed failure plane did not reveal any fault surface which would have more than a small segment present in a critical position at any one time. The β values along the discontinuities are assumed to be somewhat higher than the values of the residual shear strength along the basal surfaces. This is because these surfaces have undergone fewer differential movements than the base of the slide. Hence, some additional strength losses could presumably occur with continued displacement along the near-vertical surfaces.

In the three-dimensional analyses undertaken in this study, it is necessary to assume that differential movement may also occur between adjacent blocks. The angle of shearing resistance that can be mobilized along the sides of blocks (those near-vertical planes oriented parallel to the direction of slide movement) within the slide mass is assumed to be similar to the values used for β since the materials are the same. The frictional resistance of the steeply dipping planes forming the east end of the slide was assumed to be 36° . These values are in agreement with published data on the residual angle of shearing resistance for carbonate rocks (Patton and Hendron, 1974).

Water Pressures

The piezometric head acting on the surface of sliding along its contact with the reservoir was assumed to be equal to the reservoir level. Away from the reservoir, the piezometric head was assumed to increase above reservoir levels due to an assumed groundwater flow system where water was moving from the mountain towards the valley. The initial water level recorded in drillhole P2 in October 1961 was over 90 m above the reservoir level. This is a control point on the fluid-pressure distribution curve for the low rainfall condition. For the sections without P2, an equivalent pressure difference was assumed at positions equivalent to P2 along the surface of sliding. For high rainfall conditions, a significantly higher piezometric pressure was assumed at P2 than that measured. For both low and high rainfall conditions, the difference between the assumed piezometric level at any point on the failure surface and the elevation of that point is gradually reduced to zero between the location of P2 and the southern extremity of the slide surface. The actual piezometric levels used in these analyses are given in Appendix C.

Each reservoir condition was analyzed for a low and a high piezometric pressure distribution corresponding to a low and a high rainfall condition. The actual pressure distributions would vary for intermediate rainfalls. For each reservoir level the calculated factor of safety would be expected to differ from its real value. The amount of the correction from a known value, say at failure, would be an indication of the real fluid pressure distribution due to intermediate rainfalls, if other factors remained constant.

The groundwater table above the clay layers was assumed to equal the reservoir level at the toe of the slide and to slope gently upwards to agree with the water levels measured in P1 and P3 (and in P2 after July 1962). The water pressure distribution on the ends of the vertical slices was assumed to be consistent with a hydrostatic increase in water pressure within the slide debris.

In summary, a modified classical artesian system acting within an inclined and layered sedimentary rock sequence was assumed to be operative on the north slopes of Mt. Toc. The slide area, particularly the lower portion of the slide, was assumed to lie within a groundwater discharge area where piezometric pressures below the failure surface were significantly in excess of the groundwater table and the reservoir levels. These excess piezometric levels below the failure surface were maintained with increases in reservoir levels so as to maintain a positive head difference with respect to the reservoir. This interpretation is in agreement with the only quantitative data available (that is, the water levels recorded in P1, P2, and P3) and accounts for the behavior of the water levels observed in P2.

Geometry of the Failure Plane

The base of the slide has been assumed to correspond to a pre-historic slide surface. The position of the toe of the failure surface was assumed to agree with the contact along the Vajont Canyon given by Giudici and Semenza (1960) in their map of the preslide geology, presented in Appendix G, and shown in more detail in Figure 11. The stratigraphic sequence was used to plot the base of the slide between exposures currently visible along the back of the slide and along the toe. Location of the failure surface is further based on all available postslide drillhole data as interpreted by Broili (1967), Rossi and Semenza (1965a) and more recently by Rossi and Semenza in the preparation of Figures 15 to 20 for this report. Although the core recovery was poor in the slide material and in the thinly bedded Lower Cretaceous and Malm units associated with the failure surface, it was generally possible to recognize the top of the Dogger formation with confidence. The failure surface was assumed to be located a constant distance above the top of the Dogger formation, except near the eastern boundary. An offset distance above the top of the Dogger was similarly selected to establish the position of the failure surface along the east-west sections (Figures 21 and 22).

The sections used for the two-dimensional analyses in the first stage of the overall re-evaluation were drawn approximately parallel to the direction of the initial movement of the slide as determined by survey records. The orientation of these sections is shown on Figures 11 and 12.

The combination of low shear strength on the base of the slide and the pronounced eastward (upstream) dip of the failure surface along the base of the seat of the slide required that the shearing resistance developed along the east side of each north-south slice of the slide be considered in the analyses. In particular, this assumption was necessary to demonstrate the relative stability of the slide prior to reservoir filling.

The step-like shape of the eastern side of the basal failure surface corresponds to surface observations of the possible tectonic fault surface at locations 12-1A, 12-2, 12-3, and 24-1 (see Figure 13).

The base of the slide was assumed to be relatively continuous across the seat and the back of the slide, although the basal plane is assumed to step upwards as the eastern limit of the slide is approached.

Slide Movements

Large movements were assumed to have occurred along a pre-existing surface of rupture. This movement occurred in an alignment subparallel to the direction of slide movement.

Significant downhill movements along the failure plane are assumed to have occurred periodically during valley erosion and glacial loading and unloading in Pleistocene times. One of these movements was probably rapid and was responsible for the large remnant of slide material mapped by Giudici and Semenza (1960) on the right side of the Vajont Valley prior to the slide (see Figures 5 and 11). Additional movements of the slide mass have occurred in postglacial times with the erosion of the most recent Vajont Canyon through the slide mass and the removal of support from the toe of the slide. These movements continued into historic times and are probably the source of the tales told by local residents about the instability of the slope and the name Mt. Toc. The

latter is reported to mean "crazy" in the local dialect (Semenza, personal communication). Talus of various ages infills a large zone along the base of the top scarp of the slide providing evidence of historic and prehistoric movements. Also the aligned depressions and airphoto lineaments noted along the perimeter of the slide and within the slide in the 1960 airphotos (Figure 25) clearly reflect prehistoric slide movements.

Most of the slide, including both sides of the Massalezza Ditch, is assumed to have moved as a unit to the northeast. Previous analyses (for example, Müller 1964a and 1968) have generally assumed a difference in slide movement and other factors on either side of the Massalezza Ditch. The authors' field observations and interpretations of the preslide and postslide mapping of Rossi and Semenza, Figures 11 and 12, indicate that there was one general direction of slide movement and the main slide mass did not undergo significantly different directions of movement. This evidence also indicates that a much smaller slide came from the east side of the slide (the Eastern Lobe) in a secondary slide which was probably triggered by the loss of toe support produced by the movement of the main slide. The authors have concluded that consideration of this secondary slide is not necessary for an understanding of the main slide.

Sections 2, 5 and 10a were considered appropriate for analysis as they were taken in the approximate direction of the initial slide movement as determined by displacement vectors calculated from measurements of survey monuments. This direction of movement was in general agreement with the field observations of striations on the failure plane.

PART VIII: STABILITY ANALYSES

Purpose and Scope

The Vaiont Slide has probably been the subject of more stability analyses by more investigators than any other slide. The purpose in making stability analyses after a slide has occurred is to develop a more complete and more quantitative understanding of the factors that led to the slide. Such analyses also provide a check on one's knowledge of the principal input parameters that had an affect upon the slide. These parameters include: the shear strength along the slide surface, the geometry of the failure surface, and the distribution of water pressures along the surface of failure. For stability analyses conducted after a slide, the geometry of the failure surface is determined by pre- and postslide drillhole data and geologic mapping. The water pressure distributions may be estimated from preslide piezometric observations and geohydrologic interpretations. The shear strength data used may be based on laboratory tests or assumptions. In many cases the shear strength may be back-calculated for the failure condition, assuming a factor of safety of 1.0 at failure and assuming the geometry and pore pressures are known values.

Postslide stability analyses are in fact a quantitative means of verifying the story developed to explain the slide. For example, when significant rates of movement were recorded at various times during the history of slide movement, the various analyses should yield calculated factors of safety very near 1.0. It is equally important that the stability calculations yield factors of safety appreciably greater than 1.0 for those times in the slide history when the movements were known to be insignificant. If the results of the analyses do not agree with all the available data and with the observed movement record, then the explanation developed is incorrect or at least incomplete. Because of the importance of the Vaiont Slide as a precedent, it is essential that the stability analyses for Vaiont be in agreement with the observed facts.

Periods Examined for Stability

Stability analyses are a much more powerful tool when there has been a definite condition of failure or a significant rate of movement because the factor of safety can then be assumed to be 1.0 and various combinations of shear strength and pore pressure distribution can be investigated which will yield a factor of safety of 1.0. If several periods of movement have occurred under differing reservoir conditions, it is possible to further eliminate some of the ambiguity in the input to the stability analyses. Such is the case for the Vajont Slide where four periods of movement have been identified. None of the analyses by Mencl (1966), Kenney (1967a), and Nonveiller (1967a, 1967b), which were summarized by Müller (1968, Table 9), or the later analyses by Khan (1971), Lo et al (1972), Jaeger (1972), Trollope (1977) and Chowdhury (1978) explain the known movement record for these periods. Also these analyses did not compare the unstable behavior observed in October 1960 when the reservoir was at el 650 m with the stable behavior exhibited by the slope when the reservoir was at el 650 m during January of 1962.

The analyses performed for this study were designed to examine the equilibrium conditions of the Vajont Slide for three periods when the factor of safety was near 1.0. These periods were: (a) prehistoric times, when geologic field evidence indicates that movement had occurred; (b) October 1960, when the perimeter cracks developed; and (c) October 9, 1963. Two groundwater conditions were considered for each period, one representing periods of high rainfall and the other low rainfall. In addition, the case of a dry slide was included for control purposes. Differences in the behavior of the slide between October 1960 and January 1962 are explained by differences between the "high" and "low" rainfall groundwater conditions for a reservoir at el 650 m.

Basic Assumptions and Sections Analyzed

Table 9 gives a summary of the basic assumptions as well as the results of two-dimensional stability analyses conducted by some of the previous investigators (Müller, 1968). The typical cross-sections

previously analyzed are also shown in Figures 8 and 34. As Table 9 shows, these analyses indicated that "effective" angles of shearing resistance ranging from 17° to 29° were necessary along the two-dimensional failure surfaces to achieve a factor of safety of 1.0 when the cohesion was assumed to be zero. For many of the published analyses, the angles of shearing resistance necessary for equilibrium would have been calculated to be even higher if these authors had assumed higher and more realistic piezometric levels along the failure surface during periods of high rainfall.

The values of shearing resistance back-calculated and shown in Table 9 are high compared to the angles of residual shearing resistance which can be ascribed to the clays on the failure plane described in Parts III and IV. It is apparent that there was too much of a difference between the values of back-calculated angles of shearing resistance reported in Table 9 and the angles of residual shearing resistance for the clays which are presented in Part IV of this report. The difference seemed too large to be attributed to the roughness along the failure plane, in this case bedding planes, particularly since the geological evidence suggests that the Vajont Slide is a reactivated old slide mass. Thus, it seems that an important element has been missing from previous two-dimensional stability analyses.

Upstream dip of failure surface

An examination of Sections 16 and 17 (Figures 21 and 22) taken nearly perpendicular to Sections 2, 5, and 10A reveals that the bedding planes adjacent to the surface of sliding dip from 9° to 22° upstream in a direction perpendicular to Sections 2, 5, and 10A. These sections were taken in the direction of observed slide movement and are similar to the sections on which two-dimensional analyses have been conducted. From Sections 16 and 17 it is obvious that the upstream dip of the bedding results in large normal forces acting on vertical planes oriented parallel to the direction of slide movements (Sections 2, 5, and 10A). These forces will increase in magnitude from west to east. The shear forces on these planes should be significant and will also

increase from west to east. Therefore, a three dimensional stability analysis is required.

Schematic illustration of the three-dimensional slide

Figure 35 is a schematic diagram which illustrates the three-dimensional nature of the possible failure wedges discussed above. In Figure 35 the plane a-e-d is taken as a vertical plane in the direction of movement and would be parallel to Sections 2, 5, and 10A. The surface a-d-c-b is the basal bedding plane failure surface, the trace a-b is the outcrop of the bedding planes on the wall of the Vajont Gorge, and the trace b-c is the western extent of the slide. The shearing force τ_1 is the shearing resistance mobilized on the base plane parallel to the direction of movement and is the resisting force calculated in normal two-dimensional analyses. The shearing force τ_2 is the shearing resistance mobilized parallel to the direction of movement on the vertical plane a-e-d due to the normal force PN_2 . PN_2 is the supporting force required on plane a-e-d to prevent movement upstream down the apparent dip of the bedding surfaces in a direction perpendicular to plane a-e-d.

Angles of shearing resistance

For the analyses considered in this report, the angle of shearing resistance used for the bedding planes along the base of the slide was from 10° to 12° (see Part VII). The angle of shearing resistance on planes parallel to plane a-e-d on Figure 35 was assumed to be about 36° since these planes cross strata of limestone, chert, siltstone, claystone and clay interbeds. Later in this section of the report, the resisting force τ_2 , as shown schematically in Figure 35, is shown to be significant and necessary for equilibrium of the slide at all times. This would be true even before the filling of the reservoir, assuming the shear strength along the bedding planes was governed by the clays and was in the range of 8° to 12° .

Section locations and orientations

Geologic Sections 2, 5 and 10A, as updated for this study by Rossi and Semenza, correspond to those used for two-dimensional analyses. The

locations of these sections are shown in Figure 11; the sections before the slide are shown in Figures 15, 17, and 19. Each of these sections represents about one third of the slide. The directions of these sections were taken from the direction of initial sliding as determined from the vectors of initial movement. These directions were later confirmed by the authors in the field in those locations where striations were measured on the exposed failure surface. For limit equilibrium analyses it is important that the orientation of the section agree with the observed direction of movement because only then will the friction forces on the base of the mass be oriented parallel to the section as assumed, since friction forces are parallel but opposite to the direction of movement.

Two-Dimensional Stability Analyses

The two-dimensional analyses conducted for this study used a variation of the method of slices which is shown schematically in Figure 36. The analyses of the three cross sections chosen as representative of the different portions of the slide were carried out by means of a computer program which calculated the factor of safety by considering the surface of sliding as a series of planes. Each cross section was subdivided into slices with vertical boundaries between slices as shown in Figure 36a.

Shear forces between slices were considered in this analysis. The maximum obliquity permitted of the resultant lateral force, F , acting on a vertical plane between slices is defined as β (Figure 36b) and is representative of the shearing resistance across strata of limestone, chert, siltstone, and clay. The values of β used in these analyses ranged from 30° to 40° . Consideration of the shearing forces between slices is important for the Vajont Slide because of the abrupt change in the slope of the failure surface between the portion which is nearly horizontal and that portion which dips from 25° to 44° .

It should also be noted that in the two-dimensional analyses a distinction was made between the water levels measured above the clayey

failure surface and the piezometric levels acting on the failure surfaces. This is shown schematically on Figure 36b.

The magnitude of the value β is input to the program. The resultant effective forces between slices may be inclined at an angle β above or below the horizontal as shown in Figure 36b. The angle will depend on the relative changes in the slope of the base planes which support adjacent slices. The analyses satisfied the equations of horizontal and vertical equilibrium but rotational equilibrium was not considered. As described in Appendix B, the shear force resisting movement at the base of each slice is R , given by

$$R = \frac{(C'L_s + N \tan \phi')}{F.S.}$$

where: C' = cohesion,
 L_s = base length of the slice,
 N = "effective" normal base reaction,
 ϕ' = angle of shearing resistance, and
F.S. = factor of safety.

The computation involves the assumption of an initial factor of safety, and an iterative process is employed in which the factor of safety is changed until the slide mass is computed to be in equilibrium for all slices at the same factor of safety. The program also determines the horizontal force which would have to be applied to the downhill side of the lowermost slice to bring the slide to a factor of safety of 1.0. If the factor of safety is less than 1.0, the force, designated as F_δ , would be compressive. If the factor of safety is greater than 1.0, F_δ would be a tensile force. A more detailed description of the inputs, procedures, and steps used in the program is given in Appendix B.

Cases Analyzed

Cross sections 2, 5, and 10A were each analyzed for seven different cases which corresponded to different combinations of reservoir

elevation and rainfall. These cases are summarized below and include the case of no reservoir and the instances when the reservoir elevation was at 650 m and 710 m. For each reservoir elevation considered, both low and high groundwater levels in the slope are considered to account for low and high periods of rainfall. The low and high piezometric elevations along the failure surface were obtained from the piezometric elevations recorded in piezometer P2 in the fall of 1961, as discussed in Part VII. In addition, as a reference calculation for the cases cited above, each cross section was analyzed for the case of no pore pressure on the failure surface.

Cases Analyzed for Sections 2, 5 and 10A

<u>Case</u>	<u>Groundwater Level or Rainfall Condition</u>	<u>Reservoir Elevation, m</u>
1	Low	None
2	High	None
3	Low	650
4	High	650
5	Low	710
6	High	710
7	No Pore Pressures on Failure Surface	

The cross sections and piezometric elevations considered are shown in Figures C1 to C18 in Appendix C.

Results of Two-Dimensional Stability Calculations

The factors of safety calculated from the two-dimensional slope stability analyses for Sections 2, 5, and 10A are summarized in Table 10. For Sections 2 and 5, analyses were conducted for all seven water level conditions listed above for ϕ values of 8° , 10° , and 12° and β values of 30° and 40° . For Section 10A all seven cases listed above were calculated for a ϕ value of 12° and β values of 30° and 40° .

An inspection of the values of the factor of safety given in Table 10 indicates that even for no reservoir the factors of safety are low for the shear strength used. If the values for $\phi = 12^\circ$ and $\beta = 40^\circ$ are

studied for the no reservoir case, Section 2 has a factor of safety ranging from 0.63 to 0.73, Section 5 has a factor of safety ranging from 1.04 and 1.18, and Section 10A has a factor of safety ranging from 0.51 to 0.57. In all cases Section 5 is more stable than Sections 2 and 10A because Section 5 is closer to the Massalezza Ditch where the volume of material on the steep backslope is less than for Sections 2 and 10A.

Influence of reservoir and groundwater levels

It is also interesting to study the results for Section 5 for $\phi = 12^\circ$, $\beta = 40^\circ$ for Cases 1 through 6. In comparing Cases 1 and 2, the difference between high and low groundwater levels makes about a 14 percent change in the factor of safety for no reservoir. In comparing Cases 1 and 5 and Cases 2 and 6, there is a 12 to 14 percent change in the factor of safety caused by the reservoir changing from river level (450 m) to 710 m. A comparison of Cases 5 and 6 shows that at a reservoir elevation of 710 m the difference in high and low rainfall could change the factor of safety by about 16 percent. Thus, it appears that for the unstable slope the changes caused by rainfall are just as significant as changes in reservoir level.

Forces required to maintain equilibrium

All calculations show a significant increase in the calculated factor of safety as the value of β is increased from 30° to 40° . This is because of the abrupt change in orientation of the failure surface from the steep to the flat portion of the Vajont Slide.

Table 11 summarizes the calculated forces, F_δ , for Sections 2, 5 and 10A which are required to maintain the slide at a factor of safety of 1.0. The calculated forces, F_δ , are assumed to be applied horizontally to the lowermost slice. As indicated in this table, raising of the reservoir level results in the need for a larger force, F_δ , to maintain the equilibrium of the two-dimensional cross sections. A similar need developed when periods of intense rainfall resulted in changes in groundwater levels from low to high. A drop in the friction angle, β , between adjacent vertical surfaces (which can result from relative displacement of the surfaces once movement of the slope has begun) also

resulted in a substantial increase in the force, F_δ , required to maintain the equilibrium of the cross section. Negative values of the equilibrium force, F_δ , indicate that the factor of safety of the cross section is larger than 1.0, and a tensile force in a downhill direction is required for the cross section to reach an equilibrium condition.

Discussion

Taken as a whole, the two-dimensional calculations shown in Tables 10 and 11 indicate that the factors of safety are too low for the slide mass to have been stable over much of its history. Therefore, the shear strengths must have been higher, the pore pressures lower, or an important element has been omitted from the two-dimensional analyses. The pore pressure distribution assumed seems quite reasonable and the angle of shearing resistance of 12° is consistent with measured residual shear strengths plus an increment to the angle of shearing resistance to account for surface irregularities. It seemed reasonable, therefore, to check the effects of the three-dimensional nature of the slide surface before abandoning the assumed values of shearing resistance and pore pressure distributions.

Three-Dimensional Nature of the Slide Surface

Stability analyses that included the three-dimensional wedge effect resulting from the bowl-shaped nature of the sliding surface are described below.

Forces acting on planes parallel to sections

Figure 37 illustrates a crossection taken at right angles to the two-dimensional sections identified by Sections 2, 5, and 10A. The triangular wedge a-e-b in Figure 37 corresponds closely to the east west section shown as a-e-b in Figure 35. The surface shown as b-a in Figure 37 represents the eastward dipping failure surface as shown in Figure 22. The total horizontal normal force PN_2 required on section a-e, Figure 37 to prevent upstream movement (eastward movement) down the apparent dip of the bedding planes is given by:

$$PN_2 = W \tan \theta$$

where: w = weight of the slide mass to the west of the cross section being considered, and

θ = average upstream dip of the sliding plane in a direction perpendicular to planes containing Sections 2, 5, and 10A.

The effective normal force $\bar{P}N_2$ is then equal to

$$\bar{P}N_2 = PN_2 - Uh$$

where: Uh = horizontal hydraulic force against the face of the cross section.

The frictional force acting parallel to the face of the cross section can be calculated then as:

$$\bar{P}N_2 \tan \phi_R$$

where: ϕ_R = the friction angle along the vertical surface between adjacent cross sections.

It should be noted that the frictional force on the slide plane a-b (Figure 37) does not have a component downhill along a-b perpendicular to Sections 2, 5 and 10A. The frictional force in the bedding plane base of the slide is parallel and opposed to the direction of movement; therefore, it is parallel to planes 2, 5, and 10A.

Factors of safety

Factors of safety of the cross sections considered to be representative of the sliding mass under the seven different conditions investigated were calculated as follows.

Stability analyses of the three cross sections chosen as representative of the sliding mass were carried out with the modified slice method explained in Appendix B. These analyses resulted in the factors of safety and equilibrium force, F_s , per unit width of the slope given in Tables 10 and 11. The resisting force along the failure plane and the driving force acting on each unit width of slide represented by that particular cross section were then estimated as follows.

$$\frac{\text{Resisting force}}{\text{Driving force}} = \frac{\sum (N_i) \tan \phi}{\sum W_i \sin \alpha_i} = F.S. \quad (1)$$

where: W_i = weight of each slice in the cross section,
 α_i = angle of inclination of the bottom of the slice,
 ϕ = effective angle of friction along failure plane, and
 N_i = effective normal force at the base of slice i

When the factor of safety = 1.0 with the equilibrium force acting, equation (1) becomes

$$\frac{\sum (N_i) \tan \phi + F_\delta}{\sum W_i \sin \alpha_i} = 1.0 \quad (2)$$

Equations 1 and 2 result in:

$$\frac{F_\delta}{\sum W_i \sin \alpha_i} = 1.0 - F.S. \quad (3)$$

where the driving force is given by

$$\sum W_i \sin \alpha_i = \frac{F_\delta}{1 - F.S.} \quad (4)$$

and the resisting force along the failure plane is given by

$$\sum (N_i) \tan \phi = \frac{F_\delta}{\frac{1}{1 - F.S.} - 1} \quad (5)$$

Equations 4 and 5 were then used to calculate the resisting as well as the driving force for various sections of the sliding mass. The total driving, resisting and restoring forces acting on the entire sliding mass were then obtained from the product of each force per unit width, times the width of slope represented by the typical cross section where those forces were calculated.

Factors of safety of the entire mass, including the frictional force along the eastern wall boundary, were then redefined as

$$F.S. = \frac{\sum (N_i) \tan \phi + \overline{P} N_2 \tan \phi_R}{\sum W_i \sin \alpha_i} \quad (6)$$

Calculated values of this redefined factor of safety of the entire mass were carried out as shown in Appendix D for the different water elevations considered in this study. These results are listed below.

A friction angle of 12° along the failure surface was considered to be the most representative of the in-situ materials at the slip surface. The friction angle along the eastern wall boundary where displacements took place between rock surfaces (as indicated by the traces in the exposed wall) was estimated to be 36°. The friction angle, β , along vertical rock surfaces between slices used in the calculation of these revised factors of safety was taken as 40°.

Results

Factor of Safety of Sliding Mass Calculated from Three-Dimensional Stability Analyses

<u>Case No.</u>	<u>Description</u>	<u>Factor of Safety</u>
6	710 m Reservoir, High Rainfall	1.00
5	710 m Reservoir, Low Rainfall	1.10
4	650 m Reservoir, High Rainfall	1.08
3	650 m Reservoir, Low Rainfall	1.18
2	No Reservoir, High Rainfall	1.12
1	No Reservoir, Low Rainfall	1.21

Discussion of Three-Dimensional Analyses

Adjustments for non-uniform rainfall

As the values shown above indicate, failure ($F.S. = 1.00$) would occur under the combined effect of a heavy rainfall (developing a high

groundwater level) and a reservoir elevation of 710 m. The slope would remain marginally stable, factor of safety of 1.10, during periods of high reservoir levels up to 710 m and low rainfall. Marginal slope stability, factor of safety of 1.08, would also develop if heavy rainfalls occurred at reservoir elevations near 650 m. The movements of October 1960, corresponding to a factor of safety of 1.0, may have developed because of the abnormally heavy rainfalls during this period. It is probable that the groundwater levels in October 1960 were above the levels considered as "high" groundwater levels in these computations.

As discussed in Part VII, the "high" groundwater levels were derived in part from the observation that piezometer P2 was 90 m above reservoir elevation at about October 20, 1961. The rainfall for 7, 15, 30, and 45 days before October 20, 1961 was 59, 205, 208, and 246 mm, respectively. The rainfall for 7, 15, 30 and 45 days before October 31, 1960 was 109, 170, 495, and 697 mm, respectively. Thus, it is clear that the rainfall preceding October 31, 1960 was much heavier than the rainfall preceding October 20, 1961 when the P2 piezometer was operational and yielded data which were used in establishing the "low" and "high" groundwater elevations for these analyses.

If the groundwater elevations were adjusted to take into account the heavier rainfall in October 1960, the factor of safety of 1.08 would more appropriately be reduced to near 1.0. The factor of safety of 1.18 for the 650 m reservoir elevation and low rainfall (see list above) is indicative of the stable conditions which were observed in January 1962 when the reservoir was raised through el 650 m and no movement was observed. Marginal slope stability, factor of safety of 1.12, was estimated for periods of heavy rainfall even without the presence of the reservoir. Over periods of several hundreds of years it is very likely that there were periods of rainfall which raised piezometric levels high enough to reduce the factor of safety from 1.12 to 1.0 so that at times the original slope, with no reservoir, was unstable.

The factors of safety presented in the above list indicate that the stability of the slopes of Vajont for any level of the reservoir was

significantly influenced by rainfall. These observations were also pointed out in Part VI without the benefit of stability calculations. Thus, the movement or lack of movement at any level of the reservoir was influenced greatly by the intensity of rain for the preceding 15 to 30 days. The other mechanism, discussed by Müller (1964a) and Müller (1968), in which it was inferred that new movements only occurred when the reservoir was raised to new elevations exceeding previous reservoir elevations, would appear to be a result of making interpretations from movement and reservoir data without attaching the importance to rainfall that these calculations would suggest.

Uniform behavior of the slide

The schematic diagram in Figure 38 shows the three-dimensional nature of the blocks selected for the calculation of forces acting in the upstream (easterly) direction. These are designated as Block I, Block I + II, and Block I + II + III. In Appendix D the factor of safety of Block I (Figure 38a) is shown to be 1.07 for $\phi = 12^\circ$, $\beta = 40^\circ$, $\phi_R = 36^\circ$ and high rainfall with reservoir elevation at 710 m. The factor of safety of Block I + II is 1.31 (Figure 38b) and the factor of safety of Block I + II + III is 1.00 (Figure 38c). These three-dimensional analyses, which consider the shear forces between sections caused by the upstream dip of the strata, account for the fact that the entire slide came down at one time. This was not apparent from the two-dimensional analyses which yielded calculated factors of safety for Sections 2, 5, and 10A which were quite different for each section. The three-dimensional calculations also account for the fact that if the strength on the bedding planes was as low as 12° , the slide mass could have been stable, but not greatly above a factor of safety of 1.0, before the reservoir was built. However, this condition required a large resistance along the eastern boundary of the slide. The epicenters of small tremors reported near the eastern boundary of the slide during the history of movement agree with the conclusion that a significant resistance was developed at this boundary.

PART IX: KINEMATIC CHARACTERISTICS OF THE VAIONT SLIDE

Introduction

For a given geometry of failure surface, the distance travelled by a slide mass, such as the Vaiont Slide, is a measure of the loss in strength which occurred during slide movements. Various investigators, such as Ciabatti (1964), Müller (1964a), Jaeger (1968a, 1972), Romero and Molina (1974), Habib (1975), and Chowdhury (1978), have shown that a significant loss of shear strength was necessary to account for the total distance travelled by the slide as determined from the preslide and postslide cross sections. The high velocity acquired by this slide mass was easily the most unforeseen phenomenon associated with the Vaiont Slide.

A satisfactory explanation of the mechanism that resulted in the unexpected high velocity of the sliding mass at Vaiont needs to be developed. Estimates of the final velocity of the sliding mass and the method used by different authors in calculating this velocity are given in Table 12. As indicated in this table, it appears that the total displacement, approximately 400 m horizontally, took place in less than a minute and that the maximum velocity of the sliding mass was 20 to 30 m/sec.

To justify such high estimated velocities some authors suggested that the residual angle of friction along the sliding surface was reduced to values below 5°. Others, Romero and Molina (1974) and Habib (1975), discussed the possibility that the Vaiont Slide generated sufficient heat in a thin layer on the slide plane to cause the water in the shear layer to boil.

Mechanisms Investigated

A number of mechanisms were investigated by the authors to explain the high velocity of the sliding mass at Vaiont. First, calculations were made to estimate the loss of strength and the maximum velocity of the slide that must have existed for the slide mass to come to rest in

its final position. These calculations on the geometry of the Vajont Slide surface were conducted by D. L. Anderson using the method given in Appendix E.

Next, possible mechanisms which could result in the required strength losses were examined. One of these was a mechanism whereby effective stresses are reduced by increases in pore pressure in the failure zone along the basal plane as a result of heat generation. This mechanism is presented in detail by Anderson in Appendix F.

Since the clays on the base plane were already considered to be at residual shear strength, a further reduction of the shear strength parameter on the failure plane was not considered reasonable. Thus, the shear strength losses on the basal plane were considered to be due only to a reduction in "effective" stresses since pore pressures were increased as a result of heat generated along the failure plane. The static stability calculations show that the factor of safety of the slide is quite sensitive to the angle of shearing strength, β , acting between slices because of the significant change in the failure surface orientation between the back and the seat of the slide. Therefore, a reduction in β with displacement was also considered as a possible mechanism for strength loss.

Static calculations have also shown that the shearing forces on the eastern boundaries of the slide were significant. The value of the angle of the shearing resistance ϕ_R used on the boundary was 36° . A reduction of this value of ϕ_R with displacement was investigated as another possible source of strength loss during failure.

Loss of Strength and Maximum Velocity of the Slide

After a review of the pre- and postslide ground profiles reported by Selli et al. (1964), Anderson selected the section shown in Figure 39 for analysis. The water and piezometric levels were assumed to be the same as shown. It was also assumed that the water and piezometric levels remained at the same position in the slide mass as the mass moved down the slope, except in the toe region which is discussed below.

Comparing the pre- and postslide profiles in Figure 39, it appears that the toe of the slide moved laterally about 400 m while the upper portion moved farther. Although this movement is larger than reported by Müller (1964a) on the basis of identification of specific surface features, it is in reasonable agreement with the postslide ground profile and will provide a conservative estimate of the loss of strength and maximum velocity.

Figure 40 illustrates the configuration of the slide at various stages. At each stage the static analysis was used to determine the acceleration and velocity as described in Appendix E.

Bounding toe conditions

From Figure 39 it is apparent that immediately after the beginning of movement the toe of the slide would begin to displace, and perhaps ride over, the water in the reservoir. The pore pressure at the slide surface in the toe region (the toe region is defined to be that part of the slide that has progressed beyond the original toe position) is very difficult to estimate and so two bounding conditions have been assumed. What has been defined as the "dry toe" condition assumes that the pore pressure in the toe region is zero. The "wet toe" condition, which is envisaged as a hydroplaning of the toe, assumes pore pressures in the toe region sufficient to reduce the effective stress and the resulting frictional strength to zero.

Definition of loss of strength

The dynamic calculations were carried out for the two boundary toe conditions and the results are shown in Figure 41. It shows plots of slide velocity and reservoir slide displacement for different values of percentage strength loss along the failure surfaces. The loss in strength is defined as the change in strength from that strength required for an initial static factor of safety of 1.0. If cohesion is neglected, and if ϕ is the friction angle for a factor of safety of 1.0, then a 60 percent loss in strength could be achieved by taking $\tan \phi_d = 0.4 \tan \phi_{cr}$, where ϕ_d is the dynamic angle of shearing resistance and ϕ_{cr} is the static angle of shearing resistance for a factor of

safety of 1.0. The value of β was constant for the examples calculated and plotted in Figure 41.

Results of calculations

It is apparent from the results shown in Figure 41 that the toe friction condition is not an important parameter for this slide. It would then appear for the case analyzed that if the slide moved laterally about 500 m, it must have suffered a loss in strength of about 50 percent. The maximum slide velocity consistent with this loss in strength would be about 20 m/sec.

Mechanisms of Strength Losses

The strength losses along the sliding surface which resulted in the unexpected high maximum velocity of the slide probably originated from three mechanisms: (a) a displacement induced reduction in the friction angle, β , between adjacent vertical surfaces of the sliding mass, especially at the back of the slide at the abrupt change from a steep to a flat failure plane; (b) a reduction from peak to residual shear strength along the eastern side of the slide where the sliding surface did not follow the bedding planes but sheared across the bedding; and (c) a reduction in shear strength along the basal sliding plane parallel to the bedding caused by heat-generated increases in the water pressure along this plane. A more detailed description of the mechanisms involved for each of the three main sources of possible strength loss follows.

Reduction of friction angle

Stability analyses of two-dimensional cross sections of the slide indicated that reductions in the friction angle, β , between adjacent vertical slices of the sliding mass resulted in a substantial increase in the force, F_g , required to maintain the equilibrium of the cross section. These two-dimensional static analyses were used to estimate the acceleration of the sliding mass resulting from a reduction in the friction angle from $\beta = 40^\circ$ to 30° . This estimate was made by determining the increase in the force, F_g , that would have been required to maintain the sliding mass in equilibrium if the angle β dropped from 40° to 30° .

It was then assumed that this increase in the force, F_δ , required to maintain equilibrium was equivalent to a loss in the resisting force acting on the sliding mass. The acceleration, a , of the sliding mass was then estimated by

$$a = \frac{\Delta F_\delta}{m} \quad (7)$$

where: ΔF_δ = increase in equilibrium force F_δ , resulting from a reduction of the β angle from 40° to 30° and
 m = mass of the slide.

The increase (ΔF_δ) in equilibrium of force, F_δ , for the conditions immediately before and after the movement at each one of the two-dimensional cross sections of the slide analyzed in this report are listed below.

Equilibrium Forces, F_δ , for Conditions Immediately Before and After Movement Began

Section	$\beta = 40^\circ$ F_δ , Before Movement, 1b/ft	$\beta = 30^\circ$ F_δ , After Movement 1b/ft	ΔF_δ 1b/ft	Length of Slide Along the River Represented by the Two Dimen- sional Cross Section, ft
2	22.73×10^6	38.46×10^6	15.73×10^6	1036
5	3.58×10^6	13.24×10^6	9.66×10^6	1353
10A	41.32×10^6	51.7×10^6	10.38×10^6	1517

The equilibrium forces, F_δ , required at each cross section immediately before movement corresponds to those calculated for a high rainfall with a reservoir level at 710 m, a friction angle of 12° along the sliding surface, and β equal to 40° . The equilibrium forces, F_δ , after movement correspond to those calculated under similar conditions except for the angle β which has been reduced to 30° .

The total reduction in the resisting force acting on the sliding mass was calculated as

$$\Delta F_{\delta} \text{ total} = \sum \Delta F_{\delta i} l_i \quad (8)$$

where: $\Delta F_{\delta i}$ = the change in the equilibrium force calculated at cross section i and

l_i = the width of the slide represented by cross section i .

Therefore:

$$\begin{aligned} \Delta F_{\delta \text{total}} &= 15.73 \times 10^6 \times (1036) = 16.29 \times 10^9 \text{ lbs} \\ &\quad 9.66 \times 10^6 \times (1353) = 13.07 \times 10^9 \text{ lbs} \\ &\quad 10.38 \times 10^6 \times (1517) = \underline{15.74 \times 10^9 \text{ lbs}} \\ \Delta F_{\delta \text{total}} &\quad = 45.10 \times 10^9 \text{ lbs} \end{aligned} \quad (9)$$

The estimated volume of the sliding mass is approximately equal to 250 million cubic yards. Therefore the weight, W , of the sliding mass can be estimated as

$$W = 250 \times 10^6 \text{ yd}^3 \times \frac{27 \text{ ft}^3}{\text{yd}^3} \times \frac{140 \text{ lbs}}{\text{ft}^3} = .95 \times 10^{12} \text{ lbs} \quad (10)$$

The initial acceleration of the sliding mass resulting from the reduction in the β angle is then equal to

$$a = \frac{45 \times 10^9}{.95 \times 10^{12}} \text{ g} = .048 \text{ g} = .47 \text{ m/sec}^2 \quad (11)$$

Calculations of the velocity and acceleration of the sliding mass by Ciabatti (1964), which were based on a simplified schematic of the sliding phenomena, indicated that an initial mass acceleration of 0.1 g would have resulted in a maximum velocity of the slide of approximately 17 m/sec. Thus, it appears that a reduction of β of about 10° would only account for maximum velocities on the order of 7 m/sec which is considerably below those consistent with a movement of 400 to 500 m.

Reduction of shear strength at the eastern slide boundary

As previously indicated, shear strength losses due to displacement-induced reduction of the friction angle from a value of about 36° to say a residual value of about 25° at the boundary of the eastern wall of the slide could also be a possible mechanism for a significant loss of strength. This loss of strength on the eastern

boundary could also have been caused by an eastward movement of the failure surface until the eastern boundary coincided with a pre-existing fault. In that case, the shear strength on the boundary could have been reduced from 36° to about 25° . This loss of strength can be evaluated by computing the change in the frictional force acting along the eastern boundary, F , defined as

$$F = \overline{PN}_2 \tan \phi_R \quad (12)$$

where: \overline{PN}_2 = effective force acting normal to the eastern boundary, resulting from the upstream dipping of the sliding surface and

ϕ_R = friction angle along the eastern boundary.

The change in this frictional force, before and after the slide, was computed as

$$\Delta F = \overline{PN}_2 (\tan \phi_{R1} - \tan \phi_{R2}) \quad (13)$$

where: ϕ_{R1} = friction angle before the slide, assumed to be equal to 36° and

ϕ_{R2} = residual frictional angle, once slide started, estimated to be close to 25° .

The effective force normal to the eastern boundary, \overline{PN}_2 , calculated as the horizontal component of the weight of the sliding mass normal to this boundary minus the horizontal hydraulic force acting against this face was estimated to be approximately equal to 120×10^9 lbs.

Therefore,

$$\Delta F = 120 \times 10^9 \text{ lbs } (\tan 36^\circ - \tan 25^\circ) \quad (14)$$

$$\Delta F = 120 \times 10^9 \text{ lbs } (0.741 - 0.466) = 33 \times 10^9 \text{ lbs} \quad (15)$$

The initial acceleration, a , on the sliding mass resulting from this loss in shear strength would be about

$$a = \frac{33 \times 10^9 \text{ lb}}{.95 \times 10^{12} \text{ lb}} \times g = 0.035 \text{ g} \quad (16)$$

The initial acceleration produced by the combined effect of a displacement-induced reduction in the friction angles β and ϕ_R between adjacent vertical surfaces within the sliding mass and along the eastern boundary, respectively, can then be calculated as

$$a_i = \frac{\Delta F_\delta + \Delta F}{m} \quad (17)$$

where

$$a_i = \frac{45.1 \times 10^9 + 33 \times 10^9 \text{ lbs}}{.95 \times 10^{12} \text{ lbs}} = 0.08 \text{ g} \quad (18)$$

The magnitude of the initial acceleration is about 20 percent smaller than the initial mass acceleration of 0.1 g calculated by Ciabatti (1964) as the required initial acceleration for the mass to achieve a maximum downward velocity of approximately 17 m/sec. Thus, the combined effect of reductions in β and ϕ would result in maximum velocity on the order of 12 m/sec. This is still substantially lower than the 20 m/sec calculated by Anderson as necessary for the slide mass to move the distance observed. It follows then that, although the factors above are significant, another mechanism must be involved.

Heat-generated pore pressures

A third source of strength loss due to slide displacements is a heat-generated pore pressure increase as a result of an increase in temperature in the shear zone. The idea that a heat generated mechanism might account for the loss of strength of large rock or earth slides has been discussed by Romero and Molina (1974), Habib (1975) and Gougel (1978). The mechanism considered is one where enough heat is present to boil some of the pore water to create steam, which then, of course, would greatly reduce the shear strength. In fact, it can easily be shown that in large slides there is certainly enough energy available, once the slide gets moving, to boil a considerable amount of water and provide a mechanism for large losses of strength. The theory has been advanced to explain how slides can attain high velocities and achieve long runouts.

The analysis presented in Appendix F by Anderson considers a heat generated mechanism. He considers the generation of pore pressures due to increased temperatures which cause expansion of the pore water even when it is below the boiling point. For more details see Anderson (1980).

The analysis considered a rigid block of slide material resting on a thin inclined shear zone. A time step analysis is performed where the equations of motion of the slide mass are solved for a small time increment and the resulting relative motion between the slide mass and foundation is used to determine the heat generated in the shear zone. The heat generated increases the temperature which in turn increases the pore pressure. The reduction of pore pressure due to pore water flow is considered as is the reduction of temperature due to conduction and convection in the pore water.

Analytical model

The sliding mass is assumed to move as a rigid body with all the deformation taking place in a small or narrow shear zone as shown in Figure 42a. For purposes of calculation, the foundation, shear zone, and the sliding mass are divided up into a number of thinner layers as shown in Figure 42b.

The displacement of the slide is denoted as v . For the shear zone the displacements are given by v_n which represents the displacement at the top of the n^{th} layer as shown in Figure 42c. T_n and p_n represent the temperature and pressure, respectively, at the center of the n^{th} layer.

At the beginning of a time step, Δt , the known quantities are T_n , p_n , v , \dot{v} (the velocity of the slide) and τ_{\min} (the minimum shear strength which will occur in one of the layers of the shear zone). The acceleration of the slide mass \ddot{v} , which depends on the inclination of the slide and τ_{\min} , can be calculated using an explicit integration scheme, which assumes \ddot{v} is constant and allows Δv and $\Delta \ddot{v}$ to be calculated for the time step.

The pressure change from the fluid flow, Δp_{pn} , must be calculated using an implicit time integration scheme if the time step, Δt , is to be

suitably large. For this reason it is calculated separately, and the resulting pressures are used to calculate the pore water flow (seepage) during the time increment.

The heat transfer, both by convection in the pore water and conduction, is used along with the heat generated in the shear zone, to determine the change in temperature, ΔT_n . The change in pressure caused by the increased temperature, Δp_{Tn} , is then calculated and the total change in pressure, $\Delta p_n = \Delta p_{pn} + \Delta p_{Tn}$, is determined. From this τ_{\min} can be found. Thus, at the end of the time step there are new values of p_n , T_n , v , \ddot{v} , and τ_{\min} .

The implicit flow equations, the heat generation mechanism, and the pressure temperature relations are given in Appendix F.

Input and results of heat generation analysis

An initial factor of safety of 0.99 was used in this idealized two-dimensional analysis. Particulars of the idealized slide mass are:

Depth, 250 m (on the basis of a total mass per unit volume of 2.7 gm/cm³ for the slide material)

Average slope, 17°

Initial piezometric head, 154 m

Initial temperature, 12° C

The foundation and sliding mass were each divided into eight layers of 5, 10, 15, 20, 25, 25, 50 and 100 cm thickness. Beyond 100 cm it was assumed there would be no change. The shear zone was divided into five equal layers of 4 cm thickness.

The permeability of the shear zone as well as the adjacent foundation materials was assumed to be equal to 10⁻⁶ cm/min. The elastic modulus, K_n , for the shear zone materials was estimated to be 10,000 kg/cm². Other material properties assumed are given in Appendix F.

Results from this analysis, shown in Table 13, and Figure 43, indicate that the slide velocity increases very slowly during the initial stages of the movement, but picks up rapidly after the slide has displaced about 12 m.

The analysis also indicates that the pore water pressure increases available from the heat generation mechanism can account for very large losses of strength along the sliding plane. Table 13 shows that a 66 percent loss in strength could occur after a movement of 19 m.

It can be concluded that the combined action of three phenomena (displacement-induced reduction of the friction angle along adjacent vertical surfaces in the slide, as well as along the eastern wall boundary, plus the shear strength reduction due to heat-generated pore water pressure along the sliding plane) can explain the unexpected high velocities of the sliding mass at Vajont. The changes in β and ϕ need only serve as a trigger for movement to begin which can produce heat-generated pore pressures on the base plane parallel to the bedding. These calculations also indicate that the lower the permeability, the lower the rate of movement that is required to produce heat-generated pore pressure. Thus, the results of these calculations also point out another way in which the clays on the failure plane at Vajont were important.

PART X: CONCLUSIONS

General Geology

The 1963 Vajont Slide was a reactivation of an old slide. The age of the old slide is unknown, but it probably occurred in postglacial times but before the period of recorded history of the Vajont Valley. The evidence for an old slide is strong and diverse. It includes many aspects of the surface morphology, the talus infilling of a reoccurring crack at the headscarp which formed breccias of differing characteristics, the basal rupture plane, and remnants of a previous slide mass or masses on the north side of the valley. The elements of the surface morphology, which are indicative of an old slide, include deranged drainage, enclosed depressions, bulging slopes, and other related alignments and patterns evident on the airphotos.

The slide mass moved upon one or more clay layers which were continuous over large areas of the surface of sliding. Multiple clay interbeds occur near the base of the Lower Cretaceous stratigraphic units and were observed at many locations within the slide. Clays occur on the slide surface, below the slide surface, and also form the matrix of the lower portions of the slide mass. Thick clay fragments and layers are abundant in the debris. Clay interbeds were found outside the slide area in stratigraphic positions corresponding to the surface of sliding of the 1963 slide. The authors find the field evidence for the presence of clay along the surface of sliding compelling because of the number of locations where clays were noted on the failure surface and because of the details of the geology at these locations. It is apparent that clay, which is predominantly calcium montmorillonite or a closely related clay mineral, occurs on the failure surface in many more locations than those noted in this study.

The lower portion of the failure plane, which is commonly seen as a near horizontal "seat" in cross sections of the Vajont Slide, actually dips to the east (upstream) about 9° to 22°. This upstream dip is very

significant in the stability analyses and is well documented by the geologic mapping of Giudici and Semenza (1960) before the slide and by drillholes made after the slide.

The failure surfaces of the 1963 slide and the prehistoric slides appear to correspond closely to one or more faults of possible tectonic origin formed much earlier in geologic times. A well-cemented breccia with a grooved and striated surface described here as a "tectonic breccia" is believed to have been formed by this faulting. This breccia can be observed at many locations throughout the exposed portions of the failure surface. The eastern boundary of the slide appears to have been formed by one or more lateral faults associated with or postdating the décollément-fault suggested above. Such a lateral fault is shown on the geologic maps of Rossi and Semenza (1964, 1965a). A "stepping up" to the east of the basal "fault" surface and the surface of sliding can be observed in the field. The direction of the grooving in the basal "fault" corresponds with the inferred direction of movement of a gravity tectonic structure mapped by Semenza on the map given in Leonardi et al (1967).

The great majority of the slide both east and west of the central Massalezza Ditch moved as a unit. The evidence for this is the surface morphology of the slide and the geologic features of the area mapped before and after the slide by Rossi and Semenza. A secondary slide movement formed an area called the Eastern Lobe. This movement was presumably triggered by the loss of toe support caused by the movement of the main slide. The resulting unstable mass overran a large area on the uphill side of the eastern part of the slide. The authors have concluded that an analysis of the main slide is not appreciably affected by a consideration of this secondary slide movement. As the main slide came to rest, differential movements developed within it as a result of differences in the geometry of the valley in the toe areas and differences in the momentum of various sections of the slide mass.

Hydrogeology

A significant area of pronounced karstic and/or combined karstic and glaciated terrain exists above the slide near the top of Mt. Toc. Evidence of minor and incipient karstic terrain is found just above the slide and on its western boundary. The bedding in these areas also dips towards the slide at angles of 13° to 45° or more. Solution features were observed at three areas immediately below the main surface of sliding. Undoubtedly more solution features existed. This evidence strongly suggests that the conditions were present to enable the transmission of high water pressures developed due to infiltration from precipitation or snowmelt on the mountain above. These high water pressures could therefore develop along the surface of sliding.

High groundwater pressures with respect to the reservoir levels were measured in piezometer P-2 in the vicinity of (probably just above) the failure surface. These measurements were taken prior to the slide and apparently before sufficient slide movement occurred to damage the piezometer. This water pressure fluctuated both with changes in the reservoir level and with rainfall. Initially the piezometer level in P-2 was 90 m above reservoir level. This represents a water pressure difference which was probably lower than the real difference because the piezometer tip was not well sealed. Also, this 90 m difference was observed in a period of low to moderate rainfall and could have been higher in periods of higher rainfall.

The lower permeability of the clay layers and the higher permeability of the intervening limestones and cherts must have combined to significantly increase the hydraulic conductivity along the bedding relative to that across the bedding. This effect results in a near classic case of an inclined multiple-layer artesian aquifer system at and below the surface of sliding. Such a system would be expected to produce the high piezometric levels observed at P-2.

Shear Strength of Clays

The values of the drained residual angle of shearing resistance of the clays measured in the laboratory varied from 5° to 16° with most values of the clay-rich layers ranging from 6° to 10°. These values are consistent with the Atterberg limits of the clay sampled from a large number of areas throughout the slide and from the same formation located outside the slide area. To account for irregularities along the clay layers and a limited number of rock-to-rock surfaces of contact, an average value of the residual angle of shearing resistance of about 12° would appear to be reasonable and consistent with the laboratory test results.

Stability Analyses

Three-dimensional analyses were required due to the magnitude of the upstream inclination of the clay layers which form the base of the slide. These analyses show that a significant proportion, approximately 40 percent, of the total shearing resistance acting on the slide mass was supplied by near-vertical faces which formed the eastern boundary of the slide. This particular slide is especially sensitive to this three-dimensional effect because the clay layers along the base have a very low strength and the eastern boundary has a higher strength.

The history of slide movements, the record of reservoir levels, the shape of the failure surfaces, and the assumed distribution of pore water pressures and water levels used in this study are consistent with the following shear strength values:

residual angle of shear resistance (ϕ_r) on basal planes $\sim 12^\circ$,

angle of internal shearing resistance (β) acting between slices on the slide $\sim 40^\circ$, and

angle of frictional shearing resistance acting along the eastern surfaces of the slide $\phi \sim 36^\circ$.

Only small variations in the above parameters appear to be possible for the results of the analyses to yield factors of safety

consistent with the four periods of movement and the intervening periods of relative stability.

The 1963 slide occurred because of the combined effects of a rising reservoir and increases in piezometric levels as a result of rainfall. The reduction in the factor of safety caused by reservoir filling alone is calculated to be approximately 12 percent. The reduction in the factor of safety due only to an assumed increase in pore water pressures chosen to account for a variation in rainfall and snowmelt is calculated to be a minimum of about 10 percent.

Precipitation and Reservoir Levels

Plots of cumulative precipitation vs reservoir levels just prior to periods of movement have resulted in a well defined "failure" envelope. This envelope gives those combinations of reservoir level and precipitation which yield a pore pressure distribution that would cause significant slide movement. The results of this correlation explain why the slide was observed to be stable at a given reservoir level and yet at a later date was unstable at that same reservoir level. The results of this correlation indicate that "pre-wetting" of the slide debris was not a significant factor in the slide behavior.

An extrapolation of the failure envelope enables an estimate to be made of: (a) the rainfall which would cause failure without a reservoir, and (b) the reservoir level which would cause failure with little or no rainfall on the Mt. Toc slopes.

The cumulative 30-day rainfall which would cause failure without a reservoir is about 700 mm. Since a monthly rainfall of almost 500 mm was recorded in the four-year period of record, it seems likely that the 700 mm rainfall has been exceeded during the postglacial life of the slope. Therefore, significant movements must have occurred without a reservoir. The reservoir level that would cause failure without rainfall is about 710 to 720 m. This may be compared to the full supply level of the Vajont Reservoir which was to have been 722.5 m.

Therefore, had the reservoir been filled to its design level, the slide might have moved during a period without any significant preceding rainfall.

The results of the stability analyses are consistent with the conclusions that can be drawn from the precipitation vs reservoir level correlations and the available movement record of the slide.

Slide Velocity Studies

Calculations by Anderson in Appendix E suggest that there was about a 50 percent decrease in shear strength required for the slide to reach its present position. These calculations indicate that the maximum velocity reached by the slide mass was about 20 to 25 m/sec.

Increases in pore pressure due to increases in temperature on the failure planes, such as described in Appendix F, are required to explain the losses in strength necessary to achieve the velocities calculated. Increased fluid pressures due to friction-generated thermal effects are slower to dissipate in low permeability materials. Hence, slides resting on clays, such as those present at Vaiont, are more susceptible to this strength loss mechanism than those resting on more permeable and thinner strata.

General Conclusions and Remarks

Casual studies of important precedent case histories, such as the Vaiont Slide, should not be accepted by the geological and geotechnical professions. Back-analyses and speculations on slide causes should not be made without a reasonably valid geologic, hydrogeologic, and historic reconstruction of the significant events into a model. Because of the great diversity in geologic and hydrogeologic environments among projects, it is difficult and perhaps misleading to attempt to set rules for analyses and field exploration programs which would cover all landslide studies.

Previous studies of the Vaiont Slide vary from useful factual accounts to misleading fiction. However, among the studies that consistently stood the test of time are those by Giudici and Semenza

(1960), Semeza (1965b) and Rossi and Semenza (1965a). These studies have been reliable because these geologists spent considerable time in the field at Vajont, both before and after the slide. The most misleading accounts in the literature have generally been given by those who have not visited the site or who are not familiar with the geology.

It is apparent that any damsite investigation should include a detailed study of the proposed reservoir slopes. If old slides or areas susceptible to sliding are identified, a detailed evaluation of their relative stability under reservoir conditions should be required. The lesson afforded by Vajont need not be relearned by another generation. However, it should not be a foregone conclusion that reservoir slopes will always be less stable with increased reservoir levels.

The analyses and evidence compiled strongly suggest that the slide was an "Act of God" (Müller, 1963) only in-so-far as the frequency and duration of the precipitation was concerned. The history of sliding and the final collapse of the slope can be examined in quantitative terms. Conventional methods of analyses by limit-equilibrium techniques appear to be reliable if the input data are consistent with the geologic and hydrologic controls.

The greatest gaps in the data accumulated on the Vajont Slide involve: (a) the lack of substantive water pressure data, and (b) the lack of reliable movement records along the failure plane. Fluid pressure measurements taken from piezometers installed at multiple levels within and below the slide would have provided the essential data for correlation with slide movements and reservoir levels. Reliable measurements of the depth of the failure plane and the magnitude of displacements along it would have helped to confirm the depth and size of the slide mass and would have brought more reliability to the correlation studies.

In hindsight, it appears significant that an early (1960-61) diagnosis of the kinematics of the lower part of the slide as similar to that of some glaciers (having zero horizontal velocity at the base increasing to a maximum at the glacier's surface) led those involved to

divert their attention away from field exploration required to locate the failure plane, as well as away from instrumentation and analytical efforts. Subsurface borehole deformation measurements would have shown the error in this hypothesis.

The accumulated evidence also suggests that the slide could have been stabilized by drainage.

PART XI: LITERATURE CITED

- Ajemian, R. 1963. There the dam stood, proud and beautiful. Life Magazine. Vol. 55, No. 12, pp. 30-41.
- Anderson, D. L. 1980. An Earthquake Induced Heat Mechanism to Explain the Loss of Strength of Large Rock or Earth Slides. International Conference on Engineering for Protection from Natural Disasters, Bangkok, January.
- Boyer, R. A. 1913. Étude géologique des environs de Longarone (Alpes Vénitiennes). Bull. Soc. Géol. France. S. 4, Vol. 13, pp. 451-485, plus geologic map (1:50,000).
- Bozzi, C., G. Merla, L. Trevisan, R. Sellì and M. Viparelli. 1964. Comissione di inchiesta sulla sciagura del Vajont. Relazione al Ministro Dei Lavori Pubblici. (Bozzi Commission Report.) 108 pp.
- Broili, L. 1967. New knowledge on the geomorphology of the Vajont Slide slip surfaces. Rock Mechanics & Engr. Geol., Jour. Int. Soc. Rock Mechanics. Vol. V, No. 1, pp. 38-88.
- Carloni, G. C., and R. Mazzanti. 1964a. Aspetti geomorfologici della frana del Vajont (Geomorphological aspects of the Vajont Slide). Révista Geografica Italiana, Firenze. Vol. 71, No. 3, Sept., pp. 201-231 (with summary in English).
- Carloni, G. C., and G. Mazzanti. 1964b. "Rilevamento geologico della frana del Vajont," pp. 105-138 including color maps; scale 1:5,000 and 1:25,000 in La Frana del Vajont. Annali del Museo Geologico di Bologna. Ser. 2, Vol. 32, Fasc. 1.
- Chowdhury, R. 1978. Analysis of the Vajont Slide - new approach. Rock Mechanics, Jour. Int. Soc. Rock Mechanics. Vol 11, pp. 29-38.
- Ciabatti, M. 1964. "La Dinamica Della Frana Del Vajont" (The Dynamics of the Vajont Slide), pp. 139-154 plus illus. in La Frana del Vajont. Annali del Museo Geologico di Bologna. Ser. 2, Vol. 32.
- Dal Piaz, G. 1928. Relazione di massima su due sezioni della valle del Vajont prese in considerazione per progetti di barramento idraulico. Unpublished report for S.A.D.E. 4 pp.
- Frattini, M., F. Arredi, A. Boni, C. Fasso, and F. Scarsella. 1964. Relazione sulle cause che hanno determinato la frana nel serbatoio del Vajont (9 Ottobre 1963). Frattini Commission Report. Prepared for E.N.E.L. 92 pp.

- Gervasoni, A. 1969. Il Vajont e le responsabilità dei manager. Bramante Editrice, Via Carducci 15, Milano, 166 pp.
- Giudici, F., and E. Semenza. 1960. Studio geologico del serbatoio del Vajont. Unpublished report. Part A, text, 21 pp; Part B, photographs, 68 with discussions, 42 pp; and 2 maps and sections prepared in 1959 (1:5,000).
- Goguel, J. 1978. "Scale-Dependent Rockslide Mechanisms, with emphasis on the role of pore fluid vaporization," Ch. 20, pp. 693-705 in Developments in Geotechnical Engineering, Vol. 14a, Rockslides and Avalanches, 1, Natural Phenomena. Barry Voight, ed., Elsevier.
- Gruner, E. C. 1969. Vigilance over reservoirs. Water and Water Engineering. Sept., pp. 369-373.
- Habib, P. 1975. Production of gaseous pore pressure during rockslides. Rock Mechanics, Jour. Int. Soc. Rock Mechanics. Vol. 7, pp. 193-197.
- Jaeger, C. 1965a. The Vajont rockslide, Part I. Water Power. March, pp. 110-111.
- Jaeger, C. 1965b. The Vajont rockslide, Part 2. Water Power. April, pp. 142-144.
- Jaeger, C. 1968a. The dynamics of the slide, discussion of paper by L. Muller on new considerations on the Vajont Slide. Rock Mechanics and Engr. Geol., Jour. Int. Soc. Rock Mechanics. Vol. 6, No. 4, pp. 243-247.
- Jaeger, C. 1968b. Discontinuous creep of masses. Water Power. May, pp. 197-198.
- Jaeger, C. 1972. "The Vajont Slide," Ch. 14, pp. 340-361 in Rock Mechanics and Engineering. University Press, Cambridge. 417 pp.
- Kenney, T. C. 1967a. Stability of the Vajont valley slope, discussion of paper by L. Müller (1964) on the rock slide in the Vajont valley. Rock Mechanics and Engr. Geol., Jour. Int. Soc. Rock Mechanics. Vol. 5, No. 5, pp. 10-16.
- Kenney, T. C. 1967b. The influence of mineral composition on the residual strength of natural soils. Proc. Geotechnical Conference, Oslo, 1967. Norwegian Geotechnical Institute. Vol. 1, pp. 123-129.

- Khan, S. B. 1971. Effect of Changes in Reservoir Level on the Stability of Natural Slopes. M.Sc. Thesis. Dept. Civil Engr., Univ. Alberta, Edmonton. 98 pp. plus appendices.
- Kiersch, G. A. 1964. Vajont reservoir disaster. Civil Engineering. Amer. Soc. Civil Engrs. March, pp. 32-39.
- Kiersch, G. A. 1965a. Vajont reservoir disaster. Geotimes. Geol. Soc. Amer. May-June, 1965, pp. 9-12.
- Kiersch, G. A. 1965b. "The Vajont reservoir disaster," pp. 136-145 in Landslides and Subsidence. Geologic Hazards Conference, Los Angeles, Calif., May 26-27, 1965. The Resources Agency, State of California.
- Leonardi, P. et al. 1967. Le Dolomiti, Geologia dei monti tra Isarco e Piave. Vol. 1, 552 pp; Vol. 2, 1019 pp. plus colored maps and geologic sections, regional geologic map (scale 1:100,000). Manfrini, Rovereto.
- Leonardi, P., and E. Semenza. 1967. "Zona di Longarone," Ch. 72, pp. 925-936 in Le Dolomiti, P. Leonardi et al., Vol. 2, 1019 pp. Manfrini, Rovereto.
- Lo, K. Y., C. F. Lee, and P. Gelinas. 1972. "Alternative Interpretation of the Vajont Slide," pp. 595-623 in Stability of Rock Slopes. E. J. Cording, ed. Proc. 13th Symposium on Rock Mechanics, Univ. Illinois, Urbana, Aug. 30-Sept. 1, 1971. ASCE, New York.
- Loriga, C. B., and M. G. Mantovani. 1965. Le biofacies del Cretacico della Valle del Vajont (Belluno). Riv. It. Paleont., Milano. Vol. 71, No. 4, pp. 1225-1248, tav. 110-114.
- Loriga, C. B., and M. G. Mantovani. 1970. Microbiostratigrafia della serie affiorante nella massa scivolata dal M. Toc (Vajont) il 9 ottobre 1963 e alcune osservazioni su Foraminiferi, Radiolari, Calcisfere e Nannoconus. Museo Tridentino di Scienze Naturali, Trento. Sez. A., Vol. 47, No. 2, pp. 202-285.
- Martinis, B. 1964. Stratigrafia della Valle del T. Vajont. Unpublished AGIP report. 30 pp.
- Mencel, V. 1966. Mechanics of landslides with non-circular slip surfaces with special reference to the Vajont Slide. Géotechnique. Vol. 16, No. 4, pp. 329-337.

- Morgenstern, N. R., and V. R. Price. 1965. The analysis of the stability of general slip surfaces. *Géotechnique*. Vol. 15, No. 1, pp. 79-93.
- Müller, L. 1961. Talsperre Vajont 15, Baugeologischer Bericht: "Die Felsgleitung im Bereich Toc". Unpublished report to S.A.D.E.
- Müller, L. 1963. Discussion of Differences in the Characteristic Features of Rocks and Mountain Masses. Proc. 5th Int. Conf. of Int. Bur. Rock Mechanics, Leipzig, Germany.
- Müller, L. 1964a. The rock slide in the Vajont Valley. *Rock Mechanics and Engr. Geol.*, Jour. Int. Soc. Rock Mechanics. Vol. 2, pp. 148-212.
- Müller, L. 1964b. Relazione Geomeccanica sulla Frana di Roccia del 9 Ottobre 1963. Italian translation by E.N.E.L.-S.A.D.E. of Müller's Report of 2/9/64, 89 p.
- Müller, L. 1967. Discussion on question 32. Proc. 9th Int. Congress Large Dams, Istanbul, Turkey, Sept. 4-8, 1967. Vol. VI, pp. 124-134.
- Müller, L. 1968. New considerations on the Vajont Slide. *Rock Mechanics and Engr. Geol.*, Jour. Int. Soc. Rock Mechanics. Vol. 6, No. 1, pp. 1-91.
- Nonveiller, E. 1967a. Discussion of paper by V. Mencl on mechanics of landslides with noncircular surfaces with special reference to the Vajont slide. *Geotechnique*. Vol. 17, No. 2, pp. 170-171.
- Nonveiller, E. 1967b. Shear strength of bedded and jointed rock as determined from the Zalesina and Vajont slides. Proc. Geotechnical Conference, Oslo, 1967. Vol. 1, pp. 289-294.
- Nonveiller, E. 1967c. Zur Frage der Felsrutschung im Vajont-Tal. *Rock Mechanics and Engr. Geol.*, Jour. Int. Soc. Rock Mechanics. Vol. 5, No. 1, pp. 2-9.
- Nonveiller, E. 1968. Discussion (in German) of paper by L. Müller on new considerations on the Vajont Slide. *Rock Mechanics and Engr. Geol.*, Jour. Int. Soc. Rock Mechanics. Vol. 6, No. 4, pp. 237-242.
- Olson, R. E. 1974. Shearing strengths of kaolinite, illite and montmorillonite. *Jour. Geotech. Engr. Div.*, Proc. ASCE. Vol. 100, No. GT11, pp. 1215-1229.

- Patton, F. D., and D. U. Deere. 1970. "Significant Geological Factors in Rock Slope Stability," pp. 143-151 in Planning Open Pit Mines, P. W. J. Van Reusburg, ed. Proc. Symposium on the Theoretical Background to the Planning of Open Pit Mines with Special Reference to Slope Stability. Johannesburg, 1970. 388 pp.
- Patton, F. D., and A. J. Hendron, Jr. 1974. General report on "mass movements." Proc. 2nd Int. Congress Int. Assoc. Engr. Geol. (AIEG), Sao Paulo. Vol. 2, pp. 1-57.
- Romero, S. U., and R. Molina. 1974. Kinematic aspects of the Vajont Slide. Proc. 3rd Congress Int. Soc. Rock Mechanics, Denver, Colo. Sept. 1974, Vol. II, Part B, pp. 865-870.
- Rossi, D., and E. Semenza. 1964. Relazione definitiva sulle condizioni di stabilita' della Costa Delle Ortiche (Vajont). Unpublished. 18 pp., 11 photos, geologic map and sections (1:5000), and stratigraphic columns.
- Rossi, D. and E. Semenza. 1965a. "Carte geologiche del versante settentrionale del Monte Toc e zone limitrofe, prima e dopo il fenomeno di scivolamento del 9 Ottobre 1963. Istituto di Geologia dell'Universita di Ferrara. Scale 1:5000; 2 maps, colored.
- Rossi, D., and E. Semenza. 1965b. Note illustrative delle carte geologiche e delle serie di profili del versante settentrionale del M. Toc, precedenti e posteriori allo scivolamento del 9 Ottobre 1963. Unpublished. 11 p.
- Rossi, D., and E. Semenza. 1965c. Colonna stratigrafica e caratteristiche chimico-mecaniche di una parte della serie corrispondente alla massa scivolata dal M. Toc il 9 Ottobre 1963 (in collaborazione with R. Dal Cin, M. Novi and A. Venturini). Unpublished. Scale 1:50.
- Rossi, D., and E. Semenza. 1967. "La bassa Valle del Vajont e lo scivolamento gravitativo del 9 Ottobre 1963," Ch. 78, pp. 937-944 in Le Dolomiti. P. Leonardi et al., Vol. 2, 1019 pp. Manfrini, Rovereto.
- Schnitter, G. 1973. The Disaster of the Vajont River. Translation No. 73-6. U.S. Army Corps of Engineers, Waterways Exp. Sta. 13 pp. plus illustrations (from Das Unglück am Vajont, Schweizerische Bauzeitung, Vol. 90, No. 39, pp. 948-954, 1972.)
- Selli, R., L. Trevisan, G. C. Carloni, R. Mazzanti and M. Ciabatti. 1964. "La Frana del Vajont," pp. 1-63 in La Frana Del Vajont. Annali del Museo Geologico di Bologna. Ser. 2, Vol. 32.

- Selli, R., and L. Trevisan. 1964. "Caratteri e interpretazione della Frana del Vajont," pp. 8-104 in La Frana Del Vajont. Annali del Museo Geologico di Bologna. Ser. 2, Vol. 32, Fas. 1.
- Semenza, E. 1960. Nuovi studi tettonici sulla Valle del Vajont e zone limitrofe. Rend. Acc. Naz. Lincei, Roma. S. 8. Cl. Sc. Fis. Mat. Nat. Vol. 28, Fas. 2, pp. 223-229, 2 tavv.
- Semenza, E. 1964. Studio geologico della massa scivolata dal M. Toc il 9 Ottobre 1963 e delle zone limitrofe. Unpublished.
- Semenza, E. 1965a. La tettonica del fianco sinistro della Valle del Piave fra Lozzo e Pieve di Cadore. Memorie Geopaleontologiche Dell' Università di Ferrara. Vol. 1, Fas. 11, No. 4, pp. 113-145 plus illus.
- Semenza, E. 1965b. Sintesi degli studi geologici sulla frana del Vajont dal 1959 al 1964. Memorie del Museo Tridentino di Scienze Naturali. A. XXIX-XXX 1966-67, Trento. Vol. 16, No. 1, pp. 1-52.
- Semenza, E. 1967. "Zona del Duranno," Ch. 74, pp. 945-953 in Le Dolomiti. P. Leonardi et al. Vol. 2, 1019 pp. Manfrini, Roverto.
- Skempton, A. W. 1966. Bedding-plane slip, residual strength and the Vajont landslide. Letter to the editor. Géotechnique. Vol. 16, No. 1, pp. 82-84.
- Spencer, E. 1967. A method of analysis of the stability of embankments assuming parallel inter-slice forces. Géotechnique. Vol. 17, March, pp. 11-26.
- Trollope, D. H. 1977. "An Approximate Design Method for Slopes in Strain-softening Materials," pp. 45-51 in Design Methods in Rock Mechanics. C. Fairhurst and S. L. Couch, ed. Proc. 16th Symposium on Rock Mechanics, Univ. Minnesota, Minneapolis, Sept. 22-24, 1975. pp. 45-51.
- Weber, E. 1964. Die Katastrophe von Vajont in Oberitalien, Wasser-und Energiewirtschaft. Vol. 56, No. 2/3, pp. 61-69.
- Weiss, V. E. H. 1964. Vajont - Geologische Betrachtungen zur Felsgleitung in den Stausee. Steirische Beiträge zur Hydrogeologie, 1963/64, No. 15/16, pp. 11-36.

Table 1
Summary of Observations in Clay Layers and Related Features, Valont Slide

Location No.	Clay Layer Noted in Slide Debris No. and Thickness, cm	Clay Layer on 1963 Failure Surface No. and Thickness, cm	Other clay layers, + = above 1963 surface - = below 1963 surface (no thickness noted)	Tectonic Breccia or Fault Surface Present	Old Talus or Cemented Talus Present (from Scarp)	Solution Features Present
9-1	1, -	-	-	-	-	-
9-2	-	-	-	-	-	-
9-3	-	-	-	-	-	-
9-3A	-	-	possibly -> 0.2-0.5	-	-	-
9-3B	-	-	-	-	-	-
9-4	-	-	-	-	-	-
9-5	-	-	-	-	-	-
10-1	1, -	-	-	-	-	-
10-2	-	-	-	-	-	-
10-2A	1, 1-2	1, 0.5-2	-	-	-	-
10-3	-	-	1, -	-	-	-
10-3A	6 layers, 1-10	1, 1-10	-	-	-	-
10-4	Several	1, 2-4+	-2 cm, 1-2	-	-	-
10-4A	Several	1, 1-2	-	-	-	-
10-4B	Several	1, 1-2	-	-	-	-
10-5	1, -	1, 4-6	-	-	-	-
10-6	-	1, 1-3	± 5 layers, 0.4-1.5	-	-	-
10-6A	-	1, 1-3	+ 5 layers, + 5 layers	-	-	-
11-1	>5 layers in 1.5m debris ~12 m clay rich debris	-	-	-	-	-
11-2	-	-	-	-	-	-
11-2B	-	1, 0.5-1.0	-	-	-	-
11-3	Debris has clay matrix 1, -1 cm w/slick	1, 1-2 w/slick	-	-	-	-
11-4	-	1, 1-6	-	-	-	-
11-4A	-	1, -1.5	-	-	-	-
11-5	1 - 1 m	-	-	-	-	-
11-6	1, -	-	-	-	-	-
11-7	-	1, 2-6	-2, 4-6	-	-	-
11-7A	1, 0.3-0.5 (just above f.p.)	-	-	-	-	-

* Denotes that feature designated in column is present.

(continued)

Table 1 (continued)

Location No.	Clay Layer Noted in Slide Debris No. and Thickness, cm	Clay Layer on 1963 Failure Surface No. and Thickness, cm	Other clay layers, + above 1963 surface - below 1963 surface No. and Thickness, cm	Tectonic Breccia or Fault Surface Present	Old Talus or Cemented Talus Present (from Scarp)	Solution Features Present
11-7A	-	-	1, 0.5-2	-	-	-
11-8A	-	1, -	1, 2-10	-	-	-
11-9	1, -	-	-	-	-	-
11-10	4 layers (very clay-rich)	-	1, 1-2	-	-	-
11-10A	2, 1 and 15	failure plane at base of thickest layer	-	-	-	-
12-1	-	-	-	-1, 0.1-0.5	*	*
12-1A	-	-	-	-	*	*
12-1B	-	-	-	-	*	*
12-2	2. (20 cm breccia with clay matrix)	-	1, 2	-	*0.5-3 m thick	*
12-2A	-	-	-	-	*	*
12-3	1. 50 cm clay rich matrix	1, 5-20	-	-	*	*
12-3A	2, -	-	-	-	*	*
12-4	-	-	1, 0.1-1.5	-	*	*
12-4A	-	-	1, 0.2-0.5	- 3, 0.2-0.5	-	-
12-5	-	-	1, 2-3	many, 0.2-0.4	-	-
12-6	1, 15	1, 15	1, 1-2	-	-	-
12-7	1, 15	-	-	-	*	*
18-2	1, -	-	1, 2-4	-	-	-
18-3	-	-	contact not visible	-	-	-
18-4	-	-	contact not visible	-	-	-
18-5	-	-	contact not visible	-	-	-
18-6	-	-	no clays left on failure surface (rock-debris- rock contact)	-	-	-
18-6A	-	-	cemented	*	*	*

(continued)

Table 1 (continued)

Location No.	Clay Layer Noted in Slide Debris No. and Thickness, cm	Clay Layer on 1963 Failure Surface No. and Thickness, cm	Other clay layers, ♦ = above 1963 surface - = below 1963 surface No. and Thickness, cm	Tectonic Breccia or Fault Surface Present	Solution Features Present	Old Talus or Cemented Talus Present (from Scarp) cemented
18-7	-	-	-	-	-	-
18-8	-	1, 5-10	-1, 3	-	-	-
18-9	-	1, 5	+2, trace-0.5	-	-	-
18-10	-	1, 2	-	-	-	several types
18-11	-	1, 2	-	-	-	-
18-14	1, 5	1, 2-10	-	-	-	-
22-1	-	no clay visible (cascade structure)	-	-	-	-
22-1A	1, several cm discontinuous	1, trace discontinuous	-	-	-	-
22-2	-	1, 1-4	-1 to 6 layers	*	-	-
22-3	1,-	1, 4-10	-2, trace	*	-	-
22-3A	1,-	1, 2-5 x 8 m + length	many, 0.5-8	0.5 to 1.0 m	-	-
22-4	-	1, 0-5	-	*1-2 m	0.5-1.0 cm diam	-
22-5	-	no clays visible (removed by erosion)	-	-	-	-
22-6	-	1, 1-3	-	-	-	-
22-6A	-	1, 1-4	-	-	-	-
22-7	-	1, 7-10	-	-	* -10 cm	-
22-7A	-	1, 1-2	-	-	-	-
22-7B	-	1, 2-6	-	-	-	-
22-8	-	1, 2-10	+1, 1-3	-	-	-
23-1	-	no clays visible, some buckling of rock slabs	-	-	-	-
23-2	-	-	- 3 layers, 2-1	-	-	-
23-3	-	1, 8	-	-	-	-
23-4	-	1, 8-10	-	-	-	-
23-10	-	1, 2-3	-2 layers, 1-3 & 10-15	-	-	-
23-11	-	1, 2-3	-	-	-	-
23-12	-	1, 1-5	-	-	-	-
23-13	-	partial of old adit	-	* (float) - - - - - or - - - - - *? cemented	-	(continued)

Table 1 (continued)

Location No.	Clay Layer Noted in Slide Debris No. and Thickness, cm	Clay Layer on 1963 Failure Surface No. and Thickness, cm	Other clay layers, above 1963 surface + below 1963 surface No. and Thickness, cm	Tectonic Breccia or Fault Surface Present	Solution Features Present	Old Talus or Cemented Talus Present (from Scarp)
23-14	-	top of Dogger (no clays visible)	-	-	-	-
23-15	-	no clay visible - in Dogger Form, (fault in Dogger)	-	-	-	-
23-16	-	no clay readily visible (access difficult)	-	-	-	-
23-17	-	old failure plane - (no excavation for clays made) no clay visible 1-2 m cover	-	-	-	-
24-1	several, 1	1, 0.5-1	*	*	10-50	*
24-2	-	1, 0-6	*	*	*	*
24-3	-	1, 2-4	several, 1	*	*	*
24-3A	-	1, 2-3	-	*	*	*
24-4	-	1, 2-4	-	-	-	-
24-6	(on failure plane of post Oct. 9, 1963 slide)	-	-3 layers, <0.5	-	-	-
24-7	-	2, 0.5-1.5	-	-1, 1	-	-
24-8	-	-	-	-	-	-
69-1	-	1, 2-3	-	-	-	-
69-3	-	1, 2-5	-	-	-	-
69-4	-	1, 5	-	-	-	-
67-1	1,-	-	-	-	-	-
67-2	1,-	-	-	-	-	-
522-2	1,-	-	-	-	-	-
522-3	1,-	-	-	-	-	-
522-4	-	1,-	1, 1-6 x 80 m long 2 layers	-	2-10	-
522-5	-	-	1, 0.2-1	-	-	-
522-7	-	-	1, 1-3	-	-	-

Table 2
Atterberg Limits on Clay Samples from the Vajont Slide

<u>Sample No.</u>	<u>Liquid Limit</u>	<u>Plastic Limit</u>	<u>Plasticity Index</u>	<u>Descriptive Notes</u>
8-1	67	28	39	In-situ clay, same unit as base of slide
8-1A	80	35	45	In-situ clay, same unit as base of slide
8-1B	68	36	31	In-situ clay, same unit as base of slide
8-1C	50	30	20	In-situ clay, same unit as base of slide
8-1D	72	29	43	In-situ clay, same unit as base of slide
9-1	76	32	44	Clay in slide debris
9-3A	33	20	13	In-situ clay sample on failure plane
9-5	.58	21	37	Clay on failure plane
10-2	52	30	22	Clay at rock-debris contact
10-2A	53	32	21	Same as 10-2 (4 m away)
10-3A	68	35	33	Lower 1 m of debris above failure plane
10-4	39	24	15	Clay at rock-debris contact
10-4A	40	24	16	Clay at debris-rock contact (8 m from 10-4)
10-6	38	26	12	Clay at debris-rock contact in-situ
11-1	70	21	49	Clay in debris 50 m from rock contact
11-2A	66	33	33	Clay at debris-rock contact
11-3	56	32	24	Clay layer 1-2 cm above failure plane
11-4	50	27	23	Clay layer at debris-rock contact (10 m from 11-3)
11-5A	92	36	56	Clay layer just above debris (8 m from 11-4)

(continued)

Table 2 (Continued)

Sample No.	Liquid Limit	Plastic Limit	Plasticity Index	Descriptive Notes
11-6	55	31	24	Large clay block, float in slide debris
11-7B	61	26	36	Clay layer just (1-2 cm) above failure plane
11-8	48	27	21	Clay at contact of rock and debris
11-9	76	26	50	Clay at failure plane (2 to 10 cm thick)
11-9	67	30	37	Direct shear tests by WES.
11-10	76	36	40	Clay at failure plane, 4 layers (1-10 cm thick) in debris above sample
12-1	26	16	10	Clay silt layer, east scarp
12-2	72	22	50	Clay at slide debris-tectonic breccia contact
12-3	76	22	54	Clay layer at debris-tectonic breccia contact
12-4	73	29	44	Clay in-situ in failure plane
12-5	56	29	27	Clay in-situ on main failure surface over east side of slide
12-6	72	23	49	Clay in debris about 4 m above failure plane
12-6A	35	19	16	Clay on failure plane (10 m from 12-6)
18-6	49	27	22	Clay on failure plane at scarp
18-6A	39	20	19	Clayey debris on rock surface near scarp
18-8	45	32	13	Clay in-situ forms failure plane above
18-9	37	25	12	Clay in-situ forms adjacent failure plane

(continued)

Table 2 (Continued)

Sample No.	Liquid Limit	Plastic Limit	Plasticity Index	Descriptive Notes
18-9A	48	33	15	Clay in-situ on failure plane
18-11	38	25	13	Clay in-situ forms failure plane below
18-14	43	30	13	Clay layer in debris above failure plane
22-1A	57	20	37	Clay layer on failure plane
22-3	42	14	28	Clay layer between slide debris and tectonic breccia
22-3A	50	25	25	Clay in base of debris just above tectonic breccia
22-4	54	32	22	Clay below cemented breccia on bedrock contact
22-6A	44	25	19	Clay layer, in-situ, forms failure plane above
22-7	48	26	22	Clay at debris-rock contact
22-7B	37	28	9	Clay layer, in-situ below failure plane
22-8	37	25	12	Clay layer, in-situ
23-3	46	32	14	Clay layer, in-situ, forms failure plane above
23-4	60	33	27	Clay layer between debris and rock
23-10	57	30	27	Clay layer, in-situ
23-11	57	35	22	Clay layer, in-situ forms adjacent failure plane
23-12	46	28	18	Clay layer, in-situ forms adjacent failure plane
23-17B	39	21	18	Clay layer, in-situ in fold
24-1	68	31	37	Clay layer with cemented breccia
24-2	82	22	60	Upper clay layer in cemented breccia

(continued)

Table 2 (Continued)

<u>Sample No.</u>	<u>Liquid Limit</u>	<u>Plastic Limit</u>	<u>Plasticity Index</u>	<u>Descriptive Notes</u>
24-2A	64	32	32	Lower clay layer in cemented breccia
24-3	45	23	22	Clay layer along failure plane
24-7	39	22	17	Clay layer, in-situ, in fold
25-3	55	30	25	Clay layer, in-situ in Malm
522-5A	66	23	43	Clay layer on failure plane
522-5A	81	24	57	Clay layer on failure plane

Table 3
Summary of Direct Shear Test Results on Remolded Valont Clays
Tests by: Thurber Consultants Ltd., Edmonton, Canada

Water Content of the soil as received*	Atterberg Limits LL (%)	PL (%)	PI (%)	Shear Test and Specimen Details			Post-Shear Water Contents			Effective Residual Strength Parameters				
				Test Conducted on	Type of Test	Remolded Water Content (%)	Normal Stress σ_n (psi)	Shear Strength r_{res} (psi)	Away From Shear Plane	Residual Shear Strength r' (psi)	Residual Shear Strength r'' (psi)			
Valont Sample 522-5A	26.2	66.2	22.5	43.7	Soil after removing all rock and coarse sand retained above sieve No. 10. About 13-17% by weight of total sample was removed which constituted the rock fragments and coarse sand.	Multistage direct shear test along a precut plane.	27.0	900	25.9	25.3	117.5	0.131	7.44°	
Reconstituted Valont Sample 522-5A	26.2	81.0	23.8	57.2	Reconstituted sample after adding back the coarse sand fraction between sieve Nos. 4 and 10 to the above sample. However rock fragments were not added.	Multistage direct shear test along a precut plane.	30.0	900	151.9	0.169	9.6°	4.4	0.293	16.4°

NOTE: Grain size distribution for the original sample

Gravel: 6 percent
 Sand: 7 percent
 Silt: 36 percent
 Clay: 51 percent

Table 4
Summary of Direct Shear Test Results on Remolded Valmont Clay
Tests by: Engineering Geology Lab, Department of Geology
University of Illinois, Urbana

SAMPLE 522-5		Valmont Test No.	Deform. Rate (in./min.)	Initial Normal Stress (psi)	Peak Shear Resist. ² (psi)	Displ. at Minimum Resistance (in.)	Normal Stress at Min. Resist. (psi)		Shear Resistance (psi)	Tan ϕ deg.	Remarks
Test No.	Spec. No.						1.14	103.2	20.9	0.203	
1W	3	0.0025	83.6	23.3	1.14						Added only enough water to make sample into a 1/16-in. layer.
2W	3	0.0025	83.6	20.8	0.92	98.7	101.3	0.185	10.5		Added additional water; allowed sample to soak for two days.
		0.00025			1.17	108.3	19.5	0.181	10.2		Ran sample for about 0.1 in. to test effect of deform. rate of 6%. Ten-fold decrease in deform. rate resulted in 2x drop in ϕ .
3W	3	0.0025	81.0	13.6	0.61	67.8	101.2	0.150	8.57		
4W	3	0.0025	83.6	21.3	0.78	96.4	16.6	0.172	9.8		Resistance increased slightly after passing through minimum value.
5W	3	0.0025	83.6	22.3	0.95	99.3	17.6	0.177	10.0		
6W	3	0.0025	83.5	21.7	1.17	103.4	16.5	0.167	9.5		
7W	3	0.0025	61.8	13.0	1.00	50.2	9.8	0.195	11.0		Sample was unloaded after reaching residual. Thin sample. N = 275 lb.
8W	3	0.0025	41.8	13.5	2.13	35.7	6.9	0.193	10.9		
9W	3	0.0025	22.8	7.7	2.10	63.5	12.0	0.189	10.7		
1F	4	0.0025	83.6	19.0	1.16	103.4	25.1	7.8	0.223	12.5	
2F	4	0.0025	41.8	10.3	1.05	50.7	14.3	0.139	7.8		
3F	4	0.0025	83.6	22.1	1.25	105.8	6.9	0.135	7.7		
							15.9	0.150	8.5		Sample was unloaded after reaching residual.
											N = 503 lb.
											N = 273 lb.
											N = 639 lb.

¹) 1/16-in. sample between two 2 in. x 6 in. slabs of Berea sandstone unless otherwise indicated.

²) Displacement at peak resistance assumed to be zero.

³) Whole sample.

⁴) Fraction passing #10 mesh.

Table 5
Summary of Direct Shear Test Results on Remolded Vatont Clays
Tests by: Waterways Experiment Station, Vicksburg, Mississippi

SAMPLE 11-9

Specimen No.	Initial Atterberg Limits			Dry Content			Initial Void Ratio			Saturation %	Final Water Content %	Estimated Specific Gravity	Type of Test	Normal Stress tsf	Residual Shear Stress tsf	Deform. Rate in./min.	Displ. at Estimated Shear in.	$\tan \phi$	ϕ_r
	LL	PL	PI	%	pcf	g	%	g											
1	76	26	50	35.4	85.88	0.998	97.5	30.2	2.75				Shear test	1.79 3.60 7.19	0.240 0.396 0.906	.00035	3.75 7.5 9.5	0.134 0.110 0.126	7.6° 6.27° 7.18°
2	67	30	37	30.3	88.33	0.944	88.3	27.7	2.75				along a precut surface	5.40 10.79	0.562 1.824	.00035	1.8 6.4	0.104 0.169	5.9° 9.6°

Sample description: Plastic Clay (CH), gray

NOTE: Shear Plane Precut

Table 6
Summary of Clay Mineral Analyses
on Valont Samples

Laboratory	Sample No.	Results
W.E.S. (A. D. Buck) (See Table 5)	1. Clay, 11-9	smectite-major co-component (> 50%) calcite-minor component quartz-minor component kaolinite-minor component
	2. Limestone (fine-grained greenish-gray)	calcite-major component quartz-minor clay and mica-minor "randomly mixed-layer" - smectite and vermiculite-minor
Dept. of Geology University of Illinois (Dr. Eberl) (See Table 4)	1. Whole rock (i.e., clay sample) 522-5	calcite-major component corrensite illite/smectite quartz
	2. Less than 2 micron fraction 522-5	corrensite (vermiculite/smectite type) illite/smectite (~60% smectite layers) calcite quartz-small amount *present in approximately equal proportions
Alberta Research Council (Thurber) (See Table 3)	Valont I Valont II Valont III	illite hydrus mica mixed layer clay minerals containing montmorillonite
Kenney (1967b)		Massive Kinet's (% Dry Weight)
		Qtz Feldsp Calcite Others Total
		5 5 30 10 50
		10 - 7 5 22
		5 - 40 - 45
		Clay Minerals (% Dry Weight)
		Mica Mixed Hydrous layers with Mont- morillonite Kentonite
		50
		Kaol Chl Chlorite in in Valont I - - - - Valont II - - - - Valont III - - - -
		5 30 75
		25

Table 7
Precipitation at ERT0 Station at Different Periods
Before Slope Movement

Approximate Date of Max. Rate of Slope Movements	Reservoir Elevation m	Cumulative Rainfall During Interval Before Movement, mm				Total Annual Rainfall for the Calendar Year in which Movement Took Place, mm	Cumulative Rainfall in 45-day Period Before Movement, as a Percentage of Annual Rainfall
		7 days	15 days	21 days	30 days		
October 31, 1960	645	109	170	379	495	697	2322.6 (1960)
November 30, 1962	700	60.4	94.3	313	413	480	1674.4 (1962)
October 9, 1963	700	65	81	116	127	300	1708.4 (1963)

Table 8

Precipitation at ERTO Station for Periods Preceding "Safe Arrivals"
to Elevations Where Movements Had Previously Accelerated

"Safe Arrival" Date	Reservoir Elevation m	Cumulative Rainfall in Preceding Interval mm			Total Annual Rainfall for Calendar Year, mm	Cumulative Rainfall in 45-day Period Before Date, as a Percentage of Annual Rainfall
		7 days	15 days	21 days		
December 15, 1961	640	30.6	50	85.2	230	336
June 30, 1963	700	28.4	29.8	75.2	151.3	235

* During second impounding of the reservoir

Table 9
Results of Previous Stability Analyses, From Müller (1968)

Author*	Cross-Section (See Fig. 34)	Inclination of the Water- Level	$\theta_{req.}$	$t_g \theta_{req.}$	Calculation According to ϵ	Assumed or Neglected	Premises				
							Assumed Facility Assumed or Neglected **	1	2	3	4
Mencí (1966a)	2	100	-	18.75	0.339	-	on secondary slip surfaces $\phi = 30^\circ$ or 30° resp.: $c = 50 \text{ t/m}^2$	1	2	3	5
Mencí (1966b)	2	700	-	20.5	0.364	Pettersson (like Mencí 1966a)	Prandtl's wedge	1	2	3	4
Kenney (1967)	2	600	-	17.5	0.316	Jenbu (1954)	Prandtl's wedge Zone of arching	1	2	3	5
	650	-	18.5	0.325	Mencí			1	2	3	5
	700	-	20.1	0.366				1	2	3	5
	600	-	20.7	0.378				1	2	3	5
	650	-	21.6	0.400				1	2	3	5
	700	-	22.0	0.404				1	2	3	5
Mönnellér (1965b)	2	590	$\sim 10^\circ$	22.1	0.406	Mönnellér (1965)	on the upper part of the slip surface is Kept $\phi = 25^\circ$	1	2	3	4
	650	$\sim 4^\circ$	22.1	0.406							
	700	$\sim 2^\circ$	24.0	0.445							
Mönnellér (1966a)	2 differing very much	700	$\sim 10^\circ$	27.7	0.525	Mönnellér (1967a)	same	1	2	3	4
				27.0	0.510						
				28.5	0.542						
Mönnellér (calculation according to Mencí, (1966b))	2	600	-	21.0	0.384	Pettersson	-	1	2	3	4
	650	-	21.8	0.400							
	700	-	22.5	0.414							
according to Kenney (1967)	600	-	20.4	0.372	Jenbu	-	1	2	3	4	5
	650	-	21.2	0.388							
	700	-	21.9	0.402							
according to Mönnellér (1965b) but considering the actual shape of the slip surface acc. Broili (1967)	600	$\sim 10^\circ$	18.8	0.340	Mönnellér	-	1	2	3	4	
	650	$\sim 4^\circ$	20.1	0.366							
	700	$\sim 2^\circ$	20.8	0.380							

** Description of premises

1 $c = 0$

2 $t_g \phi$ has the same value along the whole slip surface
(no zone has a higher shear resistance)

3 Stiffness of the slip mass is not considered
4 Secondary failures are not considered
5 Hydrodynamic pressure is not considered

* References given in Bibliography of Mönnellér (1968)

Table 10
Vaiont Slide, Calculated Factors of Safety

a) Section 2

Case	$\phi = 12^\circ$		$\phi = 10^\circ$		$\phi = 8^\circ$		Reservoir	Groundwater
	$\beta=30^\circ$	$\beta=40^\circ$	$\beta=30^\circ$	$\beta=40^\circ$	$\beta=30^\circ$	$\beta=40^\circ$		
1	.651	.728	.540	.604	.431	.481	none	low
2	.562	.632	.466	.524	.372	.418	none	high
3	.627	.699	.520	.579	.414	.562	650 m	low
4	.540	.605	.448	.501	.357	.399	650 m	high
5	.560	.621	.465	.515	.371	.410	710 m	low
6	.469	.520	.399	.431	.310	.314	710 m	high
7	.714	.801					no pore pressure on failure surface	

b) Section 5

Case	$\phi = 12^\circ$		$\phi = 10^\circ$		$\phi = 8^\circ$		Reservoir	Groundwater
	$\beta=30^\circ$	$\beta=40^\circ$	$\beta=30^\circ$	$\beta=40^\circ$	$\beta=30^\circ$	$\beta=40^\circ$		
1	.943	1.184	.782	.984	.624	.784	none	low
2	.838	1.038	.695	.863	.554	.688	none	high
3	.911	1.142	.756	.949	.602	.756	650 m	low
4	.801	0.991	.665	.822	.530	.656	650 m	high
5	.856	1.062	.711	.883	.566	.704	710 m	low
6	.738	0.899	.612	.746	.488	.594	710 m	high
7	1.144	1.505					no pore pressure on failure surface	

c) Section 10A

Case	$\phi = 12^\circ$		$\phi = 10^\circ$		$\phi = 8^\circ$		Reservoir	Groundwater
	$\beta=30^\circ$	$\beta=40^\circ$	$\beta=30^\circ$	$\beta=40^\circ$	$\beta=30^\circ$	$\beta=40^\circ$		
1	.530	.574					none	low
2	.471	.514					none	high
3	.514	.557	Not Run		Not Run		650 m	low
4	.456	.496					650 m	high
5	.470	.508					710 m	low
6	.410	.445					710 m	high
7	.604	.655					no pore pressure on failure surface	

Table 11
Vaiont Slide, Force Per Unit Width Required to Maintain
Equilibrium of the Slide

a) Section 2

Case	units (lbs/lineal ft of slide)					
	$\phi = 12^\circ$		$\phi = 10^\circ$		$\phi = 8^\circ$	
	$\beta = 30^\circ$	$\beta = 40^\circ$	$\beta = 30^\circ$	$\beta = 40^\circ$	$\beta = 30^\circ$	$\beta = 40^\circ$
1	20.13×10^6	12.52×10^6	26.69×10^6	18.22×10^6	33.21×10^6	23.78×10^6
2	25.61×10^6	17.35×10^6	31.38×10^6	22.38×10^6	37.09×10^6	27.25×10^6
3	21.53×10^6	13.90×10^6	27.85×10^6	19.38×10^6	34.14×10^6	24.71×10^6
4	26.94×10^6	18.69×10^6	32.49×10^6	23.52×10^6	37.99×10^6	28.19×10^6
5	24.91×10^6	17.28×10^6	30.51×10^6	22.08×10^6	36.07×10^6	26.74×10^6
6	38.46×10^6	22.74×10^6	35.67×10^6	26.89×10^6	40.45×10^6	30.88×10^6
7	16.46×10^6	9.11×10^6	Dry Case		Dry Case	

b) Section 5

Case	$\phi = 12^\circ$		$\phi = 10^\circ$		$\phi = 8^\circ$	
	$\beta = 30^\circ$	$\beta = 40^\circ$	$\beta = 30^\circ$	$\beta = 40^\circ$	$\beta = 30^\circ$	$\beta = 40^\circ$
1	3.03×10^6	-6.92×10^6	11.43×10^6	0.59×10^6	19.69×10^6	7.27×10^6
2	8.73×10^6	-1.51×10^6	16.37×10^6	5.01×10^6	23.87×10^6	11.06×10^6
3	4.58×10^6	-5.23×10^6	12.50×10^6	1.73×10^6	20.29×10^6	7.95×10^6
4	10.36×10^6	0.36×10^6	17.52×10^6	6.35×10^6	24.63×10^6	11.93×10^6
5	7.03×10^6	-2.18×10^6	14.14×10^6	3.77×10^6	21.11×10^6	9.20×10^6
6	13.24×10^6	3.58×10^6	19.58×10^6	8.78×10^6	25.78×10^6	13.58×10^6
7	-7.57×10^6	-17.96×10^6	Dry Case		Dry Case	

c) Section 10A

Case	$\phi = 12^\circ$		$\phi = 10^\circ$		$\phi = 8^\circ$	
	$\beta = 30^\circ$	$\beta = 40^\circ$	$\beta = 30^\circ$	$\beta = 40^\circ$	$\beta = 30^\circ$	$\beta = 40^\circ$
1	42.67×10^6	32.66×10^6	-	-	-	-
2	48.54×10^6	37.86×10^6	-	-	-	-
3	43.26×10^6	33.26×10^6	-	-	-	-
4	48.95×10^6	38.37×10^6	-	-	-	-
5	45.68×10^6	35.80×10^6	-	-	-	-
6	51.76×10^6	41.33×10^6	-	-	-	-
7	35.91×10^6	26.35×10^6	Dry Case		Dry Case	

Note: $\beta = 0$ between the toe element and the next uphill element for all runs on Section 5.

Table 12
Vajont Slide, Calculations of Maximum Velocities

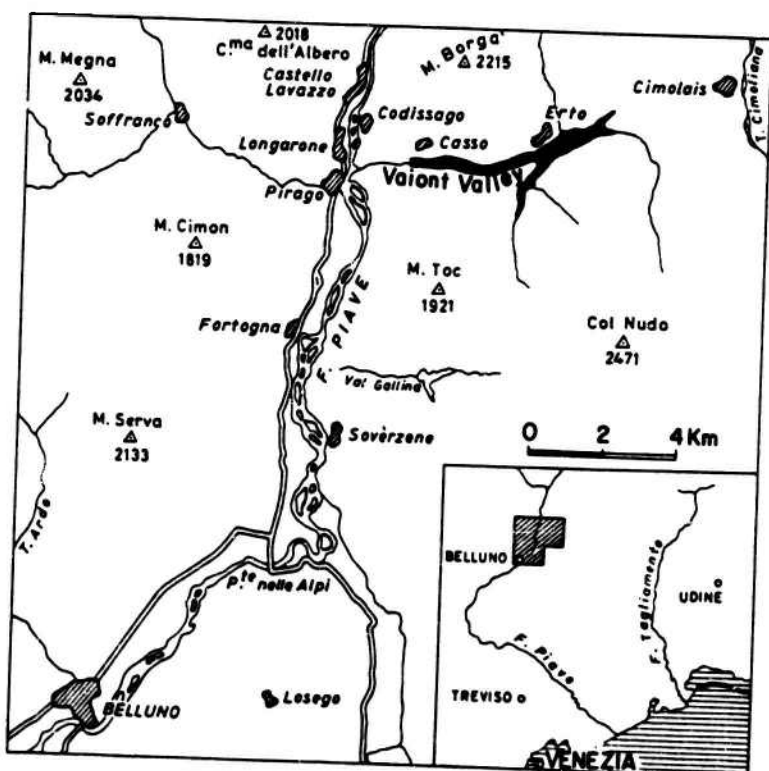
Author	Maximum Velocity meters/second	Method and Comments
Ciabatti (1964)	17	Distance travelled, external friction
Jaeger (1972)	50 upper bound	Maximum elevation of lifting of rock mass at toe of slide (~ 150 m)
Supino, Evangelisti and Datei (reported by Jaeger, 1972)	32	Wave height (Note: also calc $\phi \leq 10^\circ$)
Stragiotti (reported by Jaeger, 1972)	25	Unknown (also estimated 20 sec. duration)
Pacher (reported by Müller, 1964)	25 to 30	Rheological basis
Romero and Molina (1974)	20 to 30	External dynamic effects
Anderson (this study)	20 to 25	Distance travelled, external and internal friction and pore pressures

Table 13

Vaiont Slide, Movement Characteristics

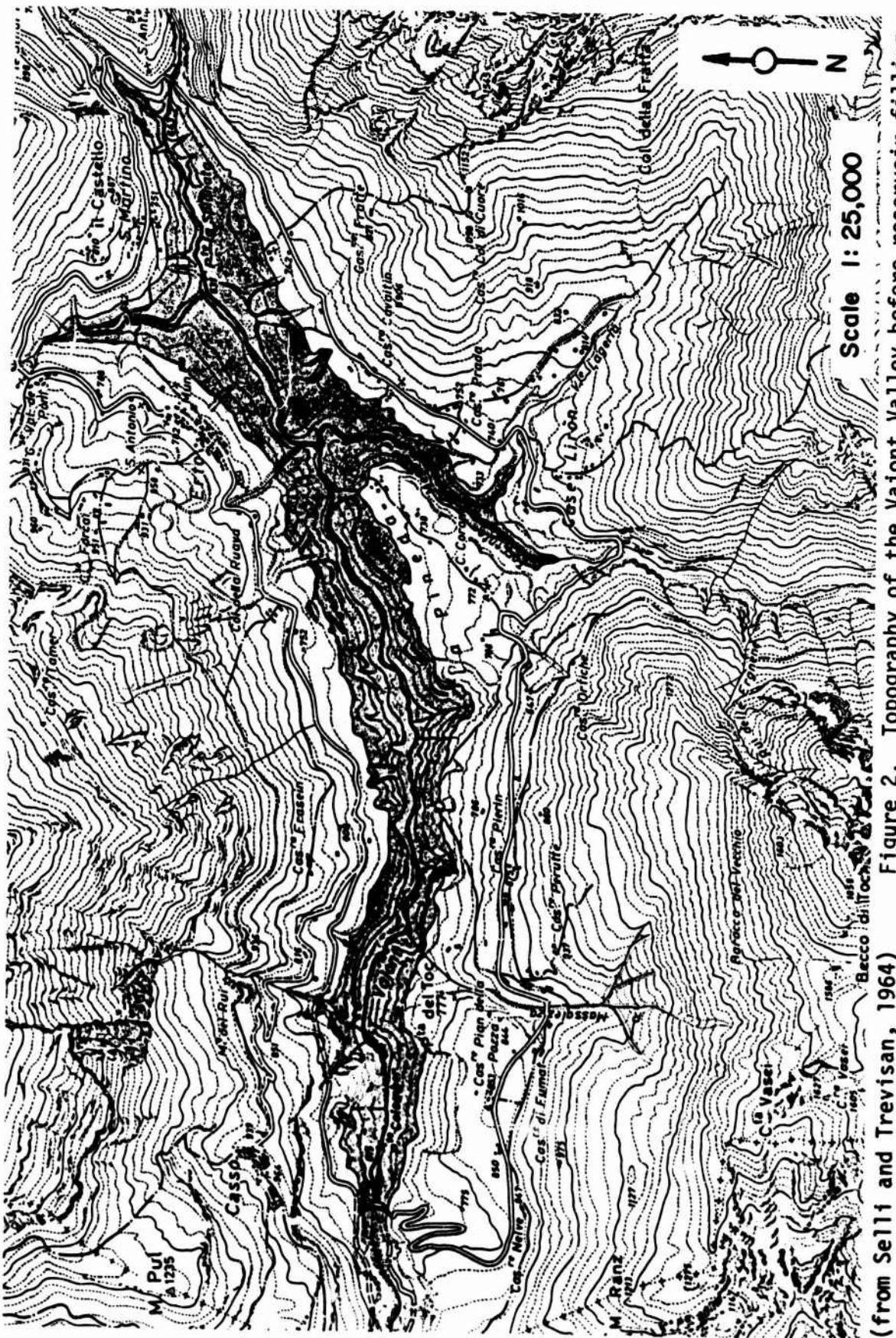
By D. L. Anderson

Time After Movement Began, sec.	Velocity of Slide .m/sec.	Horizontal Displacement of Sliding Mass, m	Factor of Safety
0	0	0	0.99
2	0.06	0.06	0.998
4	0.14	0.27	0.983
6	0.27	0.67	0.972
10	0.88	2.7	0.909
12	1.6	5.1	0.822
14	3.1	9.7	0.643
16	6.0	18.6	0.338
18	10.8	35.2	0.045

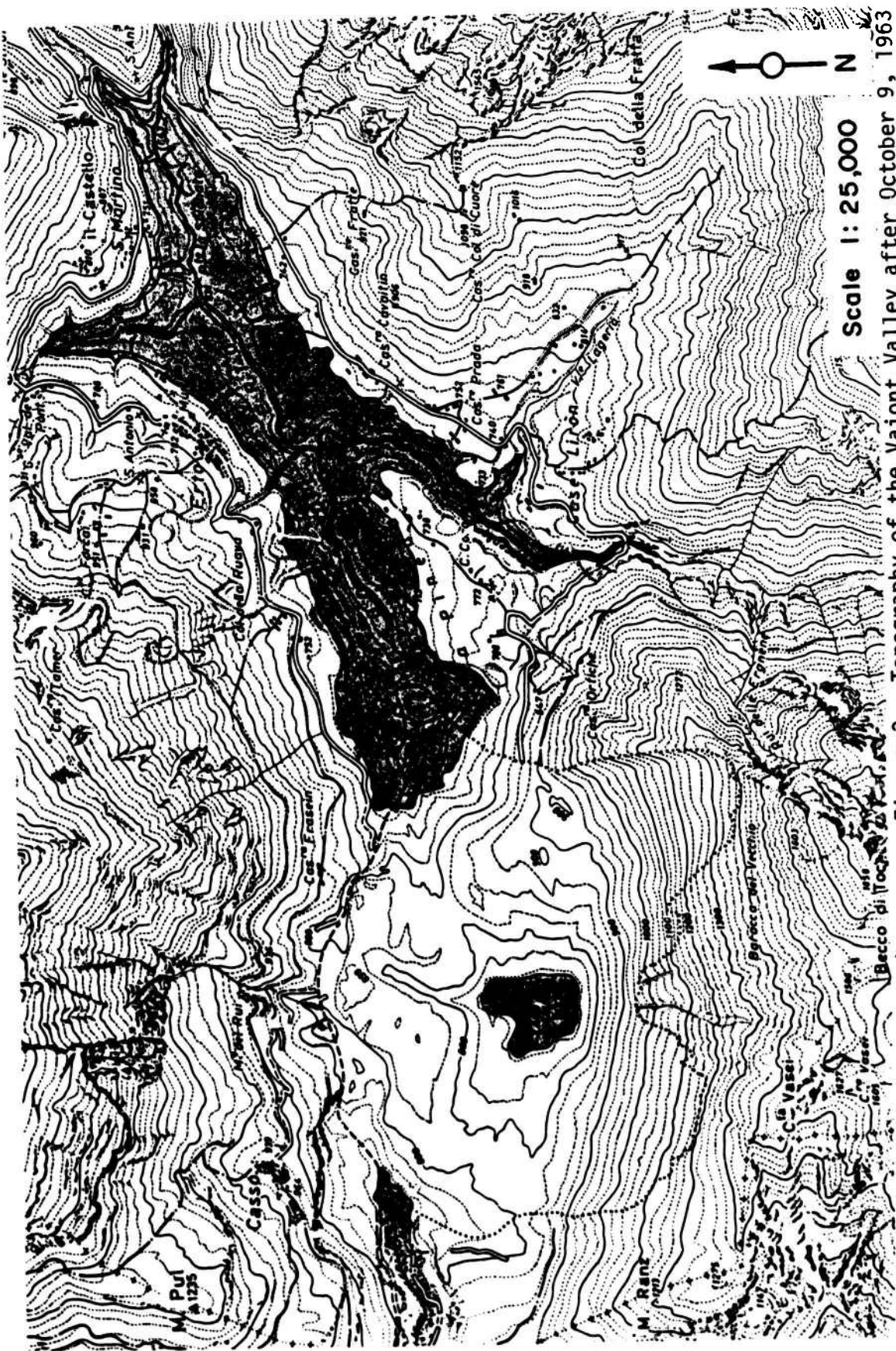


(after Selli and Trevisan, 1964)

Figure 1. Location maps of the Vaiont region, Italy

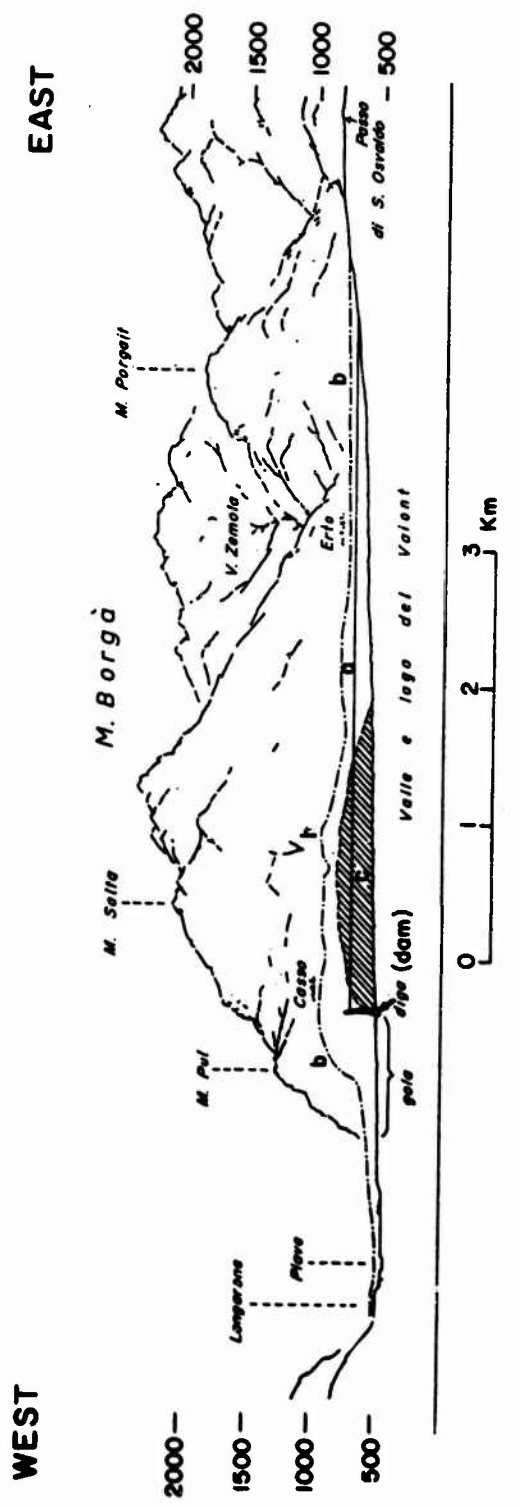


(from Selli and Trevisan, 1964) Figure 2. Topography of the Vajont Valley before reservoir filling



(from Selli and Trevisan, 1964)

Figure 3. Topography of the Vajont Valley after October 9, 1963



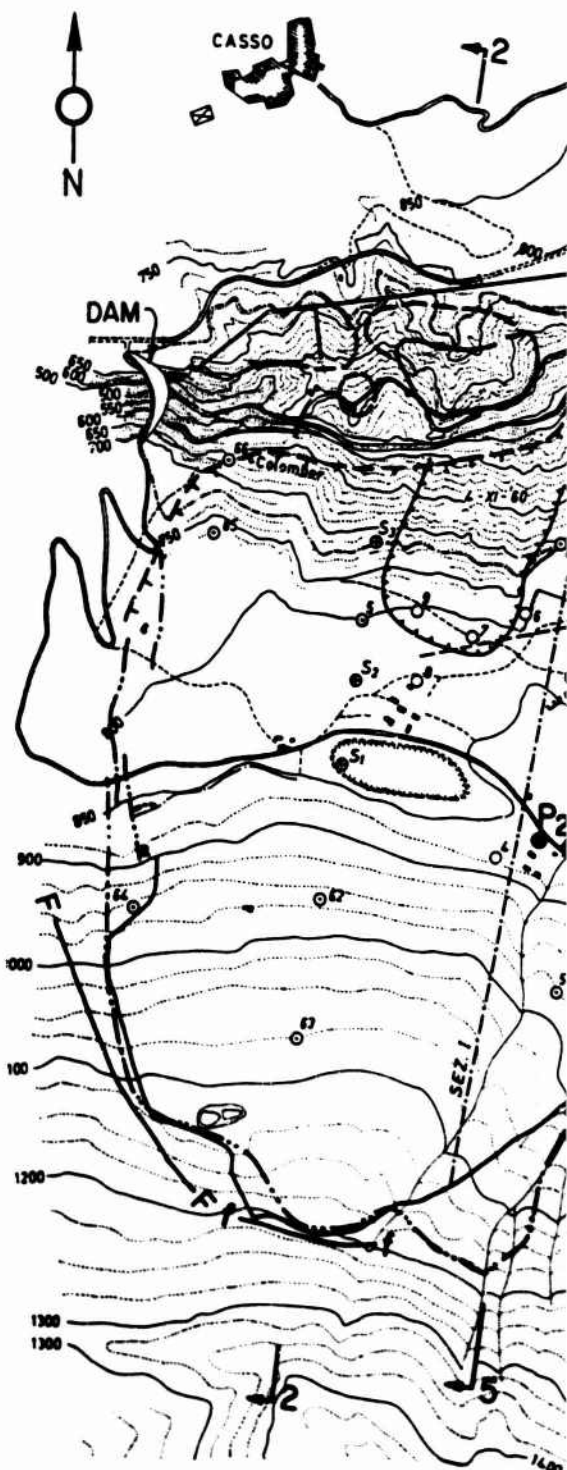
- a. Level of the lake at the time of the slide, elev. 700.4 m
- b. Maximum Level reached by the wave
- c. Slide debris

(From Selli and Trevisan, 1964)

Figure 4. Longitudinal profile along the Vaiont Valley,
looking north

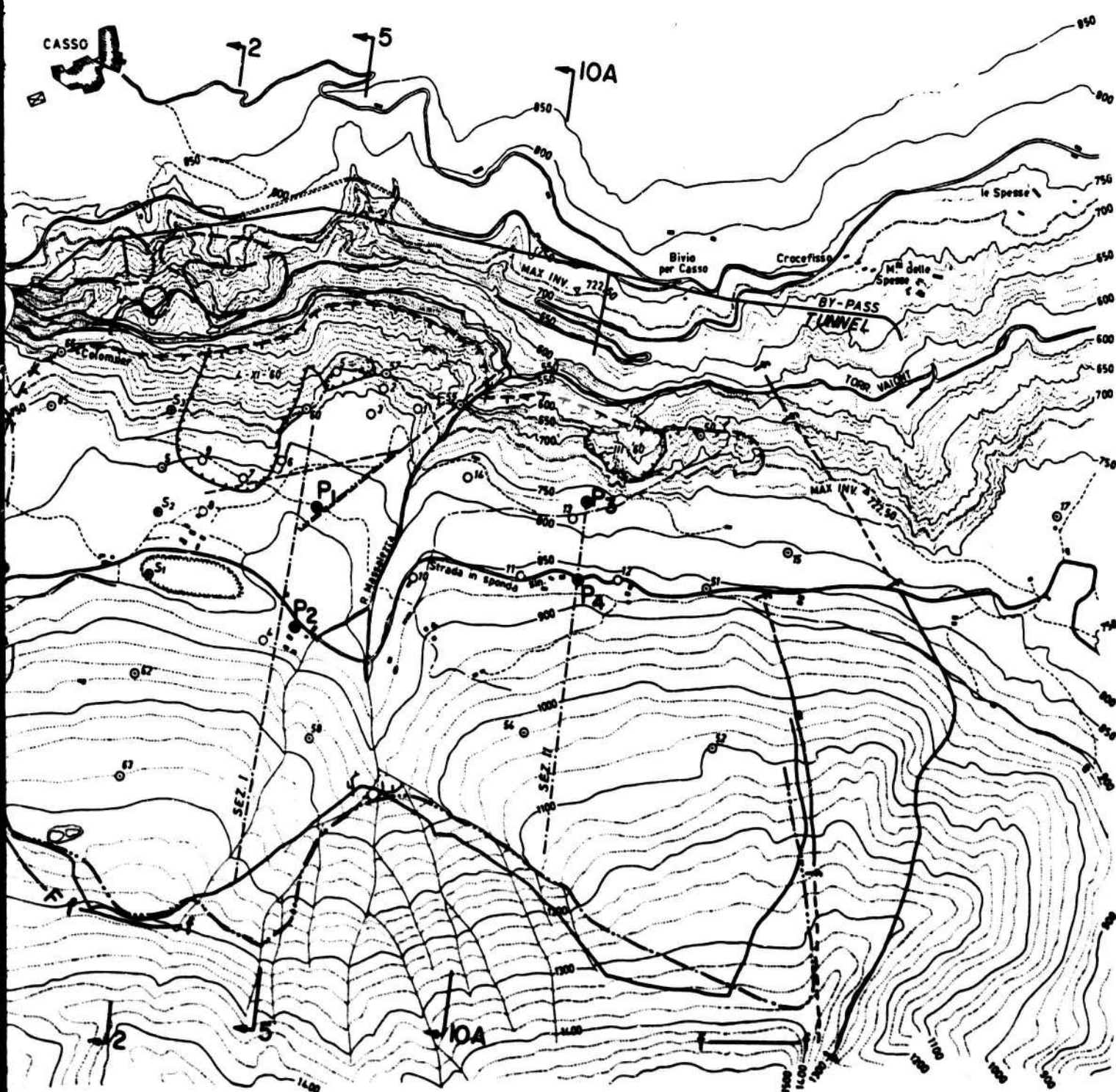
LEGEND

- ⁹ Control points installed before Nov. 1960
- ⁵ Control points installed during Nov. 1960
- 72 Location of sections, this report
- Location of other sections
- S₁ Drillholes made in 1959 - 1960
- P₂ Drillholes made in 1961 (piezometers)
- † Exploration adits near Massalezza ditch
- Seismic traverse of Nov. 1959
- Seismic traverse of Nov. 1960
- Seismic traverse of Feb. 1961
- Curve Principal slides prior to Oct. 9, 1963
- Fissures developed by Nov. 4, 1960
- After Selli and Trevisan (1964)
- After Rossi and Semenza (1965a)
- (—) Remains of pre-historic slide, right bank Giudici and Semenza (1960)
- Outcrop of slip surface of pre-historic slide, Giudici and Semenza (1960)
- Faults Rossi and Semenza (1965a)
- Faults Carloni and Mozzanti (1964)



(after Selli and Trevisan, 1964)

Figure 5. Plan view prior to slide of



Selli and Trevisan, 1964)

SCALE 1:12,500

m 0 250 500

Plan view prior to slide of October 9, 1963

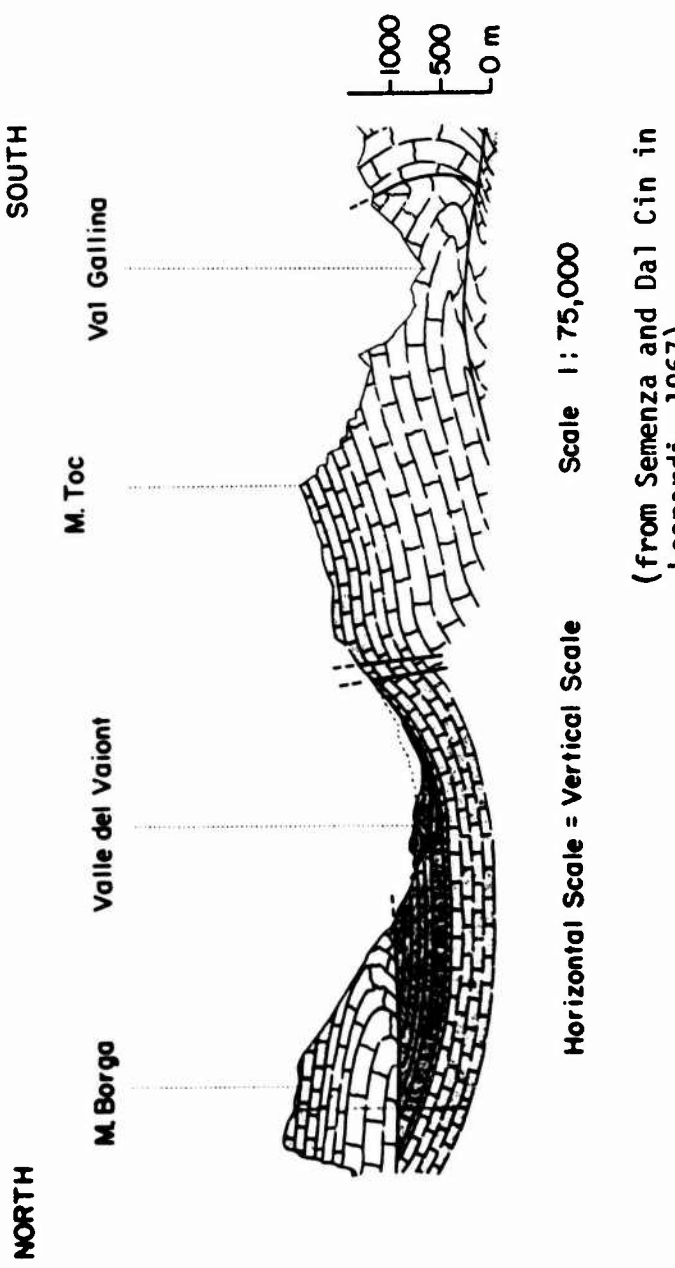


Figure 6. Regional north-south geologic section through Vaiont slide

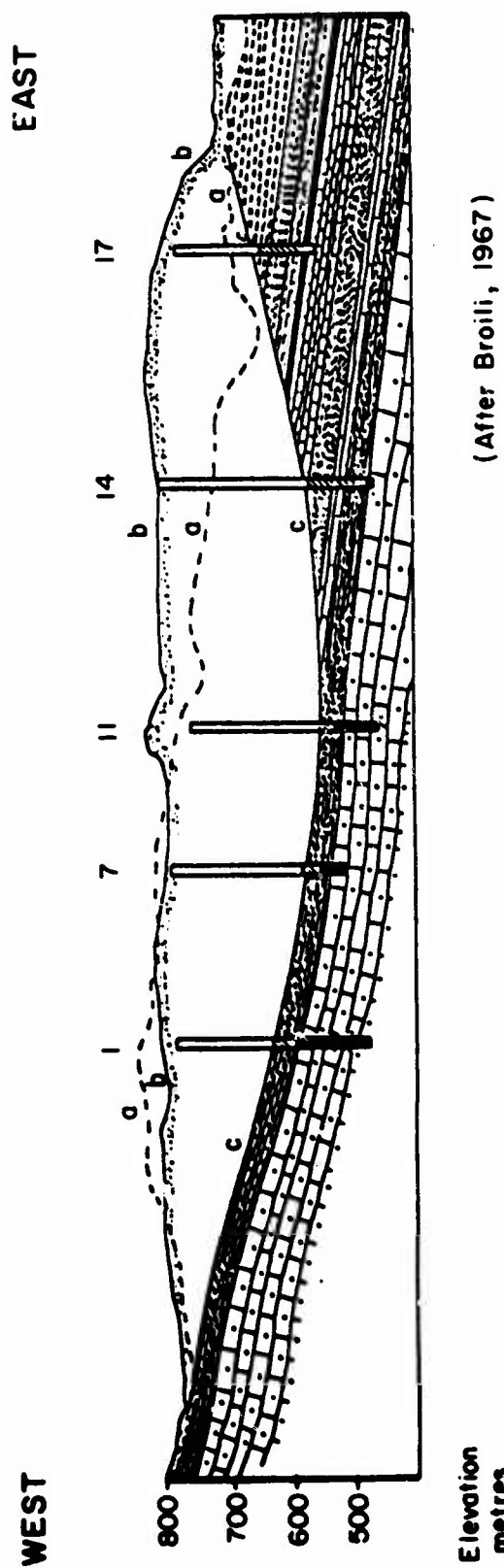


Figure 7. East-West geologic section through the toe of the slide

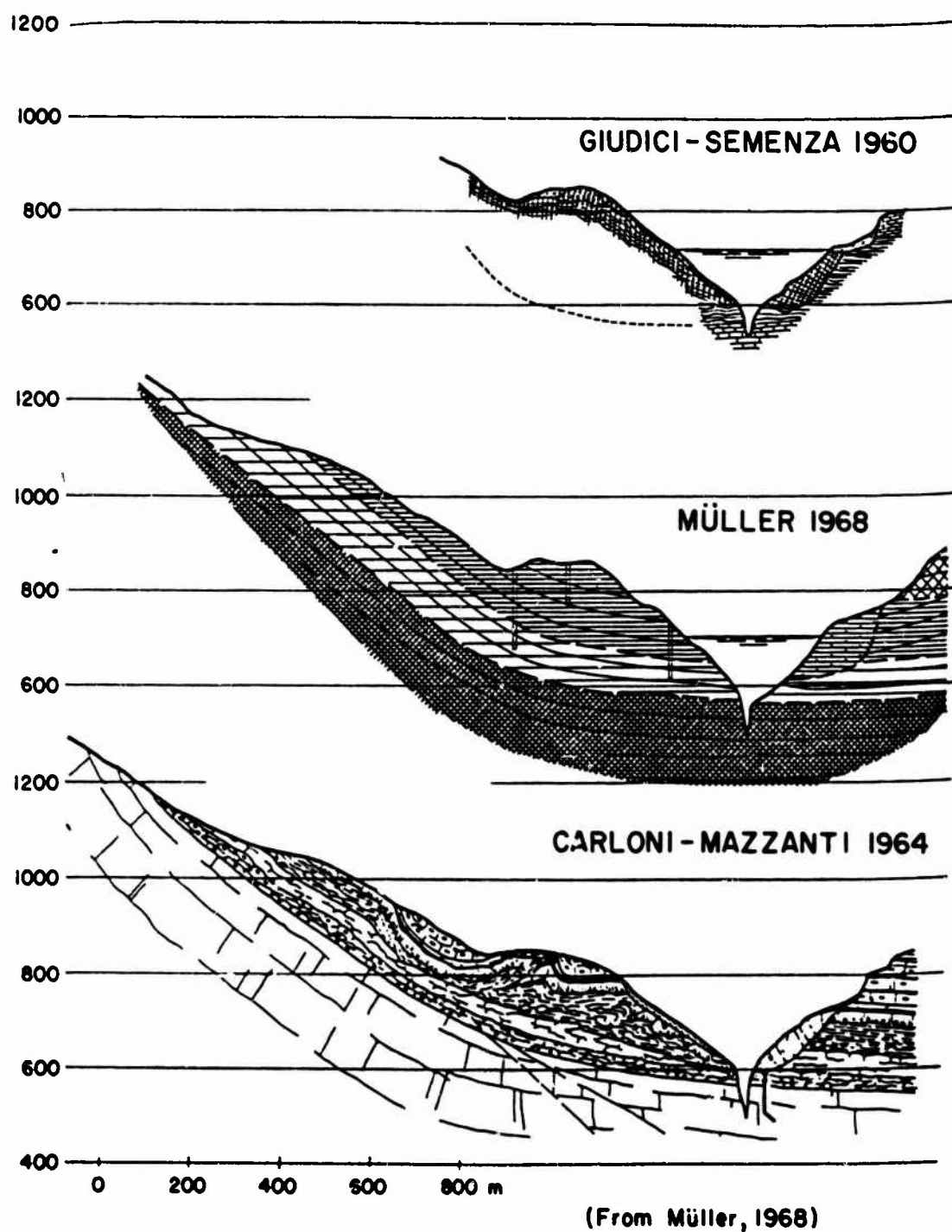


Figure 8a. Geologic sections of other investigators

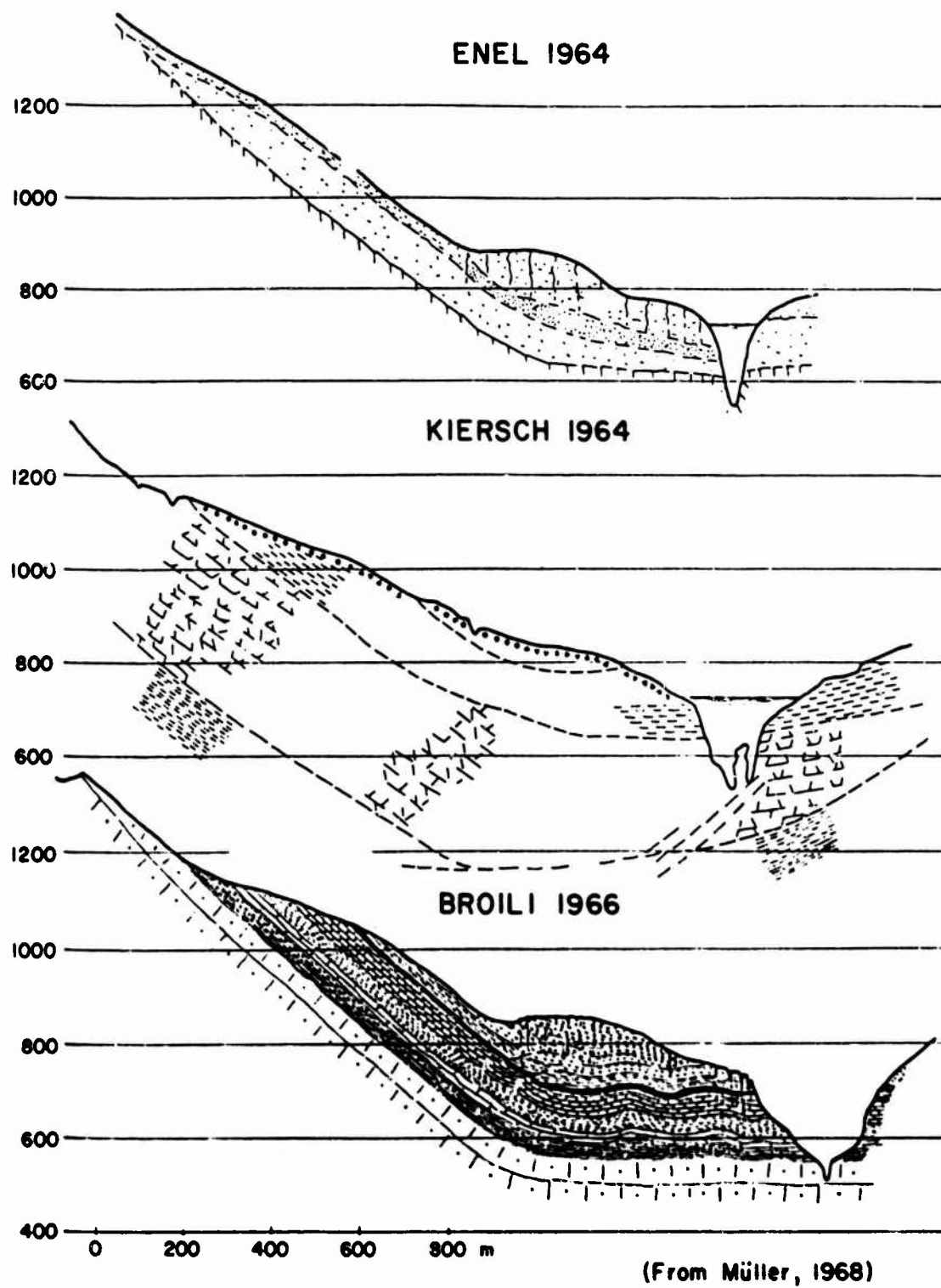


Figure 8b. Additional geologic sections of other investigators

a) DESCRIPTION OF THE STRATIGRAPHIC COLUMN
 after Carloni and Mazzanti (1964) e Brelli (1967)

UPPER CRETACEOUS

c₈ - Marly limestone, silty, pink-colored. (Scaglia Fm)
 beds - 5cm thick, total thickness 30cm

c₇ - Limestone - red-colored - (basal Scaglia Fm)
 total thickness ~ 15-20cm

c₆ - Cherry limestone, greyish to reddish, nodular beds 5-20cm
 interbeds of grey-green marly limestone to marl, age - Turonian & Lower Senonian
 total thickness ~ 10cm

c₅ - Marly limestone - pink and red, age Cenomanian,
 total thickness 1.5m

c₄ - Limestone with some green clayey interbeds, age Santonian,
 total thickness 3-4m

c₃ - Marl and marly limestone, pink, eye-fanning, thickness 3-4m (weak unit)

c₂ - Brecciated limestone and marly limestone, beds 10-100cm thick
 slump structures, age - Allian, total thickness 10-20m

Marlites - (non deposition of sediments and/or sediments eroded)

LOWER CRETACEOUS

c₁ - Marly limestone - pink and green color 5-30cm thick, nodules of dark chert,
 clastic limestone at top.
 Some green clay or marly limestone beds, age - Allian.
 total thickness 45-60cm (weak unit)

UPPER JURASSIC TO LOWER CRETACEOUS

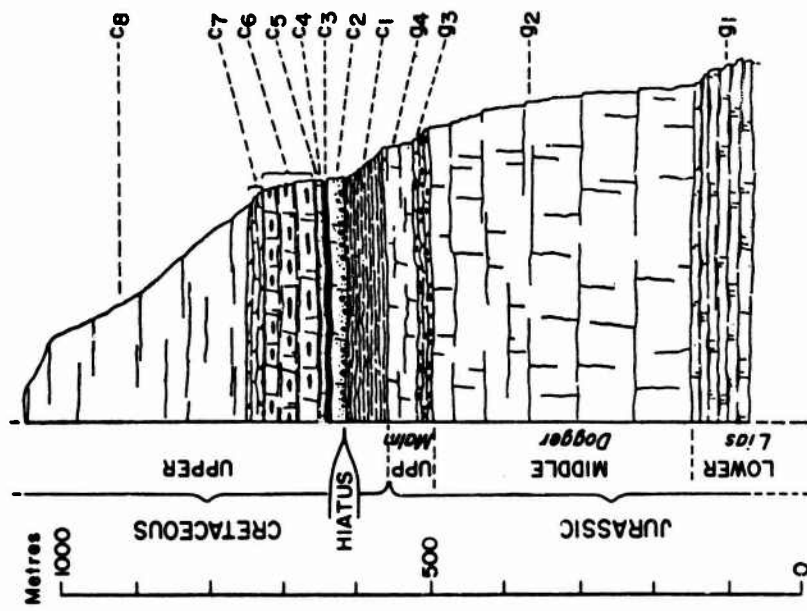
g₄ - Coarsest limestone, greyish to reddish color, sometimes with chert nodules.
 beds 30-40cm thick (in lower 2m) age - Upper Falc to Lower Cretaceous
 total thickness 40-45m (weak unit)

MIDDLE JURASSIC

g₃ - Cherry limestone, dark grey color, beds 5 to 20cm thick
 nodular reddish chert, age - Mals.
 total thickness 25-35m (weak unit)

g₂ - Calcareous dolomitic limestone, locally porous dolomite due to
 solution, beds in upper part 0.5-1.0m thick, otherwise ~ 1m, age - Dogger,
 total thickness 350m

g₁ - Limestone, grey to bluish well-stratified, beds 5-15cm thick,
 patches of bluish marl, age - Lias,
 total thickness 80-100m



GEOLOGIC COLUMN, VAIONT VALLEY

(after Carloni and Mazzanti, 1964)

Figure 9. Geologic column, Vaiont Valley

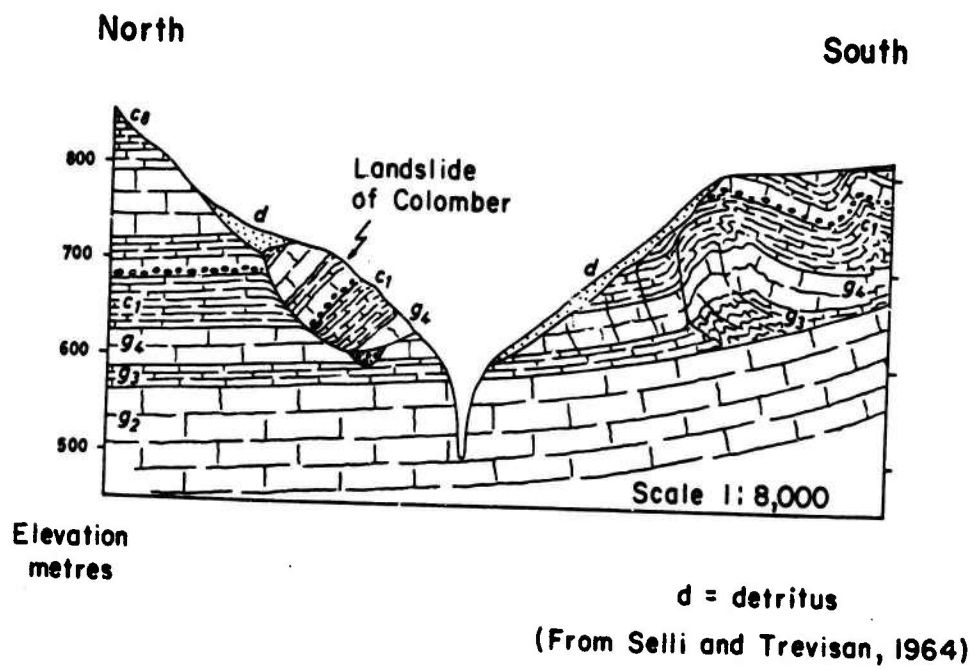


Figure 10. Geologic section looking upstream showing old slide mass covering buried alluvium

Figure 11 is in the pocket at the back of this volume.

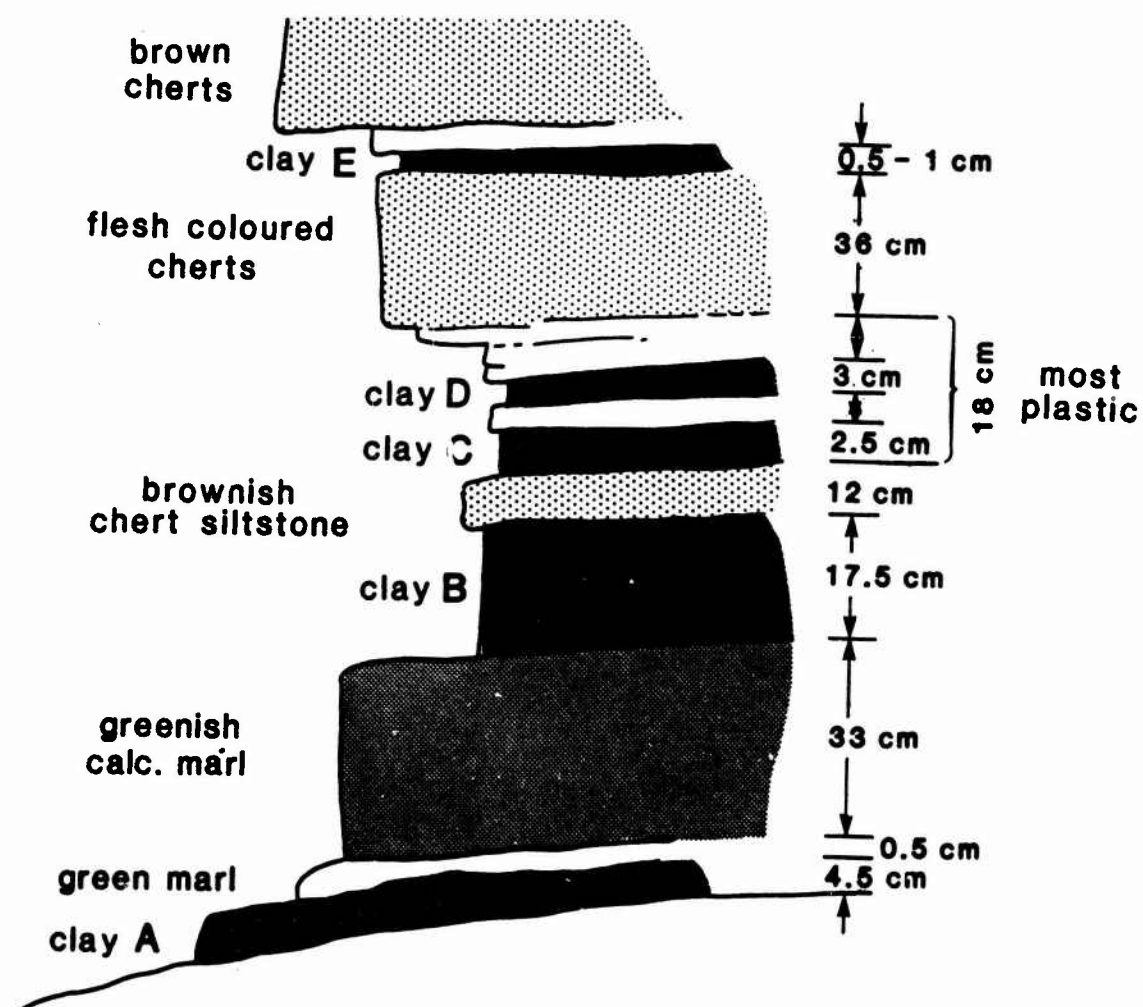
**Figure 11. Geologic map of the Vajont Slide
before the slide of October 9, 1963**

Figure 12 is in the pocket at the back of this volume.

**Figure 12. Geologic map of the Vajont Slide
after the slide of October 9, 1963**

Figure 13 is in the pocket at the back of this volume.

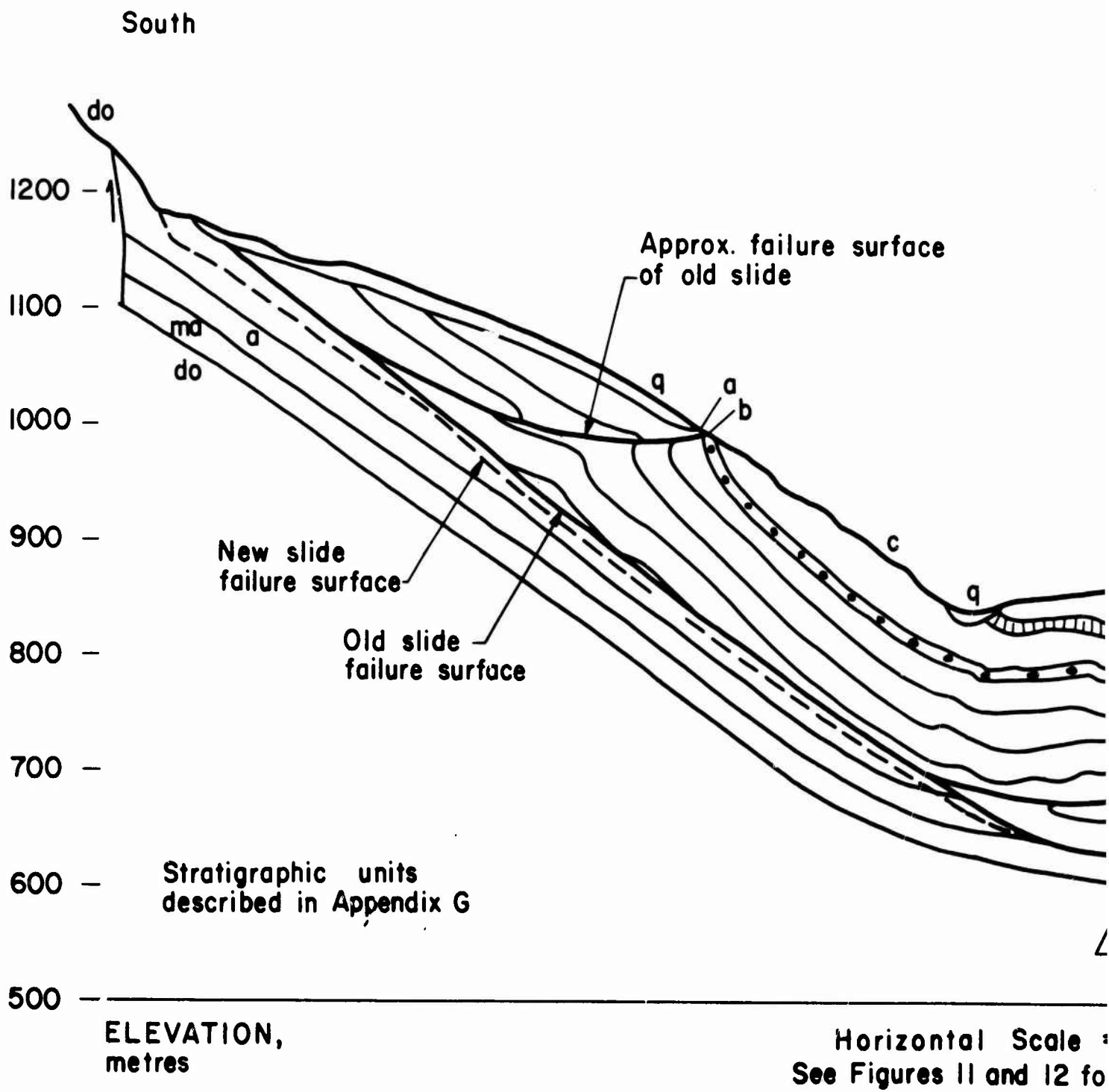
**Figure 13. Photomosaic of the upper portion
of the Vajont Slide**



For location see 8-1 on Figure 12, and
Photos 1, 2, and 3

Note: This outcrop lies in the same
stratigraphic sequence as those
at the base of Vaiont Slide.

Figure 14. Sketch of outcrop of Lower Cretaceous rocks,
southwest of Casso



North

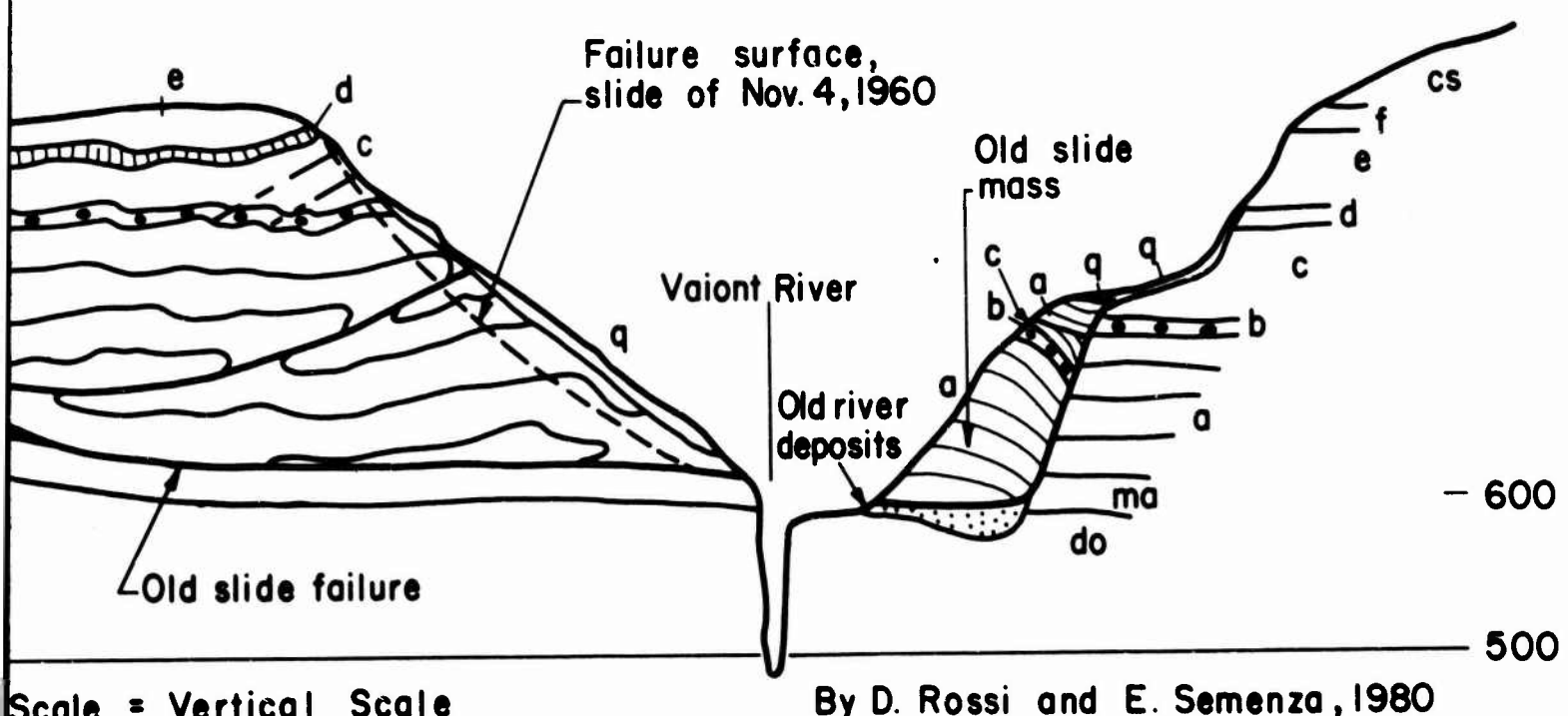
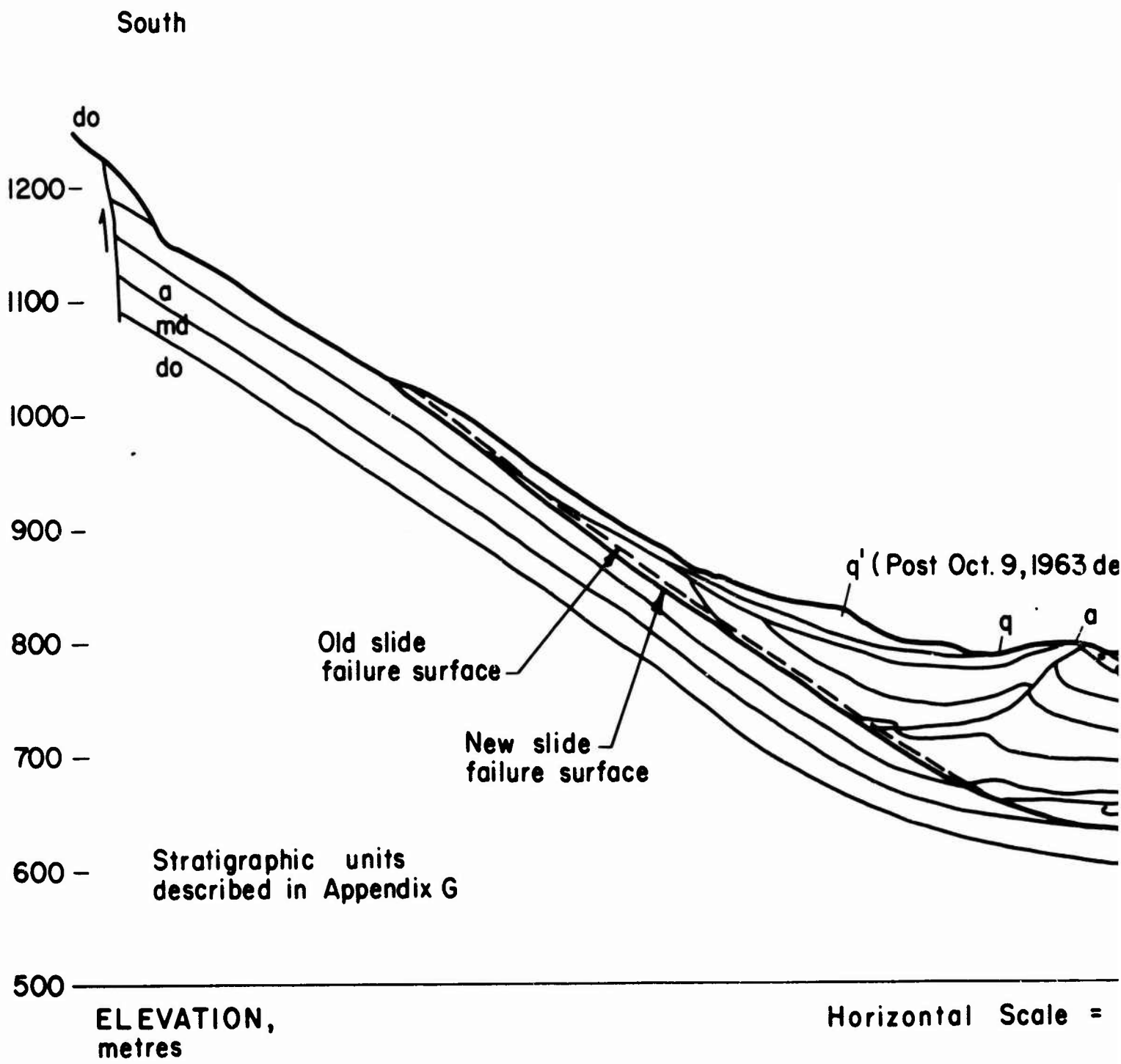


FIGURE 15
Geologic Section 2, Vaiont Slide
Before October 9, 1963



North

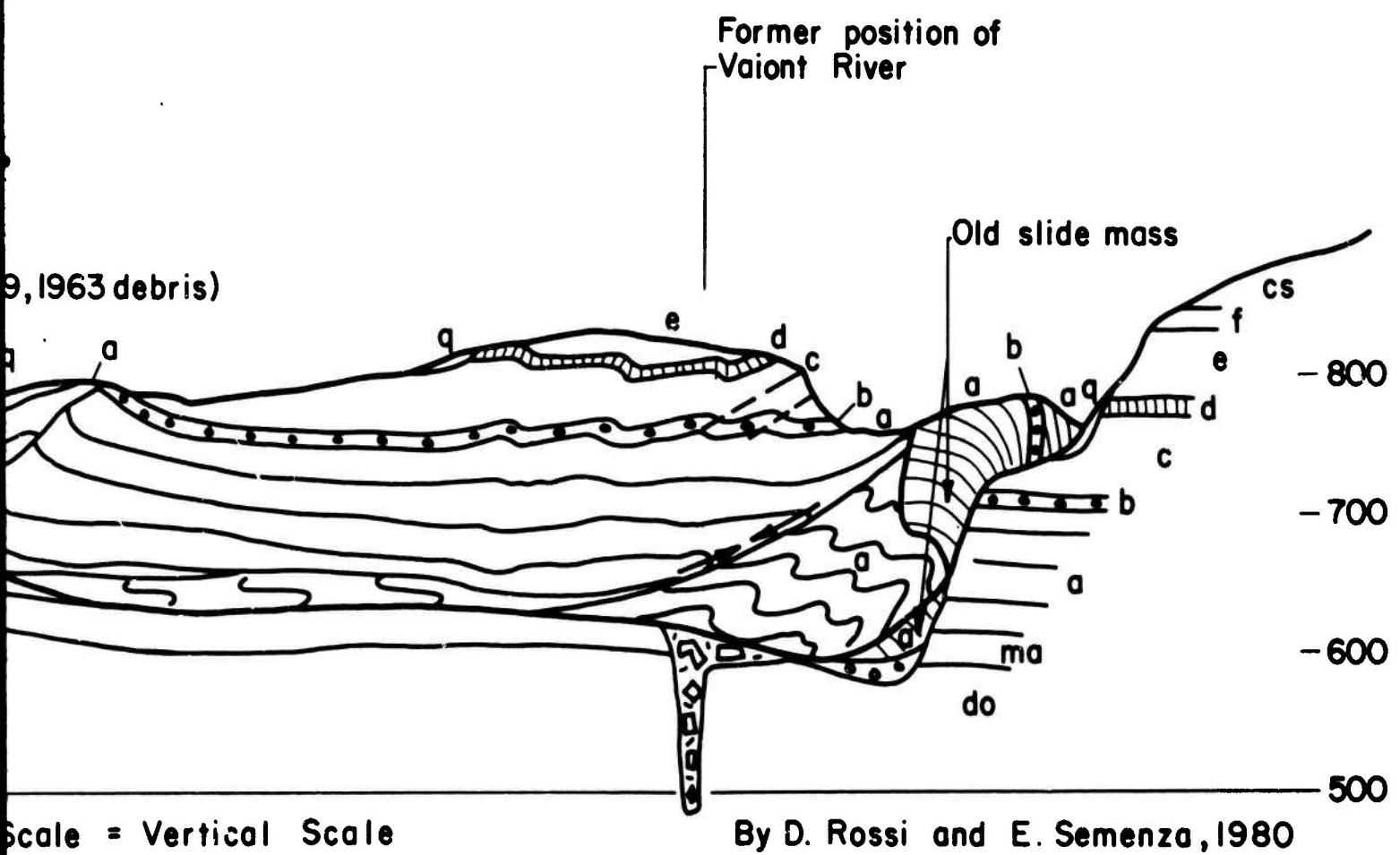
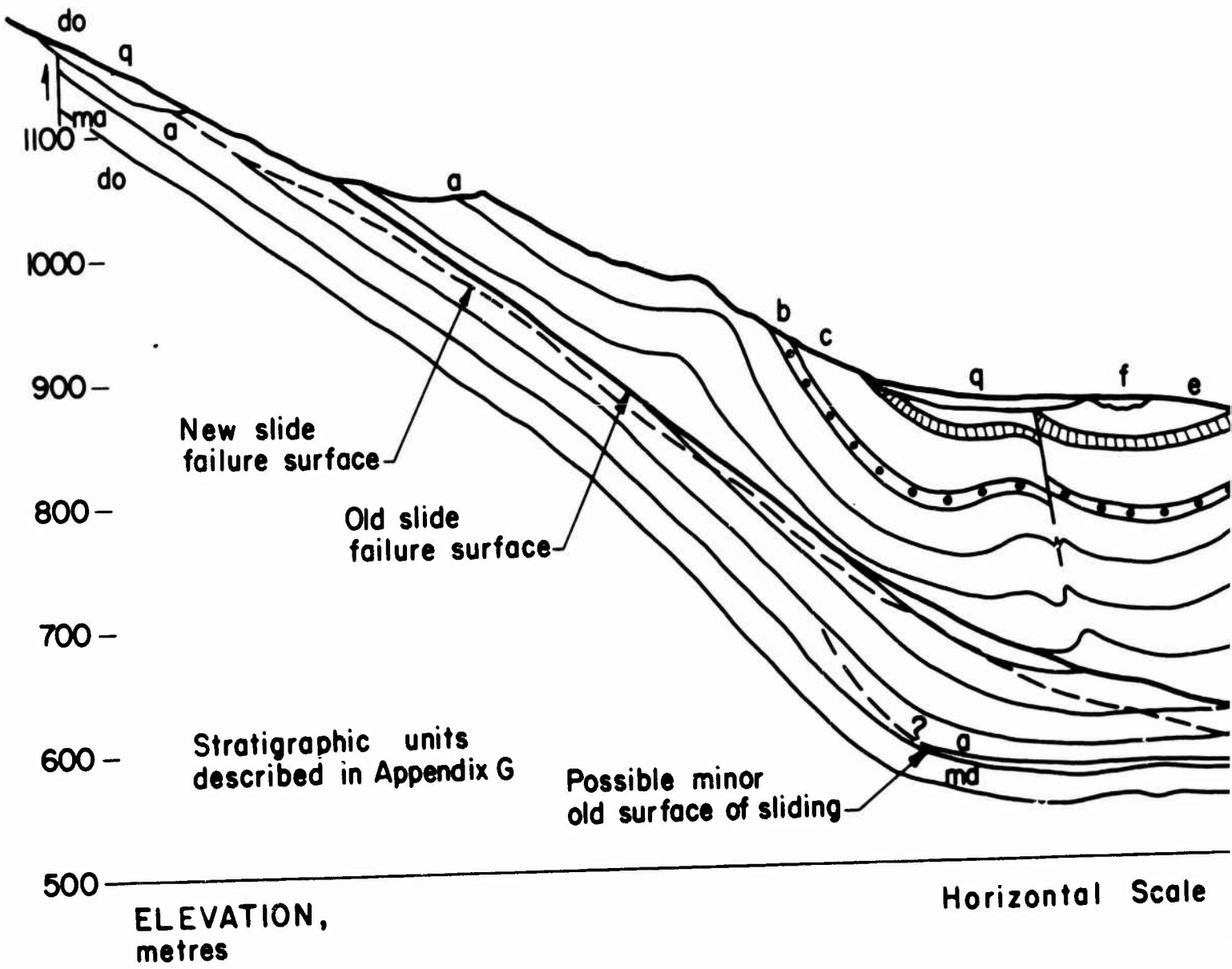


FIGURE 16
Geologic Section 2, Vaiont Slide
After October 9, 1963

South



North

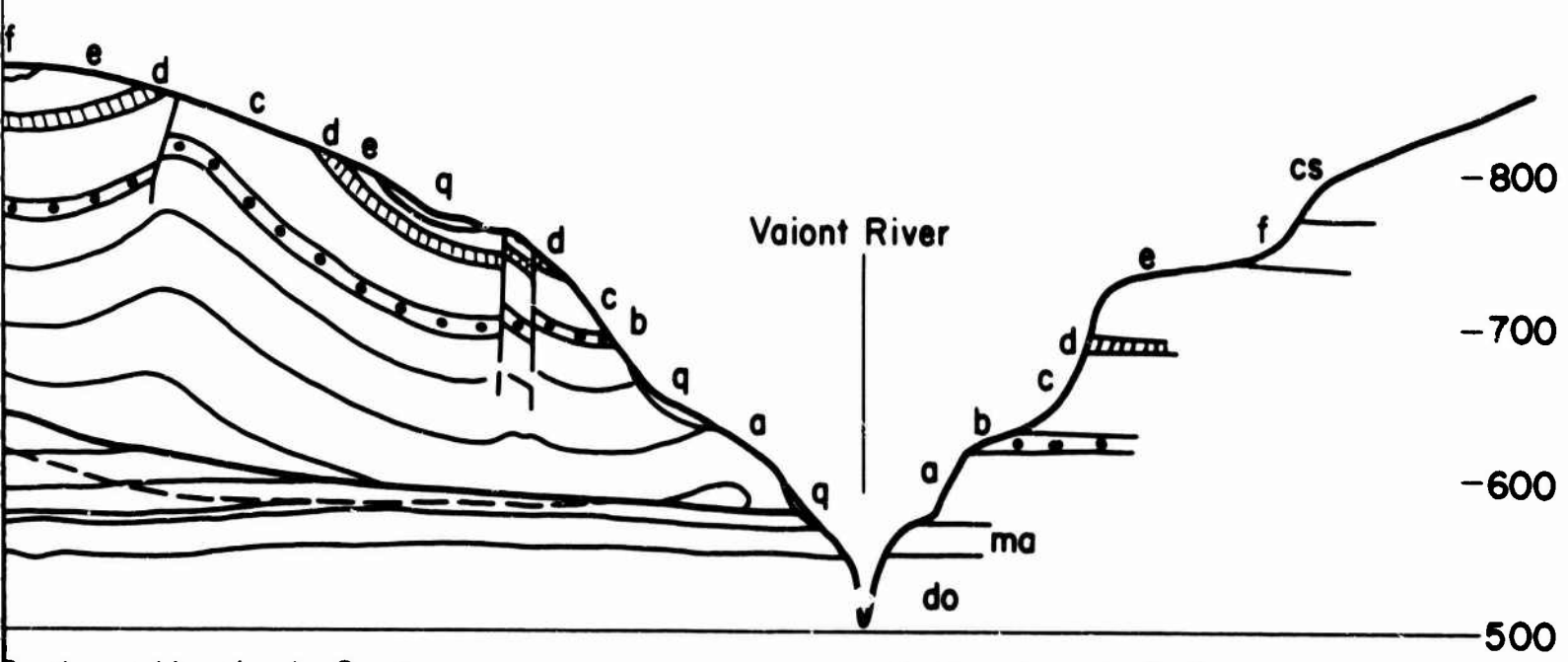
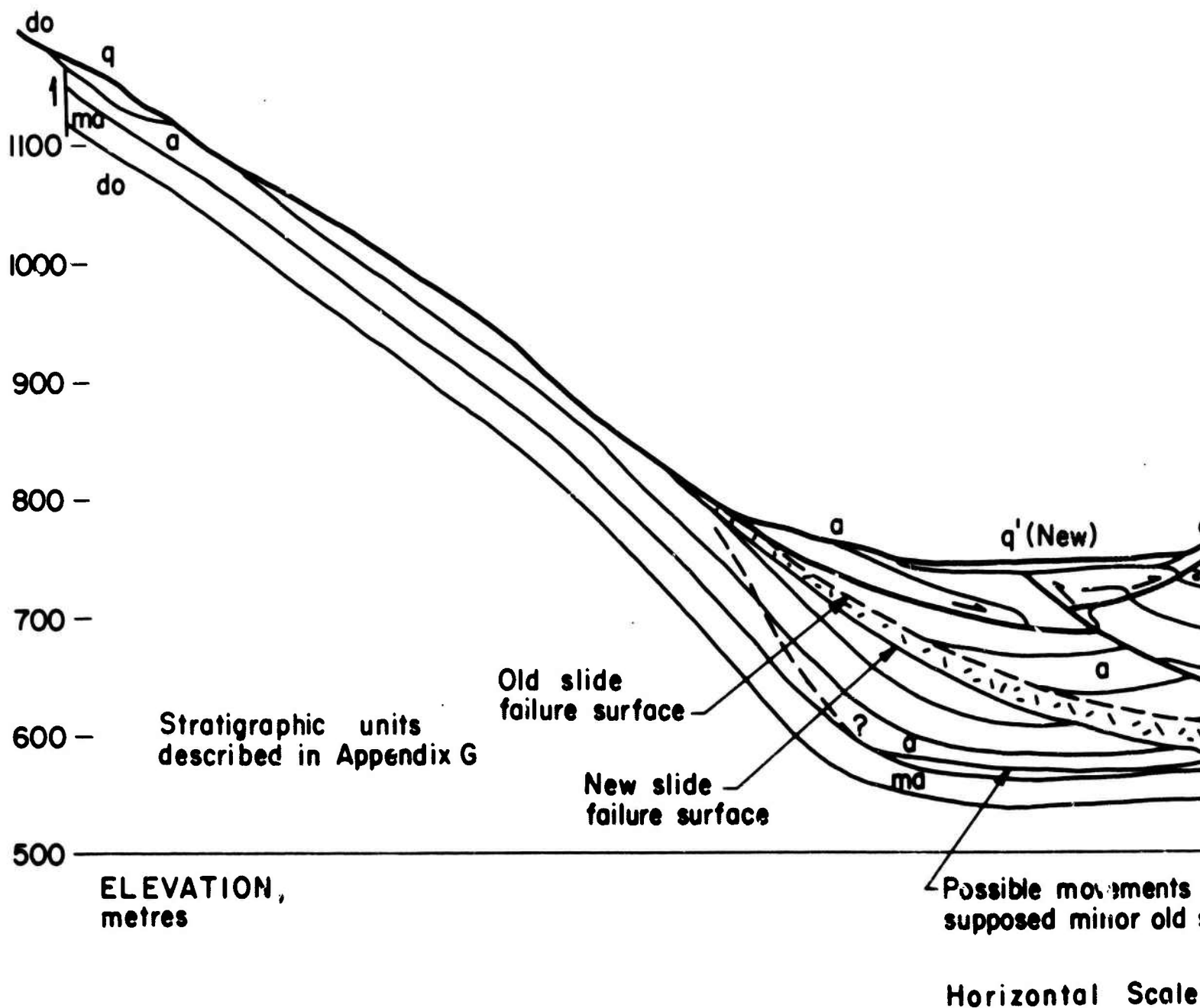
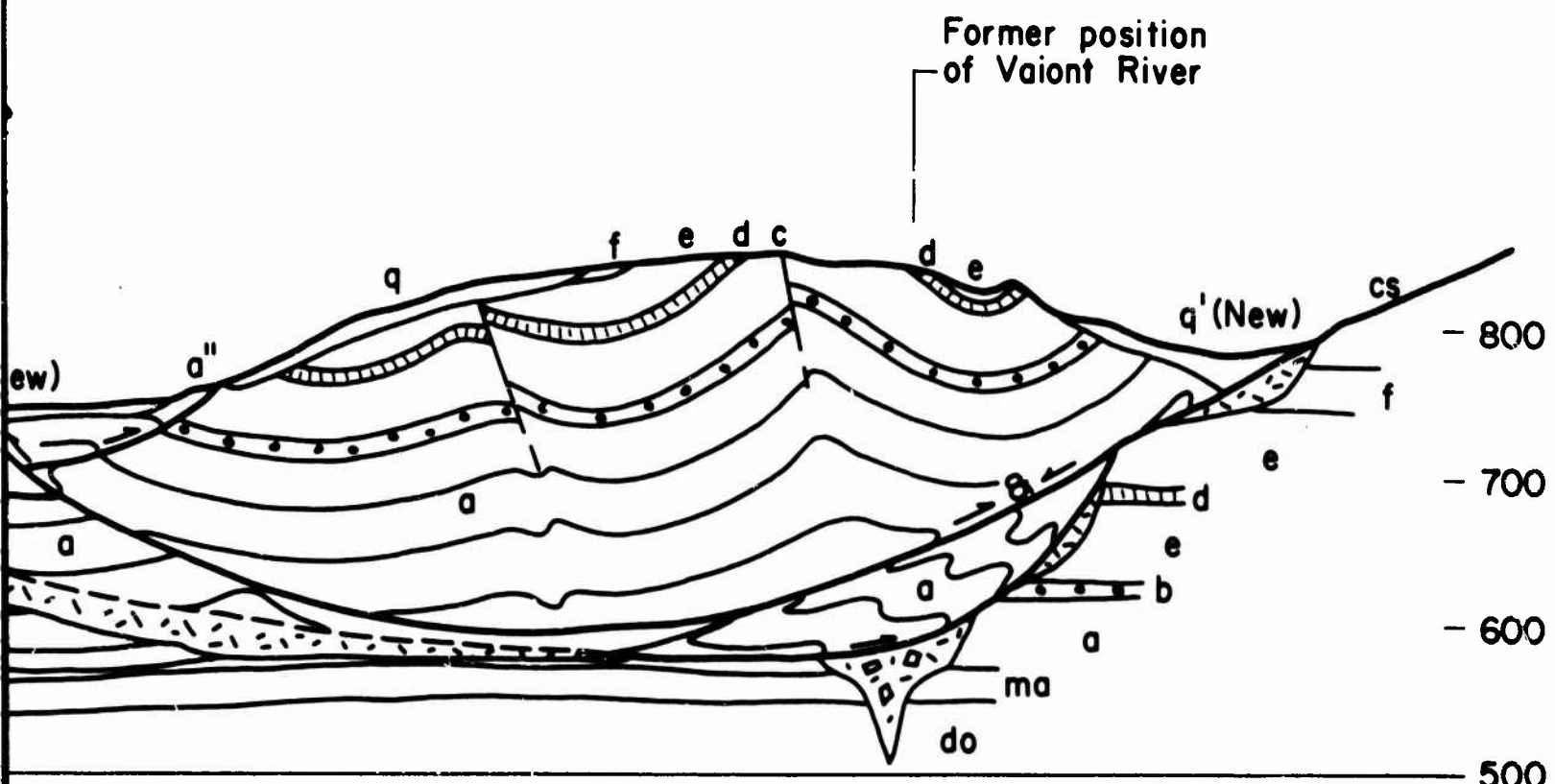


FIGURE 17
Geologic Section 5, Vaiont Slide
Before October 9, 1963

South



North



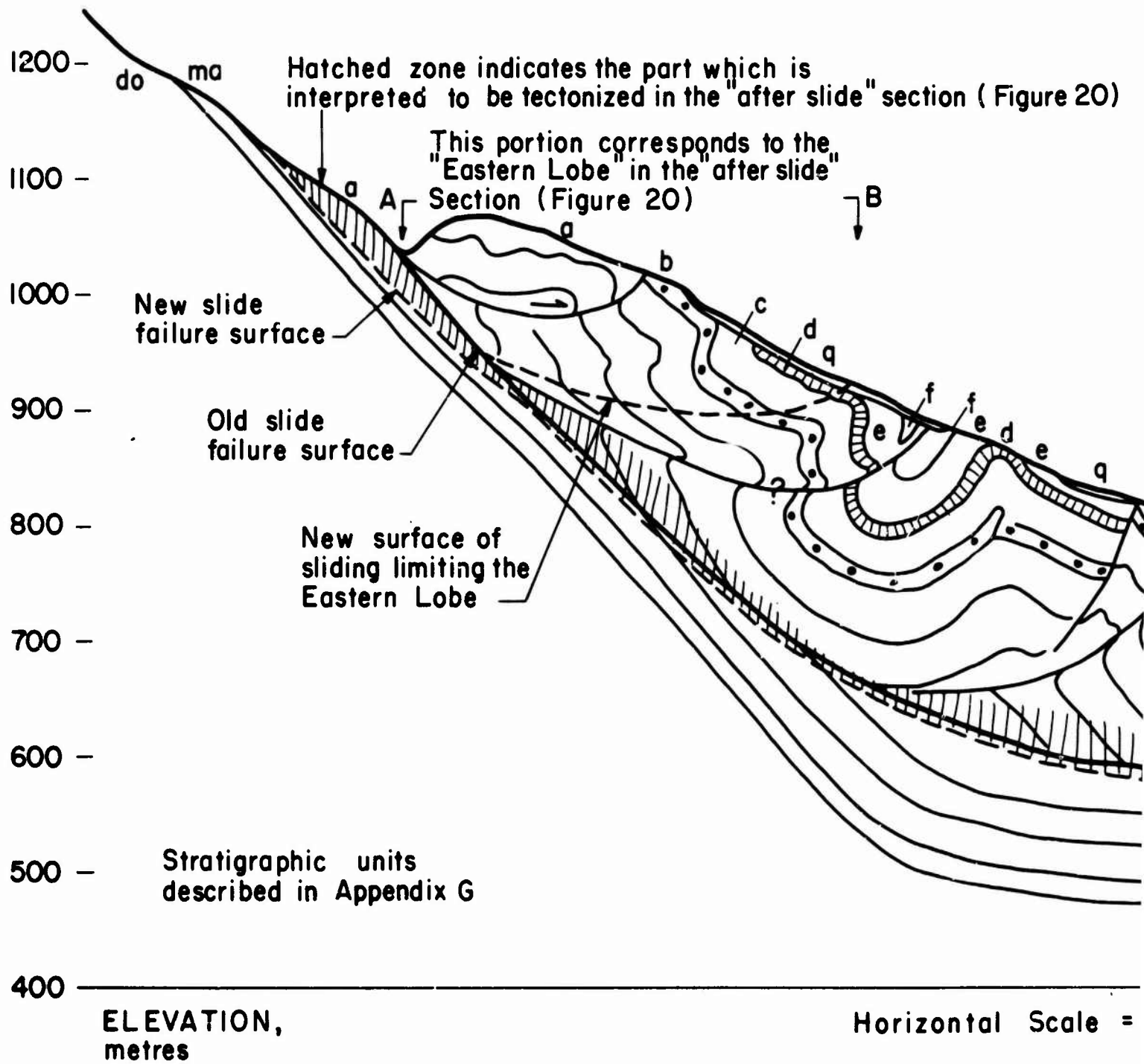
movements along this
minor old slide surface of sliding

By D. Rossi and E. Semenza, 1980

Total Scale = Vertical Scale

FIGURE 18
Geologic Section 5, Vaiont Slide
After October 9, 1963

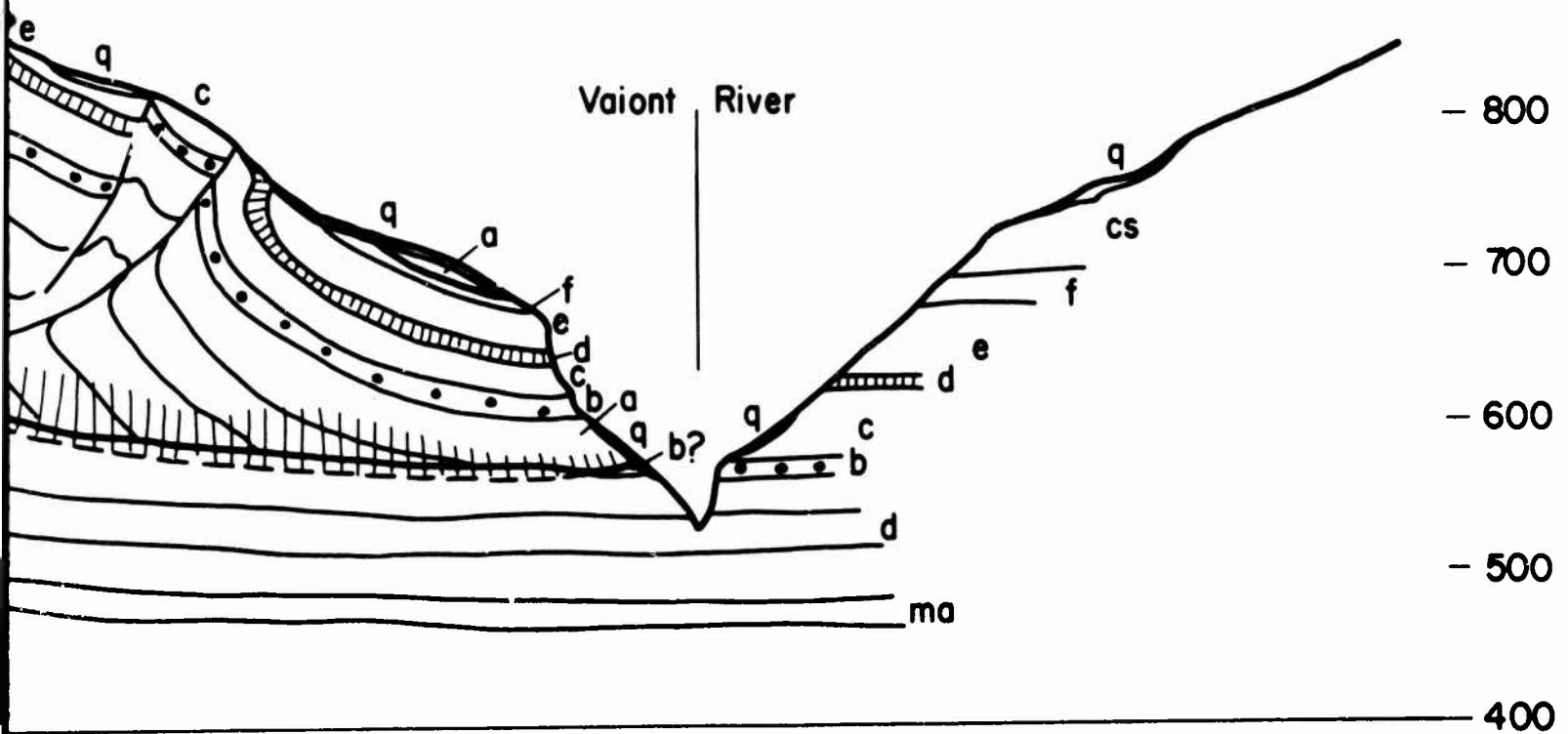
South



2

North

Figure 20)

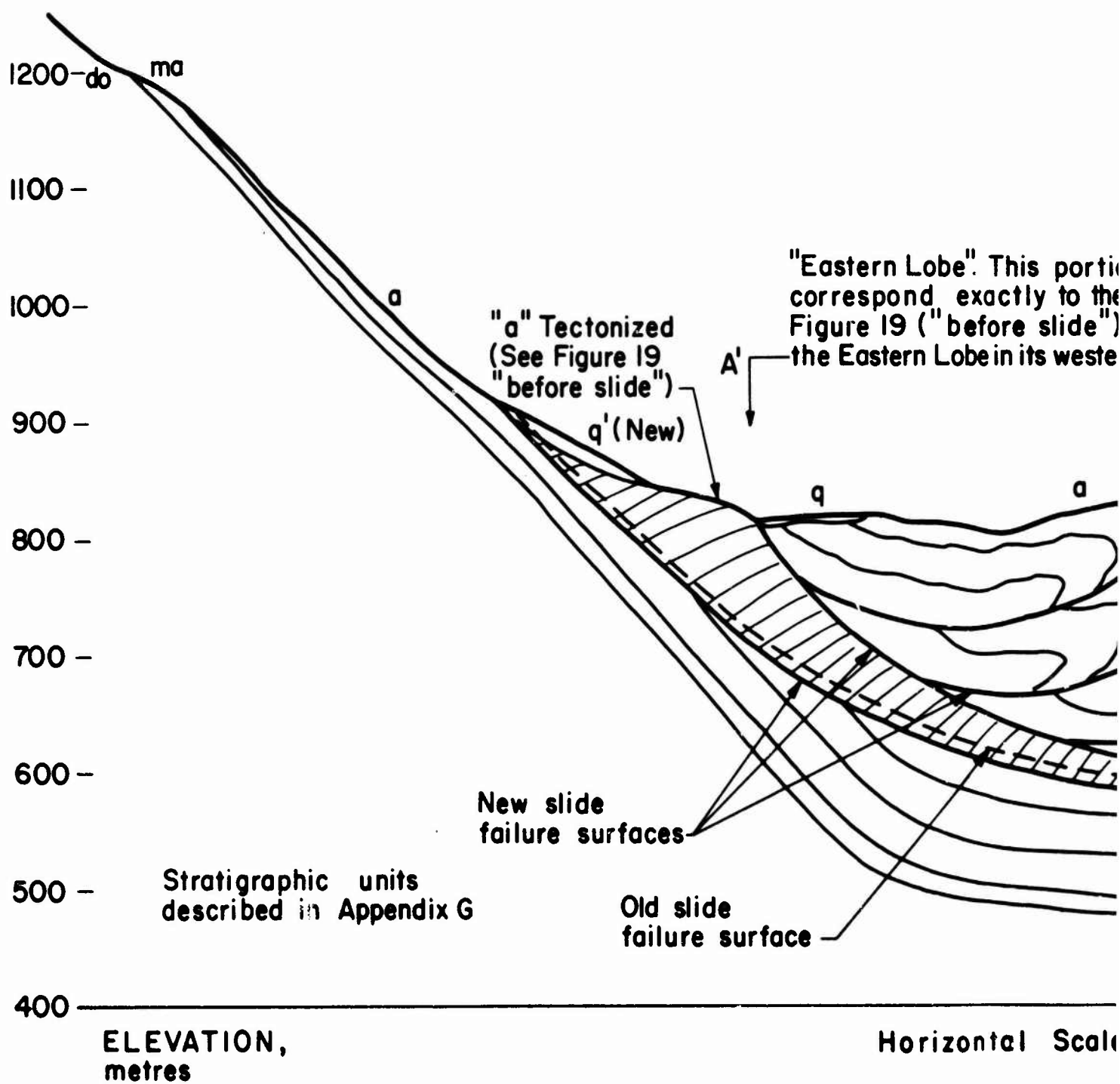


Scale = Vertical Scale

By D. Rossi and E. Semenza, 1980

FIGURE 19
Geologic Section IOA, Vajont Slide
Before October 9, 1963

South



North

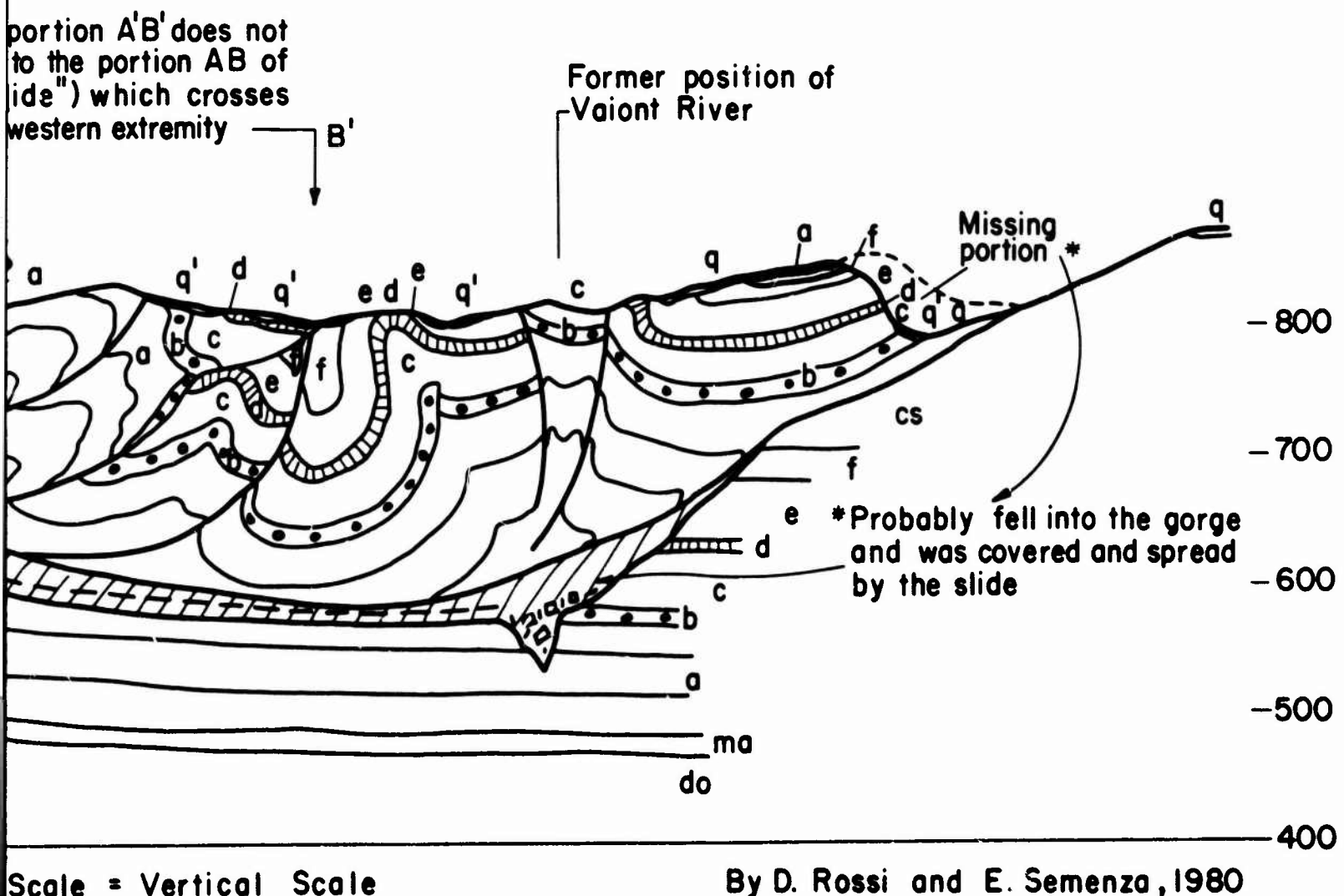


FIGURE 20
Geologic Section IOA, Vaiont Slide
After October 9, 1963

Elevation
metres

West

1000-

Section
2

Section
5

Perimetral
Cracks

800-

600-

400-

Horizontal Scale = Vertical Scale

For location of Section ..

LEGEND

— — — Surface before slide

— — Surface after slide

9

Drill Hole

-S

Slide failure surface (interpreted)

-O

Top of colluvium

1

Mapped fault

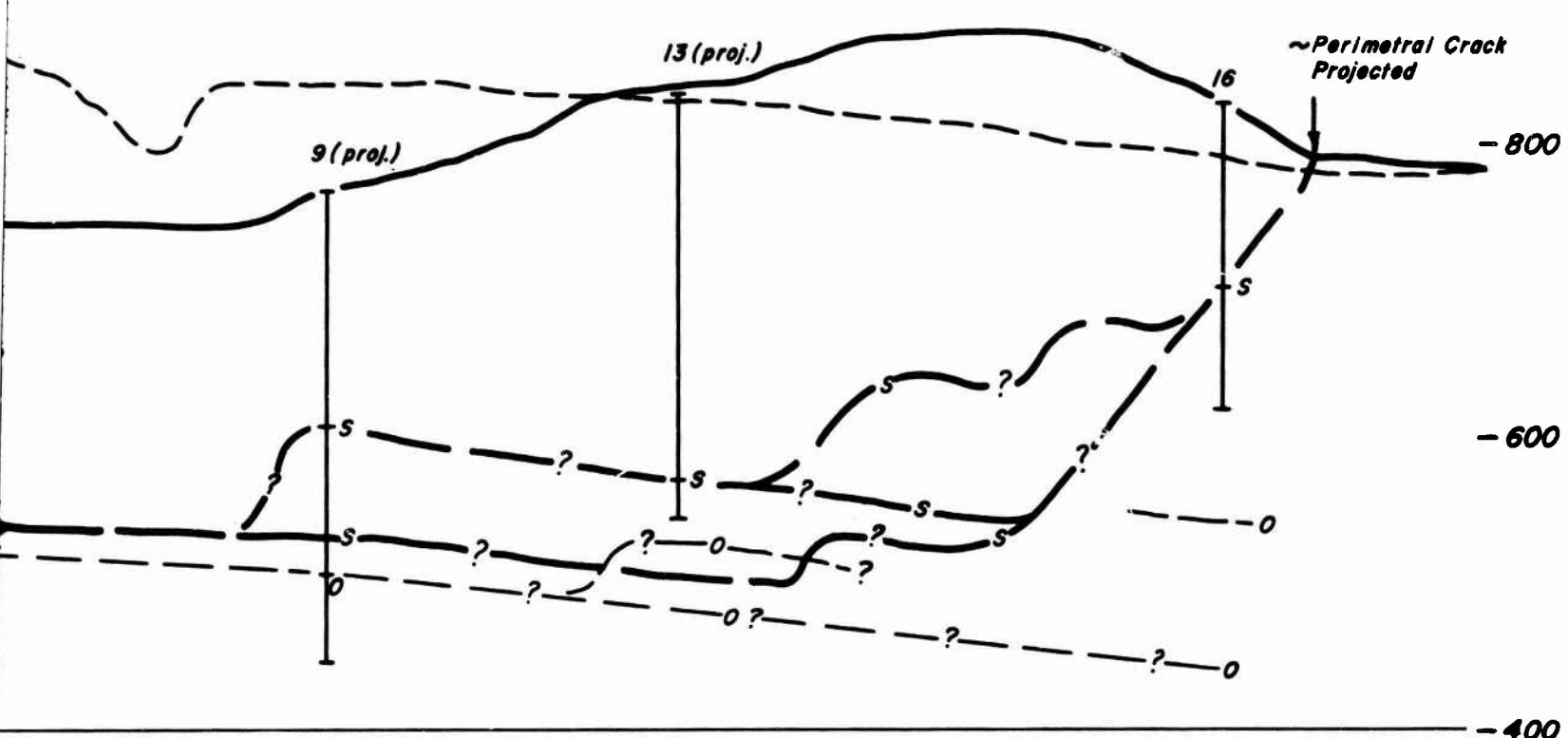
1P

Mapped fault (projected)

East

-1000

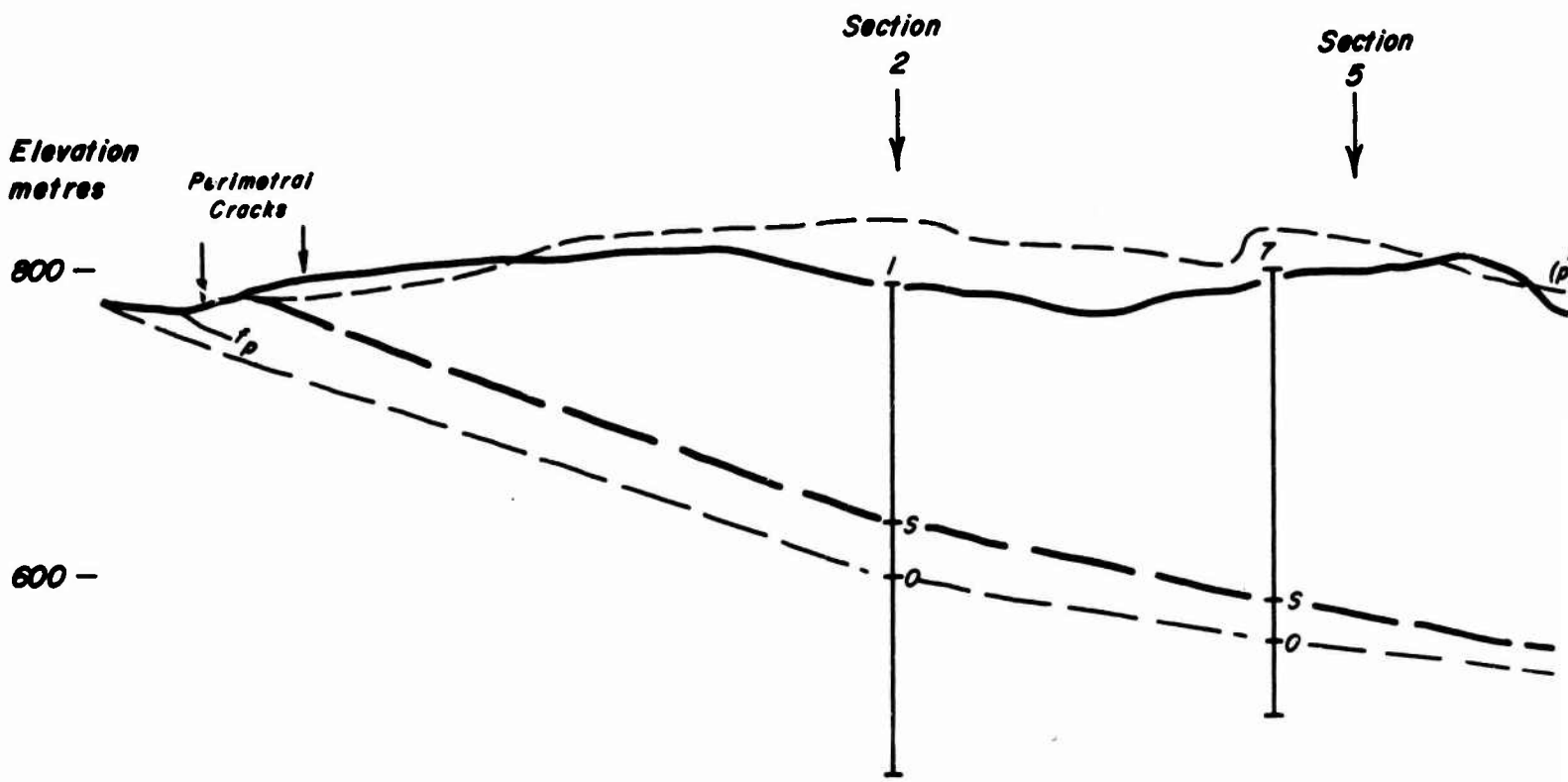
Section
10A



ction 16 see Figures 11 and 12

FIGURE 21
Vaiont Slide
Geologic Section 16

West



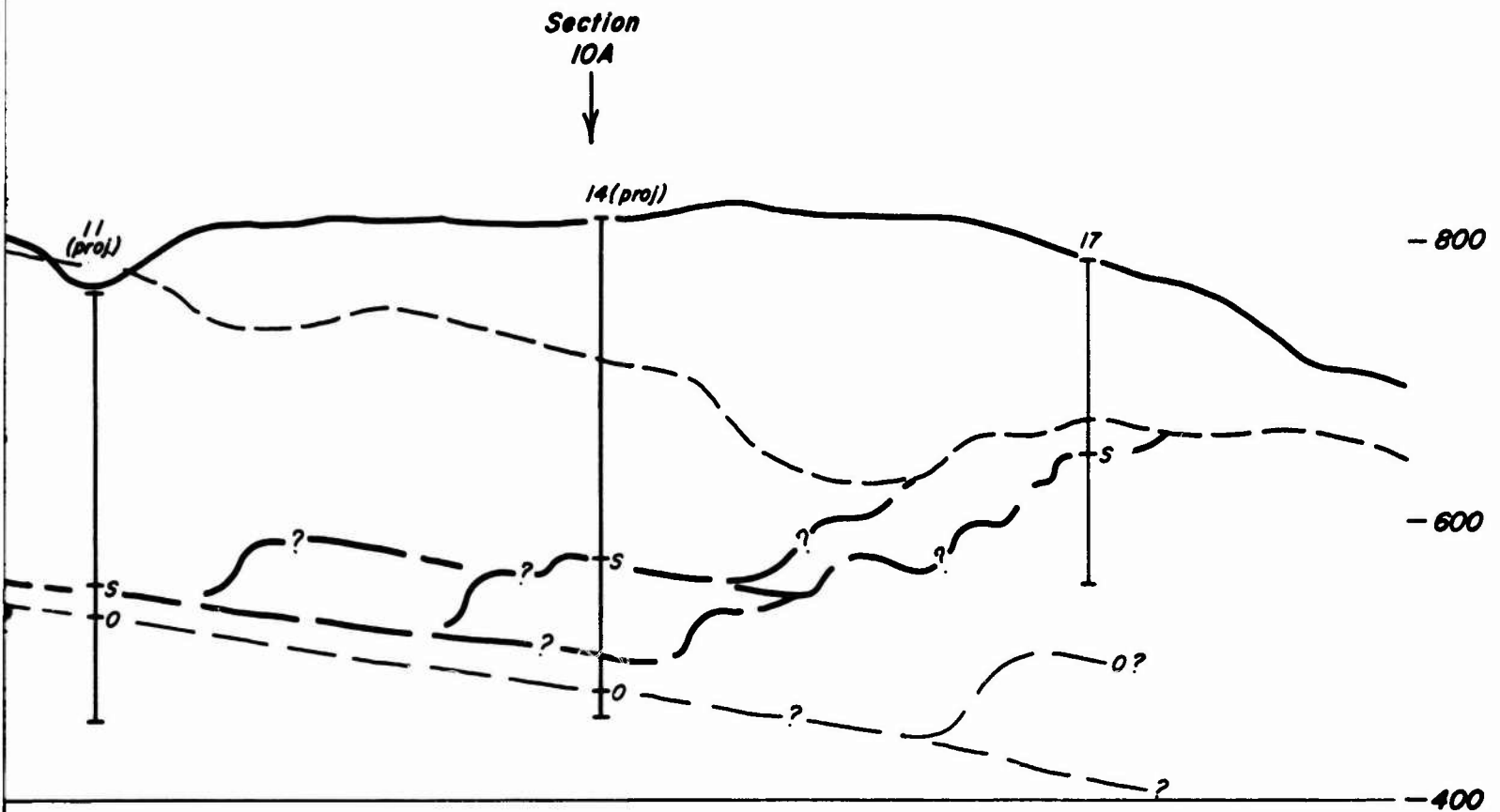
400 -
 Horizontal Scale = Vertical Scale

For location of Section 17 see F.

LEGEND

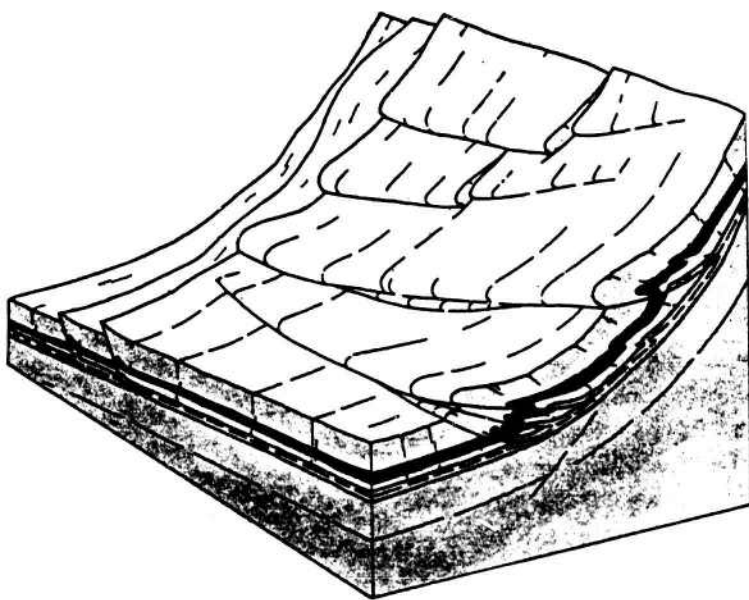
- — — Surface before slide
- — — Surface after slide
- Drill Hole
- S Side failure surface (interpreted)
- O Top of coalbeds
- Fault
- Mapped fault (projected)

East



see Figures 11 and 12

FIGURE 22
Valiant Slide
Geologic Section 17



(after Carloni and
Mazzanti, 1964b)

Figure 23. Schematic block diagram illustrating the formation of cascade structures, Vajont Slide

Figures 24a and 24b are a stereopair and are in the
pocket at the back of this volume.

Figures 24a and 24b. Airphoto of the Vajort Dam
and Reservoir taken in 1960 (stereopair)

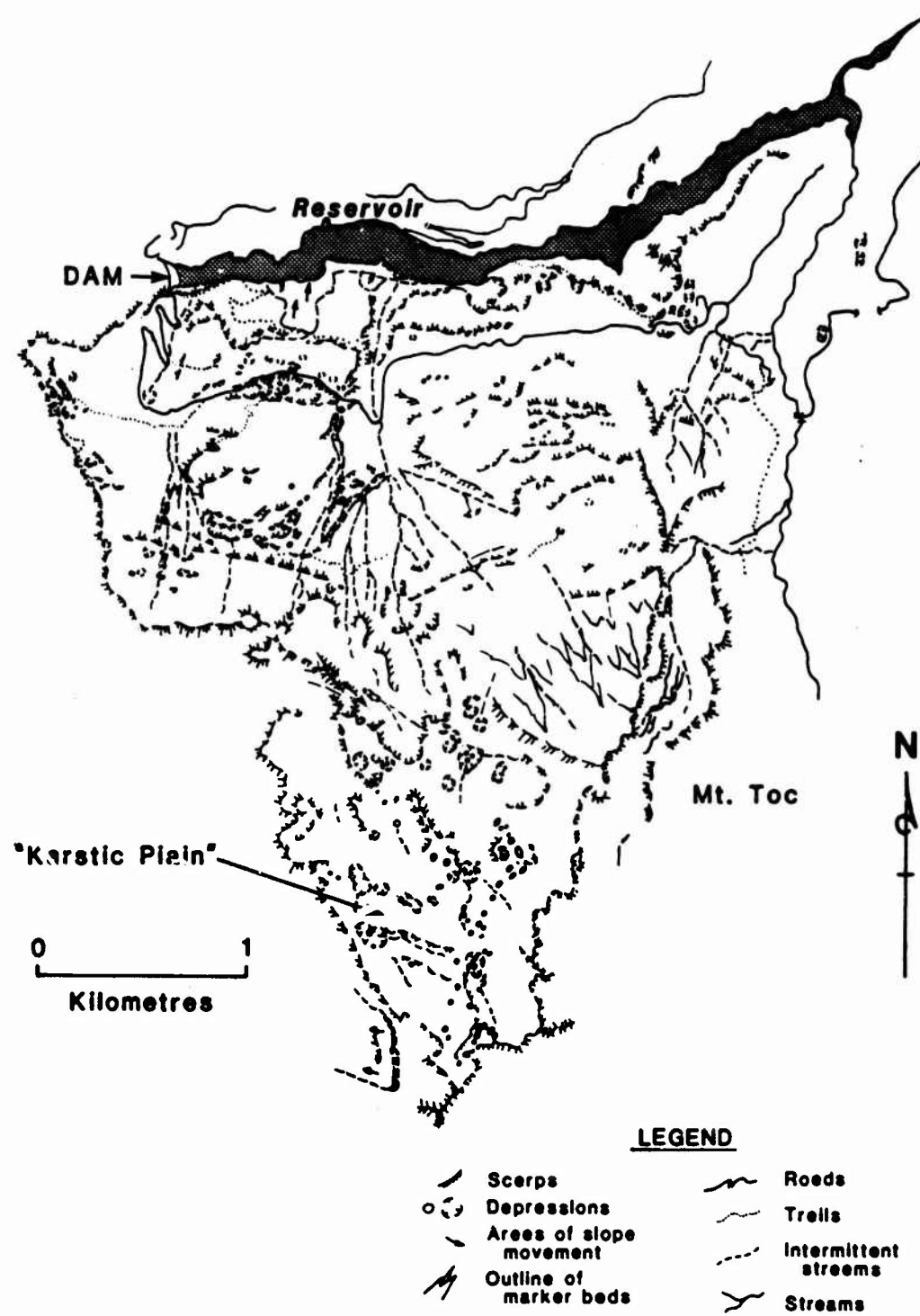


Figure 25a. Geomorphic features, Vaiont Slide, delineated from the 1960 airphotos

Figure 25b is a transparent overlay to Figure 24a and
is in the pocket at the back of this volume.

Figure 25b. Geomorphic features, Vajont Slide,
delineated from the 1960 airphotos

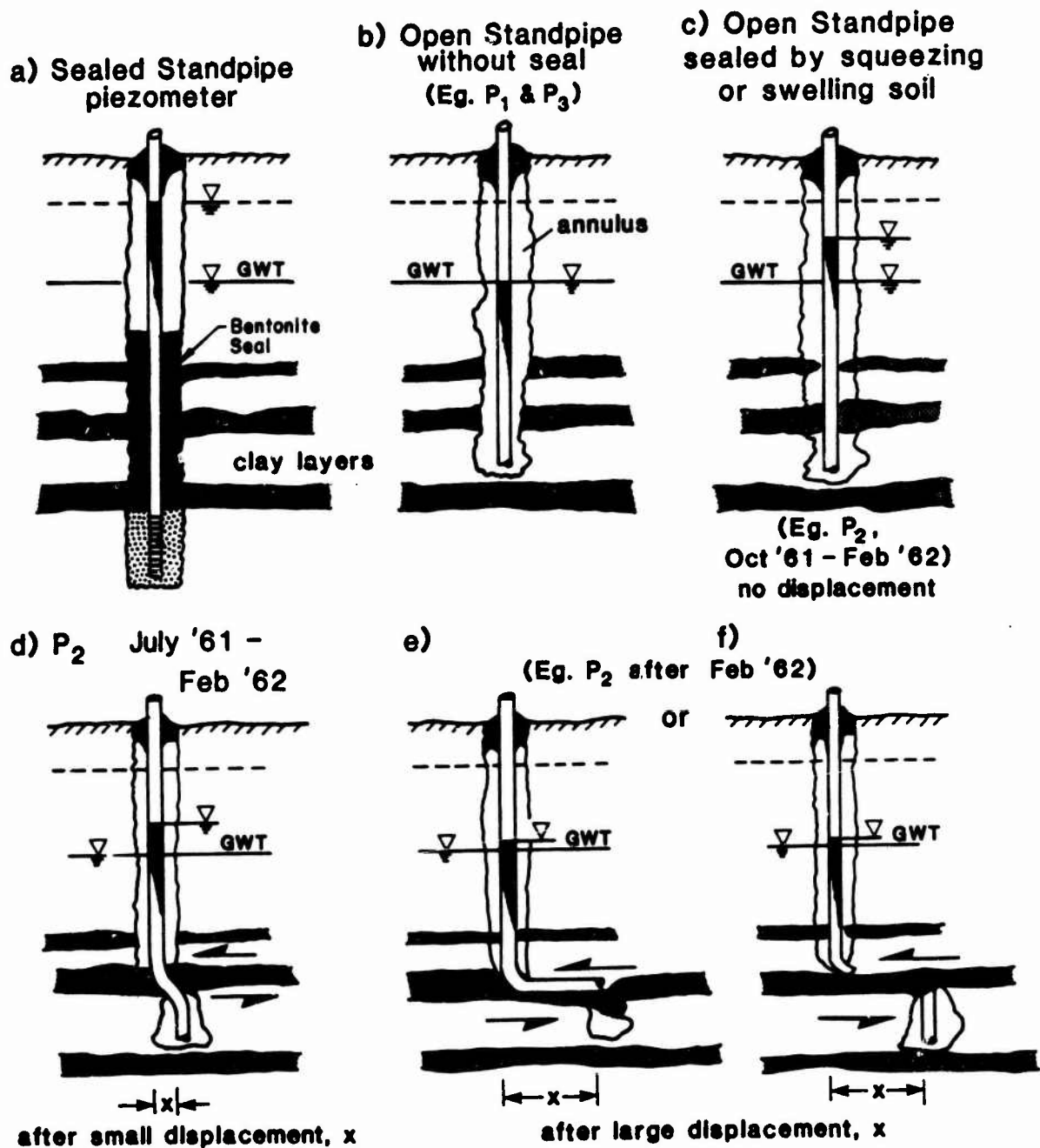


Figure 26. Sketches showing a possible explanation for water levels recorded in P-2

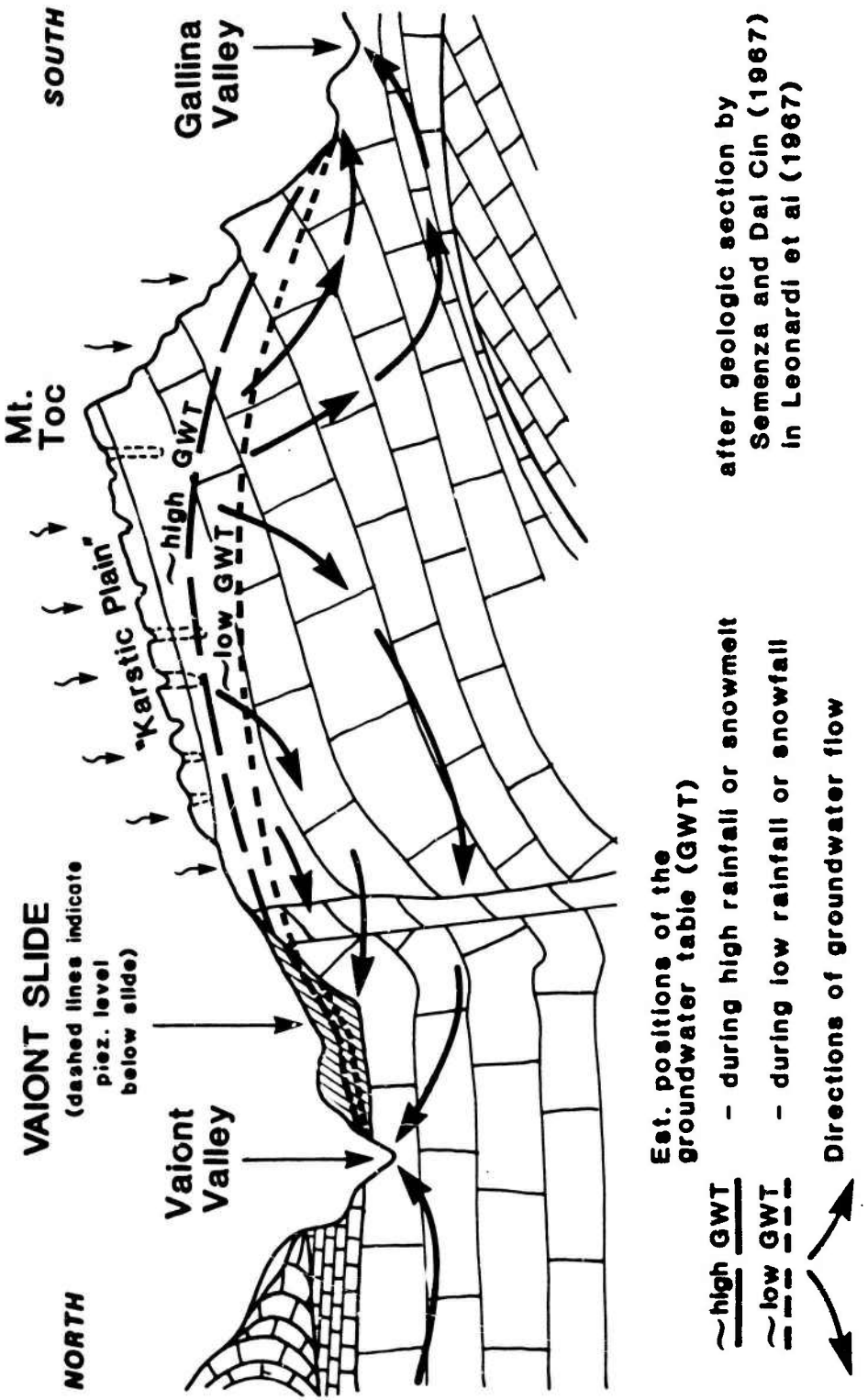


Figure 27. Schematic section through Vaiont Slide showing estimated regional groundwater flow system

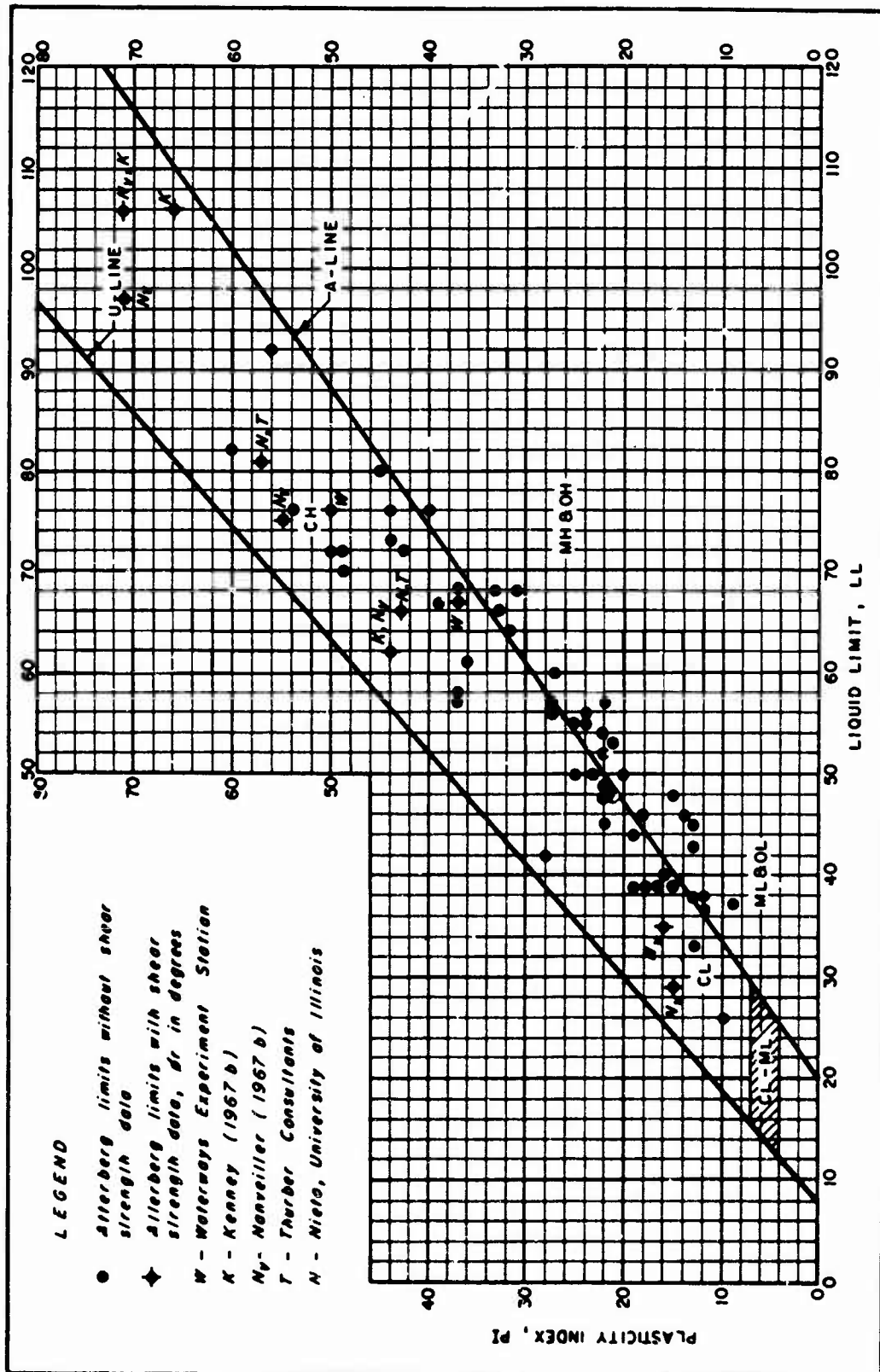


Figure 28. Plasticity chart, clay samples, Vaiont Slide

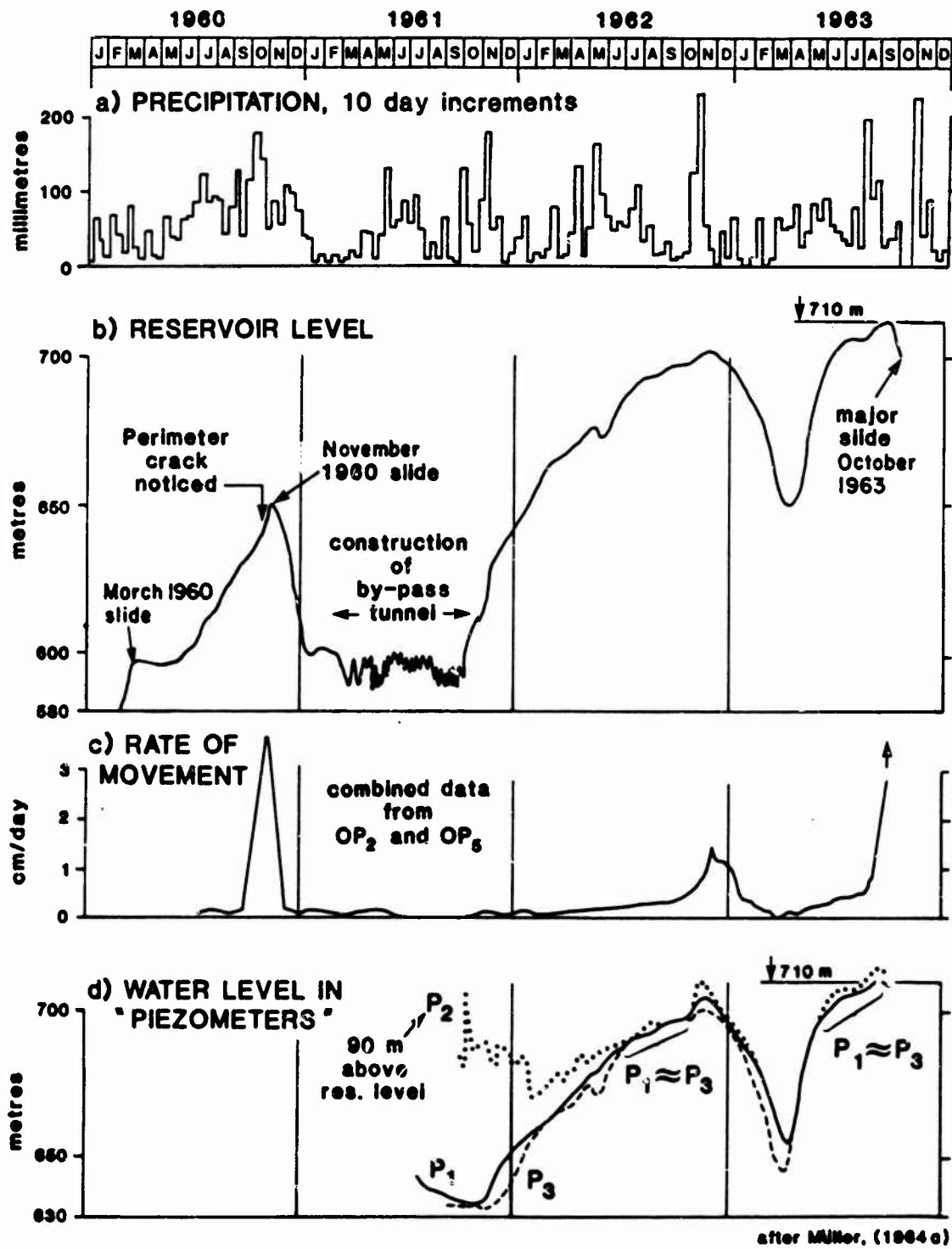


Figure 29. Vajont Slide, comparison of water levels, movements, and precipitation, 1960 through 1963

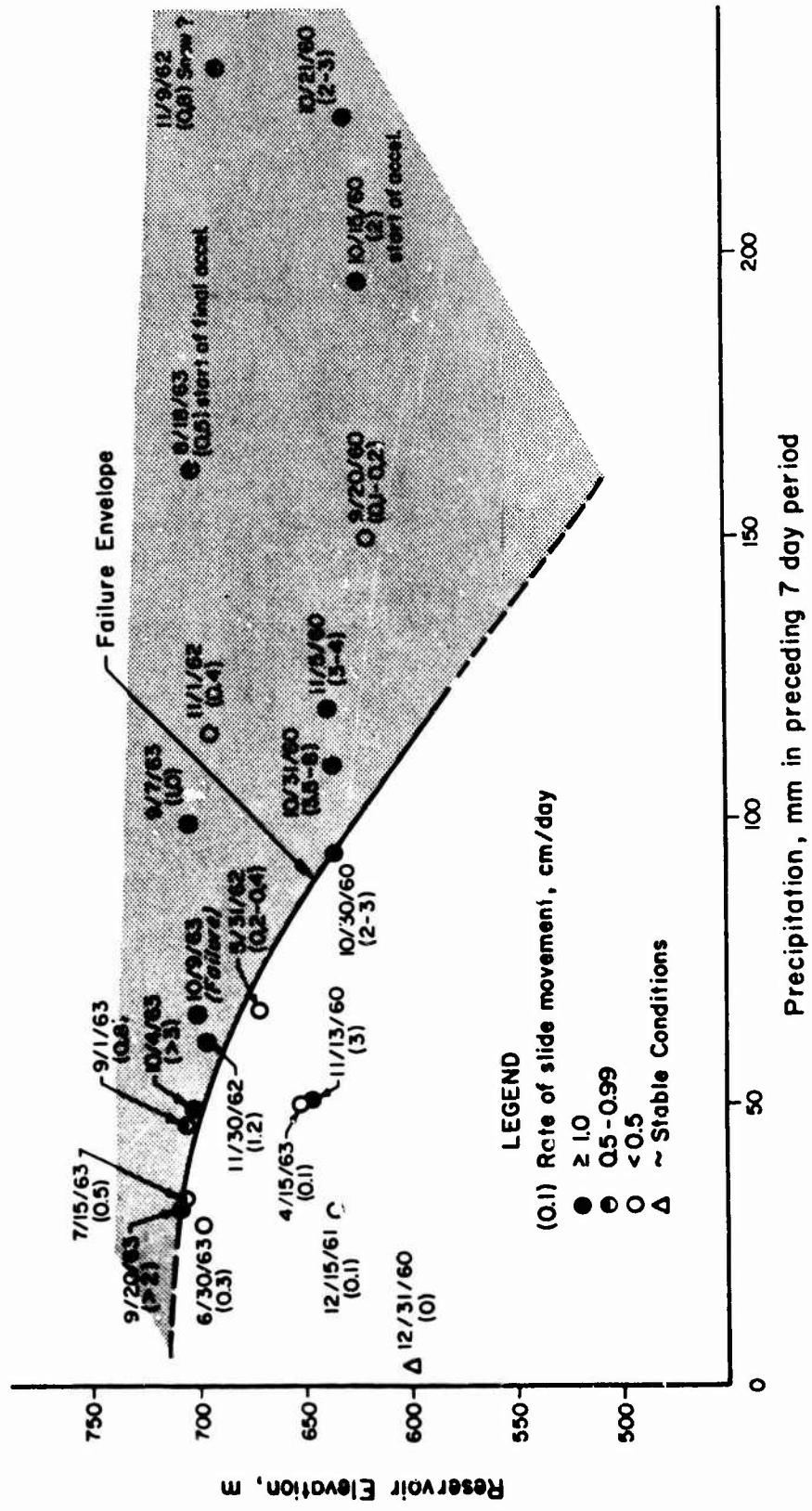


Figure 30. Stability of Vajont Slide for reservoir elevation vs. 7-day precipitation

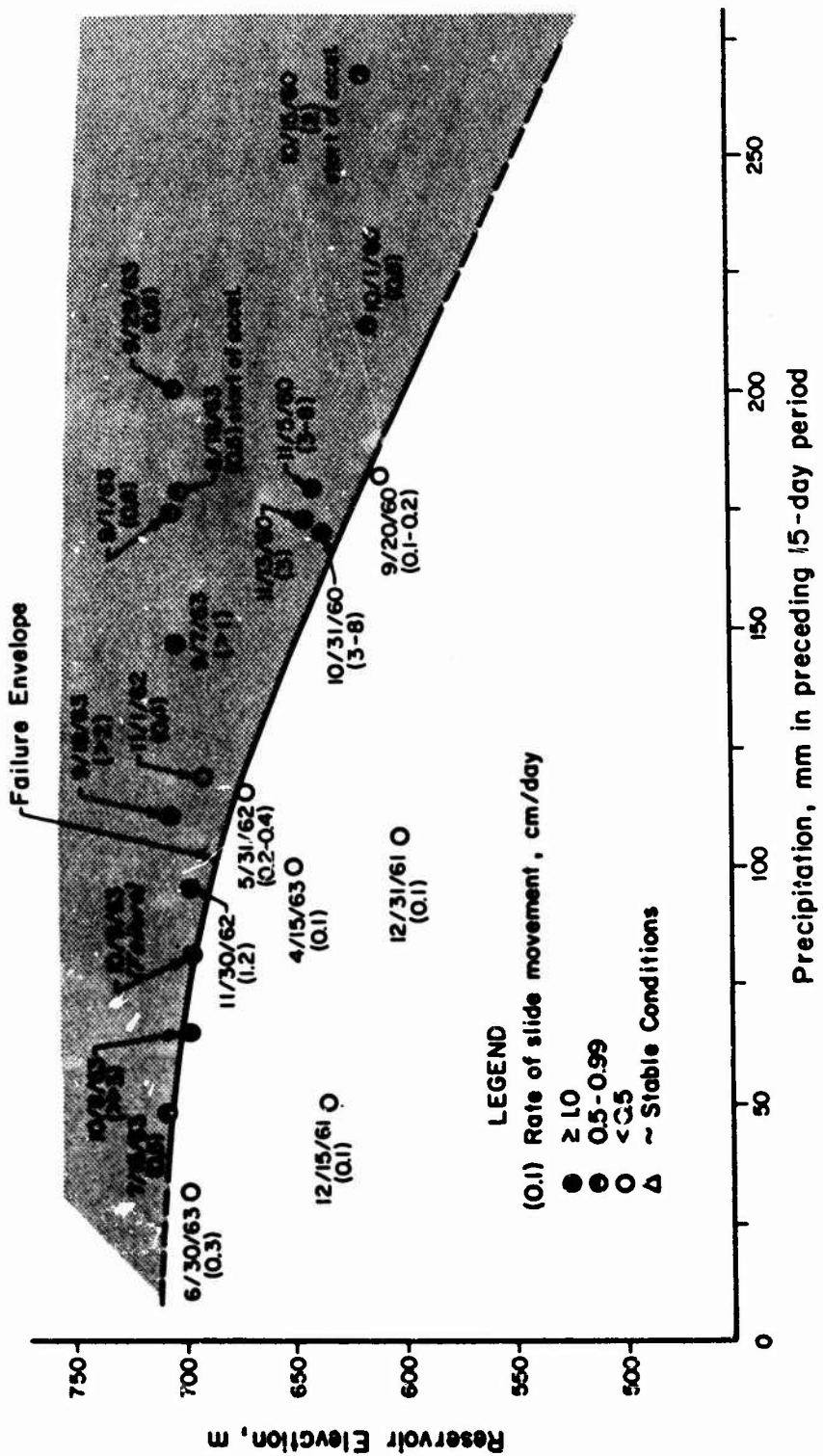


Figure 31. Stability of Vajont Slide for reservoir elevation vs. 15-day precipitation

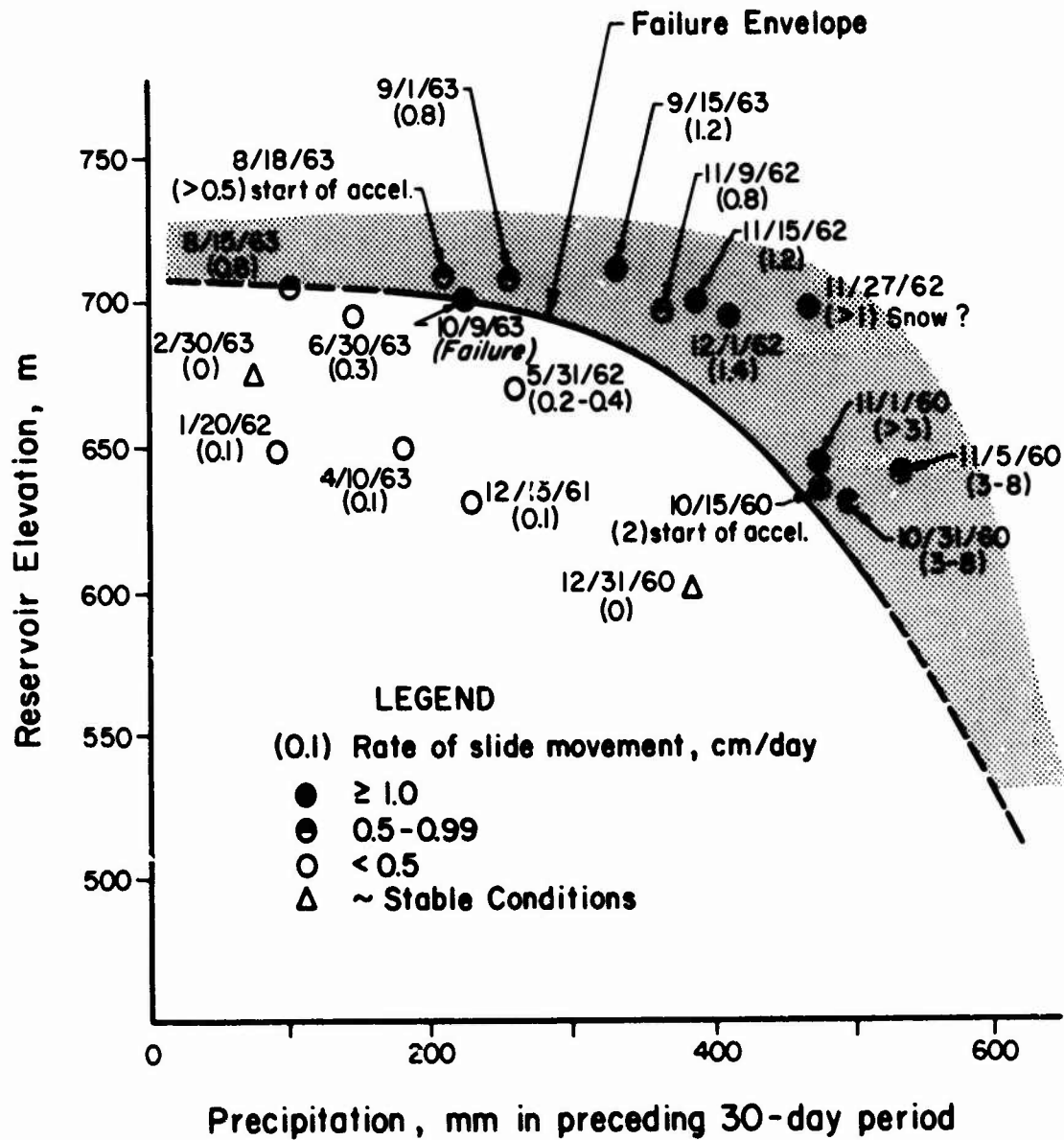


Figure 32. Stability of Vajont Slide for reservoir elevation vs. 30-day precipitation

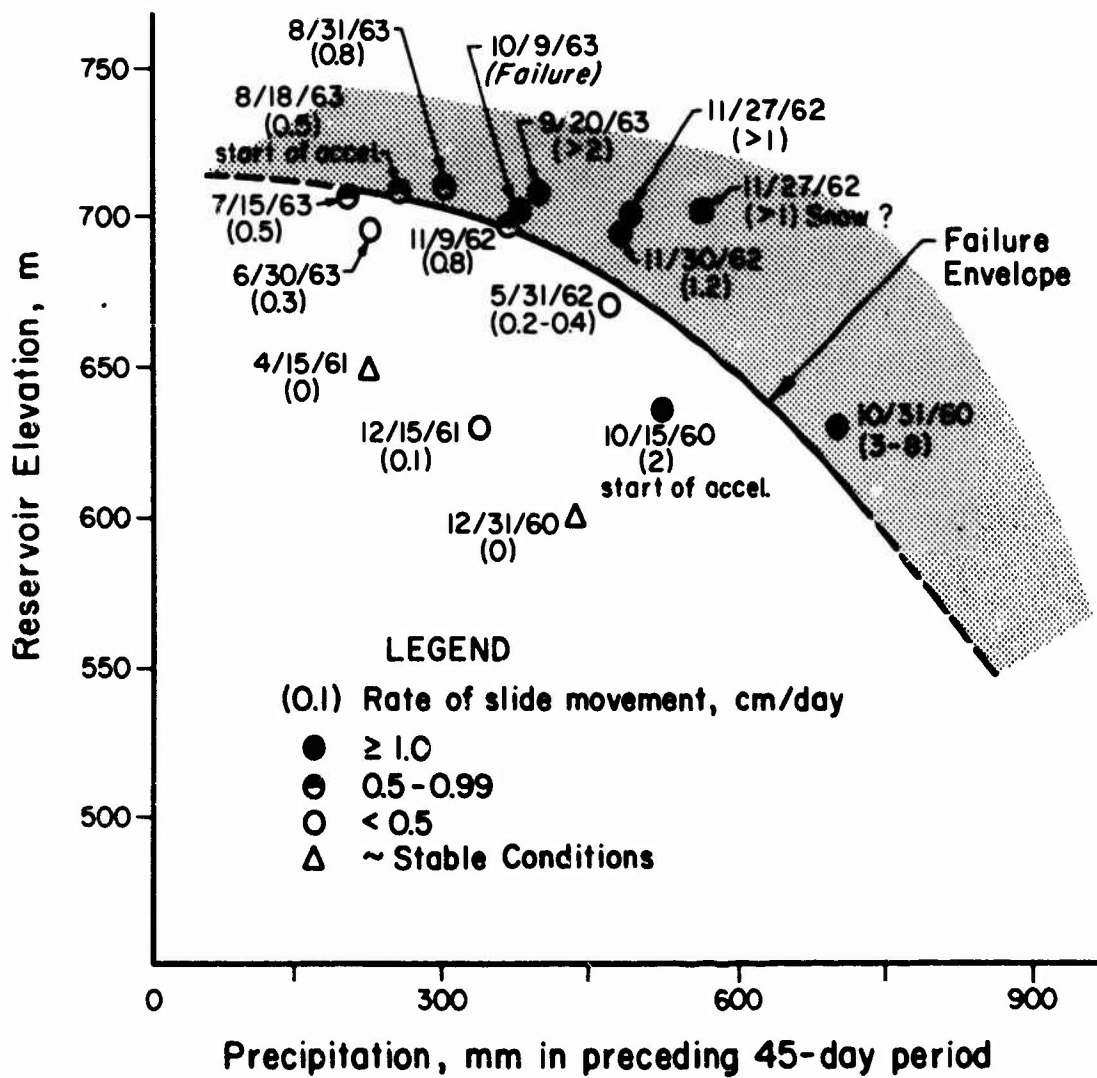


Figure 33. Stability of Vaiont Slide for reservoir elevation vs. 45-day precipitation

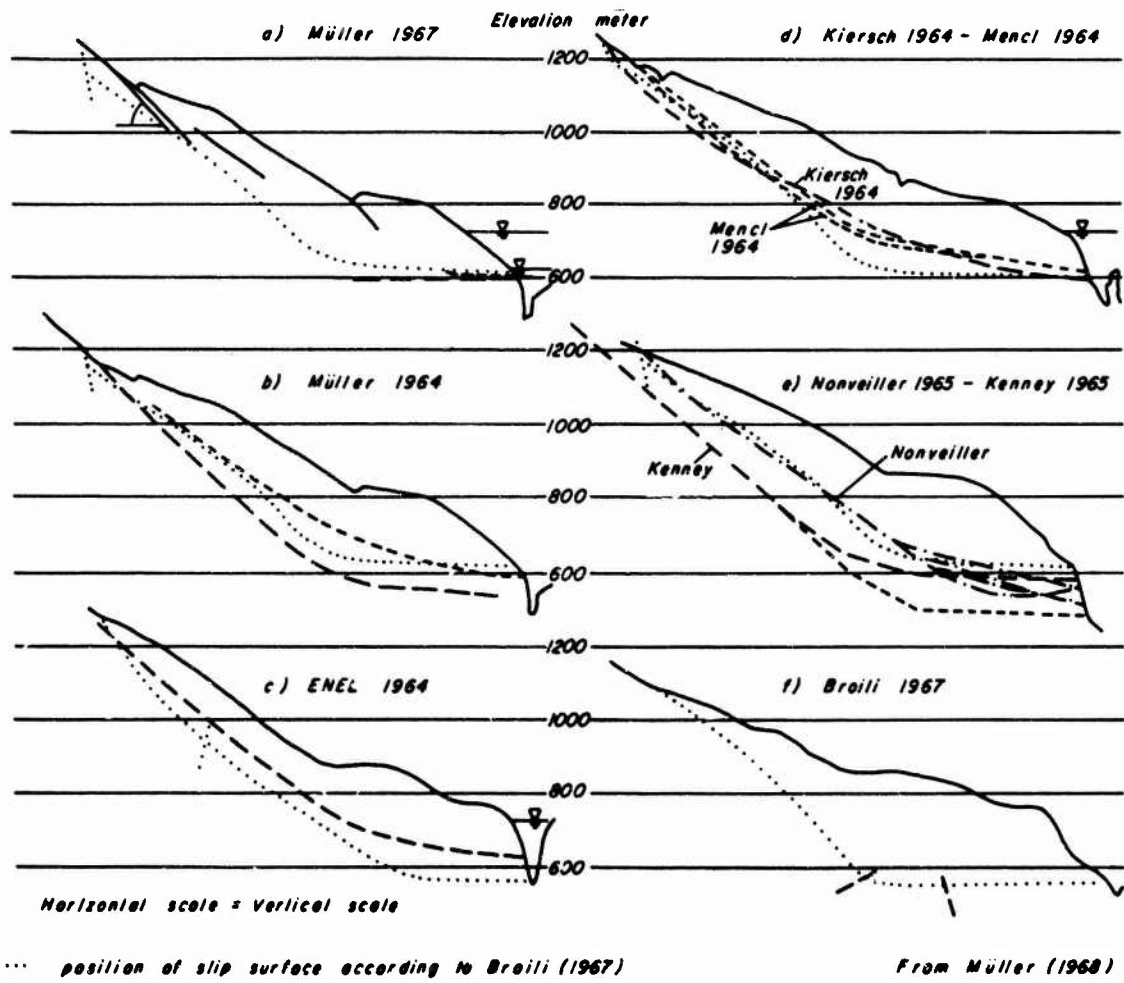


Figure 34. Slip surfaces of Vajont Slide assumed by previous authors

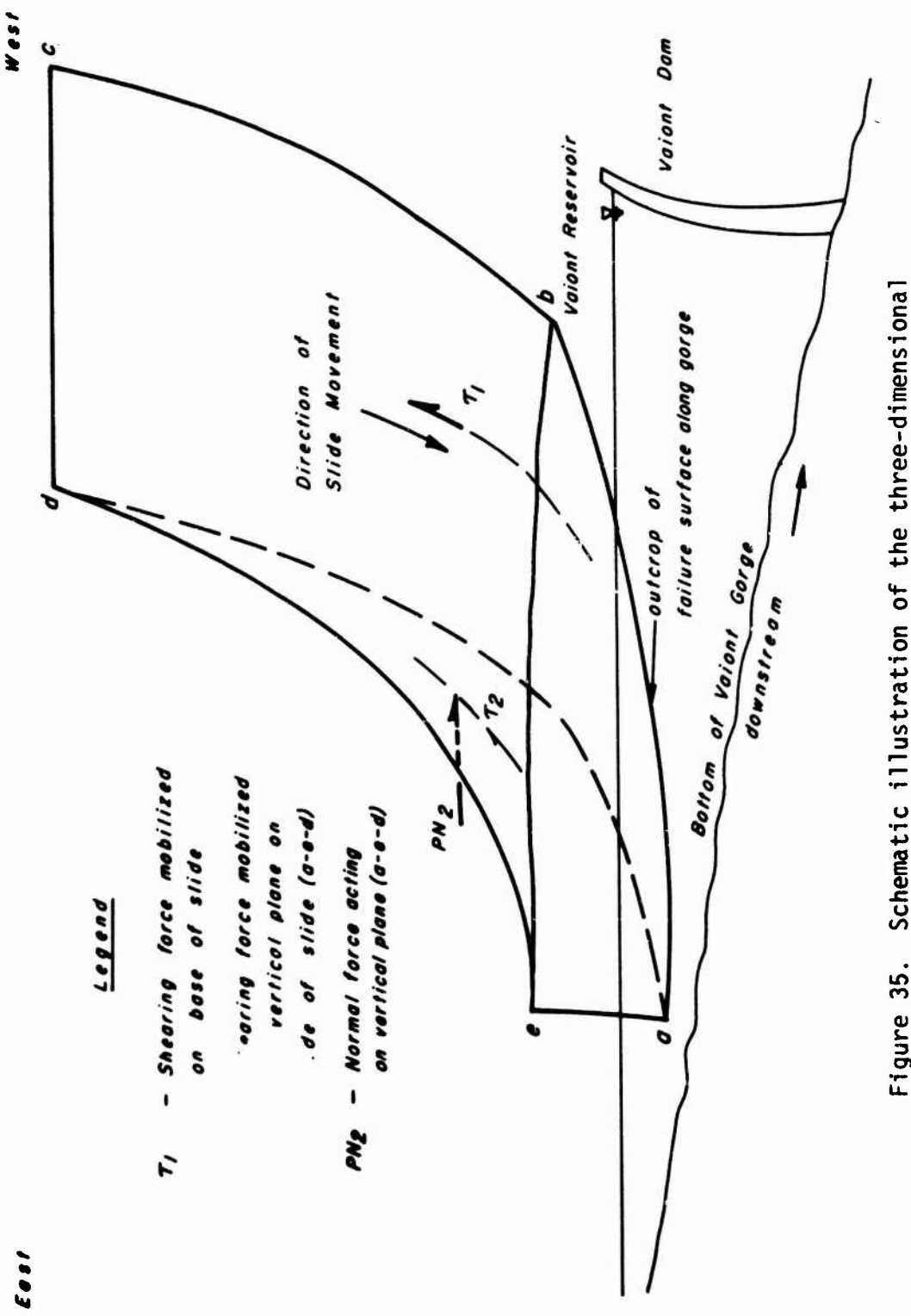
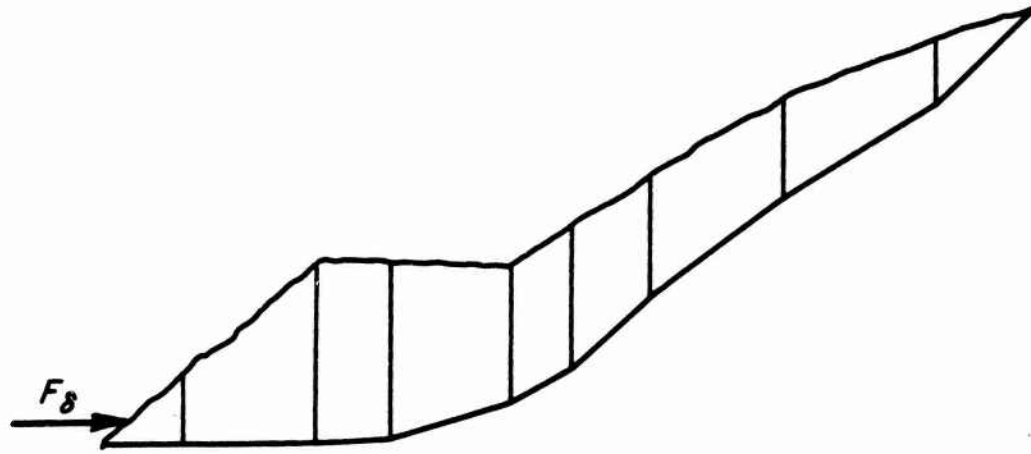
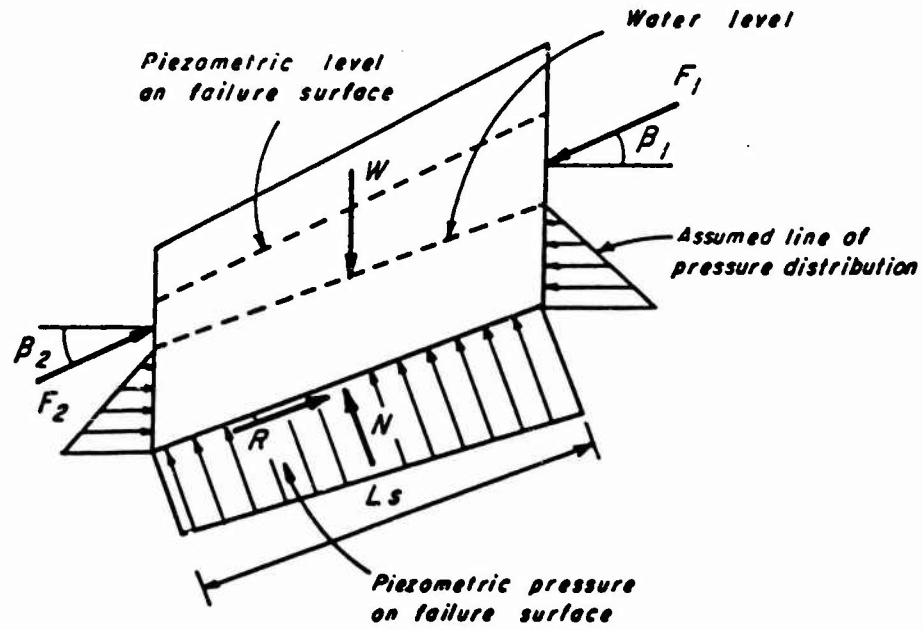


Figure 35. Schematic illustration of the three-dimensional nature of the Vaiont Slide mass



a) SUBDIVISION OF SLIDE INTO SLICES



W = total weight of soil and water above the failure surface

N = effective reaction normal to the failure surface

R = shearing resistance of the soil

F_1, F_2 = interelement forces between adjacent slices

β_1, β_2 = inclination of the interelement forces from the normals to the slice faces.

b) FORCES ON A TYPICAL SLICE OF THE SLIDE

Figure 36. Selection of typical slices and forces acting on a typical slice

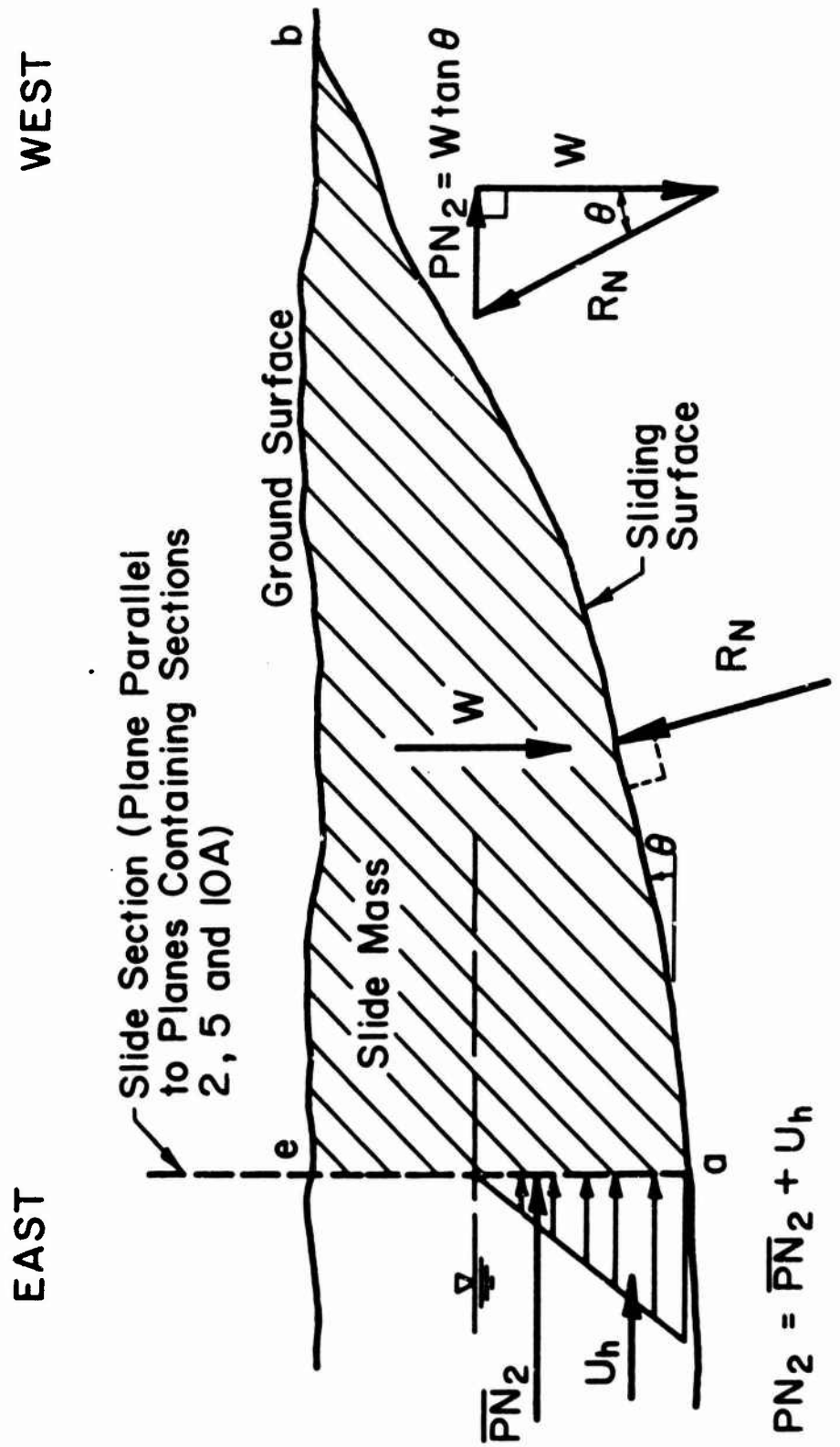


Figure 37. Schematic representation of normal forces on slide cross-section developed by the upstream dip of the sliding surface

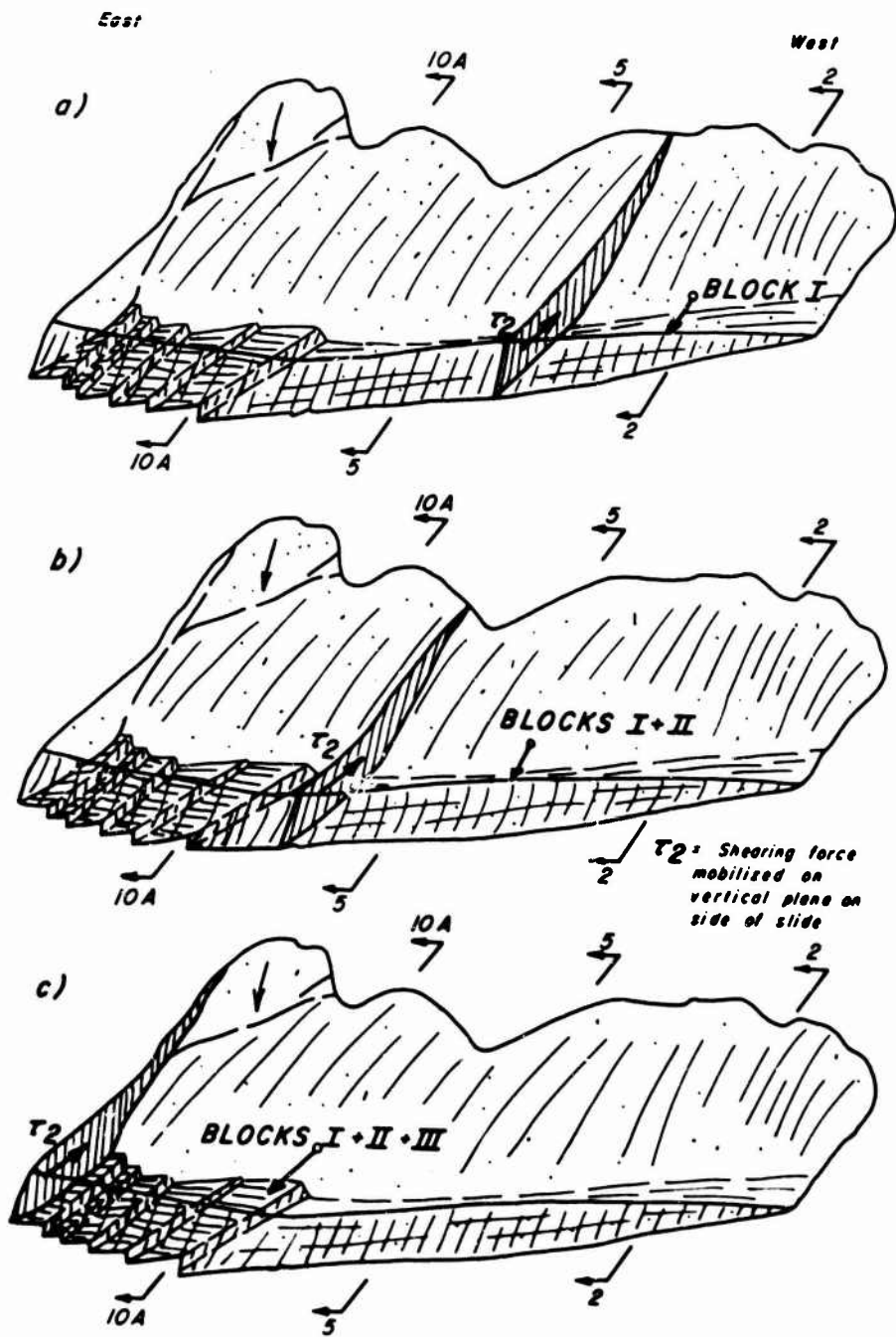


Figure 38. Vaiont Slide, schematic illustration of the three blocks used in the three-dimensional stability analysis

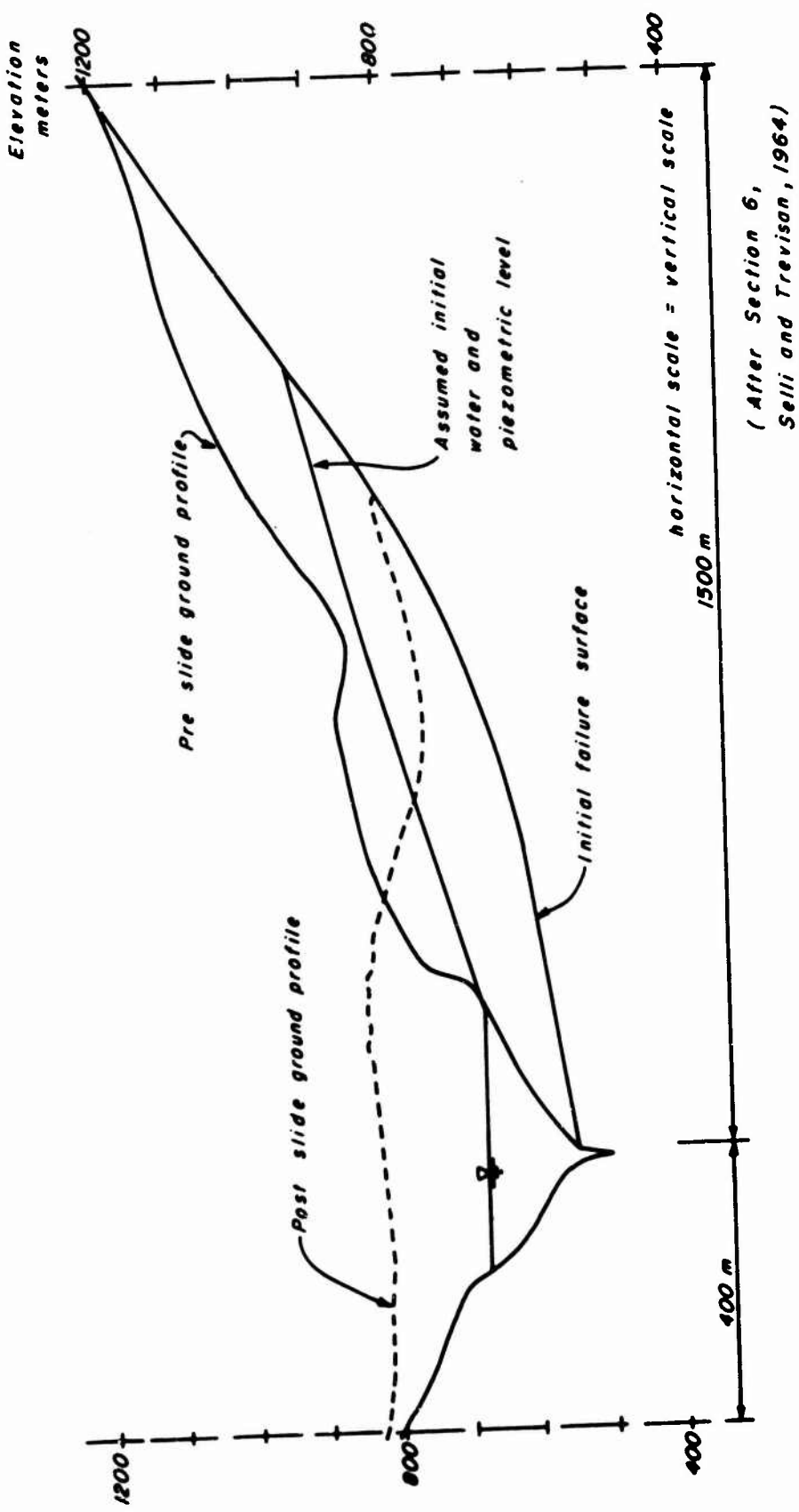


Figure 39. Vajont Slide showing pre- and post-slide ground profiles, assumed failure surface, water and piezometric levels

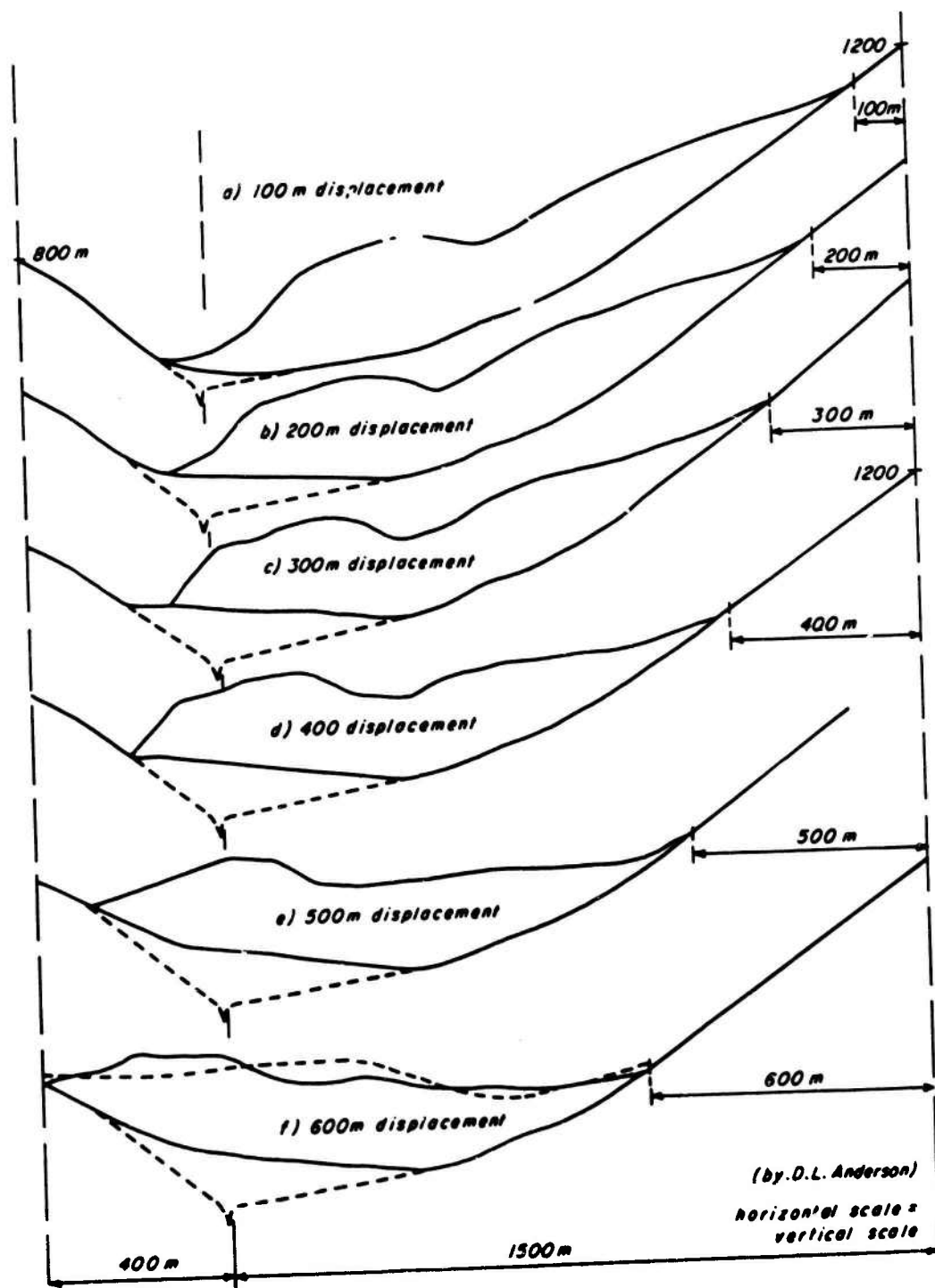
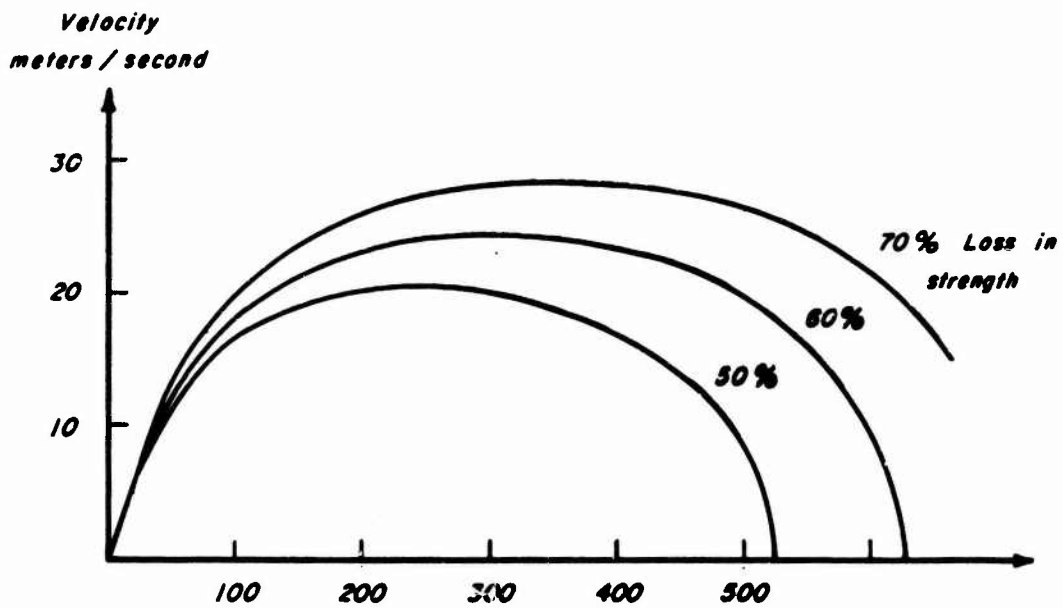
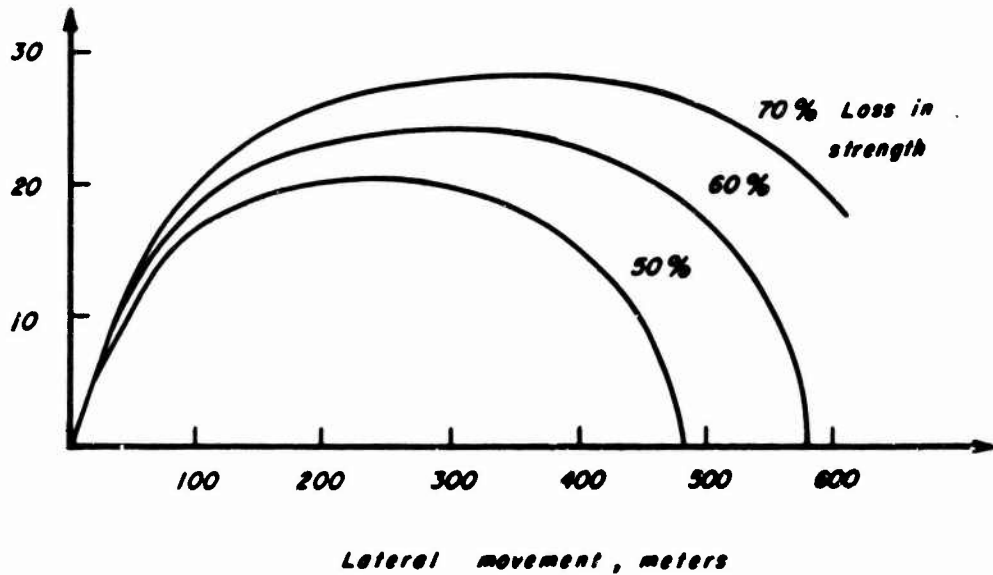


Figure 40. Vaiont Slide, assumed geometry as slide movement progresses

a) Wet toe condition

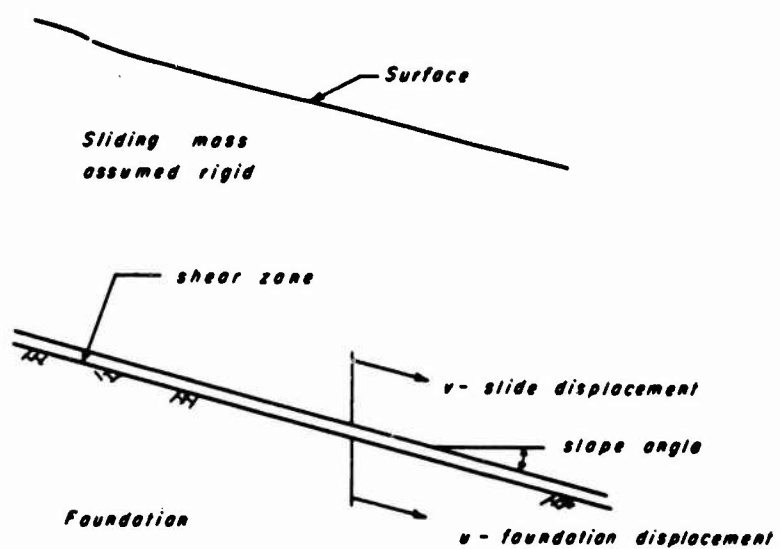


b) Dry toe condition



by D.L. Anderson

Figure 41. Vajont Slide, velocity profiles



a) Idealization of slide

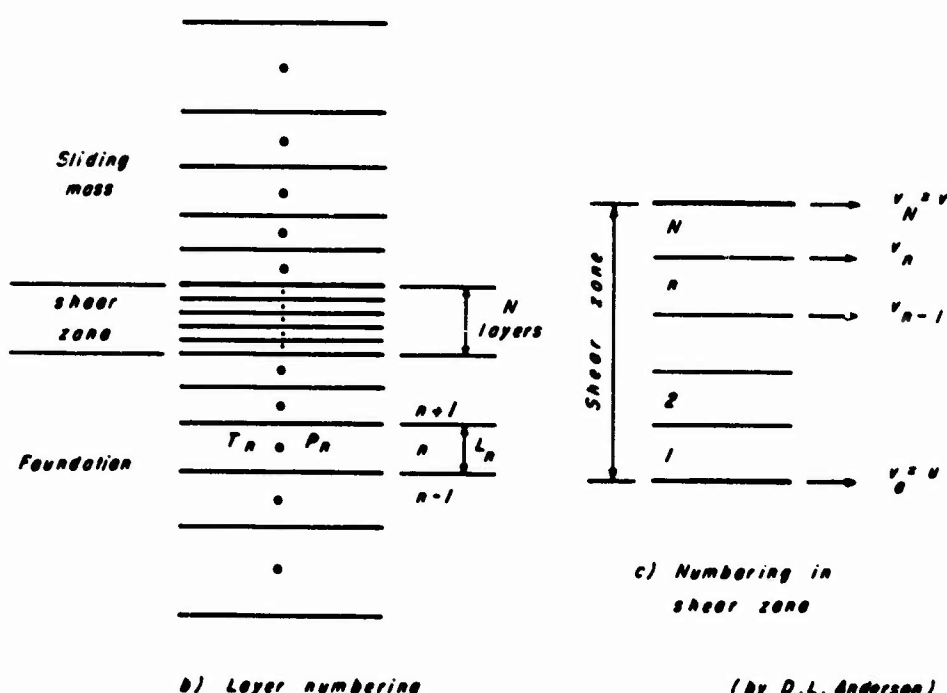
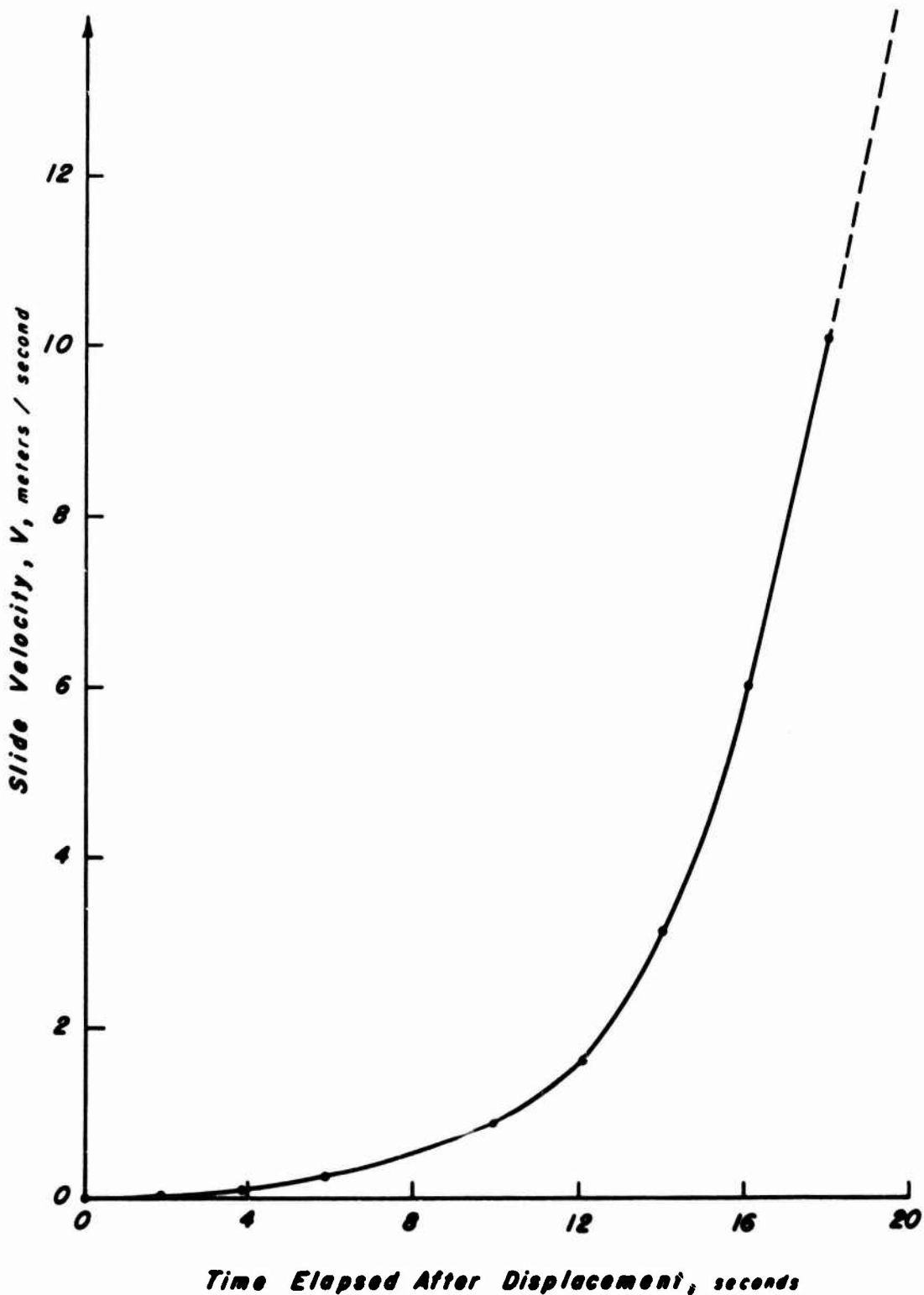


Figure 42. Assumptions used in calculations of slide induced fluid pressures



(by D.L. Anderson)

Figure 43. Vaiont Slide, results of the heat generation analysis

PHOTOS 1 - 52

Note: Most of the following photographs showing specific details of the slide can be identified by the field location numbers shown on the panorama photograph of the slide (Figure 13).

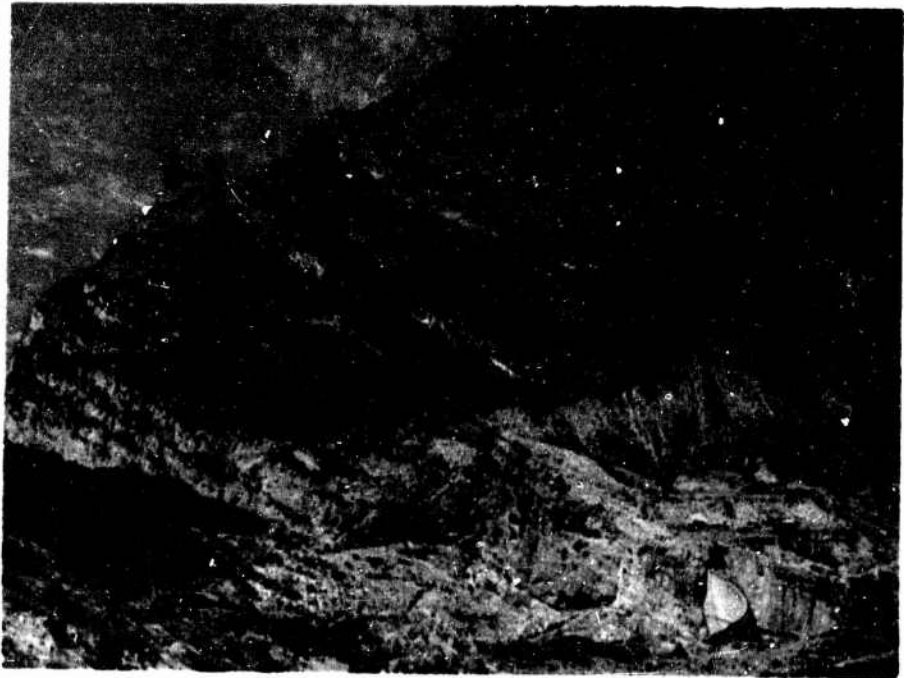


Photo 1. Location 8-1 with respect to the Vajont Dam (also shown on Figures 11 and 12); photo was taken from western part of surface of sliding near location 522-5B



Photo 2. Outcrop 8-1; five in-situ interbeds of clay were uncovered in Lower Cretaceous-Upper Malm units which correlate with approximate position of failure surface at base of slide (see Figure 14)

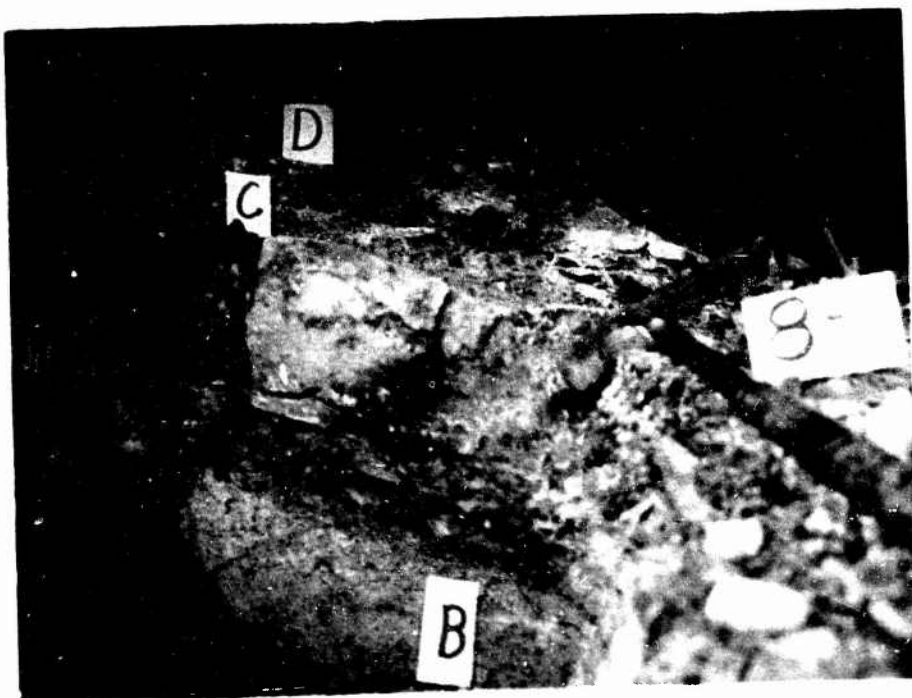


Photo 3. Close-up of three of the five clay interbeds at outcrop 8-1; thicknesses in cm: B - 17.5; C - 2-5; D - 3 (see Figure 14)



Photo 4. Location 10-2A, base of second gulley from west side of surface of sliding; clay layers 0.5 to 2 cm thick are present in slide debris and along failure surface

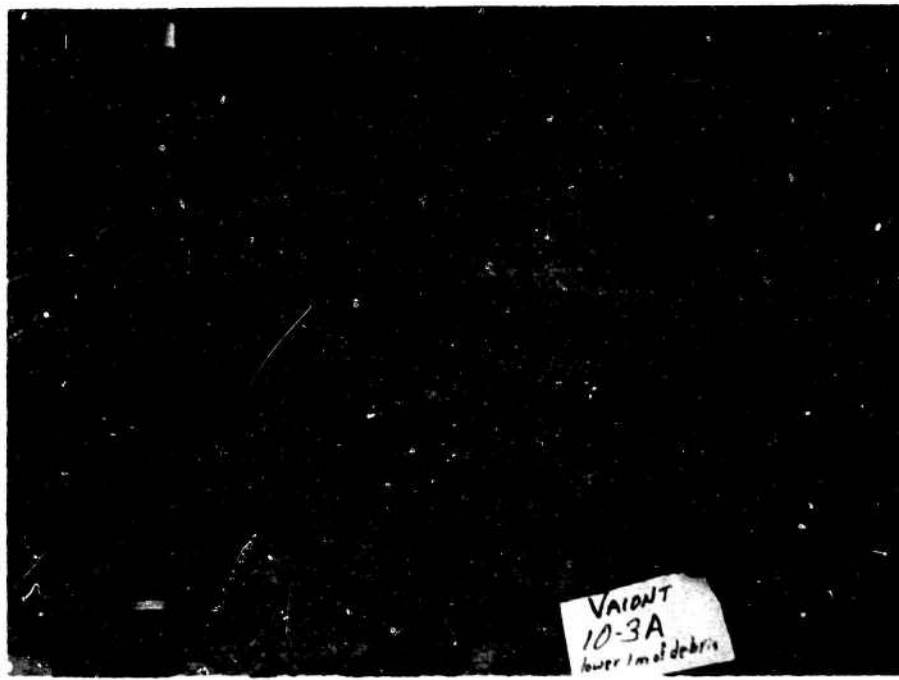


Photo 5. Location 10-3A, headscarp, western third of slide; lower 1 m of slide debris contains 7 layers of clay 1 to 10 cm thick separated by layers of crushed and sheared fragments of brown chert

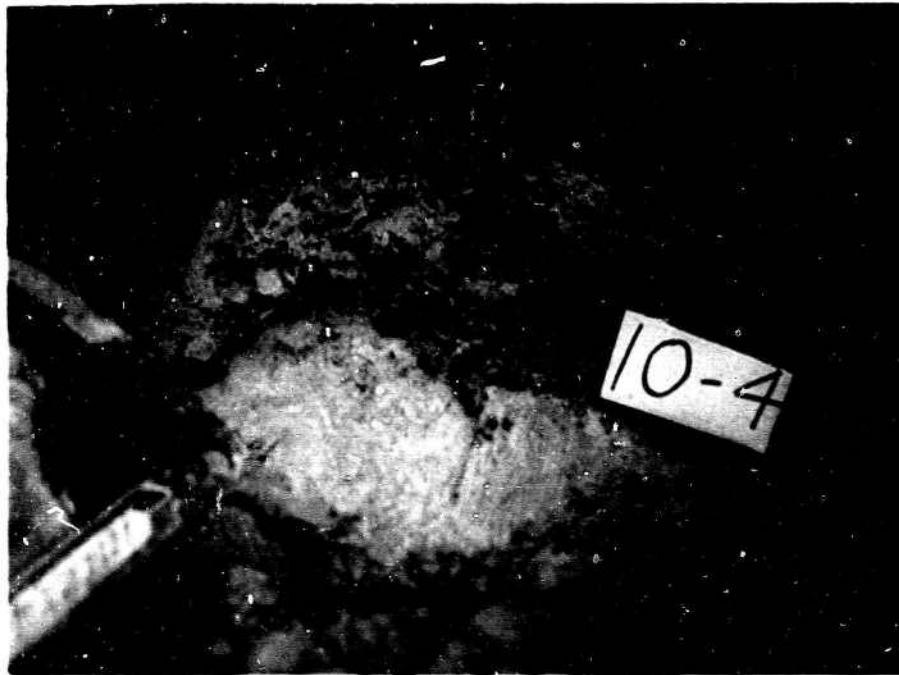


Photo 6. Location 10-4, western side of headscarp; slickensides were found in 1 to 2 cm thick clay layer at bedrock contact dipping at 23-24°N; holes indicate additional clay-rich materials in the overlying slide debris



Photo 7. Location 10-4A, western headscarp; clay layer 1 to 2 cm thick lies between undisturbed beds below and fractured, displaced bedrock above; clay layer dipping at 19-23°N formed the failure surface for rock mass missing in foreground

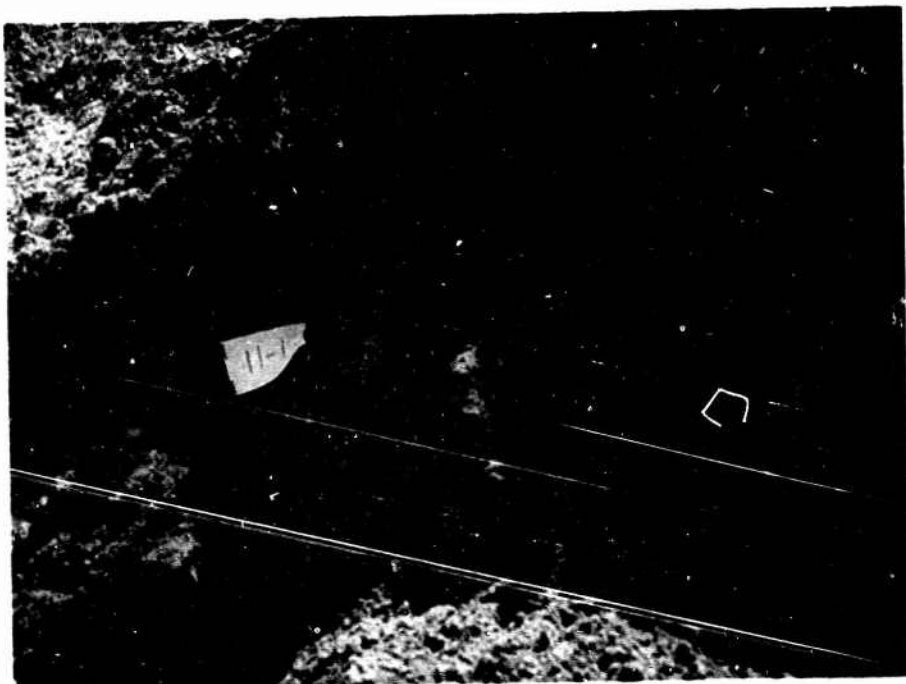


Photo 8. Location 11-1, slide debris at base of third gulley from west side of slide approximately 12 m above failure surface; five clay layers are present in the 1.5 m of debris exposed

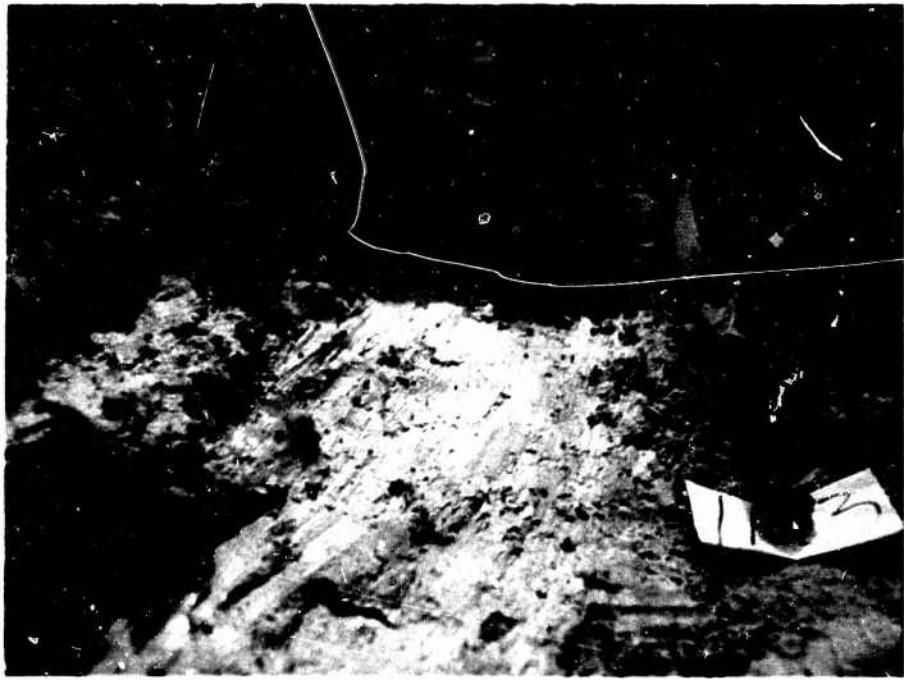


Photo 9. Location 11-3, surface of sliding near bottom of third gulley; slickensides are aligned at 100° Az and dip 30° N

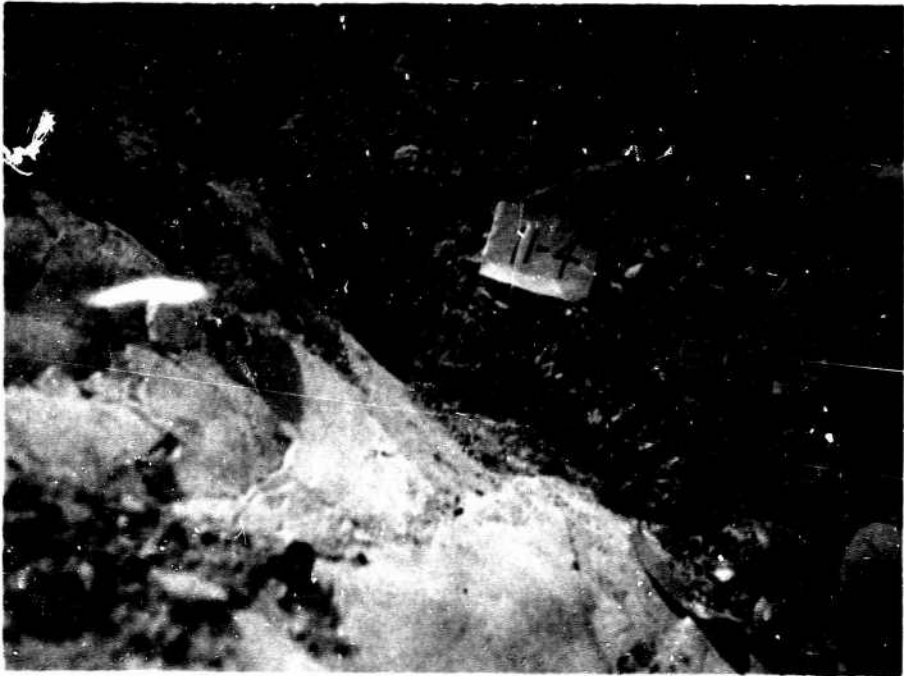


Photo 10. Location 11-4, lower portion of third gulley; clay layer along slide debris-rock contact is 0.1 to 5 cm thick, has an average dip of 36° N, and is continuous for 13 m



Photo 11. Location 11-7, lower portion of fourth gulley from west side of slide; clay layer 4 to 6 cm thick with a dip of 32-34°N forms the base of the slide debris; clay has been washed out below boulders



Photo 12. Location 11-7B (50 m above location 11-7); clay layer 10 cm thick, which lies between bedrock to right and slide mass to left, is in the same stratigraphic position as nearby failure surface, but is protected by cascade structure



Photo 13. Location 11-8A (20 m above location 11-7B); clay layer along failure surface is 0.5 to 2 cm thick with a dip of 22° N



Photo 14. Location 11-10, fourth gulley from west side of slide; five layers of clay 1 to 2 cm thick lie in lower 1.5 m of slide debris; failure surface appears in lower left corner



Photo 15. Location 11-10A; block of "nearly pure" clay in lower 1.5 m of slide debris lies adjacent to location 11-10; slickensided surface appears at top center of photo



Photo 16. Location 12-1, base of rock outcrop in second gulley from east side of slide; clay layer 2 cm thick is present in clay-rich debris 20 cm thick located above failure surface dipping at 33° N

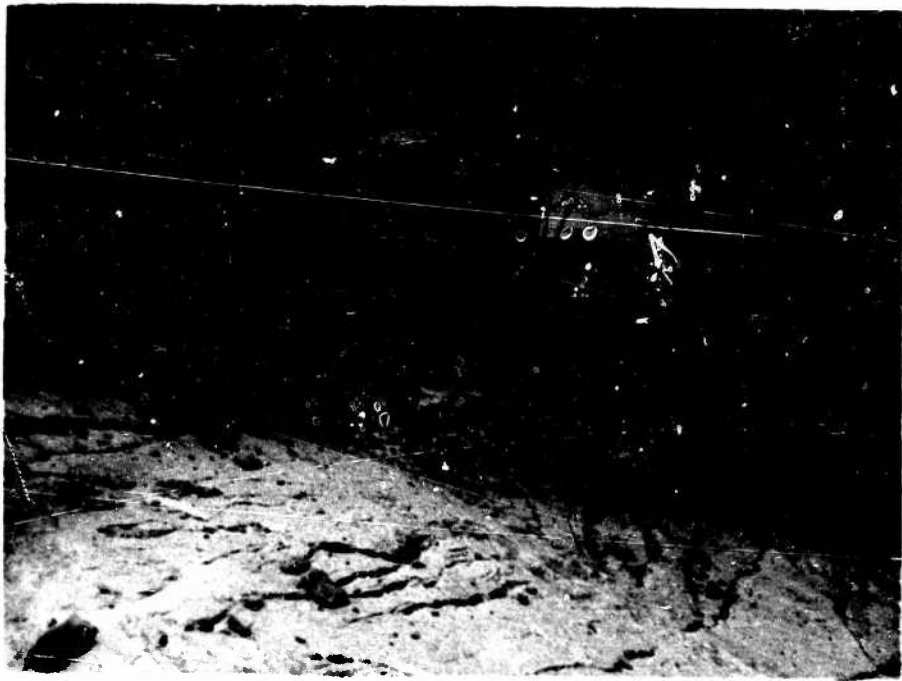


Photo 17. Location 12-3, near east side of slide; clay layer 5 to 20 cm thick overlies cemented breccia along failure surface (see Photos 38 and 39); average dip of breccia 15-20° N; approximately 50 cm of clay-rich slide debris above main clay layer

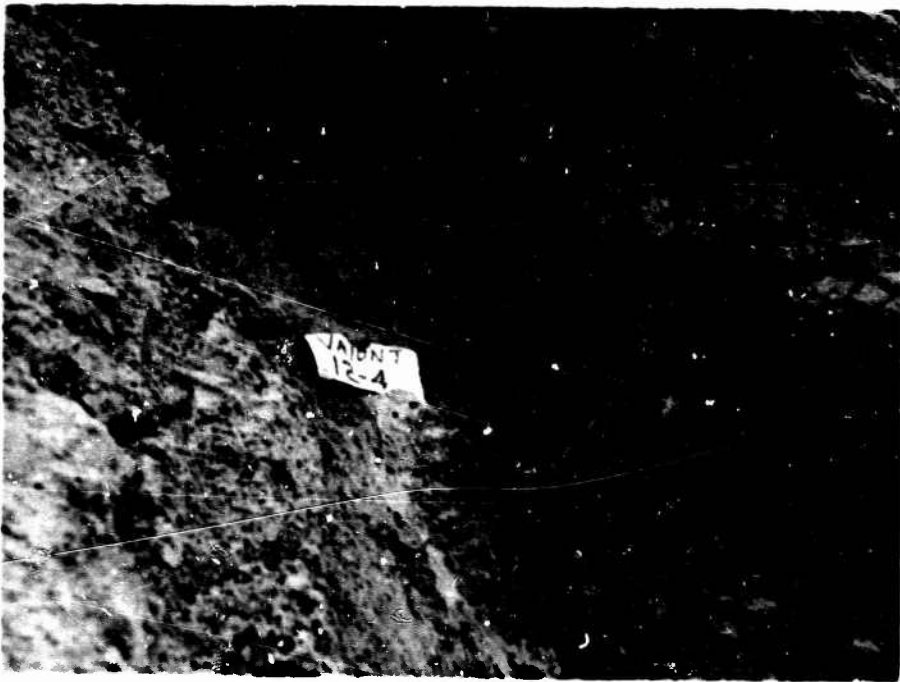


Photo 18. Location 12-4, near east side of slide approximately 70 m above location 12-3; clay layer 0.1 to 1.5 cm thick with a dip of 38° N is present on surface of sliding



Photo 19. Location 12-4A; four clay interbeds 2 to 5 mm thick with a dip of 48°N lie within first 25 cm of rock below failure surface of slide and are preserved in cascade structure (see Photos 44 and 45)



Photo 20. Location 12-5, near east side of slide; clay layer approximately 2 to 3 cm thick with a dip of 44°N is exposed at side of rock surface that forms a large part of eastern portion of the scarp; thinner clay interbeds appear in relatively undisturbed scarp above



Photo 21. Location 18-8, below western third of headscarp; clay layer 5 to 10 cm thick with a dip of 47°N is associated with failure surface of rock slab above



Photo 22. Location 18-14, below headscarp approximately two-fifths of the way from the west end; clay interbed 2 to 10 cm thick with a dip of 39°N is protected in fold associated with fault



Photo 23. Location 22-1A, east side of fourth gulley from west side of slide; clay layer (with holes) is continuous with clay layer located in the lower 4 cm of debris on slope above; dip of clay layer 35° N; dip of surface of sliding 38° N



Photo 24. Location 22-3, east side of fourth gulley from west side of slide; clay layer 10 cm thick is present on failure surface of 1963 slide (base of card); two other older (?) surfaces of sliding lie below clay layer within a partly cemented breccia

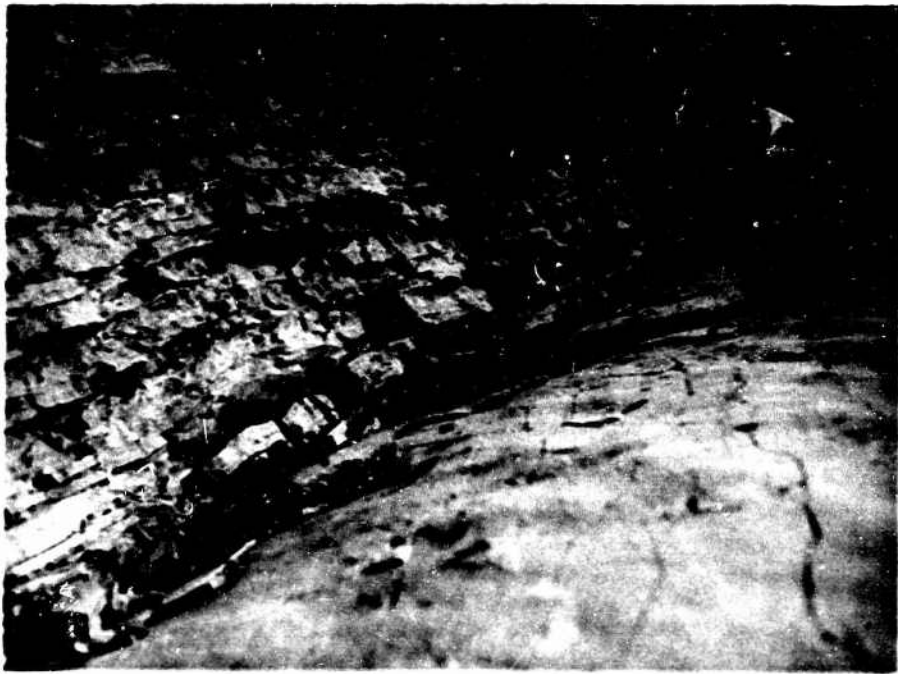


Photo 25. Location 18-9, below western third of headscarp; outcrop along edge of failure surface of 1963 slide or post-1963 slides; loose rock slabs cover clay interbed with dip of 35°N



Photo 26. Location 18-9, loose rocks were removed exposing clay interbed 5 cm thick on edge of failure surface; other thin clay interbeds to 0.5 cm maximum are exposed in rock mass above



Photo 27. Location 22-3A, clay layer, 2 to 3 cm thick and continuous for 8 m, rests on 1963 surface of sliding; clay overlies 0.5 to 1.0 m of cemented breccia dipping at 45-48° N; dips of "bedding" and clay layers in slide debris above are flatter



Photo 28. Location 22-3A, close-up of clay layer in Photo 27; thickening of clay was apparently caused by differential displacements of the material along the base of the 1963 slide mass

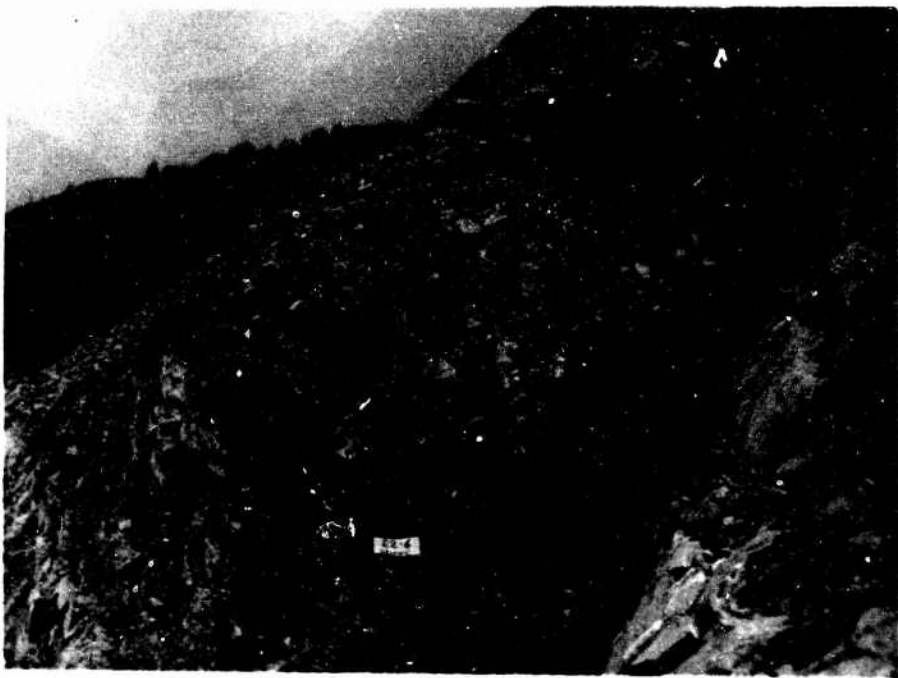


Photo 29. Location 22-6, west side of fifth gully from western edge of slide; clay layer 1 to 3 cm thick, which has been preserved along small fold with dip of 60° N, is associated with adjacent failure surfaces of 1963 slide



Photo 30. Location 22-6A; clay layer 1 to 4 cm thick associated with adjacent failure surface of 1963 slide is protected by small fold in beds (limb of fold has dip of 54-58° N)

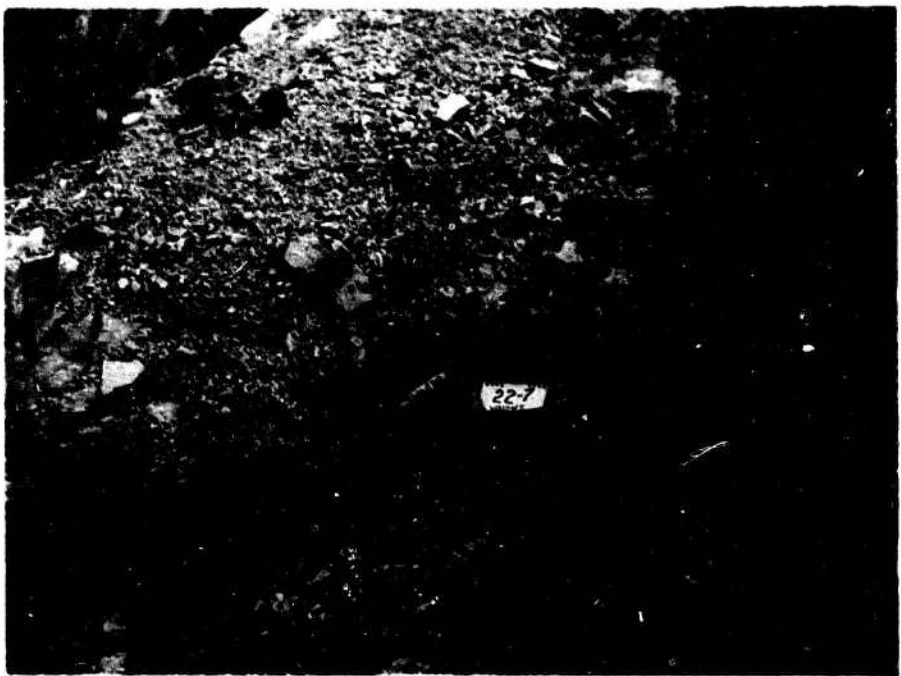


Photo 31. Location 22-7; clay layer 7 to 10 cm thick (max 20 cm) associated with adjacent failure surfaces of 1963 slide is protected by small flexure (right-hand side has dip of 54° N)

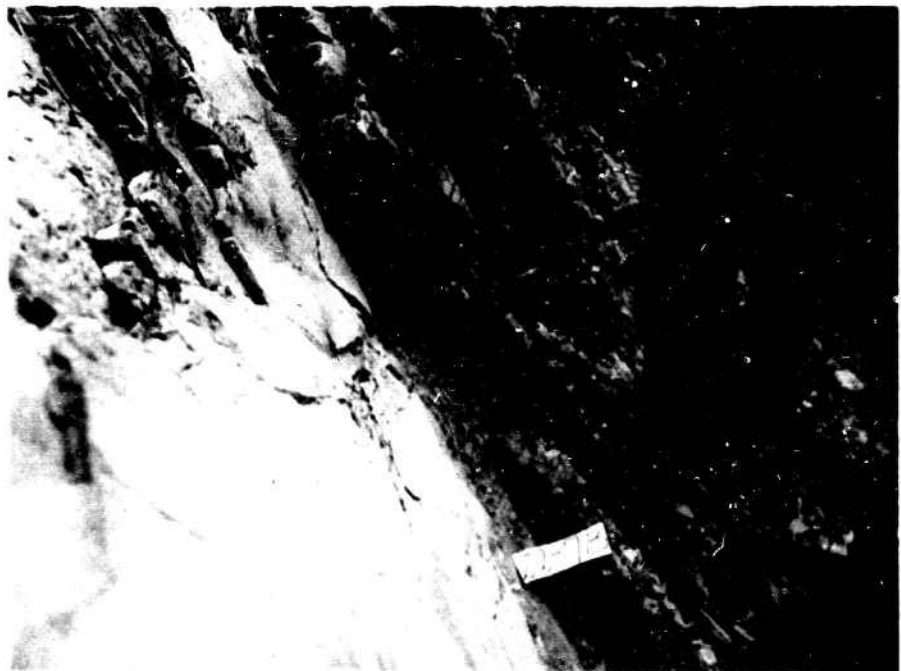


Photo 32. Location 22-7B; clay interbed 2 to 6 cm thick associated with adjacent failure surfaces of 1963 slide is protected by small flexure; clay dips at 65° N



Photo 33. Location 22-8, east side of fifth gulley from west side of slide, one-third of the way up rock face; clay interbed 7 to 10 cm thick is associated with adjacent failure surfaces of 1963 slide; second clay interbed 1 to 3 cm thick is present in overlying beds; clay has weathered and eroded to leave opening



Photo 34. Location 23-11, middle of seventh gulley from west side of slide (below Massalezza streambed); clay interbed 2 to 3 cm thick associated with remainder of adjacent failure surfaces of 1963 slide is protected by small fold



Photo 35. Location 23-12, below Massalezza streambed; clay interbed 1 to 5 cm thick associated with adjacent failure surface of 1963 slide is protected by fold with a dip of 36° N

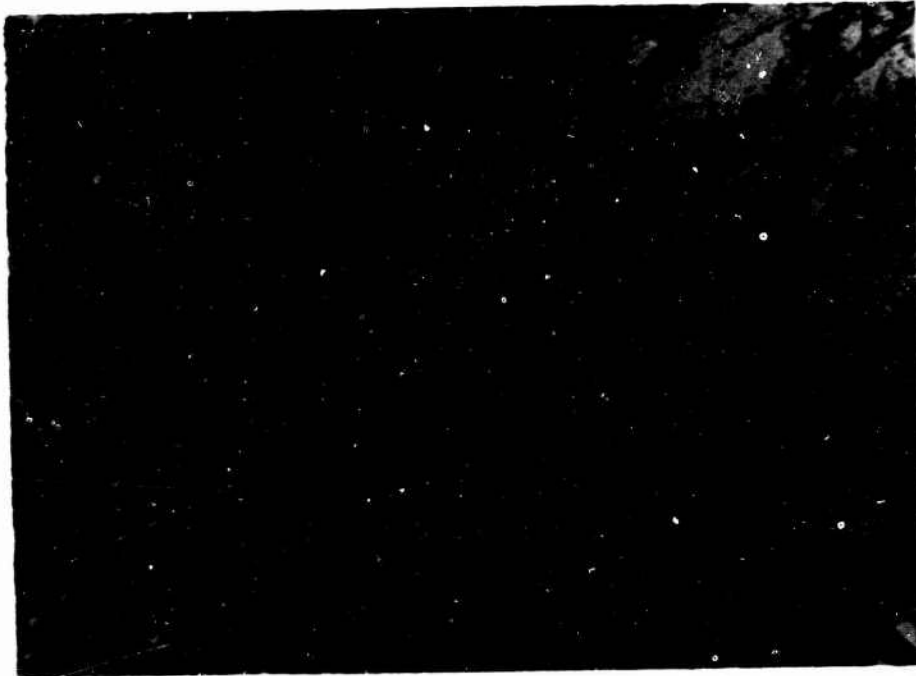


Photo 36. Location 24-3, third gully from east side of slide; several clay interbeds 1 cm thick are present in local fold below 1963 surface of sliding (at larger card); average dip of beds on failure surface above is 44° N



Photo 37. Location 24-7, middle of eastern half of slide; two clay interbeds, each 0.5 to 1.5 cm thick, were exposed by post-1963 rock slides; both interbeds were probably associated with the 1963 surface of sliding in adjacent areas



Photo 38. Location 12-1A, eastern surface of sliding; striations left by 1963 slide appear on surface of cemented breccia of possible tectonic origin; surface:strike 20° , dip 46° W; striations: 338° Az, plunge 30° N

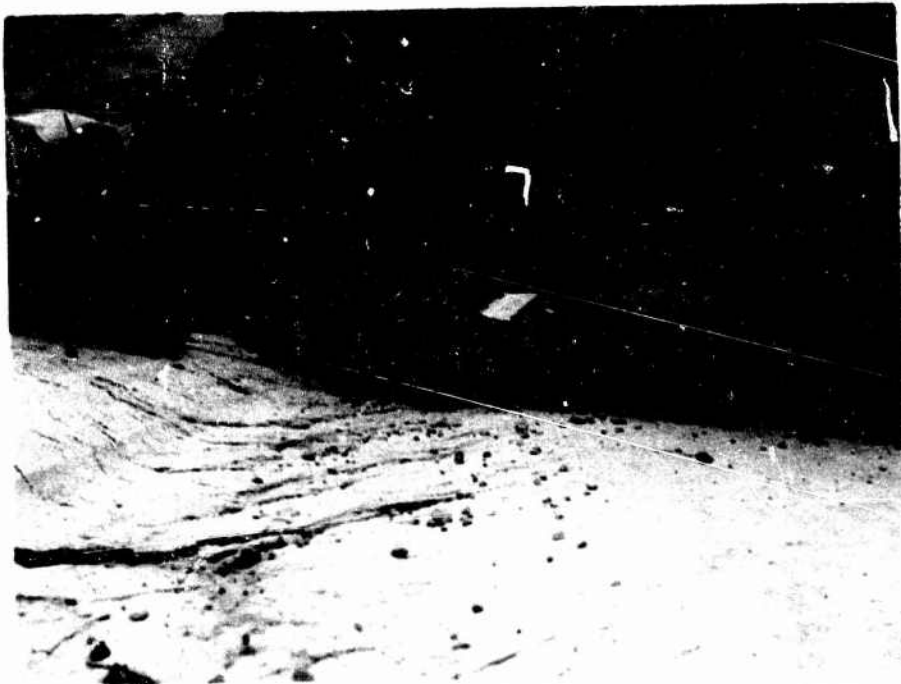


Photo 39. Location 12-3, near east side of slide; grooved surface corresponds to possible tectonic fault and to base of 1963 slide; clay layers appears along contact (see Photo 17)

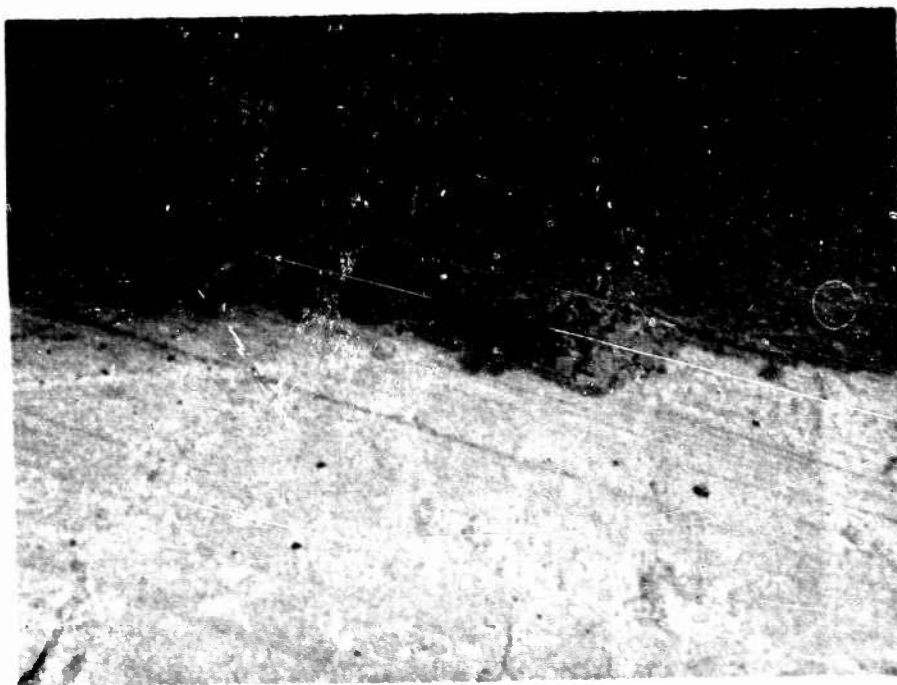


Photo 40. Location 12-3; striae believed caused by 1963 sliding of the Eastern Lobe appear in surface of cemented breccia; striae: 316° Az, plunge 20° NW



Photo 41. Location 18-10, below western headscarp; striations caused by 1963 slide or post-1963 slides cut across bedding which has a strike of 98° and dip of 30° N



Photo 42. Located approximately half-way up western part of slide with Casso and dam in background; one of several localized plunging synclinal folds now exposed along 1963 surface of sliding

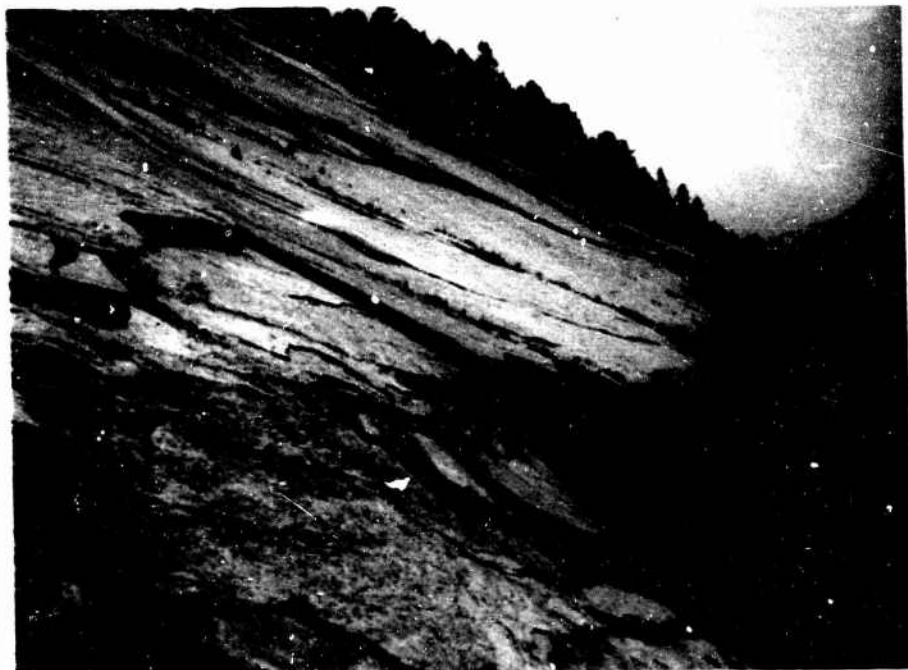


Photo 43. Locations 9-2 and 522-6, middle of western rock face of slide; monoclinal fold exposed after the 1963 slide is associated with a clay interbed 0.2 to 1 cm thick; bedding dips 36-40° above monocline and 30° below



Photo 44. Location 22-1, fourth gulley from west end of surface of sliding; the 1963 slide exposed a section through a small cascade structure; base of remnant of slide debris is just above boulders in background

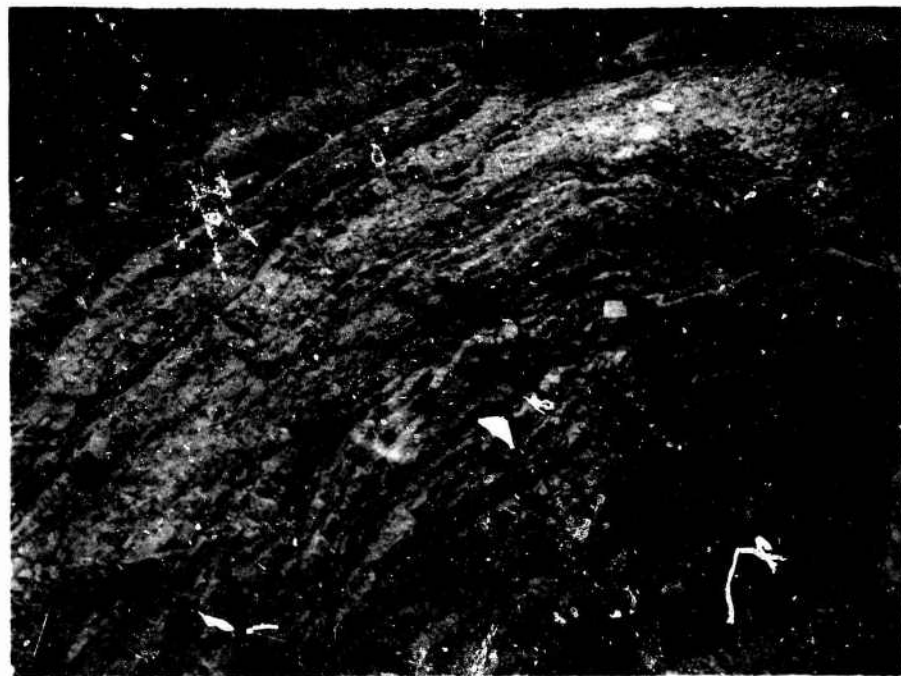


Photo 45. Location 12-2A, base of second gully from east side of slide, bedding is approximately 5 m below surface of sliding where small cascade structure was eroded by stream; rocks appear to be deformed from same period of faulting that left cemented breccia

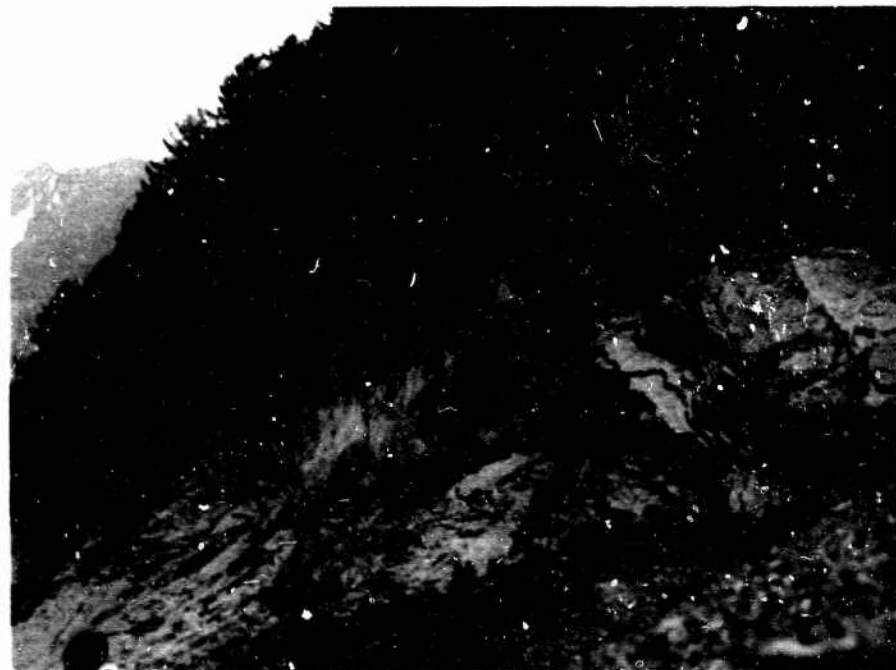


Photo 46. Location above 18-6, headscarp, western part; old headscarp visible in vegetated area above with steep monoclinal fold changing to a fault at the scarp; fragments of partly cemented breccia containing solution features remain attached to cliff above



Photo 47. Location above 18-10; old vegetated headscarp is continuous with new 1963 headscarp; two or more types of cemented breccia have infilled old "bergschrund;" solution cavities in better cemented (older?) breccia are visible on the right

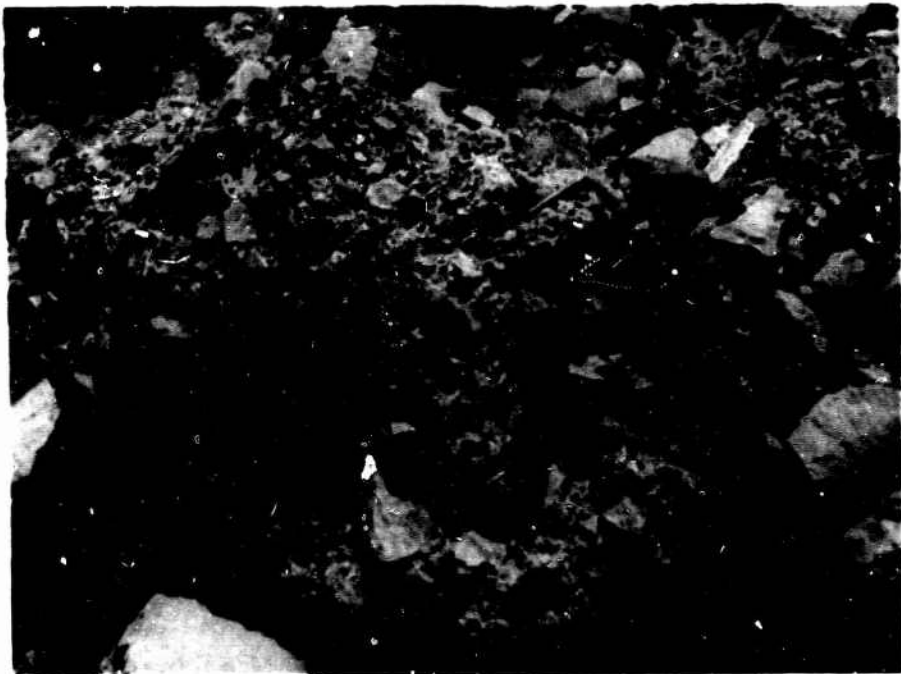


Photo 48. Float boulder of partly cemented breccia; source believed to be breccia shown in Photo 47



Photo 49. Toe of 1963 slide mass; contorted but relatively continuous Lower Cretaceous units are shown

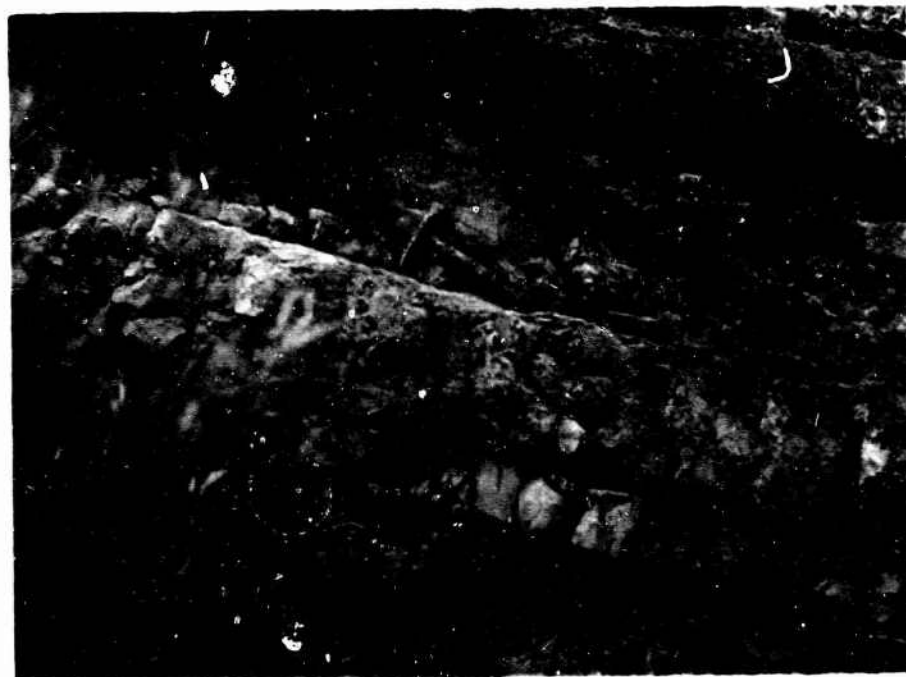


Photo 50. Malm formation in small excavation above right abutment of dam; dark gray to black chert interbeds and nodules are visible

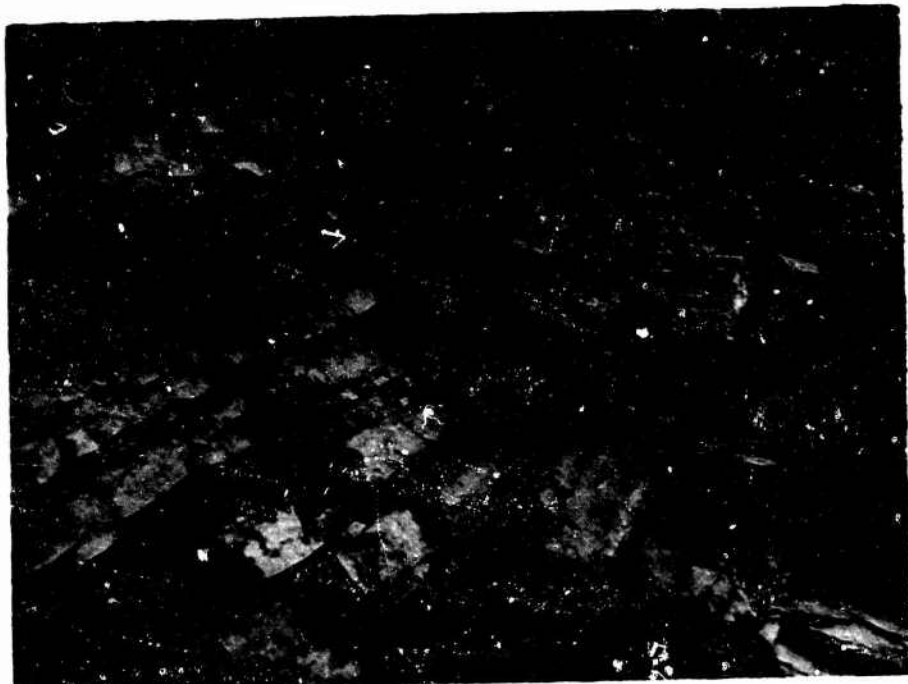


Photo 51. Location 9-3B, top of east side of first rock slab exposed at west side of slide; solution cavities up to 15 cm diameter are present along axial plane of small fold



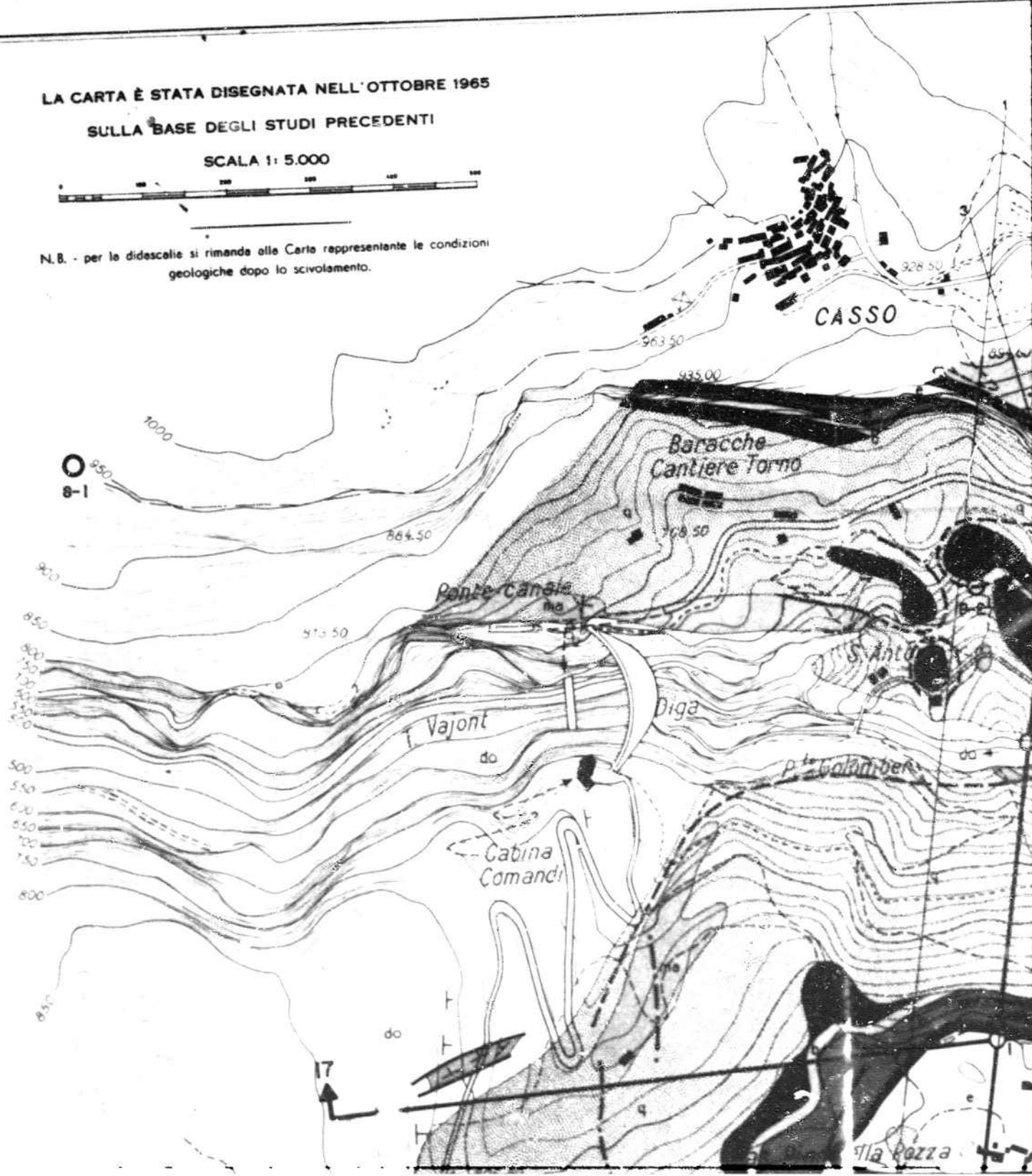
Photo 52. Location 22-4, eastern portion of slide just below surface of sliding; solution cavities 0.5 to 1.0 cm diameter developed along surface of sliding in cemented breccia of possible tectonic origin

CARTA GEOLOGICA

LA CARTA È STATA DISEGNATA NELL'OTTOBRE 1965
SULLA BASE DEGLI STUDI PRECEDENTI

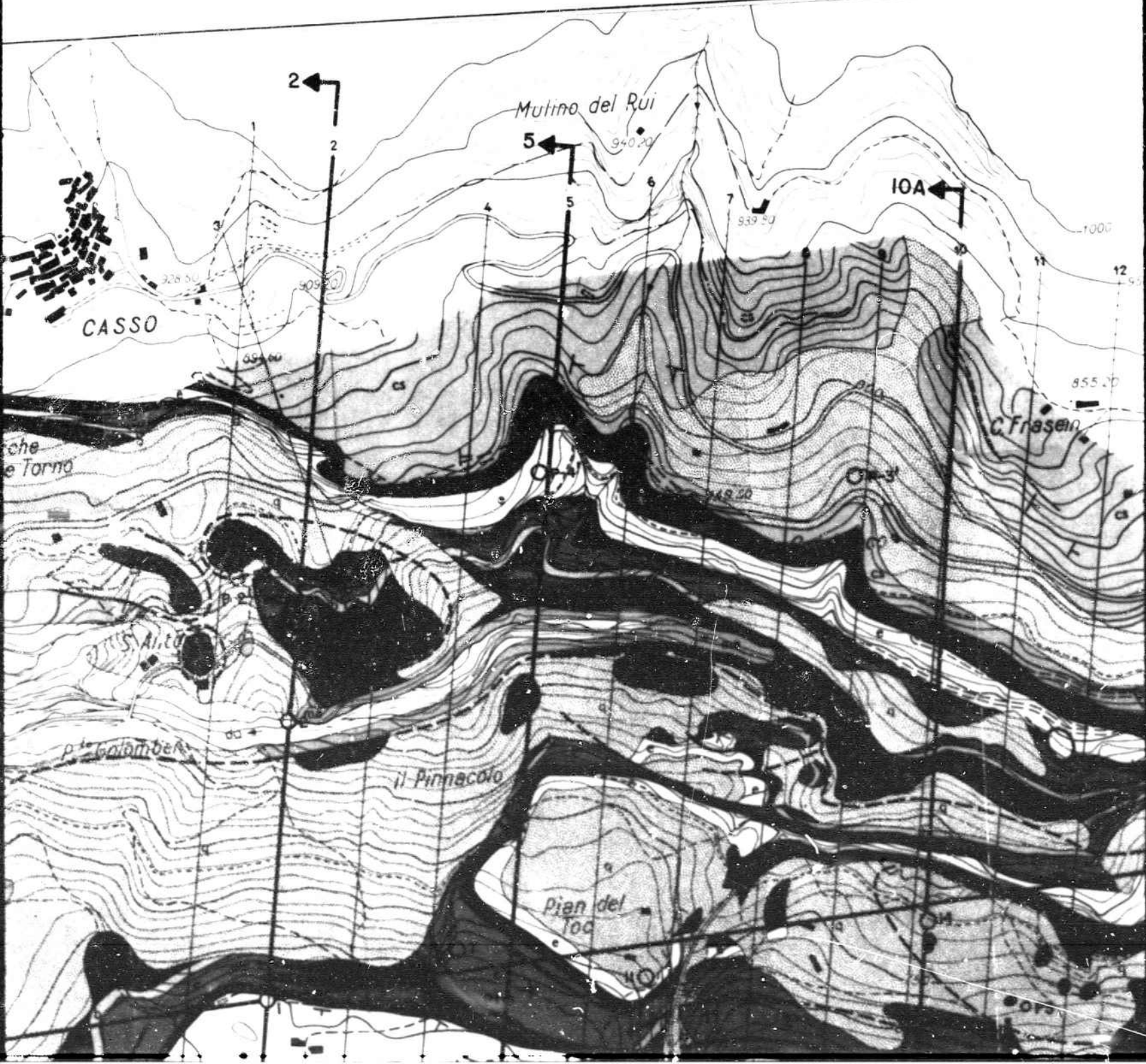
SCALA 1: 5.000

N.B. - per le didascalie si rimanda alla Carta rappresentante le condizioni
geologiche dopo lo scivolamento.

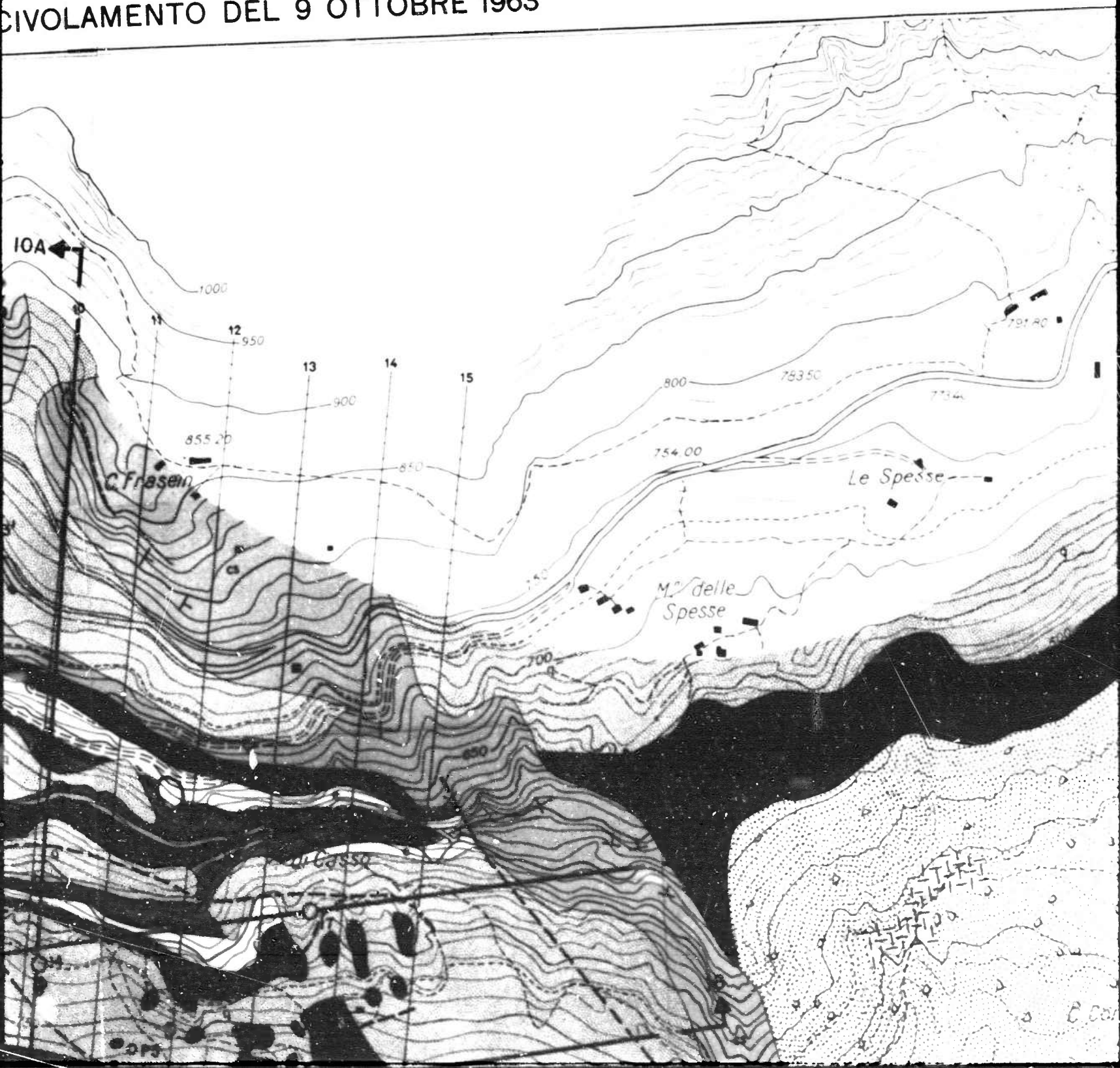


DANIELE ROSSI ED EDOARDO SEMEN

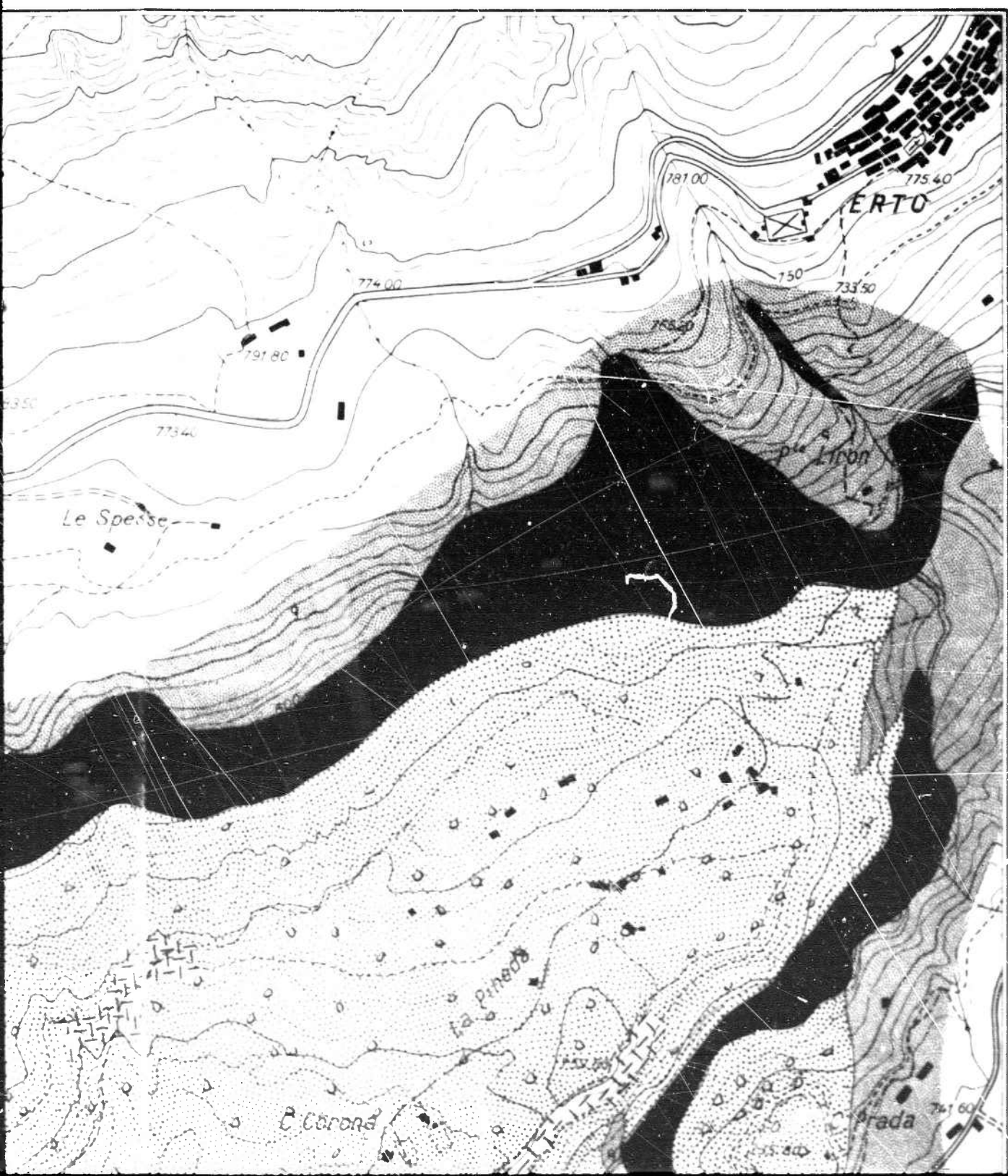
TA GEOLOGICA DEL VERSANTE SETTENTRIONALE PRIMA DEL FENOMENO DI SCIVOLAMENTO DE

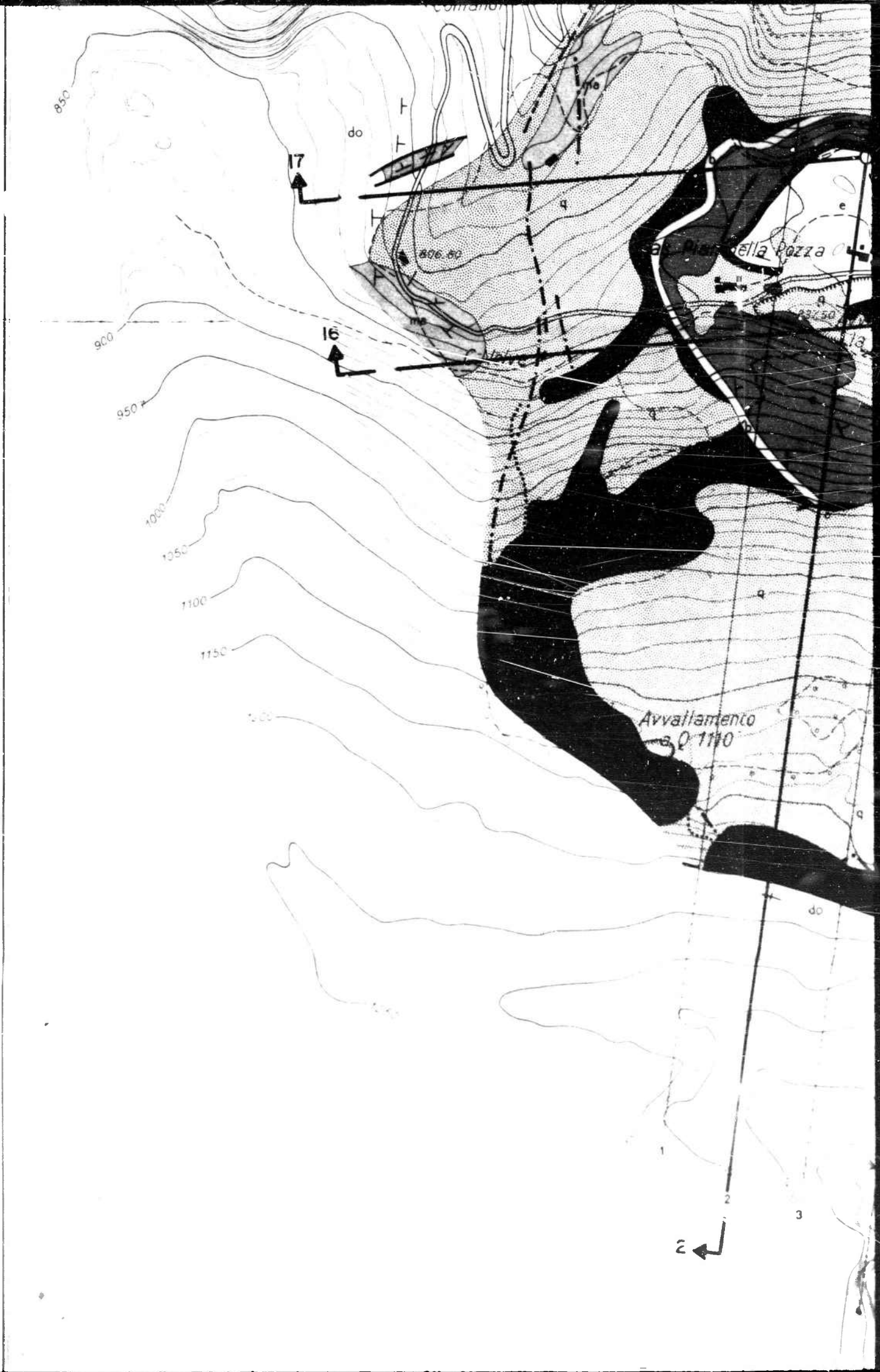


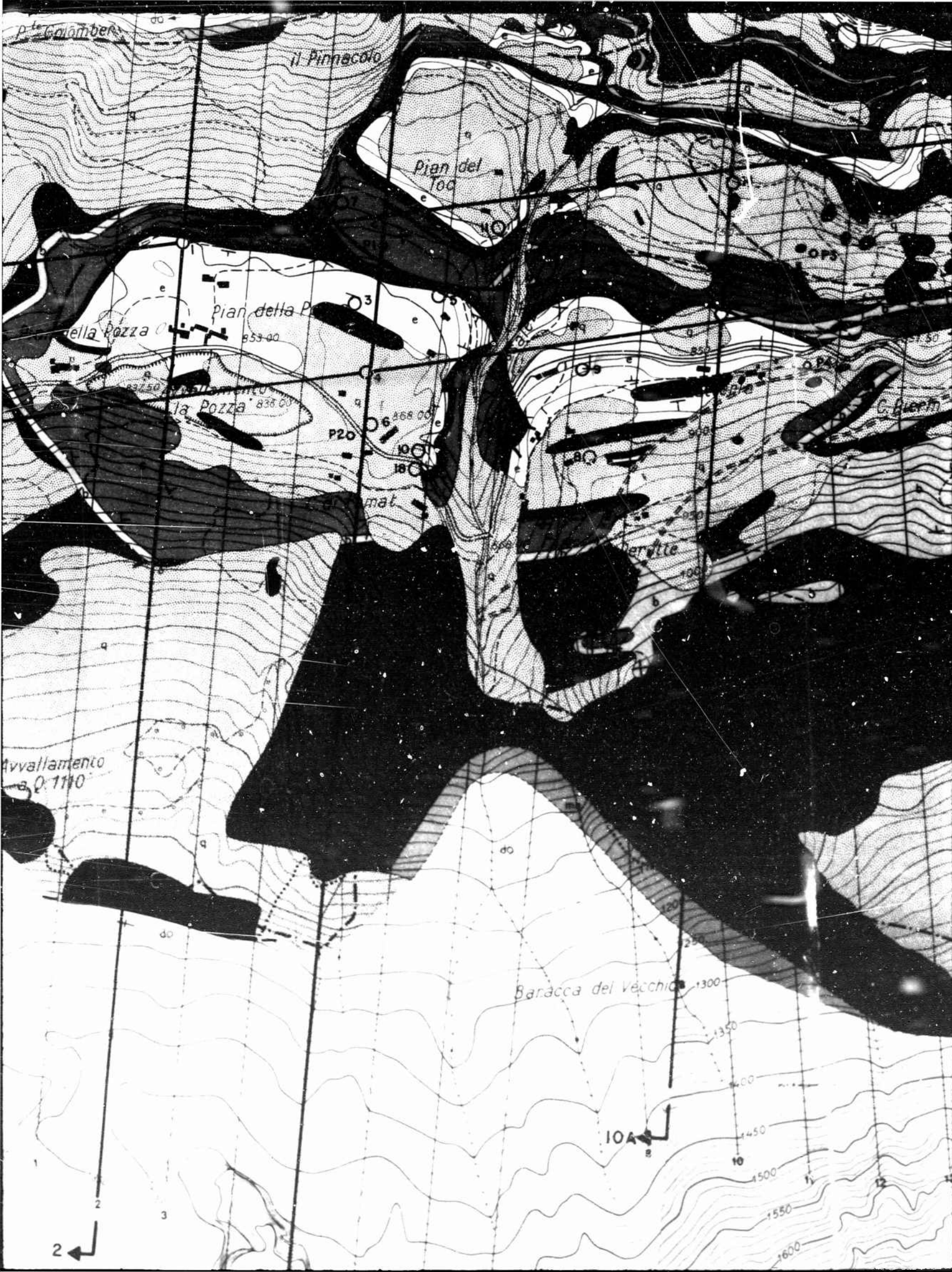
ED EDOARDO SEMENZA
CENTRIONALE DEL M. TOC E ZONE LIMITROFE
CIVOLAMENTO DEL 9 OTTOBRE 1963

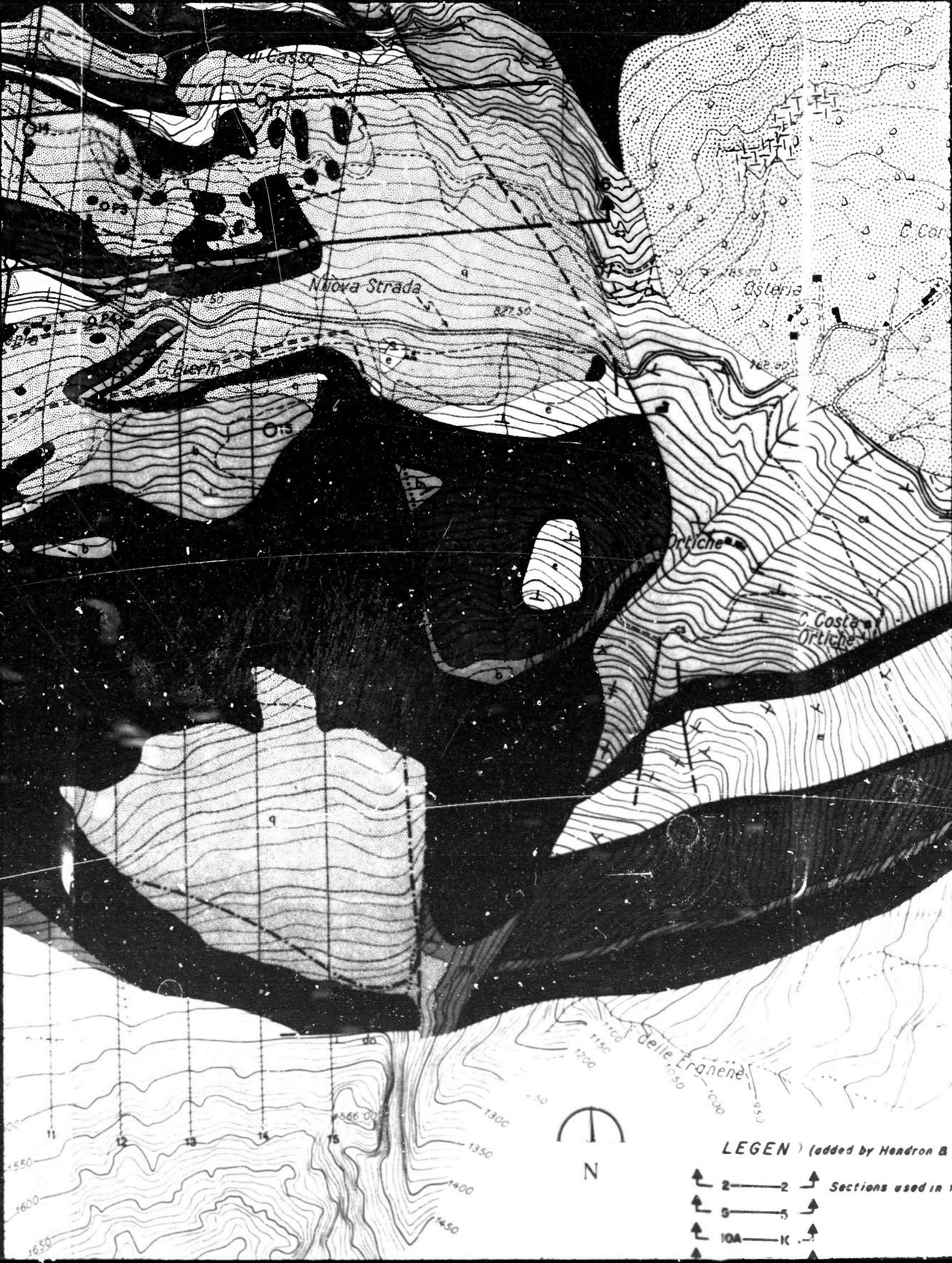


NE LIMITROFE







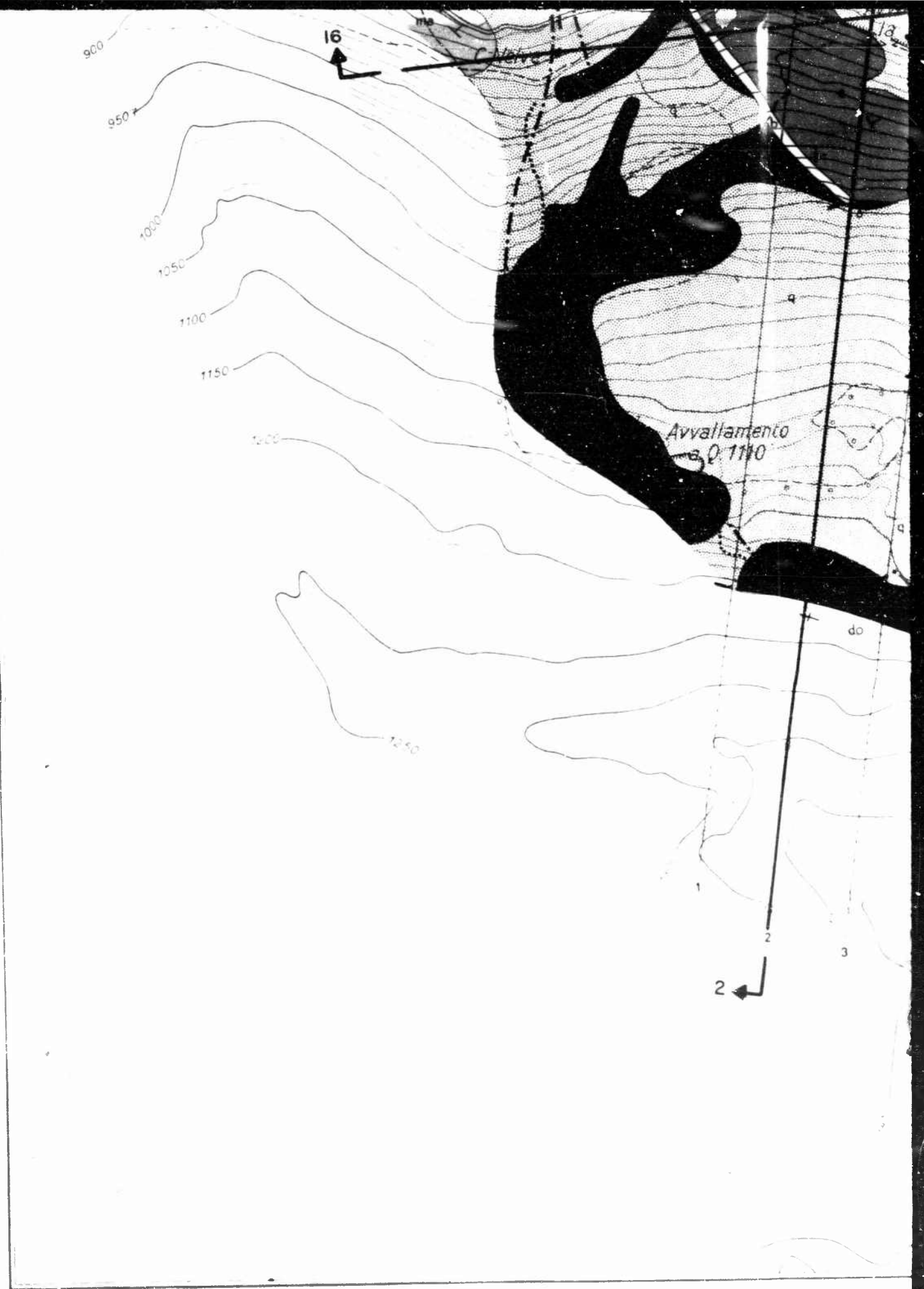


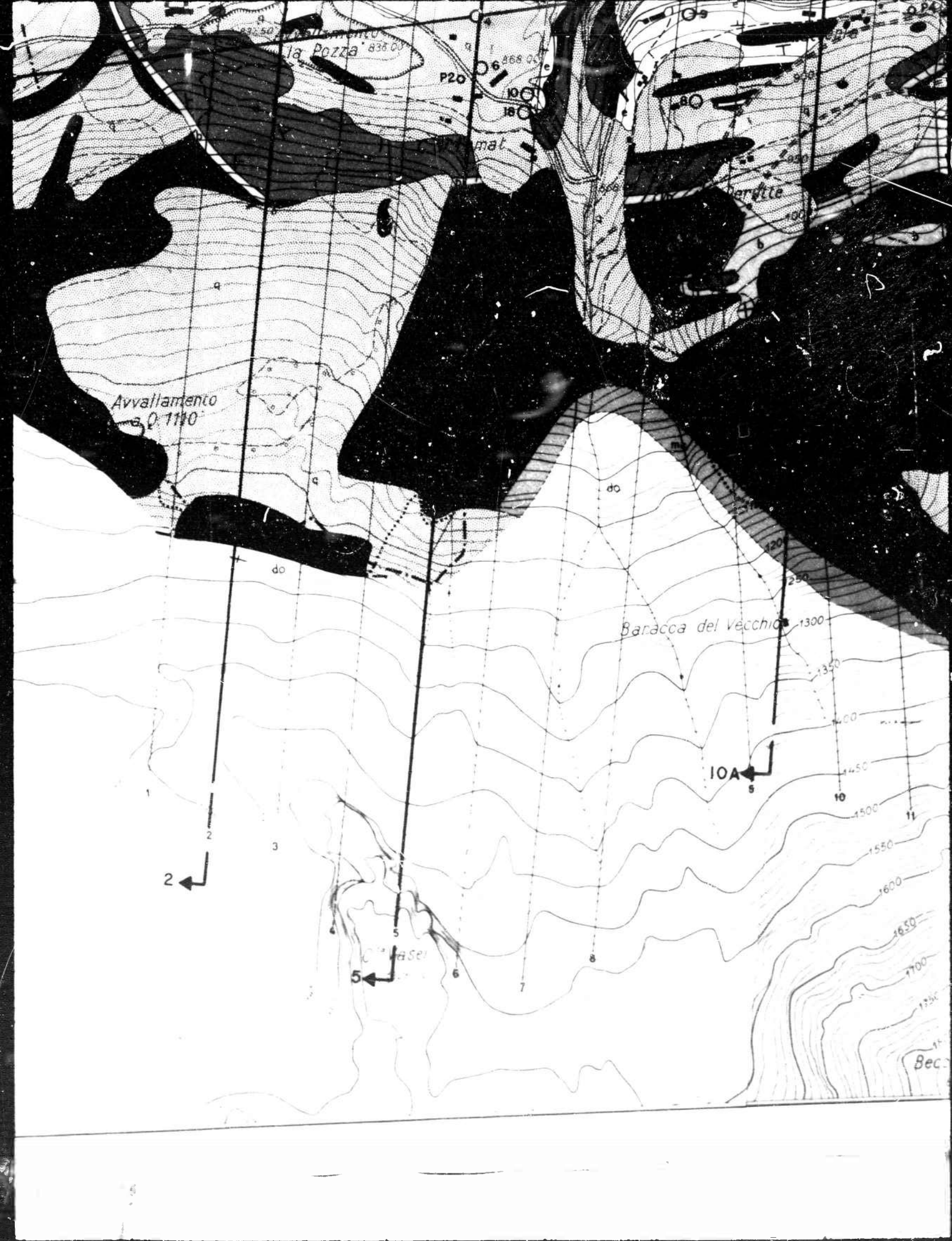


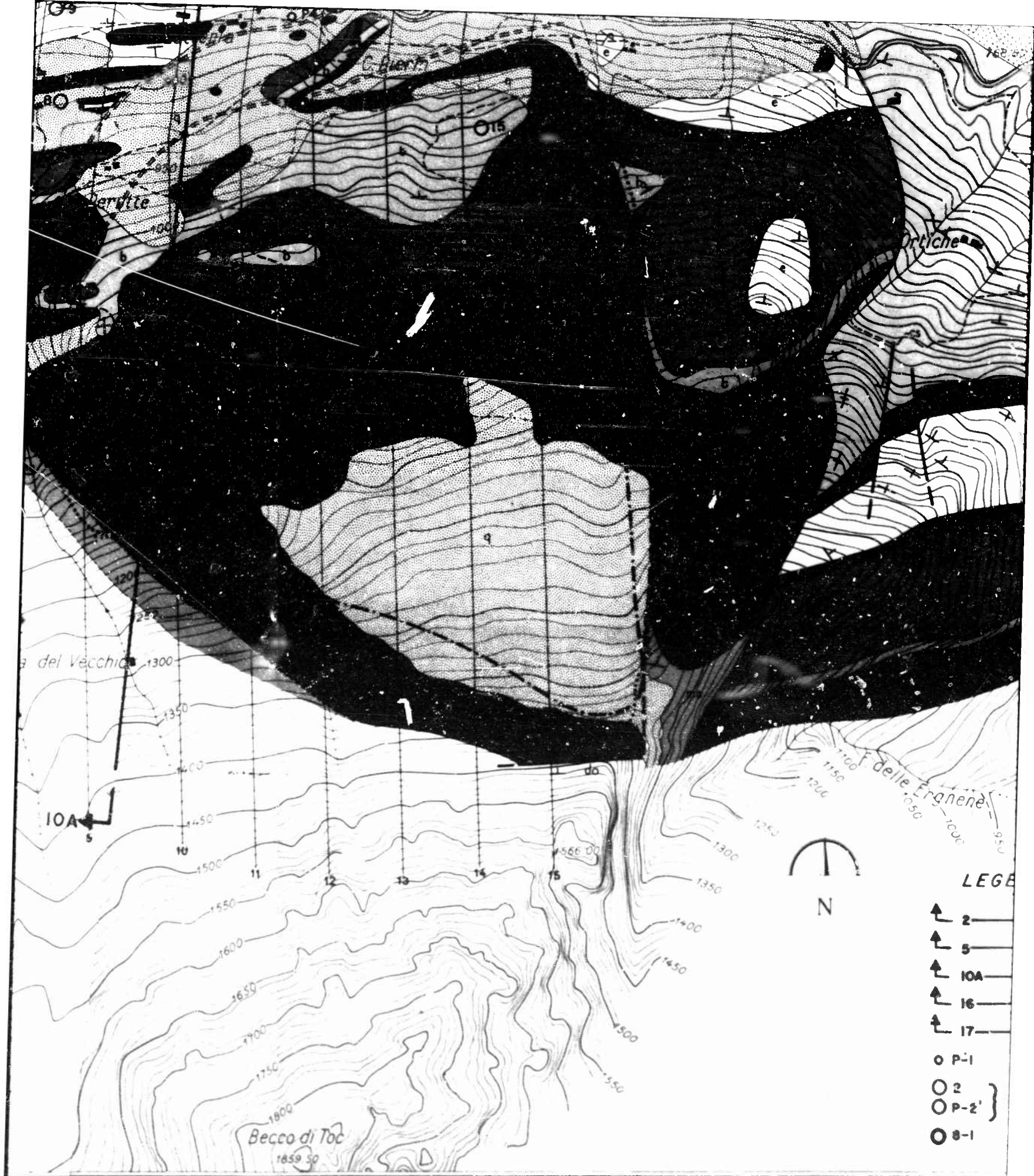
LEGEND (added by Hendron & Patton)

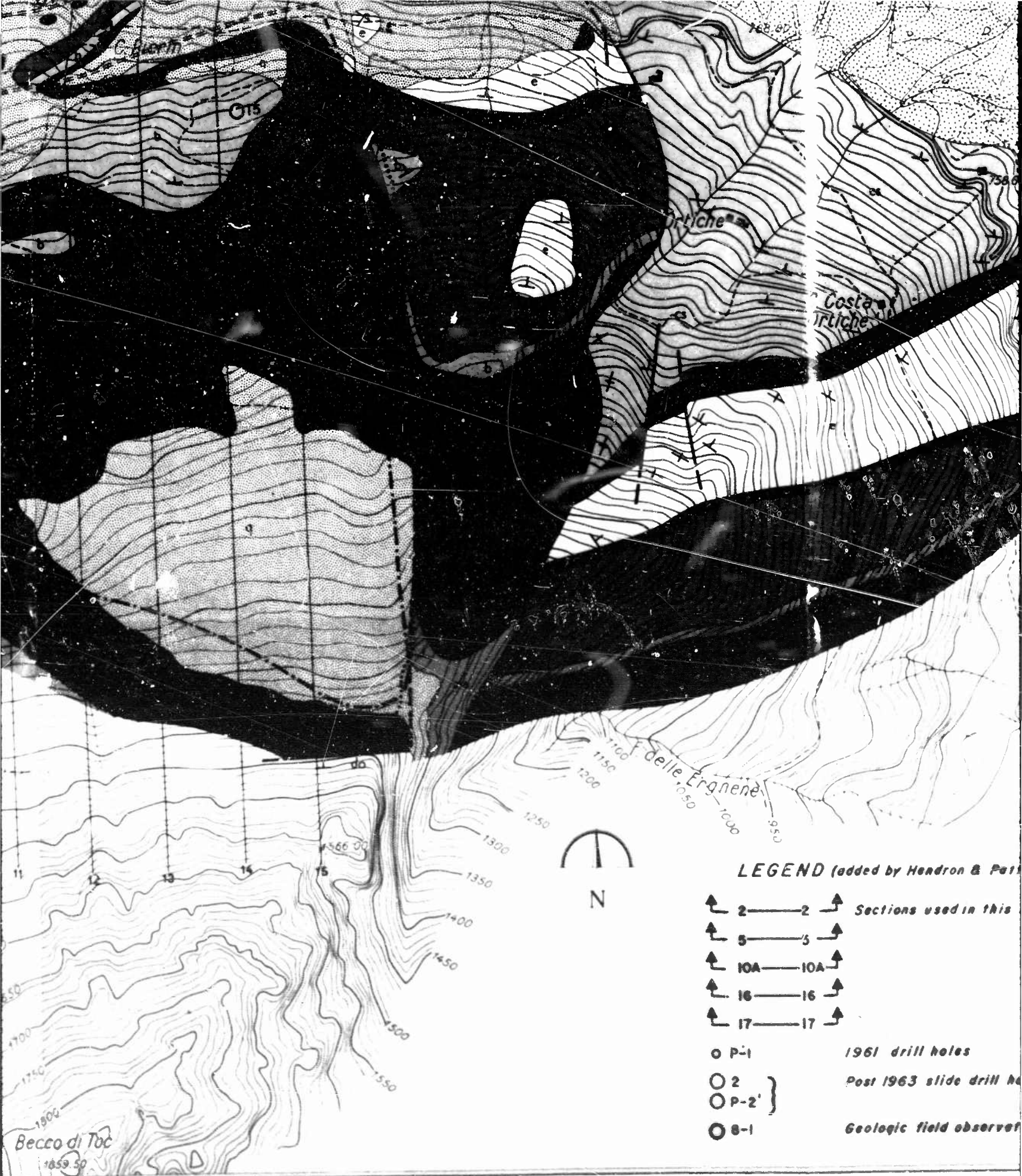
- ↑ 2 — 2 ↑ Sections used in this report
- ↑ 5 — 5 ↑
- ↑ 10A — 10A ↑
- ↑ 16 — 16 ↑

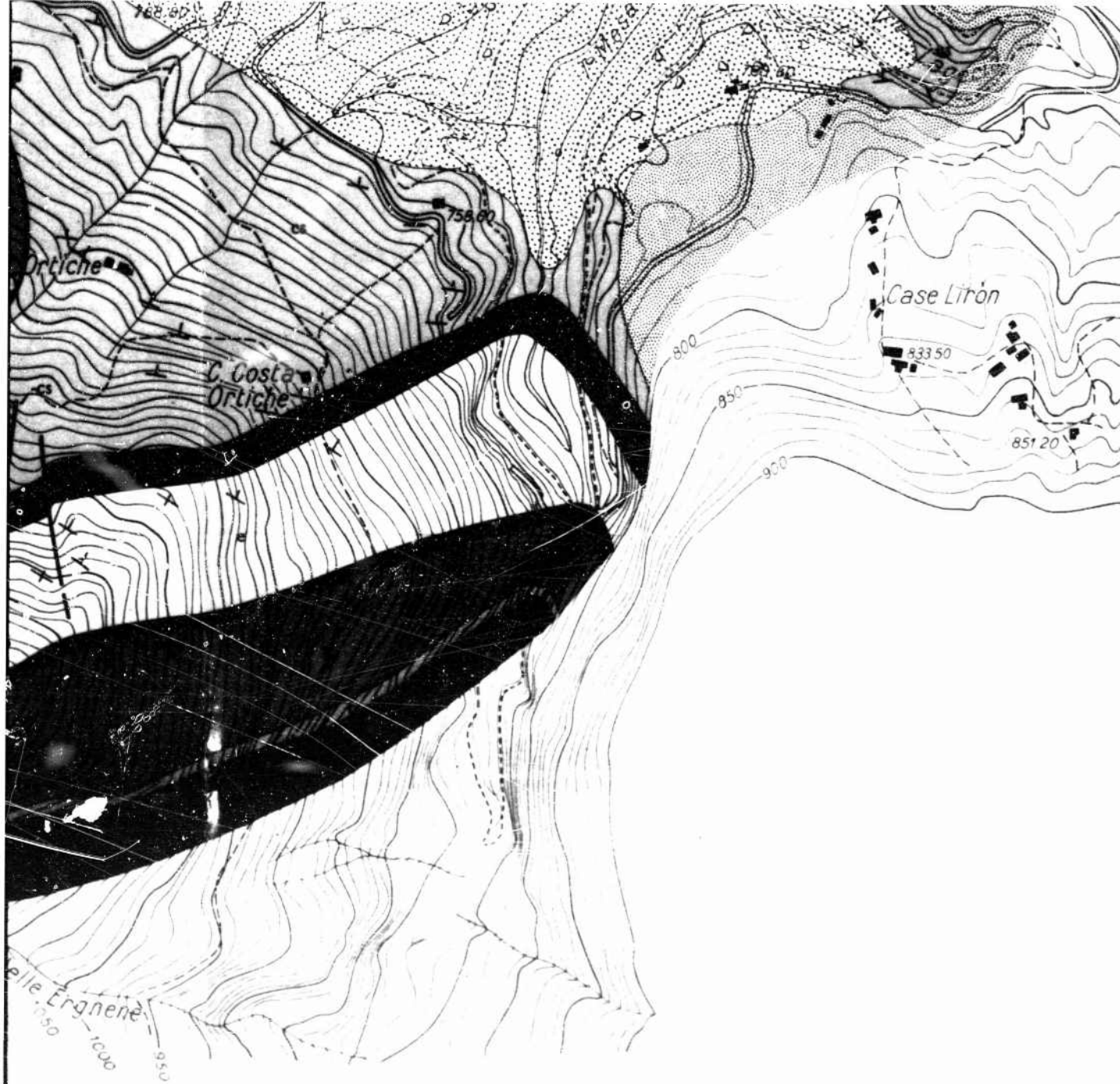
For Geologic Legend see Figure 12











LEGEND (added by Headron B. Patton)

For Geologic Legend see Figure 12

- ↑ 2 — 2 ↑ Sections used in this report
- ↑ 5 — 5 ↑
- ↑ 10A — 10A ↑
- ↑ 16 — 16 ↑
- ↑ 17 — 17 ↑
- P-1 1961 drill holes
- 2 Post 1963 slide drill holes
- P-2' } Post 1963 slide drill holes
- S-1 Geologic field observation point

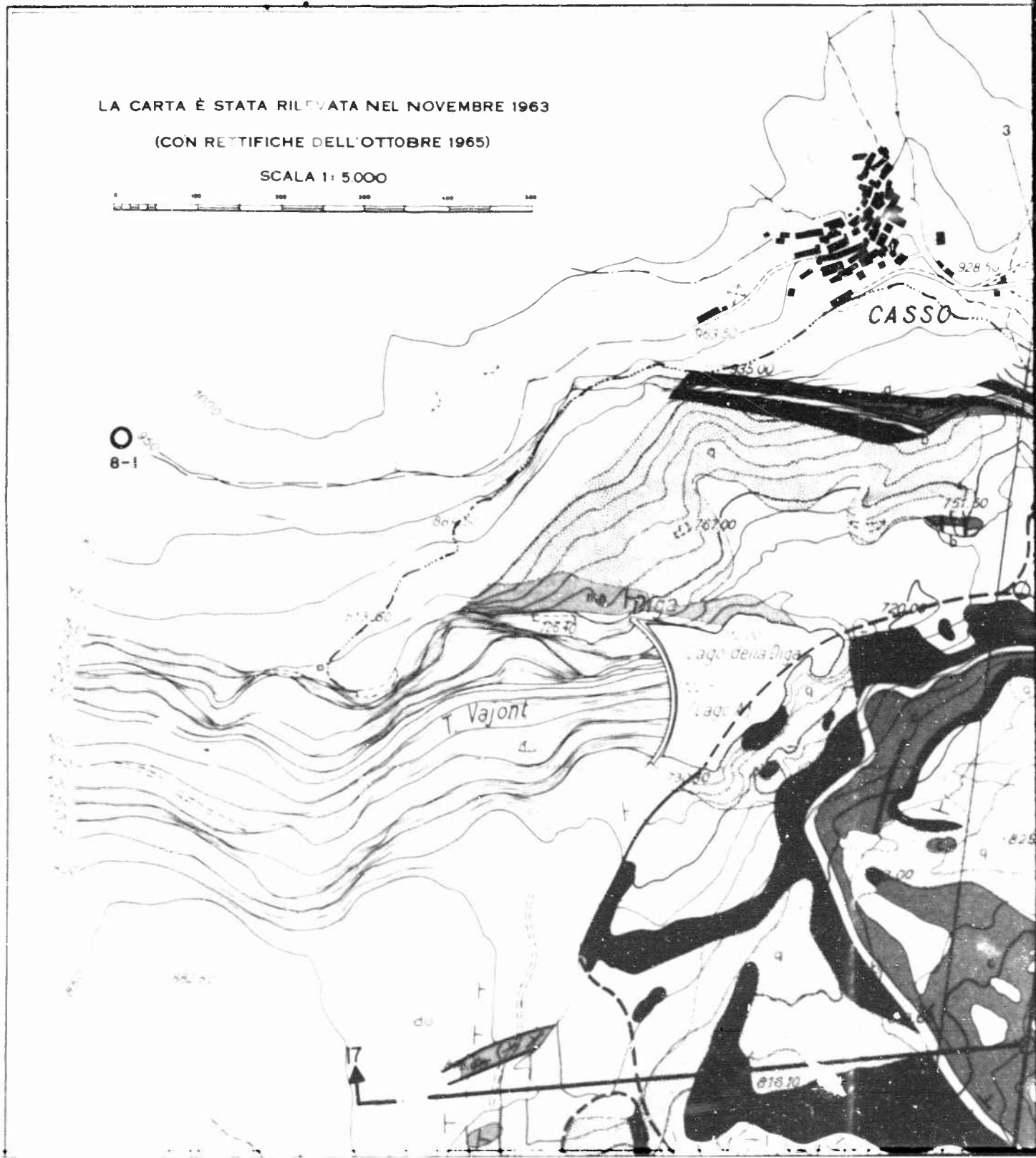
FIGURE 11

Geologic Map of the Vajont Slide
Before the Slide of October 9, 1963.

CARTA GEOL

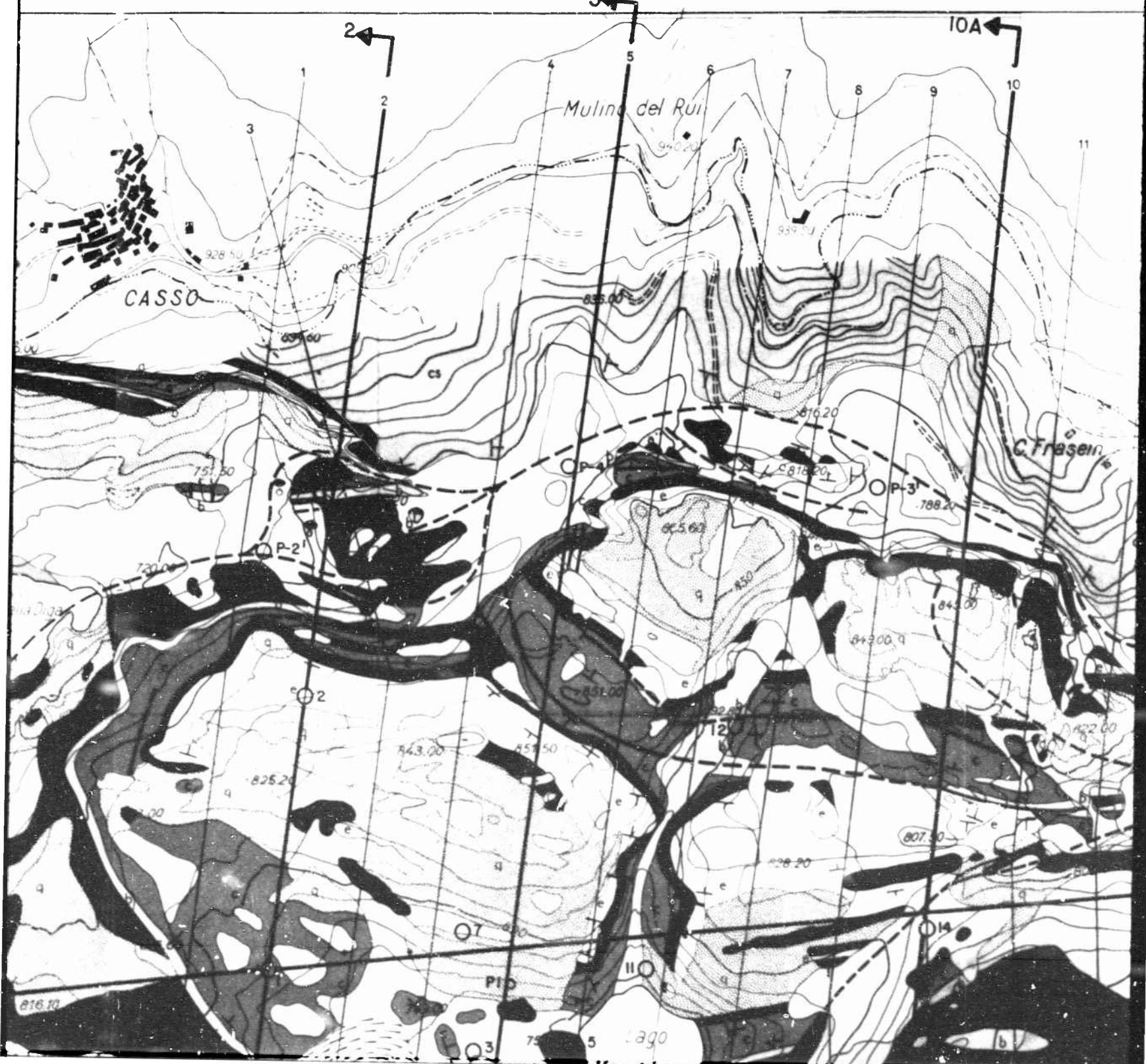
LA CARTA È STATA RILEVATA NEL NOVEMBRE 1963
(CON RETTIFICHE DELL'OTTOBRE 1965)

SCALA 1: 5.000



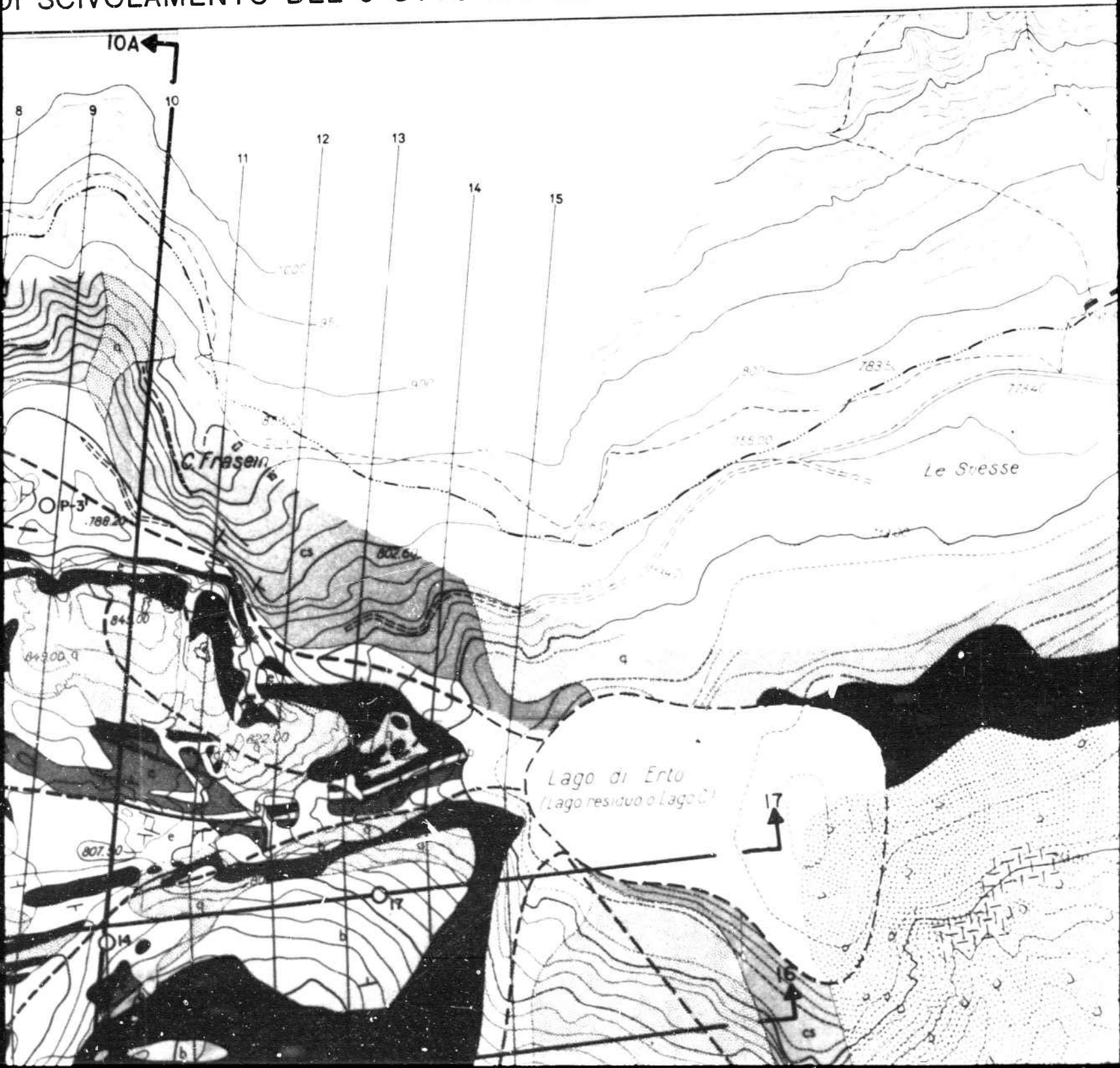
DANIELE ROSSI ED EDOARDO SEM

MARTA GEOLOGICA DEL VERSANTE SETTENTRIONALE DOPO IL FENOMENO DI SCIVOLAMENTO

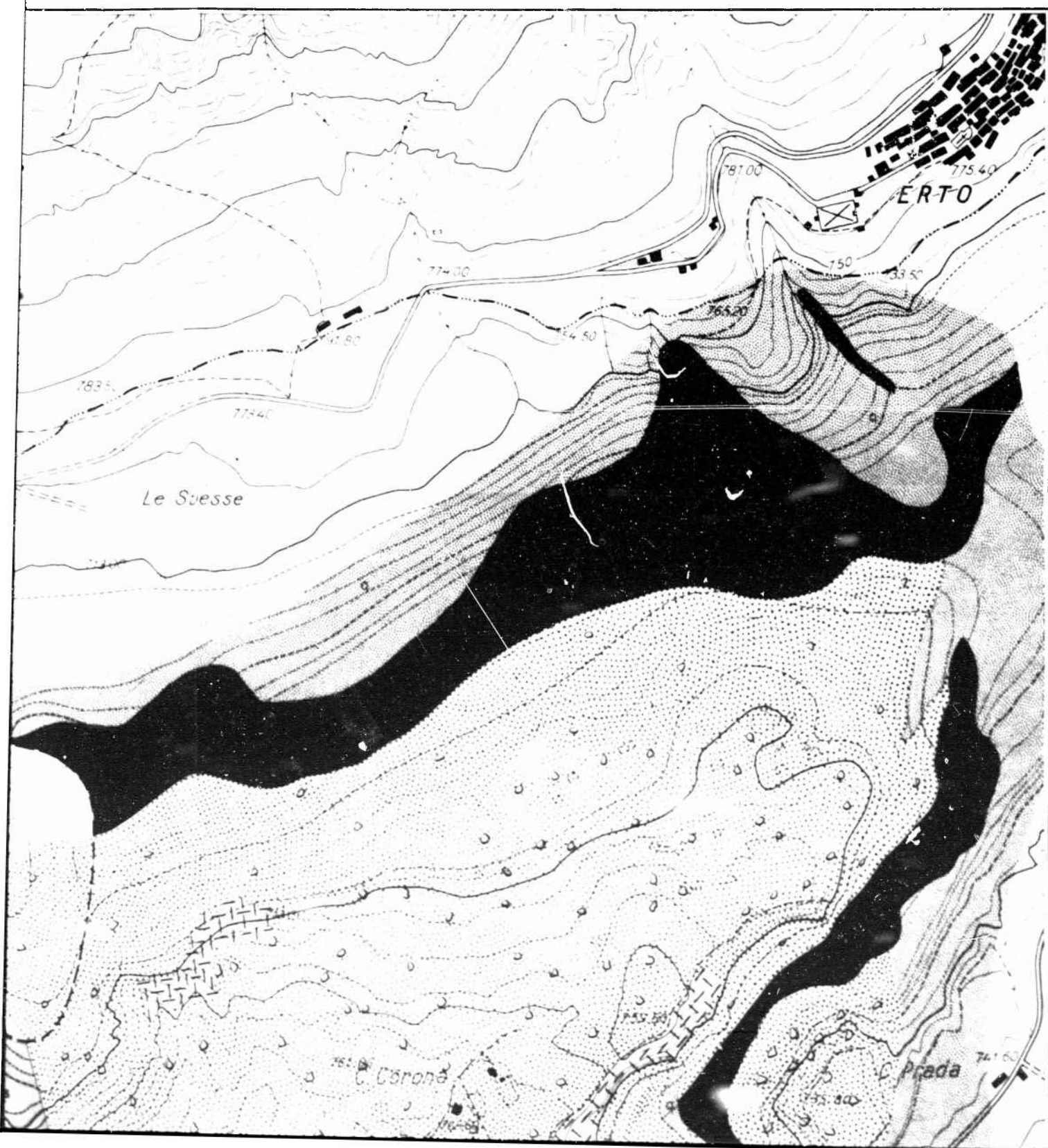


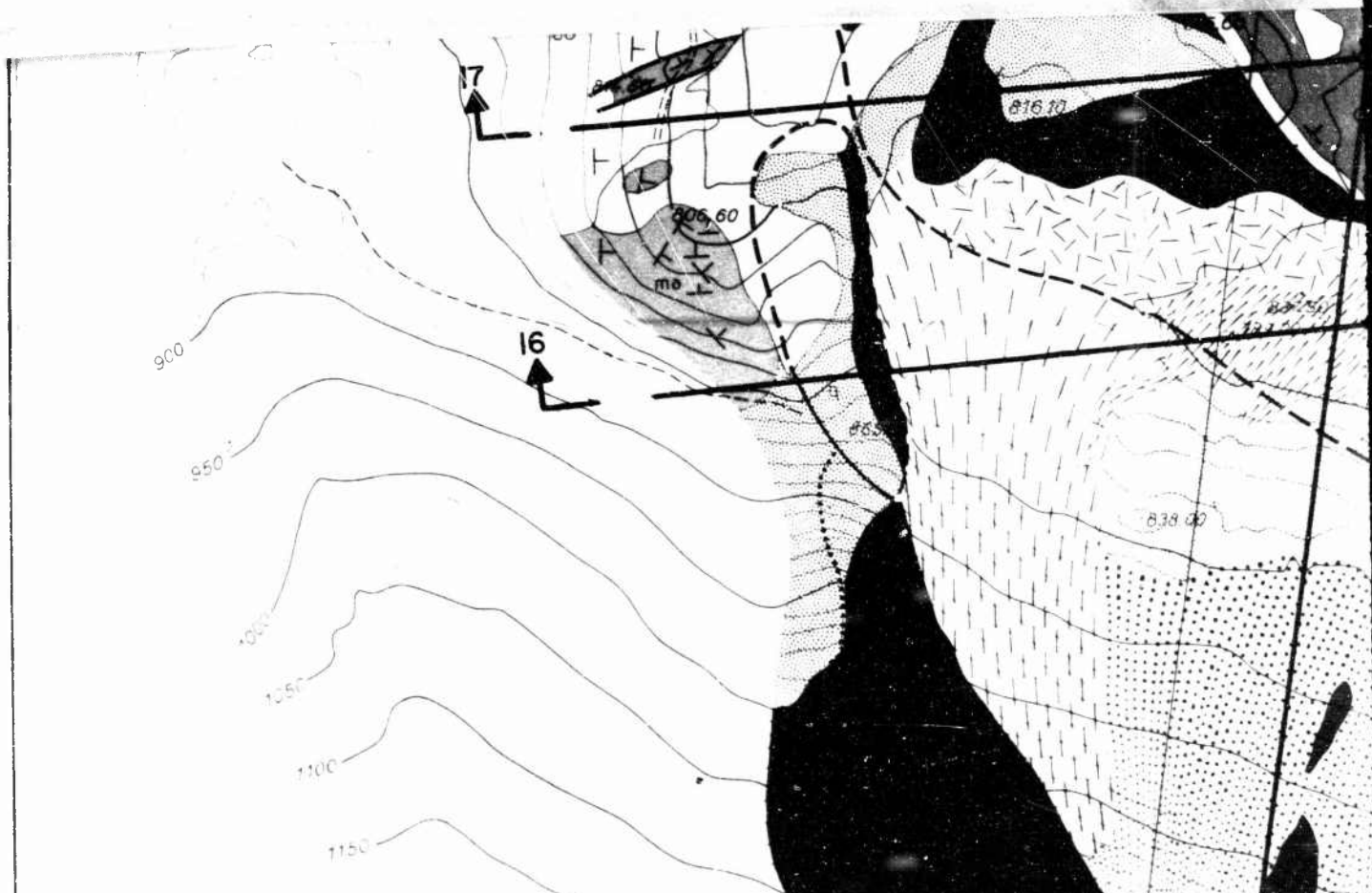
ROSSI ED EDOARDO SEMENZA

SETTENTRIONALE DEL M. TOC E ZONE LIMITROFE DI SCIVOLAMENTO DEL 9 OTTOBRE 1963



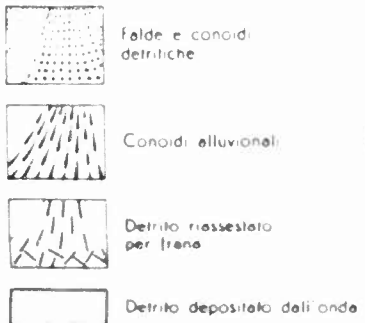
ONE LIMITROFE





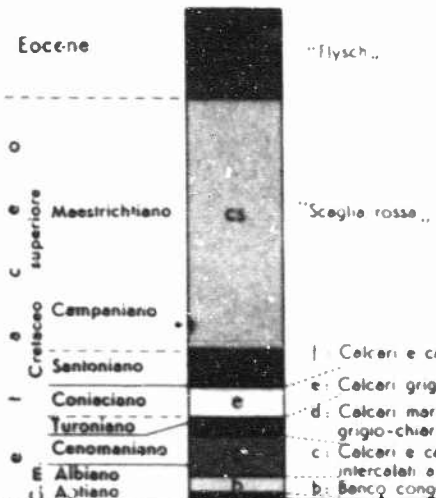
LEGENDA

Depositi posteriori
allo scivolamento



Formazioni in posto o sciolte in blocco

Eocene



Porzione sommersa della massa scivolata

Quaternario: materiali costituenti l'antica frana
della Pineda (prevolentemente Dogger, detritico
o in estese zolle più o meno calcolastiche (•) non
sempre distinte sulla carta.

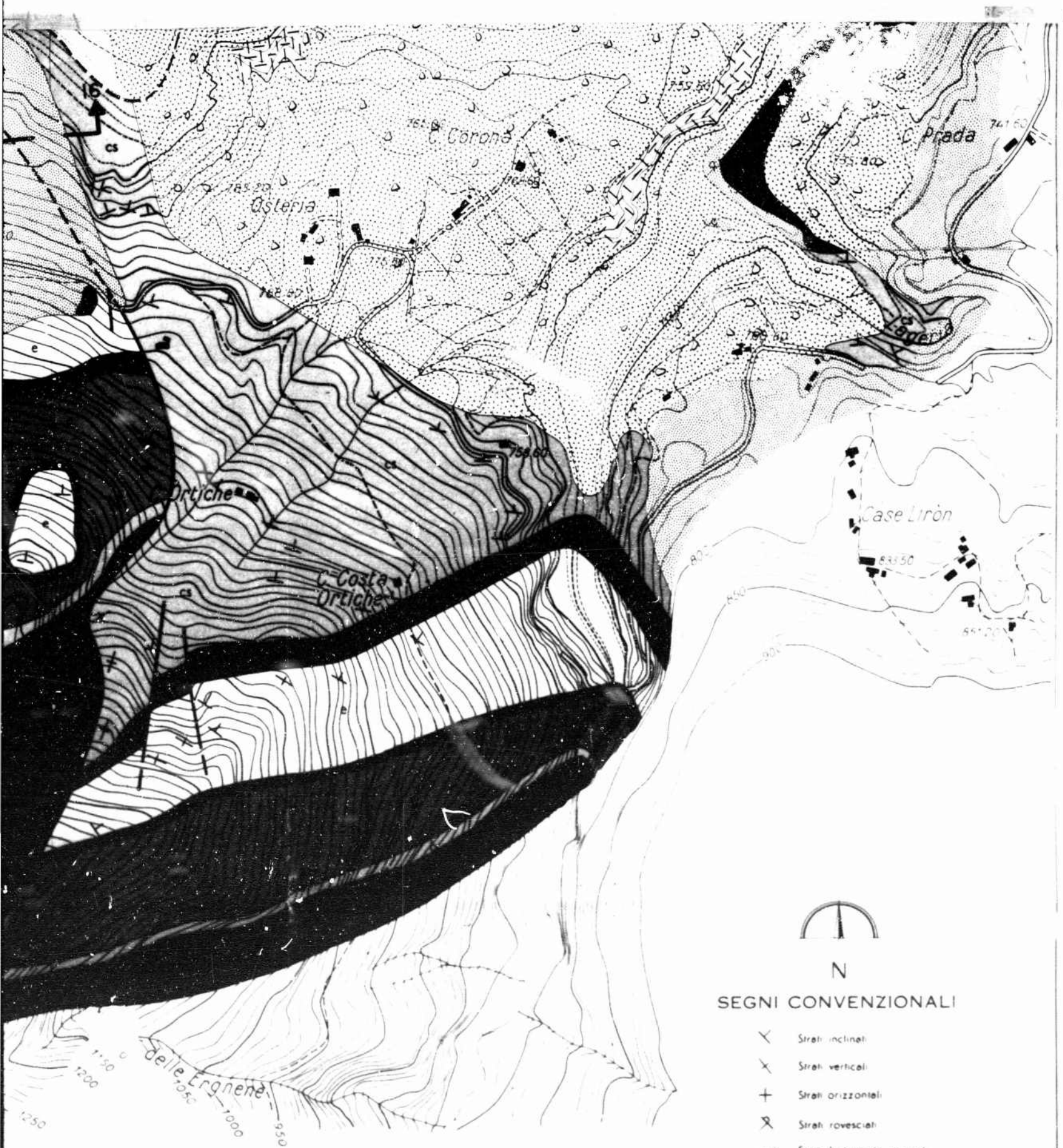
- f: Calcare e calcari marnosi rossi e verdognoli con selci rosse.
- e: Calcare grigi e nocciola con selci varicolore.
- d: Calcare marnosi e siltosi prevalentemente rossi e selce rosso con una intercalazione di calcare grigio-chiaro in parte a struttura conglomeratica o a pieghe infiformazioni.
- c: Calcare e calcari marnosi grigi o verdognoli, con frequenti interstrati calcareo-marnosi, intercalati a banchi calcarei compatti e a selce nera.
- b: Banco conglomeratico compatto.





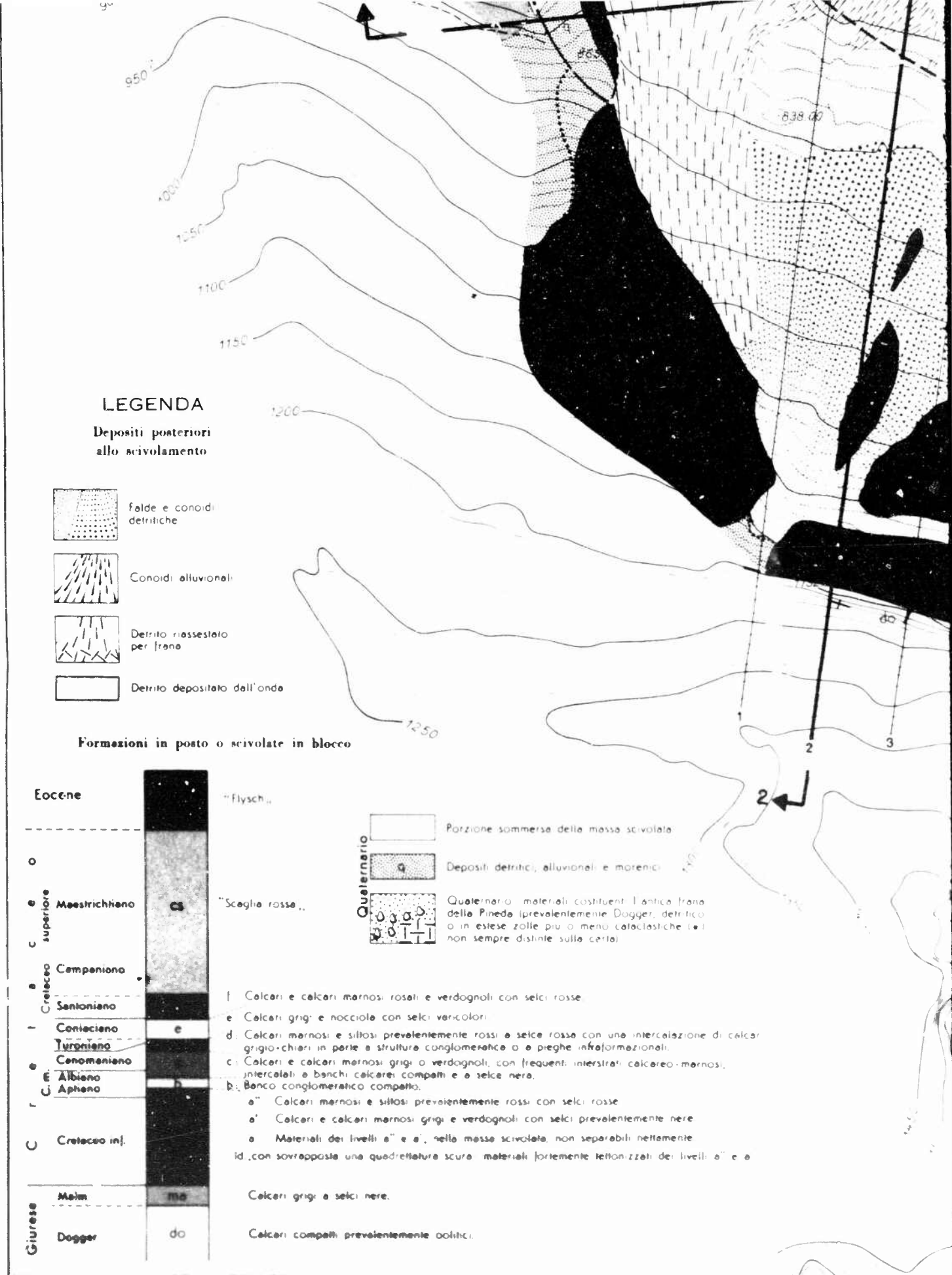
LEGEND (added by Hendron & Patton)

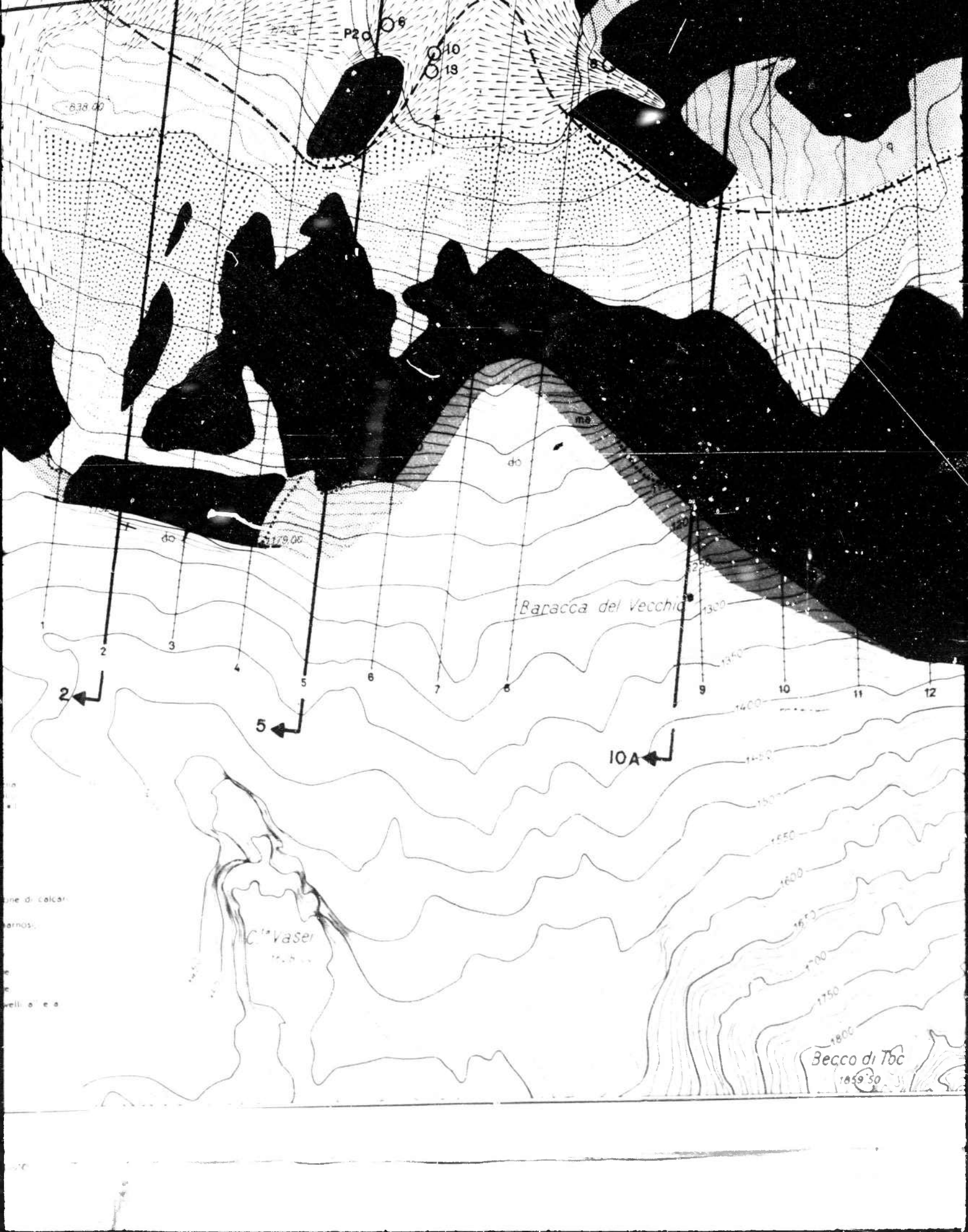
- ↑ 2 — 2 ↑ Sections used in this report
- ↑ 5 — 5 ↑
- ↑ 10A — 10A ↑
- ↑ 16 — 16 ↑

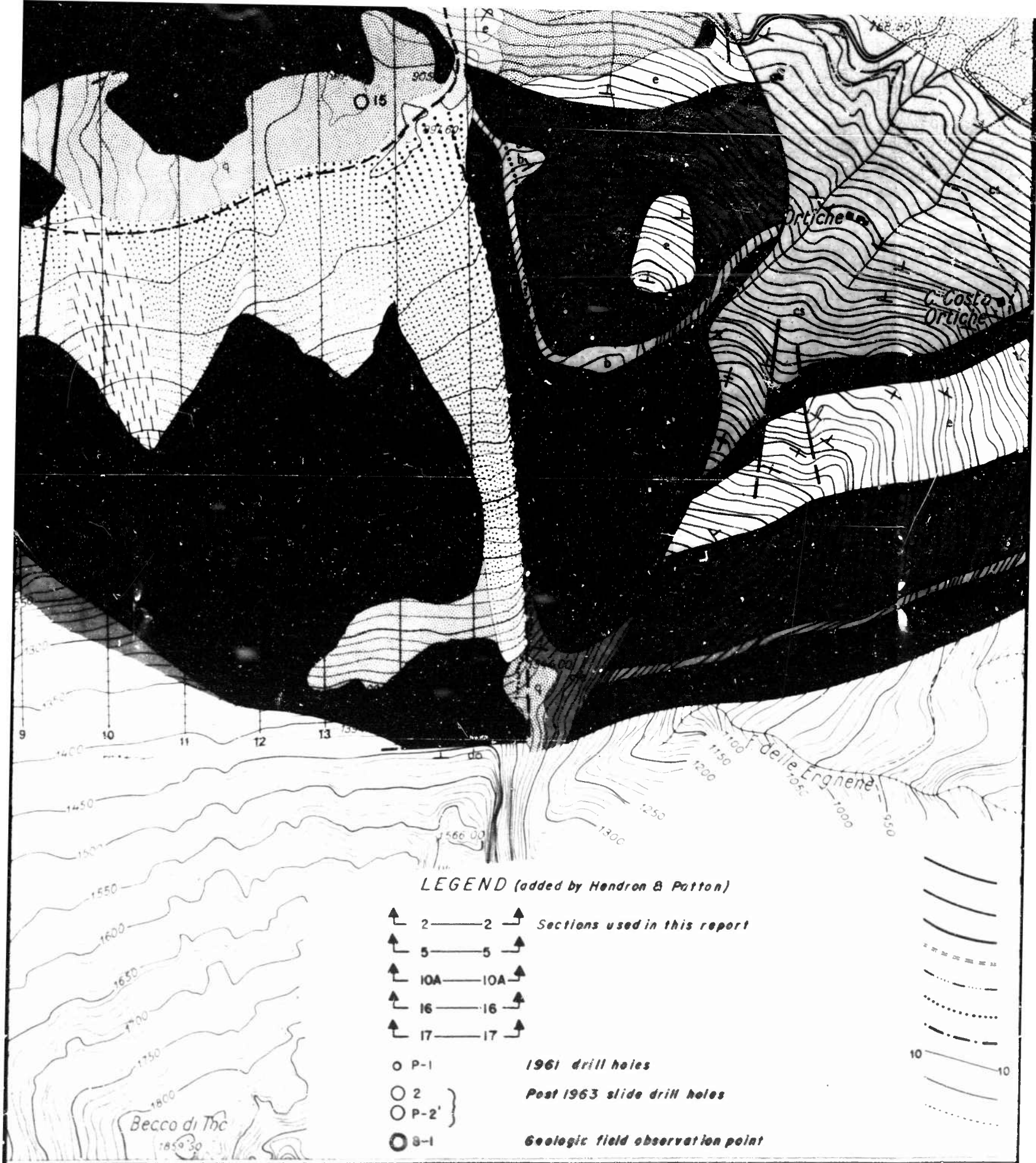


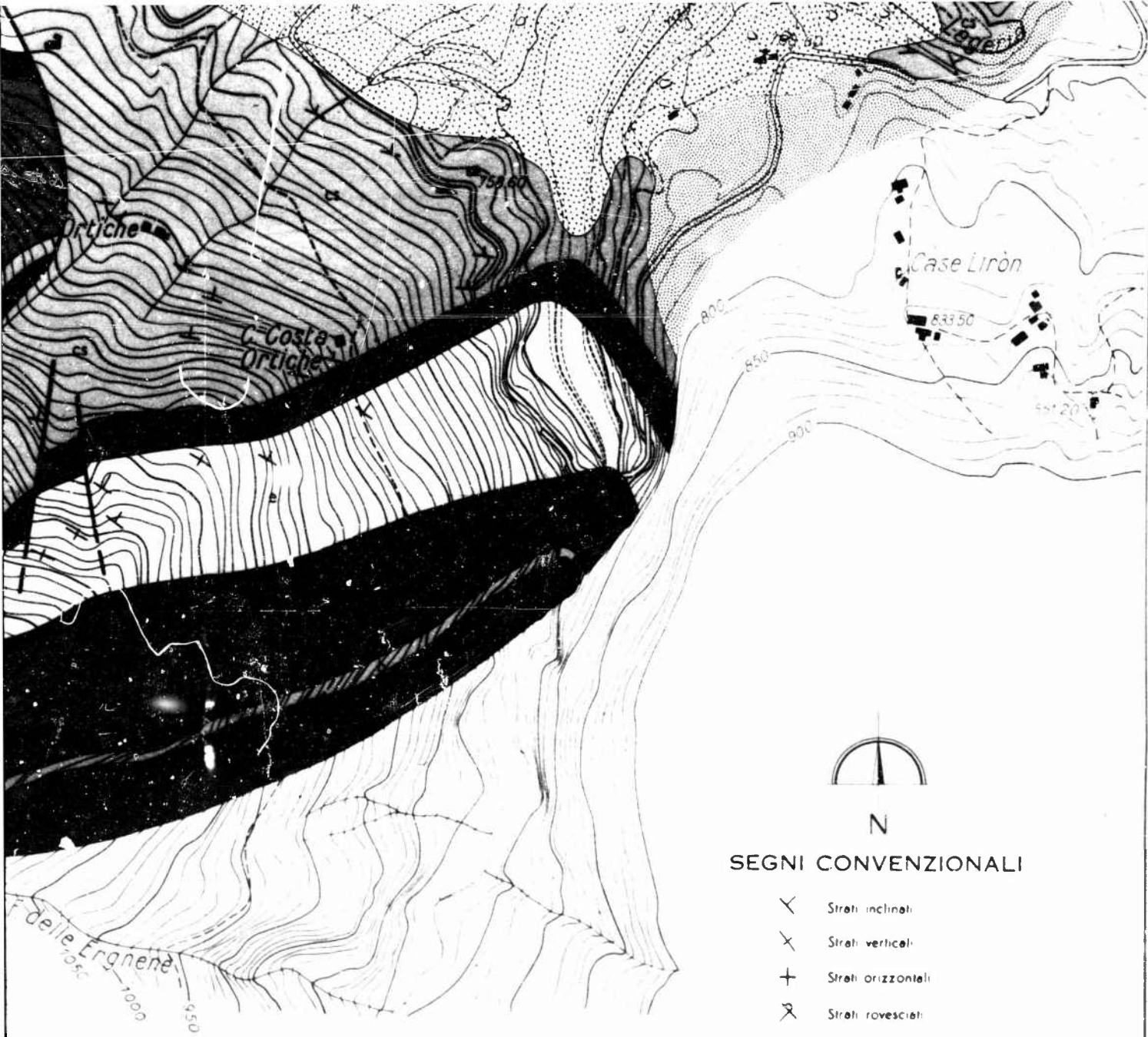
Principali linee di dislocazione precedenti allo scivolamento

determinate dallo scivolamento









N
SEgni CONVENZIONALI

- ✗ Strati inclinati
- ✗ Strati verticali
- + Strati orizzontali
- ✗ Strati rovesciati
- vvv Strati fortemente ripiegati

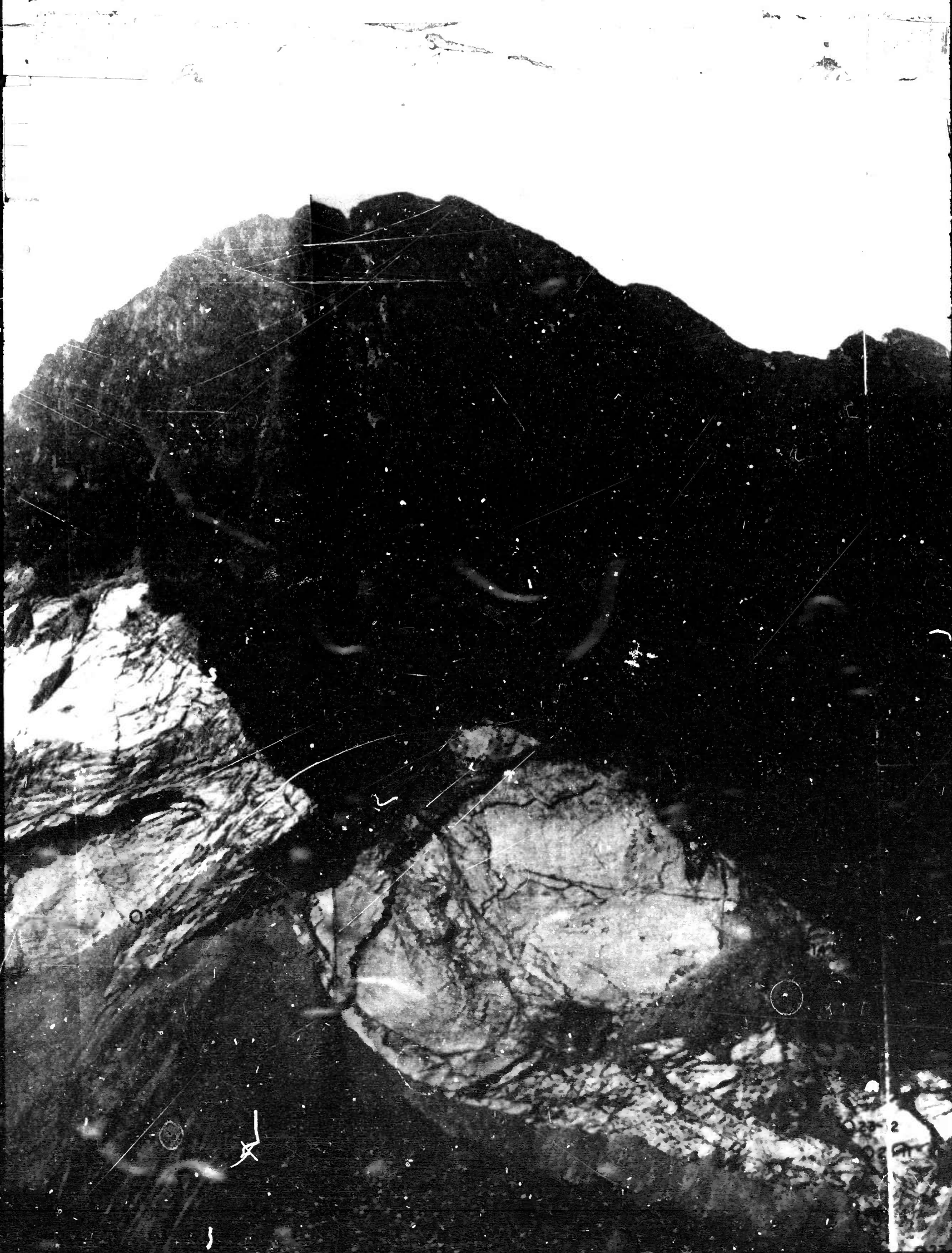
- Principali linee di dislocazione precedenti allo scivolamento
- " " " " determinate dallo scivolamento
- " " " " uniche, rinnovates: durante lo scivolamento
- Limiti della zona mascherata della successiva sovrapposizione, nella parte orientale (C. Perutti - C. Pierini)
- Limite dell'onda provocata dallo scivolamento
- Limite della superficie di distacco
- La "fessura perimetrale", compresa nell'autunno 1960
- 10 Traccia dei profili geologici
- 10 Limite dei laghi subito dopo lo scivolamento
- Linea del massimo riveso progettato

FIGURE 12

*Geologic Map of the Vajont Slide
After the Slide of October 9, 1953.*

O12-6A

24-6





LEGEND

O 23-14 Field location, sample and observation No.

Audit location

FIGURE

Photos taken Sept.

LEGEND

-14 Field location, sample and observation No.

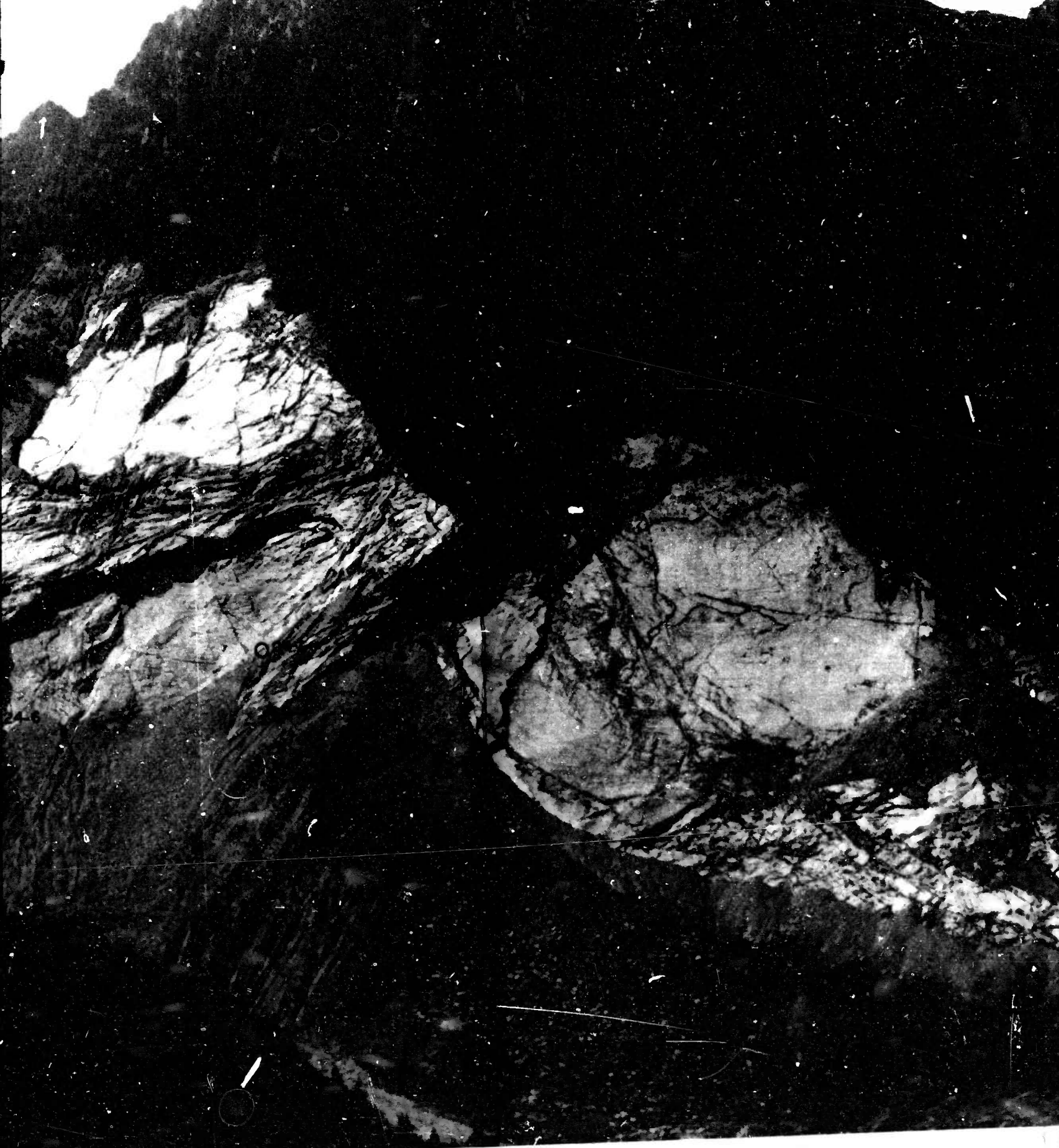
Adit location

FIGURE 13
Photomosaic of the
Upper Portion of the Valont Slide

Photos taken Sept. 19, 196





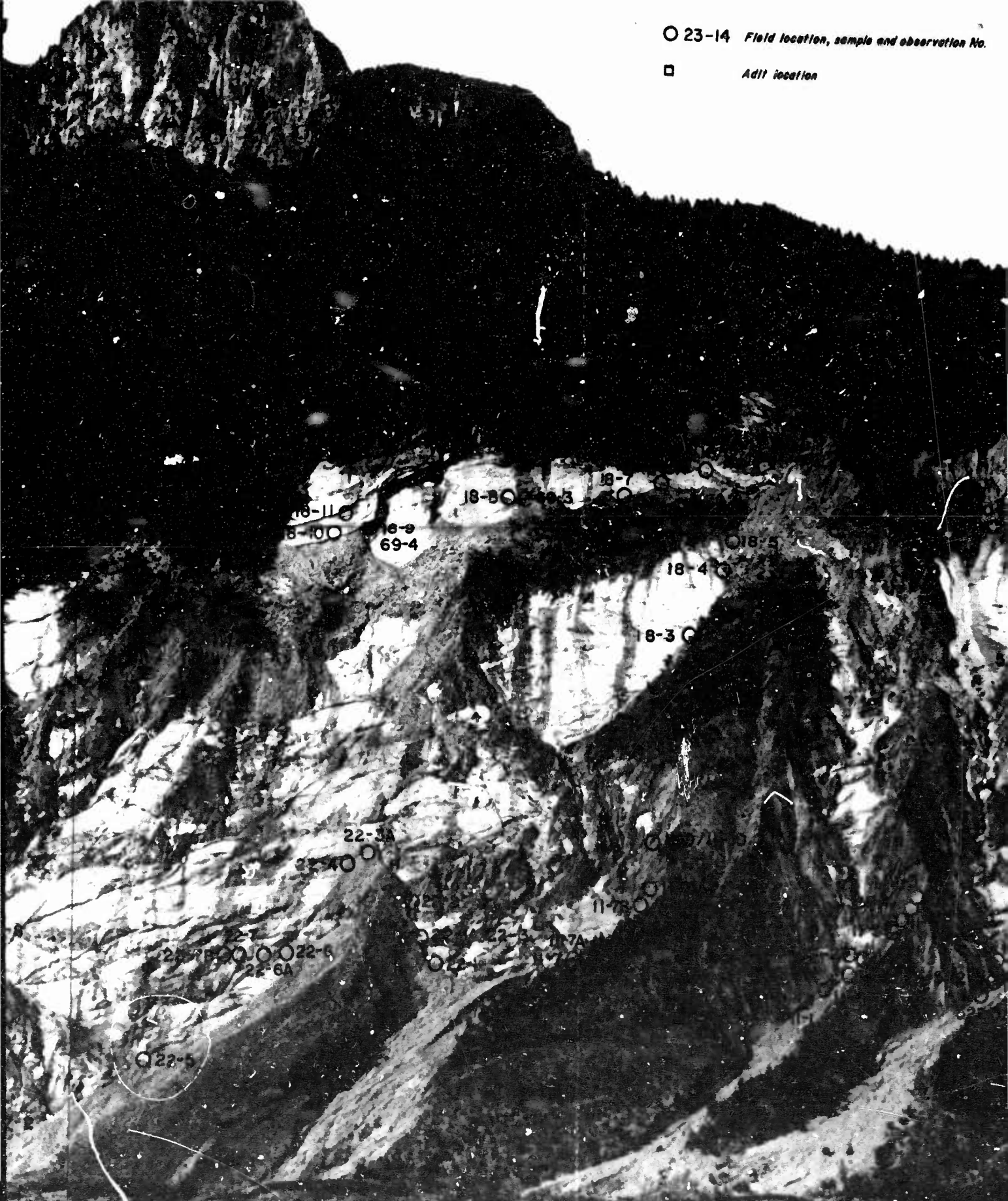




O 23-14 Field location, sample and observation No.



Addt location



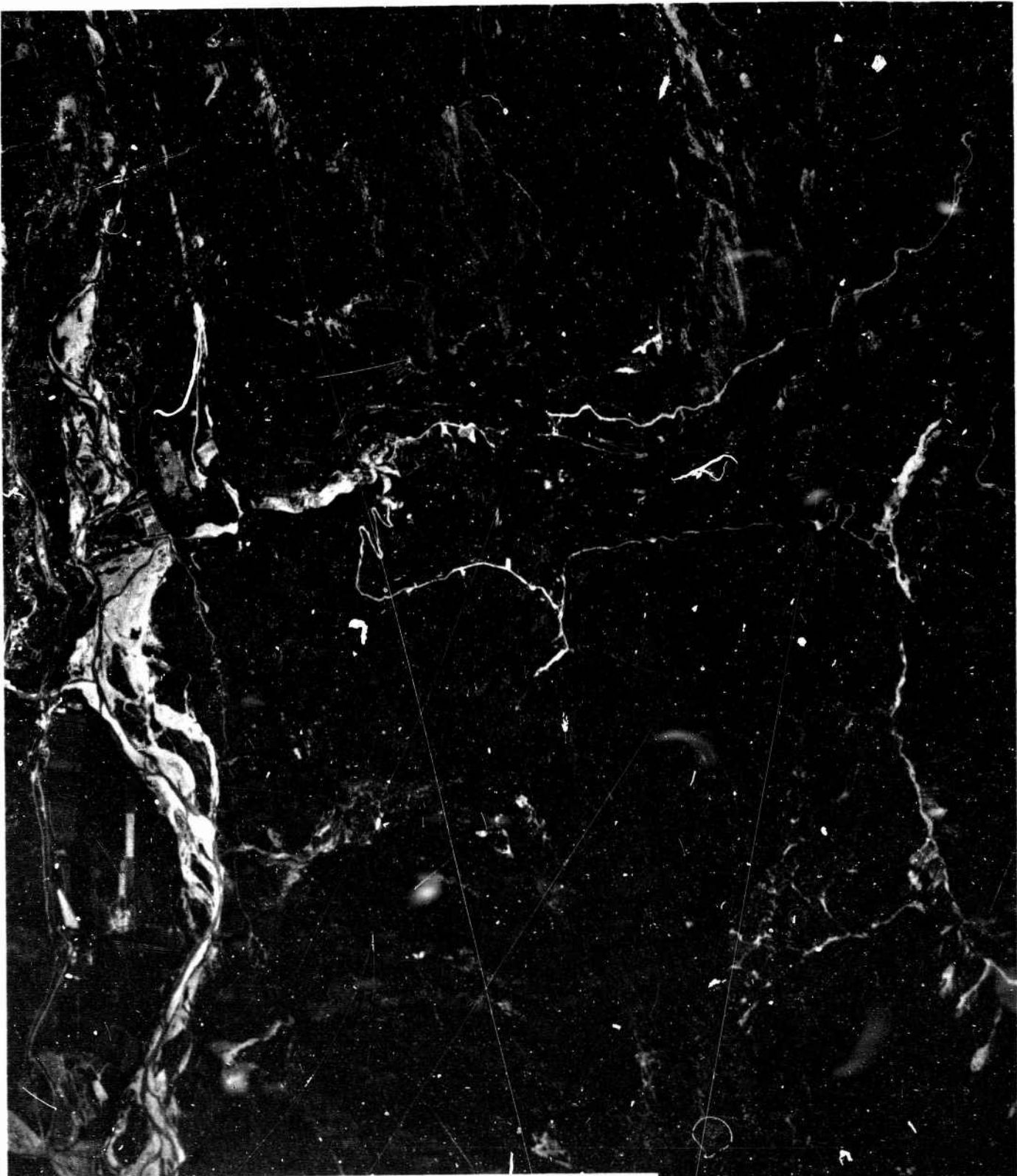


Figure 24a. Airphoto of the Vaiont Dam and Reservoir
taken in 1960

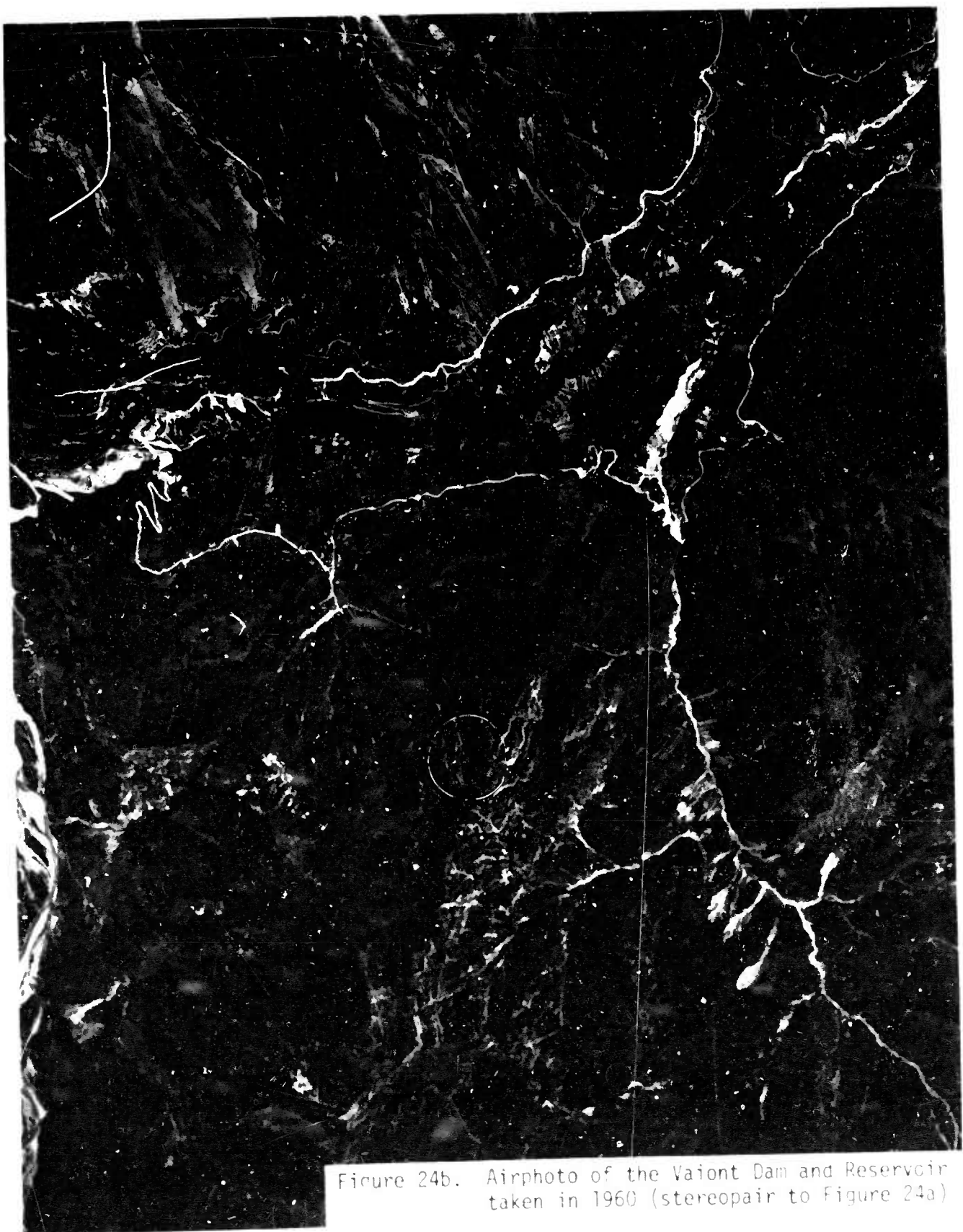
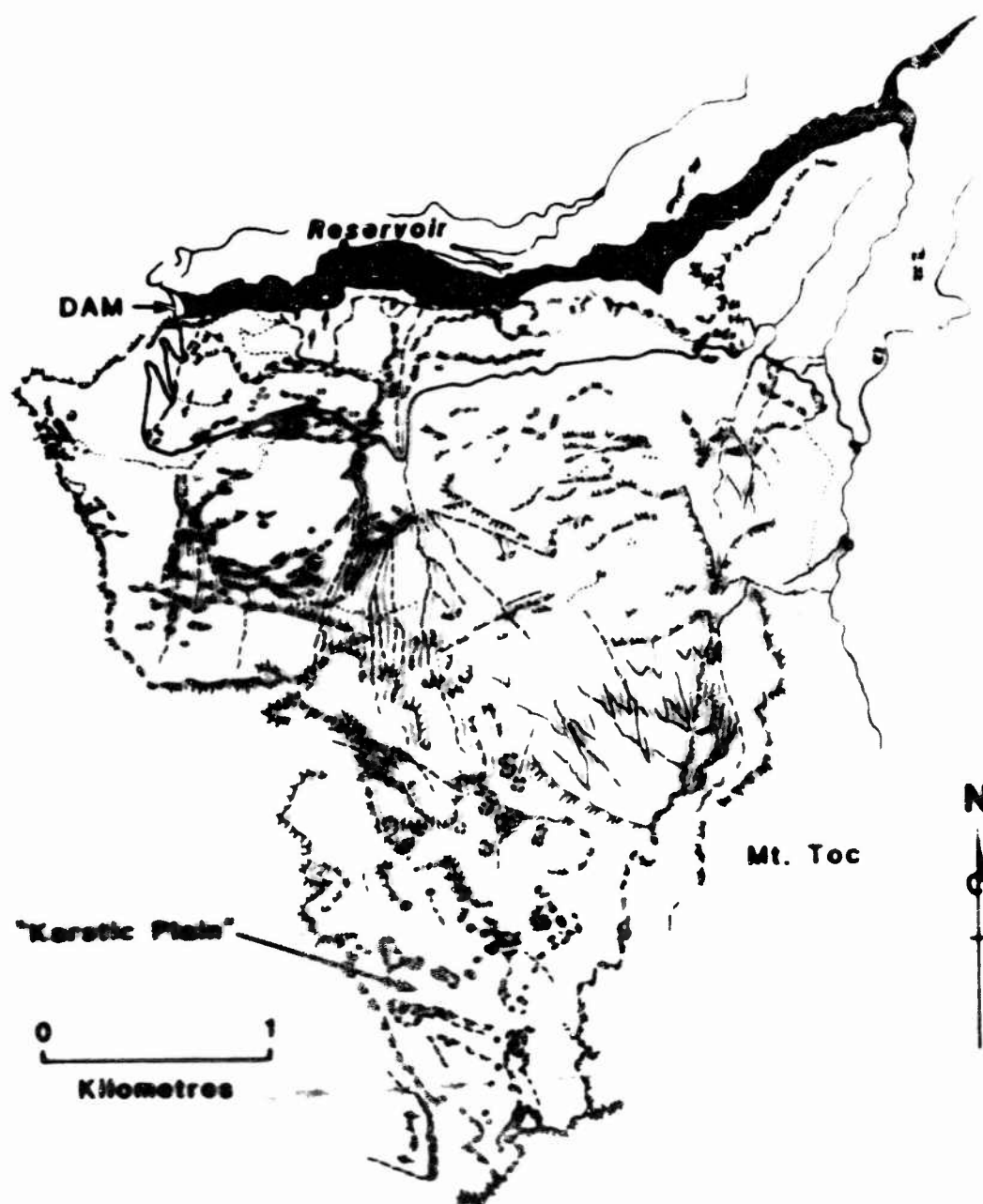


Figure 24b. Airphoto of the Vajont Dam and Reservoir taken in 1960 (stereopair to Figure 24a)



LEGEND

- | | |
|-------------------------|----------------------|
| Scarp | Roads |
| Depressions | Trails |
| Areas of slope movement | Intermittent streams |
| Outline of marker beds | Streams |

Figure 25b Geomorphic features, Valont Slide, delineated from the 1960 airphotos (transparent overlay to Figure 24a)